

A Data Fusion-based Hybrid Sensory System for Older People's Daily Activity Recognition



Yan Wang

A thesis submitted in partial fulfillment of the requirements of
Bournemouth University for the degree of Doctor of
Philosophy

October 2018

I would like to dedicate this thesis to my husband and my daughter for their unceasing love and support.

Copyright statement

This copy of the thesis has been supplied on condition that anyone who consults it is understood to recognise that its copyright rests with its author and due acknowledgment must always be made of the use of any material contained in, or derived from, this thesis.

Abstract

Population aged 60 and over is growing faster. Ageing-caused changes, such as physical or cognitive decline, could affect people's quality of life, resulting in injuries, mental health or the lack of physical activity. Sensor-based human activity recognition (HAR) has become one of the most promising assistive technologies for older people's daily life. Literature in HAR suggests that each sensor modality has its strengths and limitations and single sensor modalities may not cope with complex situations in practice. This research aims to design and implement a hybrid sensory HAR system to provide more comprehensive, practical and accurate surveillance for older people to assist them living independently.

This research: 1) designs and develops a hybrid HAR system which provides a spatio-temporal surveillance system for older people by combining the wrist-worn sensors and the room-mounted ambient sensors (passive infrared); the wearable data are used to recognize the defined specific daily activities, and the ambient information is used to infer the occupant's room-level daily routine; 2) proposes a unique and effective data fusion method to hybridize the two-source sensory data, in which the captured room-level location information from the ambient sensors is also utilized to trigger the sub classification models pretrained by room-assigned wearable data; 3) implements augmented features which are extracted from the attitude angles of the wearable device and explores the contribution of the new features to HAR; 4) proposes a feature selection (FS) method in the view of kernel canonical correlation analysis (KCCA) to maximize the relevance between the feature candidate and the target class labels and simultaneously minimizes the joint redundancy between the already selected features and the feature candidate, named mRMJR-KCCA; 5) demonstrates all the proposed methods above with the ground-truth data collected from recruited participants in home settings.

The proposed system has three function modes: 1) the pure wearable sensing mode (the whole classification model) which can identify all the defined specific daily activities together and function alone when the ambient sensing fails; 2) the pure ambient sensing mode which can deliver the occupant's room-level daily routine without wearable sensing; and 3) the data fusion mode (room-based sub classification mode) which provides a more comprehensive and accurate surveillance HAR when both the wearable sensing and ambient sensing function properly.

The research also applies the mutual information (MI)-based FS methods for feature selection, Support Vector Machine (SVM) and Random Forest (RF) for classification. The experimental results demonstrate that the proposed hybrid sensory system improves the recognition accuracy to 98.96% after applying data fusion using Random Forest (RF) classification and mRMJR-KCCA feature selection. Furthermore, the improved results are achieved with a much smaller number of features compared with the scenario of recognizing all the defined activities using wearable data alone. The research work conducted in the thesis is unique, which is not directly compared with others since there are few other similar existing works in terms of the proposed data fusion method and the introduced new feature set.

Contents

Copyright statement	I
Abstract	II
Contents	IV
List of Figures	VII
List of Tables	IX
List of Abbreviations	XI
List of Symbols	XIV
Acknowledgments.....	XV
Declaration	XVI
1 Introduction.....	1
1.1 Background and motivation	1
1.2 Aim and objectives	7
1.3 Original contributions	8
1.4 Thesis organization	11
1.5 List of resulting publications.....	13
2 Literature review	15
2.1 HAR enabled technologies in healthcare	17
2.2 Sensor modality	17
2.3 Wearable-sensor-based HAR (WSHAR).....	18
2.3.1 Overview of WSHAR	18
2.3.2 Wearable sensors	19
2.3.3 Activities of daily living	30
2.3.4 Raw data pre-processing	33
2.3.5 Features for classification	35
2.3.6 Feature dimensionality reduction and feature selection.....	43
2.3.7 Classification algorithms.....	47
2.4 Ambient-sensor-based HAR (ASHAR).....	50
2.4.1 Camera-based HAR (CHAR).....	51
2.4.2 Normal ambient-sensor-based HAR	53
2.5 Hybrid-sensory-based HAR (HSHAR).....	55
2.5.1 CHAR/Audio plus WSHAR	56

2.5.2 ASHAR plus WSHAR	56
2.5.3 CHAR plus ASHAR plus WSHAR.....	57
2.5.4 Data fusion algorithms among different sensor modalities	58
2.6 Performance evaluation and criteria.....	60
2.6.1 Performance evaluation.....	60
2.6.2 Performance criteria	60
2.7 Applications of HAR in assisted living.....	62
2.8 Research gaps.....	64
2.9 Summary	68
3 Methodology and system design	69
3.1 Introduction	69
3.2 Methodology	69
3.2.1 System design.....	72
3.2.2 Data fusion	74
3.2.3 Sensor prototype.....	75
3.2.4 Data collection and feature extraction.....	82
3.2.5 Feature selection methods used in the system.....	83
3.2.6 Classification algorithms and performance assessment	85
3.3 Summary	90
4 Data collection and data preprocessing	91
4.1 Data acquisition for the research	91
4.1.1 Activity definition and wearable data collection.....	91
4.1.2 Ambient data	95
4.2 Feature pool generation for the system	95
4.3 Data segmentation of wearable data.....	102
4.4 Summary	106
5 Identification of the contributions of the selected wearable sensors and the augmented features	107
5.1 Mutual information inspired feature selection using kernel canonical correlation analysis.....	108
5.1.1 KCCA and the proposed feature selection method mRMJR-KCCA	109
5.1.2 Experimentations and results based on the mRMJR-KCCA.....	112
5.1.3 Remarkd conclusion	117

5.2 Identification of the contribution of the selected wearable sensors	120
5.2.1 Sensor contribution identification with the MI-based feature selection methods	120
5.2.2 Sensor contribution identification with the proposed mRMJR-KCCA feature selection method	122
5.2.3 Remarkd conclusion.....	126
5.3 Identification of the augmented features from the wearable sensors	127
5.3.1 Experimental results with the MI-based feature selection methods.....	127
5.3.2 Experimental results with the mRMJR-KCCA feature selection.....	128
5.3.3 Remarkd conclusion.....	130
5.4 Summary	134
6 Data fusion of the wearable information and the ambient information	135
6.1 Daily routine derived from the PIR sensors.....	135
6.2 Data fusion between the wearable sensors and the ambient sensors.....	138
6.2.1 Experiments of the data fusion based on the MI-based feature selection	139
6.2.2 Data fusion of the hybrid sensory system using mRJMJR-KCCA feature selection	143
6.3 Summary	149
7 Conclusions and future works.....	152
7.1 Thesis summary	152
7.2 Main findings	153
7.3 Limitations and future direction.....	156
Appendix A Experimental results	159
Appendix B Participant Information Sheet.....	165
Appendix C Consent Form	169
Bibliography	171

List of Figures

Figure 1. 1 Percentage of population in broad age groups for the world and by region, 2017	2
Figure 1. 2 The thesis structure.....	12
Figure 2. 1 Literature review diagram in chapter 2	16
Figure 2. 2 Learning procedure of WSHAR.....	20
Figure 2. 3 Sensor placement on body and the associated sensors in WSHAR	27
Figure 2. 4 Deployment of wearable sensors.....	28
Figure 2. 5 An accelerometer located at the waist (Rodriguez-Martin et al., 2013)	28
Figure 2. 6 The accelerometer placed on multiple body parts (Szttyler et al., 2017)	29
Figure 2. 7 Device worn on a wrist (Mortazavi et al., 2014).....	29
Figure 2. 8 Multiple sensors placed on body (Chernbumroong et al., 2014)	30
Figure 2. 9 Sample number of each window versus window size in publications .	36
Figure 2. 10 Skeleton representations of some specific activities (Jalal et al., 2014)	53
Figure 2. 11 Samples of human depth silhouettes (Jalal et al., 2017)	53
Figure 2. 12 A study of the ambient-sensors based smart home (Tunca et al., 2014)	54
Figure 2. 13 The Experimental setup (Liu et al., 2014a).....	56
Figure 2. 14 Experiment setup in Pham et al., 2018.....	57
Figure 2. 15 Applications of HAR for daily life in healthcare	63
Figure 3. 1 The development steps of the research	71
Figure 3. 2 Conceptual framework of the proposed system	73
Figure 3. 3 Wearable sensors used in this research	77
Figure 3. 4 Ambient sensors in this research	78
Figure 3. 5 Flowchart of the Centre Unit.....	79
Figure 3. 6 Flowchart of the Receiving Terminal Unit	80
Figure 3. 7 Wearable sensor placement in this research.....	81
Figure 3. 8 Ambient sensor placement in this research	82
Figure 3. 9 Classification boundaries of SVM solution	86
Figure 3. 10 10-fold data split.....	88
Figure 3. 11 The simplified Random Forest.....	89
Figure 4. 1 Data collection examples and the recorded wearable raw data.....	97

Figure 4. 2 The wearable device on the wrist and the corresponding attitude.....	99
Figure 4. 3 Performance of different window lengths based on <i>CUFs</i> with SVM	104
Figure 4. 4 Performance of different window lengths based on <i>ARFs</i> with SVM	104
Figure 5. 1 Classification accuracies versus increasing γ (0.1~100) on Seeds and Parkinsons.....	118
Figure 5. 2 Classification accuracies versus varied γ values in the RBF kernel on <i>ARFs</i>	118
Figure 5. 3 Classification accuracies versus the number of components in ICD on <i>ARFs</i> , <i>CUFs</i> , and <i>All</i> with SVM and RF classification.....	119
Figure 5. 4 Performance of AGM and AGMBT with RF for 17 defined activities	125
Figure 5. 5 Performance of AGM and AGMBT with SVM for 17 defined activities	125
Figure 5. 6 Classification accuracy versus the number of selected features from different feature sets with SVM plus MI-based FS methods (“ <i>All</i> ” represents “ <i>CUFs+ARFs</i> ”).....	129
Figure 5. 7 Classification accuracy versus the number of selected features from different feature sets with RF plus MI-based FS methods (“ <i>All</i> ” represents “ <i>CUFs+ARFs</i> ”).....	129
Figure 5. 8 Classification accuracies of <i>CUFs</i> , <i>ARFs</i> and <i>All</i> on all 17 activities with RF+mRMJR-KCCA.....	132
Figure 5. 9 Classification accuracies of <i>CUFs</i> , <i>ARFs</i> and <i>All</i> on all 17 activities with SVM+mRMJR-KCCA.....	132
Figure 6. 1 One subject’s room-level routine over a whole day.....	138
Figure 6. 2 Classification accuracy before and after data fusion using different feature selection methods with SVM based on <i>ARFs</i>	140
Figure 6. 3 Classification accuracy of before and after data fusion with SVM+mRMJR-KCCA.....	146
Figure 6. 4 Classification accuracy of before and after data fusion with RF+mRMJR- KCCA.....	148
Figure 6. 5 Classification accuracy of all 17 activities with RF on different feature sets before and after data fusion.....	151

List of Tables

Table 2. 1 Wearable sensors used in HAR	22
Table 2. 2 Sensor platforms in WSHAR	25
Table 2. 3 Typical Sensor placement in WSHAR	31
Table 2. 4 Case studies regarding activity types in assisted living.....	32
Table 2. 5 Typical hand-crafted features used in HAR	40
Table 2. 6 Comparison between hand-crafted features and automatically learned features.....	44
Table 2. 7 Comparison of conventional and deep learning classification algorithms	50
Table 2. 8 Ambient sensors used in HAR.....	51
Table 2. 9 Summary of sensor modalities in HAR systems	59
Table 2. 10 Confusion matrix	61
Table 2. 11 Review of existing works in HAR based on sensor modality	65
Table 2. 12 Identified research gaps in HAR by the review.....	68
Table 3. 1 10-fold cross-validation procedure	88
Table 3. 2 Materials and methods used in the research	90
Table 4. 1 Daily activity defined in this research	92
Table 4. 2 Participants' demographic information	93
Table 4. 3 Raw data examples collected from wearable sensors from the first participant	94
Table 4. 4 Raw data captured by the PIR sensors.....	98
Table 4. 5 The original feature pool created in this research.....	102
Table 4. 6 Feature examples from the raw data of the first participant	105
Table 5. 1 Pseudocode of the mRMJR-KCCA.....	112
Table 5. 2 Descriptions of UCI datasets and ground-truth datasets used in the experiments.....	113
Table 5. 3 Classification accuracy (%) with SVM plus mRMJR-KCCA on the used data sets.....	114
Table 5. 4 Classification accuracy (%) with RF plus mRMJR-KCCA on the used data sets.....	115

Table 5. 5 Classification Accuracy (%) of different sensor combinations with SVM plus MI-based feature selection	121
Table 5. 6 Classification accuracy (%) of different sensor combinations with RF plus MI-based feature selection.....	123
Table 5. 7 The top 30 features selected by mRMR and mRMJR-KCCA from <i>CUFs</i> with all five wearable sensors (AGMBT).....	124
Table 5. 8 Classification results with SVM for each activity (%) on different feature sets.....	130
Table 5. 9 Classification results with RF for each activity (%) on different feature sets.....	131
Table 5. 10 The top 30 features selected by mRMR and mRMJR-KCCA from <i>All (ARFs + CUFs)</i> with three sensors (AGM)	133
Table 6. 1 Room location information from PIR sensors	137
Table 6. 2 Activity assignment in rooms for data fusion.....	139
Table 6. 3 Classification accuracy (%) with SVM before and after applying data fusion based on <i>ARFs</i>	141
Table 6. 4 Features selected by mRMR and CMIM before and after data fusion	142
Table 6. 5 Classification accuracy with RF before and after data fusion on different feature sets from AGM	150
Table A. 1 Confusion matrix based on mRMR plus SVM before data fusion (wearable sensing alone).....	159
Table A. 2 Confusion matrix based on mRMR plus SVM after data fusion (combined sensing).....	160
Table A. 3 Confusion matrix based on CMIM plus SVM before data fusion (wearable sensing alone).....	161
Table A. 4 Confusion matrix based on CMIM plus SVM after data fusion (combined sensing)	162
Table A. 5 Confusion matrix based on mRMJR-KCCA plus RF before data fusion	163
Table A. 6 Confusion matrix based on mRMJR-KCCA plus RF after data fusion	164

List of Abbreviations

AR	Activity recognition
ASHAR	Ambient-sensor-based HAR
AAL	Ambient Assisted Living
ADL	Activities of daily life
AR	Autoregressive coefficient
ANN	Artificial Neural Network
<i>ARFs</i>	The attitude related features
AGM	Accelerometer, gyroscope, and magnetometer
AGMBT	Accelerometer, gyroscope, magnetometer, barometer and temperature
BP	Blood pressure
BG	Blood glucose
CU	Centre Unit
CNN	Convolutional Neural Network
CFS	Correlation-based Feature Selection
CCA	Canonical Correlation Analysis
CMIM	Conditional Mutual Information Maximum
<i>CUFs</i>	The conventionally used features
DBN	Deep Belief Network,
DWT	Discrete Wavelet Transform
DCT	Discrete Cosine Transform
DISR	Double Input Symmetrical Relevance
DT	Decision trees
DCCA	Deep CCA
ECG	Electrocardiogram
EEG	Electroencephalograph
EMD	Empirical mode decomposition
FFT	Fast Fourier Transform
FS	Feature selection
FDA	Fisher Linear Discriminant Analysis

FMMNN	Fuzzy Min-Max Neural Network
FCM	Fuzzy C-means algorithms
FP	False positives
FN	False negatives
GMM	Gaussian mixture models
GK-FDA	Gaussian Kernel Fisher Linear Discriminant Analysis
GK-SVM	Gaussian Kernel Support Vector Machine
HAR	Human Activity Recognitions
HSAR	Hybrid-sensory-based HAR
HR	Heart rate
HMM	Hidden Markov models
IMUs	Inertial measurement units
IR	Infrared
IoT	Internet of Things
ICD	Incomplete Cholesky decomposition
JMI	Joint Mutual Information
J48	The implementation of decision tree algorithm in WEKA
KCCA	Kernel canonical correlation analysis
kNN	k-Nearest Neighbor
kPCA	Kennel PAC
LDA	Linear Discriminant Analysis
LSCCA	Samples versus Labels CCA
LSTM	Long short-term memory
MI	Mutual Information
mRMR	maximal Relevant Minimal Redundant
mRMJR	maximal Relevant Minimal Joint Redundant
MLP	Multiplayer Perceptron
MCR-CCA	Maximum Collective Relevance CCA
NNs	Neural networks
NB	Na ïve Bayes
PIR	Passive infrared

PCA	Principal Component Analysis
PD	Parkinson's Disease
RFID	Radio Frequency Identification
RTU	Receiving Terminal Unit
RF	Random Forest
RNN	Recurrent Neural Network
RBM	Restricted Boltzmann machine
RR	Respiratory rate
RBF	Radial basis function
SVM	Support Vector Machines
SpO2	Oxygen saturation
SMA	Signal magnitude area
Std	Standard deviation
SVD	Singular value decomposition
TP	True positives
TN	True negatives
VHAR	Vision-based-HAR
WSHAR	Wearable-sensor-based HAR
WPD	Wavelet packet decomposition

List of Symbols

D_t Wearable data series

DL The data length

OV Overlap size

SL Segmentation length

w_i Sub windows

\mathcal{F} Feature extraction function set

X, Y sets of random variables

f_k Feature candidate;

F The original feature set;

S The already selected feature set

f_l Any feature in S

C The class labels.

K_X, K_Y Kernel matrix

$\mathcal{O}()$ Computation complexity

ρ_{KCCA} The correlation coefficient calculated by KCCA

γ The parameter in RBF kernel

Acknowledgments

This research was partially supported by the Erasmus Mundus Fusion Project (545831-EM-1-2013-1-IT-ERAMUNDUSEMA21), CHARMED (H2020-MSCA-RISE-2016-734684), SMOOTH (H2020-MSCA-RISE-2016-734875) and Bournemouth University. I would like to express my gratitude to all the volunteers who involved in this research for data collection.

This thesis would not have been possible without the help and support of the people around me. First of all, I would like to deeply thank Prof Hongnian Yu and Prof Shuang Cang who showed me the path to the research area of machine learning and elderly healthcare. I am extremely lucky to have had them as mentors. They have been providing continuous guidance, constructive feedback, and knowledge sharing to me during my whole Ph.D. study. Their rigorous research attitude keeps driving me to work hard and aim high.

I would like to thank Dr. Emili Balaguer-Ballester and other staff in BU who either provided valuable guidance to my research and personal life or gave timely access to the research facilities. My special thanks also go to Pengcheng, Pree, Ikram and other teammates for their support of my research and all the fun we have had in the past three years. I would like to sincerely thank Emily, Rui, Damla, Rose and other friends for their generous support in my difficult times during my stay in the UK.

My colleagues at Zhongyuan University of Technology and friends in China have been supporting and encouraging me on this path. Your tremendous help and invaluable friendship are all greatly appreciated.

Last but not least, I am indebted to my whole family, you should know that your unconditional encouragement and love is worth more than I can express on the thesis.

Declaration

The work contained in this thesis is the results of my own investigations and has not been accepted nor concurrently submitted in candidature for any other degree award.

Yan Wang
October 2018

Chapter 1

Introduction

1.1 Background and motivation

The world population prospects predict that the life expectancy at birth will rise from 71 years in 2010-2015 to 77 years in 2045-2050 (United Nations, 2017). The population aged 60 or above is growing at a rate of about 3 percent per year. Figure 1.1 shows the percentage of the population in broad age groups for the world and by region in 2017. The whole world is facing the issue of population ageing. For example, in 2017, there are an estimated 962 million people aged 60 or over in the world (United Nations, 2017), comprising 13 percent of the global population. Currently, Europe has the greatest percentage of the population aged 60 or over (25 percent). Rapid ageing will occur in other parts of the world as well. Similarly, the population aged 60 or over in Asia is expected to shift from being 12 percent of the total in 2017 to 24 percent in 2050. So that by 2050 all regions of the world except Africa will have nearly a quarter or more of their populations at ages 60 and above (see Figure 1.1).

Population ageing is projected to have a profound effect on the whole world. One of the most important issues caused by population ageing is the immensely increasing expenditure on healthcare (OBR, 2017). Conventional care patterns for older people, such as younger generations caring for older generations or older generations ageing in a nursing home, have been challenging partly due to the short of carers caused by aged population structure. Most societies face the problems to ensure that their health systems are ready to adapt to the demographic shift. Some measures, such as developing new systems with medical and assistive technologies for providing long-term care or creating age-friendly environments, have been exploring to address the challenges.

Meanwhile, a large proportion of older people can take care of their daily life on their

own. And a vast majority of them (between the age of 60 and 70) say that they are confident in their abilities to live independently and can accomplish daily tasks without a caregiver (the United States, 2015). Nevertheless, aging-caused changes, such as physical or cognitive decline, could affect people’s everyday life, resulting in a lack of physical activity, injuries or mental problems. Accordingly, their family members, doctors, or the community care centre may worry about older people’s health condition, daily life, and safety status when older people live alone. Providing this group of older people with formal or conventional cares means an extra cost and even disturbances for their everyday life. Thus, certain appropriate assistive technologies can be explored to maintain or improve older people’s quality of life.

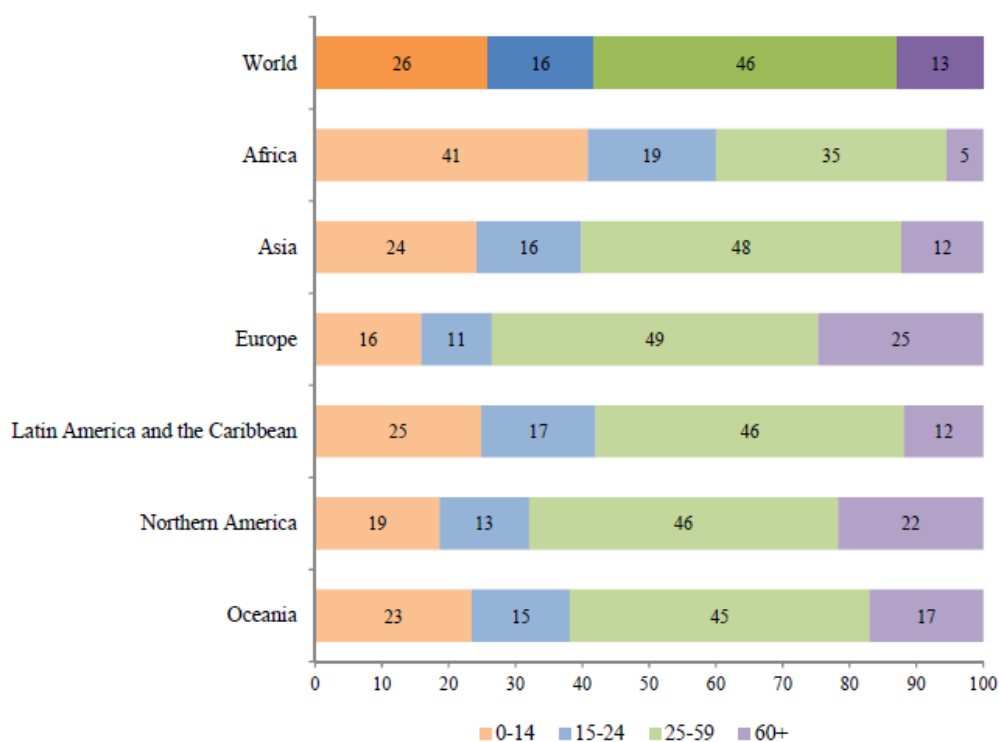


Figure 1. 1 Percentage of population in broad age groups for the world and by region, 2017
 Source: World Population prospects 2017 Revision¹

These years have been witnessing the development of assistive technologies in promoting independent, active and healthy aging thanks to the advancement of sensors, wireless communication, and machine learning techniques (Carmeli et al., 2016, Kuerbis et al., 2017, Kon et al., 2017). Among these technologies, sensor-based Human Activity Recognitions (HAR) become one of the most promising solutions to assist older people’s daily life

¹ https://esa.un.org/unpd/wpp/publications/files/wpp2017_keyfindings.pdf

(Chernbumroong et al., 2013, Janidarmian et al., 2017, Lee et al., 2017, Tunca et al., 2014). HAR learns activities from a series of observations on the actions of subjects and the environmental conditions in real-life settings, which has been enabling enormous potential in human-centred applications, such as fitness systems (Zhang and Sawchuk, 2009, Gravina et al., 2010), assisted living (Chernbumroong et al., 2014), interactive games (Terada and Tanaka, 2010), sport activity monitoring (Zhou et al., 2016), social physical interaction (Augimeri et al., 2010), factory workers monitoring (Huang and Tsai, 2007), etc.

HAR process is complex. The steps in HAR can be summarized as 1): selecting and deploying appropriate sensors to a human body or the environment to capture the user's behaviour or the change of the environment where the user is performing activities; 2): collecting and pre-processing the data from the deployed sensors based on a specific task; 3): extracting useful features from the sensor data for later classification; 4): training the classification models with appropriate machine learning algorithms to infer activities; 5) testing the learning models to give decisions and performance reports. Each step has plenty of techniques and methods available to use and also involves the corresponding research questions to tackle (Lara and Labrador, 2013, Cornacchia et al., 2017, Nweke et al., 2018). HAR is a prospective research area of machine learning. Most studies in HAR focus on indoor activities of daily life (ADL) in assisted living applications, such as walking, stairs using, lying, exercise, cooking, gaits, falls, and so on (Hannink et al., 2017, Jung et al., 2015, Zheng et al., 2014). The recognition of daily activities can help understand and assist the daily context and safety conditions of the observed.

Regarding the sensors used in HAR, the existing HAR systems can be broadly categorized into three modalities: the wearable-sensor-based HAR (WSHAR), the ambient-sensor-based HAR (ASHAR), and the hybrid-sensory-based HAR (HSHAR). The camera-based-HAR (CHAR) can be divided into ASHAR regarding the camera displacement. In CHAR, visual information extracted from images or video sequences based on cameras is utilized to recognize the human gestures or actions for specific tasks (Zhang et al., 2017). However, it is less feasible to deploy cameras everywhere at home or to use them anytime due to variable lighting conditions and other disturbances. Also, the privacy problem and the computation burden produced by image and video analysis cannot be avoided, although the researchers have been trying to minimize the privacy by using the mini-dome or integrated cameras, or reduce the computation burden by utilizing binary silhouettes instead of depth silhouettes at the price of recognition accuracy (Phillips et al., 2017). CHAR systems are therefore more suitable for an emergency, public safety surveillance, or scheduled meetings,

instead of home-based daily monitoring for older people. Other typical ASHAR systems excluding CHAR, infer human activities from the sensors that are fixed in the environment or attached to some specific objects, such as a door, a kettle, a fridge, the floor, etc., and the ambient sensors include light sensor, reed switch sensor, Radio Frequency Identification (RFID), passive infrared (PIR), temperature, flow sensor, pressure sensor, etc. (Tunca et al., 2014, Debes et al., 2016, Mehr et al., 2016). Typical ASHAR sensor modality is less obtrusive because of no on-body sensors deployed, while usually at the price of poor flexibility and complex sensor deployment. Typical ASHAR works in a limited area where the sensors are installed. Besides, systems using pure normal ambient sensors may fail to function in some situations when the user does not contact the objects attached with sensors or does not enter the functioning area of a sensor installed in the environment.

The alternative to ASHAR with fixed ambient sensors is WSHAR which identifies human activities by mining the informative data from wearable sensors using machine learning algorithms. WSHAR can function in a relatively large space. Currently, smartphone, smartwatch, smart clothes, and other specifically-designed devices are the mainstream products embedded wearable technologies in HAR (Hassan et al., 2018, Filippopolitis et al., 2017, Adaskevicius, 2014). Generally, placing more sensors on multiple body parts (e.g., head, wrists, waist, legs, feet, etc.) can benefit in improving the performance and robustness of WSHAR. For instance, Laudanski et al., 2015 investigate identifying the post-stroke-gait-related activities by putting two inertial measurement units (IMUs) on the less-affected and affected shanks individually; their experimental results show that the highest classification accuracy is achieved by using both sensor positions. Other studies (Gao et al., 2014, Chernbumroong et al., 2014) also suggest that combining multiple sensors on multiple body parts can improve the performance of HAR. However, multiple sensors with complex sensor deployment on body could cause higher costs, practical deployment difficulties, and obtrusions for older users especially those who can live independently. Meanwhile, pure WSHAR systems also have some limitations that may enable less accurate recognition for certain activities that contain similar sensor-derived attributes, such as brushing and eating (Chernbumroong et al., 2013). Also, WSHAR is less capable of identifying a user's context where he/she performs activities.

ASHAR or WSHAR has its strengths and weaknesses. Previously published works have shown that combining different sensor modalities can improve the recognition accuracy (Cornacchia et al., 2017). E.g., Atallah et al., 2007 combine the ear-worn sensors and the ambient-mounted blob sensors for the detection of patients' daily pattern changes. The

studies (Logan et al., 2007, Pham et al., 2018) report the improved performances of activity recognition by combining the wearable sensors with the infrared sensors. Zhu and Sheng, 2012 use three wearable motion sensors and two cameras installed on the wall to identify the body activities and hand gestures simultaneously. Roy et al., 2016 use ambient and mobile data in a multi-inhabitant environment for daily activities detecting. Their initial results can reach around 70%, which is much higher than the results by using the smartphone-based accelerometers alone. It is obvious that the combination of sensor modalities can capture rich information about human activities, thereby improving the performance of HAR. Nevertheless, HSHAR will increase the cost and complexity of a HAR system compared with a single sensor modality. Also, the data fusion and sensing synchronization from different sensor modalities are needed in HSHAR.

With effective monitoring systems, the daily routine and unpredictable events such as long-period sleep and falls can be alleviated to some extent. Furthermore, the recognition of human daily activity is beneficial to maintaining people's healthy lifestyle, and daily activity routine shifts during a long-term can be the assisted materials for early diagnoses, such as heart diseases, sudden death syndrome, and sleep apnoea (Lokavee et al., 2012). The existing HAR systems have been making progress in technical and practical aspects, whilst they either only focus on recognizing specific activities without tracking people's context in home (Chernbumroong et al., 2013, Biswas et al., 2015, Dao et al., 2017), or only track daily routine/location in home without detecting specific activities (Ogawa et al., 2002, JustChecking, 2014, Mainetti et al., 2017). Thus, major researches are required to provide context-aware activity detection and appropriate fusion approaches to ensure practical and accurate activity detection and health monitoring. It is possible through leveraging different sensor modalities, for example, integrating context-aware ASHAR with WSHAR to accurately recognize daily activities and context. There exist a handful of systems which consider the recognition of both activities and location at home. However, they either use complex sensor deployments or apply complex algorithms (Huynh et al., 2008, Zhu and Sheng, 2011, Luo et al., 2017).

The following research questions need to be considered to successfully develop a HAR system to assist older people's daily life:

1. Sensor modality

WSHAR is good at recognizing specific activities (Cornacchia et al., 2017). While effective HAR systems with wearable sensors require the user to wear multiple devices on multiple

body parts (Laudanski et al., 2015, Gao et al., 2014), which can cause discomfort and high cost. CHAR systems have the concerns of privacy intrusion for daily use (Jalal et al., 2017). Other typical ASHAR systems (using camera-excluded ambient sensors) are less obtrusive for daily use but work in limited environments with complex sensor deployments (Tunca et al., 2014). Combining multiple sensor modalities can catch complementary information relating to human activities and take advantage of the strengths of each sensor modality to increase performance and robustness (Roy et al., 2016). Nevertheless, older people are not born to the age of information technology, and they may refuse to use complex assistive technologies. Designing and implementing a HAR system with high performance, compact system structure and less obtrusiveness to help older people live independently is a research problem.

2. Improving the performance of HAR in practical ways

WSHAR systems tend to use more sensors placed on multiple body parts (Gao et al., 2014, cLaudanski et al., 2015) or apply complex learning algorithms (Um et al., 2017) to improve the performance. Nevertheless, these WSHAR systems normally do not fully consider the practical aspects of realizing HAR for daily use. 1): adding more wearable sensors without fully using these sensors. E.g., Chernbumroong et al., 2014 and Mortazavi et al., 2014 employ conventionally-used features derived from each sensor they choose, while, augmented features can be explored from multiple sensors to use the sensors fully. 2): enhancing feature selection. Feature selection can help select the optimal features with filter, wrapper, and embedded feature selection methods to facilitate more accurate and faster learning (Guyon and Elisseeff, 2003, Dess `and Pes, 2015, Li et al., 2017a). More effective and efficient feature selection methods can be explored to improve the performance of HAR. 3): These years, deep learning methods have been applied and shown their superior performance in HAR (Plötz et al., 2011, Lane and Georgiev, 2015, Panwar et al., 2017). However, deep learning on-board implementation on mobile and wearable devices is still challenging due to the memory constrained and a high number of parameters to tune (Nweke et al., 2018).

3. Data fusion between multiple sensor modalities

Hybrid-sensory-based HAR is explored to provide comprehensive and accurate monitoring, such as cameras plus wearable sensors (Atallah et al., 2007), wearable sensors plus ambient sensors (Logan et al., 2007, Roy et al., 2016) and so on. Data fusion is a key question when combining multiple sensor modalities. There are three basic ways found in hybrid sensory

systems to fuse multi-source sensor data, i.e., data-level fusion (Liu et al., 2014a), feature-level fusion (Pansiot et al., 2007) and decision-level fusion (In Liu et al., 2014b). Other effective feature fusion mechanisms apart from the ways listed above can be explored to enhance the implementation of hybrid sensory-based HAR.

1.2 Aim and objectives

The research aims to design and implement a more comprehensive hybrid-sensory HAR system for older people to assist them living independently, which combine the wearable sensors and ambient sensors to improve recognition accuracy and mitigate obtrusiveness.

This thesis specifically proposes and develops a hybrid-sensory HAR system for older people who live alone. The proposed system leverages the advantages of WSHAR and ASHAR, which combines the wearable sensors and ambient sensors to recognize the user's normal and abnormal daily activities as well as the daily routine in a less obtrusive way. The data from the wearable sensors are used to recognize specific activities, and the data from the ambient sensors are used to derive the occupant's room-level daily routine. Meanwhile, the captured room-level location information is also used in the data fusion we proposed in the research to trigger the subclassification models trained by wearable data. Through the fusion of the two-source sensors, each sensor modality in the system performs its own functions and plays to its own strengths for HAR and improves the whole recognition performance together.

The objectives of the research are:

1. To identify certain research gaps through an extensive literature review of the state-of-art of sensor-based HAR systems (Chapter 2).
2. To propose an innovative hybrid sensory HAR system by combining wearable sensors and ambient sensors (Chapter 3).
3. To develop the hybrid sensory networks based on the proposed system (Chapter 3).
4. To collect data using wearable and ambient sensors from the recruited participants in real home settings (Chapter 4).
5. To identify the contribution of the selected wearable sensors by comparing their performance in improving classification accuracies (Chapter 5).

6. To investigate the feature selection techniques and propose a novel feature selection method to improve the performance or reduce feature space dimension (Chapter 5).
7. To investigate the contribution of the extracted augmented features from limited wearable sensors (Chapter 5).
8. To investigate and evaluate the effectiveness of the proposed data fusion method between ambient information and wearable information. (Chapter 6).

1.3 Original contributions

This thesis makes the following contributions:

1. Conducting a fairly comprehensive review of the techniques and technologies involved in HAR, especially on wearable sensor-based HAR systems. Each sensor modality has its merits and makes significant progress in continuous monitoring, performance improvement, computation cost reduction, practicability enhancement and so on. While, each sensor modality also has its limitations, and single sensor modalities sometimes may not cope with complex situations in practice. The challenges in HAR, such as dedicated sensor modality designing, less fully using of sensors and data fusion in hybrid sensory-based systems, are identified.
2. Proposing a more comprehensive and less obtrusive hybrid-sensory HAR system. Wearable sensors make the associated HAR systems more flexible and have enabled plenty of assisted living applications. Pure WSHAR systems, however, either are confronted with the problems of complex sensor deployment on body or the limited capacity of identifying elaborate actions with simple sensor deployment. Typical ASHAR is less obtrusive because of no on-body sensors deployed, however, it usually works in a limited area at the cost of poor flexibility and complex sensor deployment. We combine WSHAR and ASHAR to build a hybrid-sensory HAR system. The system provides more comprehensive surveillance for older people by recognizing both the specific daily activities and daily routine. The unobtrusiveness can be enhanced by two ways, one is that the PIR sensors are embedded in the indoor environment to achieve ambient intelligence, which can reduce the feeling of obtrusiveness to the minimum; and the other way is the wearable sensors are placed on the wrist instead of multiple body parts. Based on the proposed system, we develop a sensor network prototype. The sensor network composes of a wrist-worn wearable sensor module and an ambient sensor module. The wearable module integrates five selected sensors inside

(i.e., the accelerometer, the gyroscope, the magnetometer, the barometer, and the temperature sensor) for motion-caused information recording, and it has an on-board processing system that can deliver three attitude values (*yaw*, *pitch*, *roll*) of the wearable device apart from another 11 readings from the five individual sensors. The ambient sensor module consists of several PIR sensor sets for room-level location information capturing. The readings obtained from the PIR sensors are processed as a series of binary digits, of which “1” represents the presence, and “0” represents the absence.

3. Collecting a ground-truth data set from real home settings. This research focuses on daily indoor activity recognition for older people to observe their routine activities and daily patterns. We define 17 daily activities that can reveal independent life skills, including basic survival tasks, the activities for maintaining an independent life at home and certain abnormal activities. These activities are assigned in different rooms according to their occurring places. The activities except Falls are collected from 21 older participants (aged from 60 to 74, 11 females and 10 males). During data collection, the wearable device is tightly attached at the participant’s dominant wrist to record the motion-caused signals. Meanwhile, we deploy a PIR sensor set in each room to capture the user’s presence and absence information. We prepare the activity list for each room. The participants are encouraged to independently perform each activity in their own way. We also recruit 21 young participants (aged from 25 to 35, 11 females, and 10 males) who replace the older participants performing natural falls to avoid injuries and safety problems. We have finally created a ground-truth data that are collected from the recruited participants, including 17 daily activities and the context information.

4. Exploring the contribution of an augmented feature set extracted from limited wearable sensors. WSHAR systems usually use one to seven and even more types of sensors and place the sensors on multiple body parts to improve the classification accuracy. These sensors are less fully used in some cases. Inertial sensors (accelerometer, gyroscope, and magnetometer) have shown their potential in HAR, whereas most associated studies only utilize the features from an individual sensor or multiple channels of a sensor, e.g., the mean of the acceleration readings along the x -axis, or the correlation between the x -axis and y -axis of the acceleration readings. Only a handful of studies use tilt, yaw or pitch angle from multiple sensors as features for activity recognition. This research explores the contribution of an augmented feature set extracted from initial sensors to improve the classification accuracy without additional sensors involved.

5. Proposing a feature selection method, named mRMJR-KCCA. Mutual information considers the correlation in pairs and uses a simple strategy to approximate the relevance between one feature/class labels and a feature set. Kernel canonical correlation analysis (KCCA) can measure the nonlinear correlation between two multidimensional datasets. We introduce the measurement of KCCA into mutual information (MI) -based feature selection method (mRMR), which maximizes the relevance between the feature candidate and the target class labels, and simultaneously minimize the joint redundancy between the feature candidate and the already selected features in the view of kernel canonical correlation analysis (KCCA). The mRMJR-KCCA omits the sum approximation \sum in mRMR when measuring the relationship between a feature and a group of features and instead measure the nonlinear correlation between two multidimensional datasets. The feature selection method experimentally performs better compared with the benchmark feature selection methods on our ground truth data and other 10 UCI classification-related benchmark datasets.

6. Proposing a unique and effective data fusion method for two-source sensors. Data fusion of information from multiple (usually two) sensor modalities in HAR can be seen in three main ways: a) data -level, b) feature-level and c) decision-level. Raw data level fusion occurs at the raw data level where incoming raw data from different sensor modalities are combined. Feature-level fusion involves carrying out data fusion after features are extracted from individual sensor modalities. Decision-level fusion refers to fusing the decisions made by individual classifiers from the corresponding sensor modalities. The data fusion from PIR sensors and wearable sensors is usually conducted by using the number of activations of PIR sensors and the features extracted from wearable sensors together as the input to the classifiers. PIR sensors have a different role in our data fusion mechanism. Instead of using it as the input of a classifier, we use the binary location information derived from infrared sensors to trigger room-level subclassification models in the data fusion. By doing this, the whole task of recognizing all defined 17 activities are skilfully separated into several subtasks by the room-level location information captured by PIR sensors. Each submodel is responsible for recognizing a smaller number of activities; this could require a smaller number of features and improve the classification accuracy in a practical way.

7. Demonstrating the effectiveness of improving the recognition accuracy of the daily activities through the following practical ways. We use Support Vector Machines (SVM) and Random Forest (RF) as the classification algorithms for system evaluation. We explore the augmented features from limited sensors to help improve recognition performance. We

propose an effective feature selection method to select more relevant features with the target classes; the data fusion method we proposed provides a practical way to fuse two-source sensor data, on the other hand, it also divides the whole recognition task into parallelly-working sub-tasks thereby reducing the requirements for submodels and improving performance.

1.4 Thesis organization

This thesis contains seven chapters. The thesis diagram is presented in Figure 1.2. A brief overview of each chapter is as follows:

Chapter 1 provides the background and motivation of the research. It gives an insight into the importance of the research topic, sets out the research aim and objectives, and highlights the contributions of the research.

Chapter 2 presents a fairly complete review of sensor-based HAR systems and the techniques involved in HAR. It gives an overview of the existing HAR sensor modalities and their characteristics as well as applications. The review highlights wearable sensor modality in terms of sensor types, sensor placement, data acquisition, feature extraction, classification algorithms, and performance evaluation, etc. The research gaps, including the system design, sensors determination, feature learning and selection, data fusion for hybrid systems, are identified in this chapter.

Chapter 3 gives an overall description of the research strategies used in this thesis. It begins with the overview of the system design and the description of the proposed data fusion mechanism in the hybrid sensory system. The development of the hybrid sensory network and the sensor placement are then explained, followed by the feature selection methods, classification algorithms, and performance evaluation approaches used in this research.

Chapter 4 looks into the data collection and the feature extraction from the wearable sensors. Firstly, the definition of the 17 daily activities for this research is described, and the activity type is large enough for our experiments purpose. Secondly, the wearable data collected in real home settings from the recruited participants are provided. Next, the ambient data acquisition is briefly described. Then, the data segmentation method of raw data for facilitating later learning is presented, followed by the creation of original features used for the research, including the conventionally-used features (*CUFs*), the attitude-related features (*ARFs*) and *All (CUFs + ARFs)*.

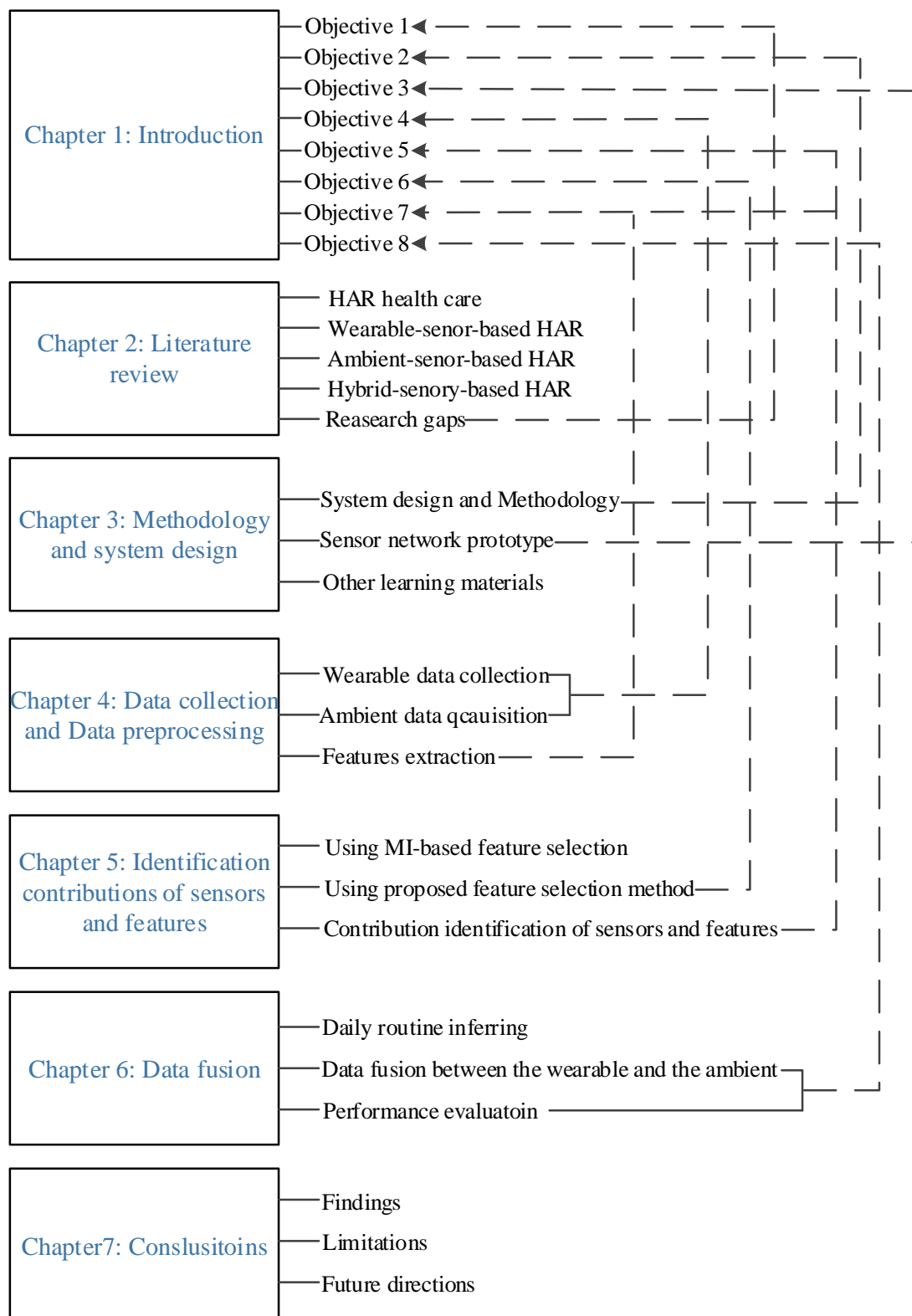


Figure 1. 2 The thesis structure

Chapter 5 investigates the contributions of the selected five wearable sensors by evaluating the performance of different sensor combinations, and the three created feature sets in Chapter 4. Chapter 5 presents a proposed feature selection method, named mRMJR_KCCA. The mRMJR_KCCA maximizes the relevance between the feature candidate and the target class labels, and simultaneously minimize the joint redundancy between the feature candidate and the already selected features in the view of the kernel canonical correlation analysis (KCCA). Experimental results demonstrate the better performance of mRMJR-KCCA on our ground truth data and other 10 UCI classification-related benchmark datasets. This chapter applies the proposed mRMJR-KCCA and other feature selection methods with SVM and RF to identify the contributions of selected wearable sensors and the three feature sets.

Chapter 6 analyses the effectiveness of the proposed data fusion between the ambient and wearable data. First, the daily routine derived from the PIR sensors are discussed. The data fusion then uses the binary location information to trigger the trained subclassification models. By doing this, the whole task of recognizing all defined 17 activities are skilfully separated into several subtasks according to the room-level location information captured by infrared sensors. Experimental results reported the improved performance using a much smaller number of features after data fusion.

Chapter 7 is the conclusion of the thesis. It proceeds with a summary of the research and a discussion of the main findings with respect to the research objectives of the thesis. The limitations and future research directions are also given.

1.5 List of resulting publications

Journal paper

1. Yan Wang, Shuang Cang, and Hongnian Yu. "A Data Fusion based Hybrid Sensory System for Older People's Daily Activity and Daily Routine Recognition." IEEE Sensors Journal PP.99(2018):1-1.

Conference paper

2. Yan Wang, Shuang Cang, and Hongnian Yu. "A noncontact-sensor surveillance system towards assisting independent living for older people." 23rd International Conference on Automation and Computing (ICAC), IEEE, 2017.

3. Yan Wang, Shuang Cang and Hongnian Yu. "A review of sensor selection, sensor devices and sensor deployment for wearable sensor-based human activity recognition

systems." 10th International Conference on Software, Knowledge, Information Management & Applications (SKIMA), IEEE, 2016.

4. Yan Wang, Shuang Cang, and Hongnian Yu. "Realization of wearable sensor-based human activity recognition with an augmented feature group." 22nd International Conference on Automation and Computing (ICAC), IEEE, 2016.

Chapter 2

Literature review

The review in this chapter aims to learn the background of the research topic and identify the associated research gaps. The review is performed from English language articles. These articles are published between January 1995 and March 2018 indexed in the following search engines: IEEE explore, web of science, ScienceDirect and Google scholar with the keywords, such as human activity/motion/behaviour recognition, assisted living/smart home, healthcare/assistive technologies, wearable/ambient/video sensors, daily activity, older/elderly people, feature, feature selection, machine learning, deep learning, etc.

This thesis proposes a hybrid sensory HAR system for older people. The system combines wearable sensors and ambient sensors for HAR but primarily uses the wearable sensor-based feature learning and classification approaches. The review, therefore, lays more emphasis on wearable sensor-based HAR systems apart from the sensor modality sections and the application section. The review follows the structure shown in Figure 2.1. The summary of technologies relating to HAR in healthcare is first briefly reviewed, followed by the glance of three different sensor modalities in HAR. It then focuses on the wearable-sensor-based HAR systems in terms of sensor types, sensor platform and placement on body, activities, data pre-processing, hand-crafted features and automatically learned features, feature dimensionality reduction, and feature selection, classification algorithms. It also looks at the ambient-sensor-based HAR systems, including camera-based systems, followed by the systems which combine the wearable and ambient sensors. Next, the performance evaluation approaches and performance criterion of HAR models are reviewed. The applications of HAR systems for assisting living are presented as well. Finally, certain research gaps are identified based on the review. And most of the research gaps identified in this chapter are based on the wearable-sensor-based HAR systems.

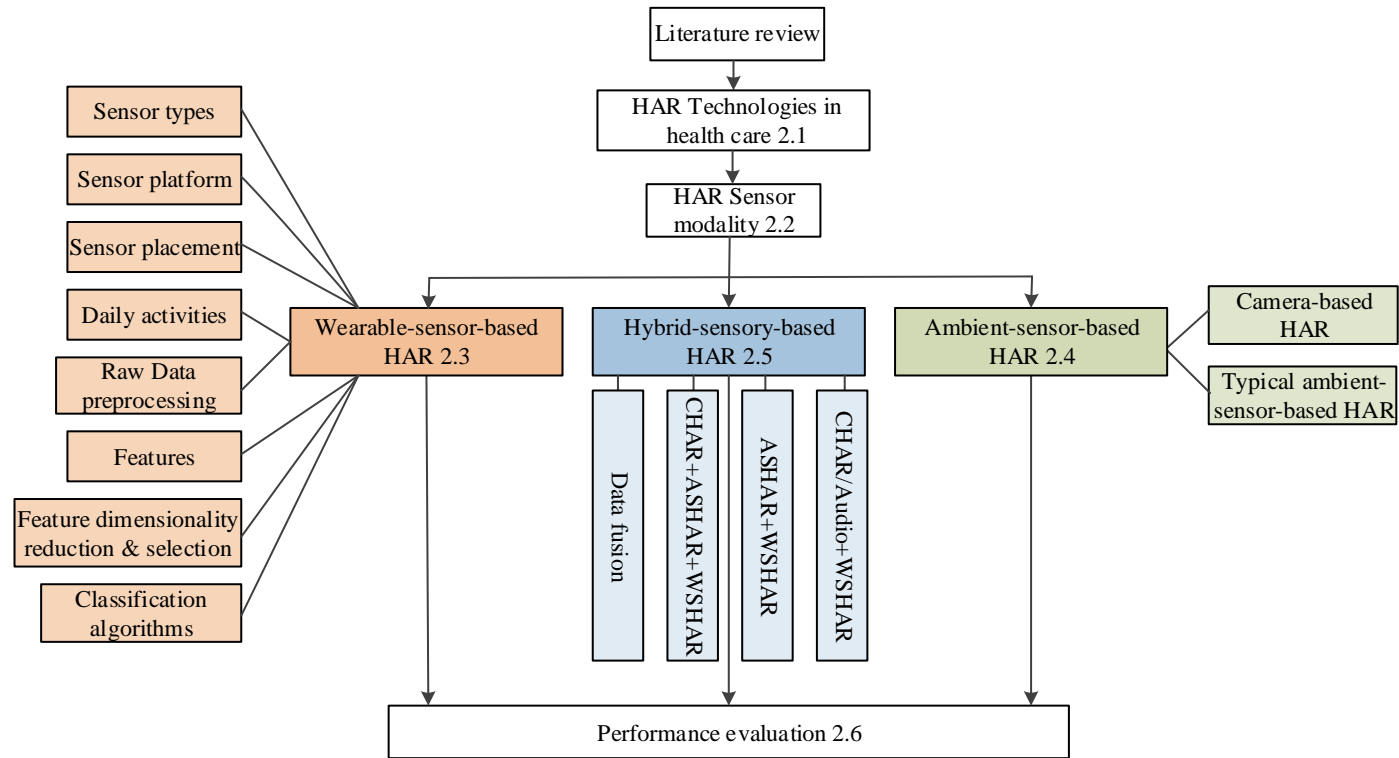


Figure 2. 1 Literature review diagram in chapter 2

(2.1, 2.2, ..., 2.6 is section 2.1, section 2.2 ..., section2.6 respectively)

2.1 HAR enabled technologies in healthcare

One of the consequences of population aging is the increasing expenditure on healthcare (OBR, 2017). The older people need more options to organize their healthcare to enhance confidence in living independently and improve the quality of living. HAR is one of the most important assisted technologies (Zhang et al., 2017, Laudanski et al., 2015). It aims to recognize a user's activities from a series of observations on the user's behaviour in real life settings. The continuous monitoring of activities for older people can detect their daily routine and abnormal situations to enhance their daily life or provide timely assistance for certain unpredictable events such as falls (Bian et al., 2015). HAR enables a variety of HAR applications to increase older people's safety, autonomy and well-being during their daily life (Tunca et al., 2014, Bian et al., 2015).

Recognizing human activities with the sensor-based approaches normally involve the procedures: 1) activities are defined in a real environment; 2) sensors provide a reliable representation of the corresponding activities; 3) useful features are extracted from the raw data presentation; 4) a classification algorithm accurately recognizes the activities. And steps 3) and 4) can be merged into one in some cases (Gordon et al., 2010, Wang et al., 2017a). Therefore, the technologies in HAR for healthcare can involve sensor and communication, data processing, feature learning, and classification. The review in this chapter puts more emphasis on the wearable-sensor based technologies in HAR due to the research interests.

2.2 Sensor modality

The advancement in sensing technologies has promoted the development of HAR systems. Sensor-based HAR learns activities from a series of observations on the actions of subjects from sensor inputs in real-life settings, which has been enabling enormous applications in assisted living, such as gait analysis (Hannink et al., 2017), rehabilitation (Hermanis et al., 2016), fall detection (Jung et al., 2015), sports assessment (Um et al., 2016), daily activity analysis (Chernbumroong et al., 2014), etc. The early study on HAR can be traced back to the work of Abowd et al., 1998 and Foerster et al., 1999. Researchers first focus on activity recognition from videos and images, but later when everyday life was considered, they start to explore tracking human behaviour by using wearable and ambient sensors (Ke et al., 2013, Bulling et al., 2014, Zolfaghari and Keyvanpour, 2016). The progress made in HAR during

the past few decades motivates the later researchers to improve the recognition performance and practicality of HAR under more realistic settings in different ways. The HAR systems can be generally categorized into three modalities based on the sensors used, i.e., ambient-sensors-based HAR (ASHAR), wearable-sensor-based HAR (WSHAR) and hybrid-sensory-based HAR (HSHAR).

Typical ASHAR systems learn activities from the information provided by the ambient sensors which are usually installed in the environment or attached to some specific objects to provide the user's context where they perform the activities. This sensor modality is less obtrusive because of no on-body sensors, but usually at the cost of poor flexibility and complex deployment (Wang et al., 2017a). The camera-based HAR (CHAR) can be classified as ASHAR, which analyses videos or images containing human motion information for HAR. The main concerns about CHAR are the privacy for daily use (Khan and Sohn, 2011). WSHAR is one of the most widely adopted sensor modality in HAR, which recognizes the human activities by mining the informative data from the sensors worn on certain body parts. The main strengths of WSHAR systems are low-cost, flexible, and easy-to-use (Cornacchia et al., 2017). HSHAR systems combine ambient sensors and wearable sensors to capture complementary information of human activities, identifying high-level activities or improving the recognition accuracy (Roy et al., 2016, Diethe et al., 2017). The following sections will look into the three different sensor modalities one by one, with the focus on the wearable-sensor-based HAR systems.

2.3 Wearable-sensor-based HAR (WSHAR)

2.3.1 Overview of WSHAR

The development of wearable devices, such as smartwatches, smartphones, wristbands, smart clothes, makes it feasible to acquire data from the ubiquitous equipment and provide continuous monitoring of human activities (Adaskevicius, 2014, Filippoupolitis et al., 2017, Hassan et al., 2018). Data-driven-based WSHAR systems share a similar procedure, as shown in Figure 2.2. Flowchart A in Figure 2.2 presents the process of using conventional approaches to realize HAR, in which the features are generated manually (Chernbumroong et al., 2014, Sani et al., 2017). First, the raw data from multiple types of body-worn sensors (accelerometer, gyroscope, heart rate sensor, etc.) are obtained at a certain sampling rate and then transmitted to a processing centre (laptop, tablet, smartphone, etc.) through specific communication technologies (Bluetooth, Zigbee, Wi-Fi, etc.). The pre-processing stage

mainly involves filtering and segmenting raw data. Informative features are then extracted in a hand-crafted way (such as mean, variance, dominant frequency, entropy and so on); followed by specific feature dimension reduction techniques or feature selection algorithms to obtain the optimal and smaller-size feature sets for further learning and computation burden reducing; finally, the optimal feature set is fed to the classifiers for classification models training and testing.

Flowchart B in Figure 2.2, on the other hand, gives the typical process of using deep learning methods for HAR, in which the features are learned automatically from different types of deep networks, such as Convolutional Neural Network (CNN), Recurrent Neural Network (RNN), Deep Belief Network (DBN), Restricted Boltzmann Machine (RBM) (Plötz et al., 2011, Panwar et al., 2017). The feature learning and learning model building in flowchart B are often performed simultaneously with these deep networks. The research in this thesis focuses on investigating the hand-crafted features; it, therefore, follows the flowchart A in Figure 2.2. Flowchart B will be the future work. Consequently, the following sections in WSHAR section will detail each stage of flowchart A in Figure 2.2, i.e., the wearable sensors, the sensor platforms, the sensor placement, the data acquisition, data pre-processing, feature extraction & feature selection, classification and so on.

2.3.2 Wearable sensors

2.3.2.1 Sensor type

These years, the advances in sensors make it possible and feasible to explore assisted living in healthcare and wellbeing with wearable sensors. Wearable sensors, different from common industrial sensors, are designed to meet certain specific requirements: high integration density, small size, low power consumption as well as high measurement accuracy, etc. The sensors are integrated into a small-size device for conveniently being attached to the user's body parts.

Wearable sensors can include inertial sensors, physical health sensors, environmental sensors, camera, microphone, etc. Table 2.1 lists the most popularly deployed wearable sensors in HAR. Motion-based inertial sensors have been well applied in WSHAR, such as accelerometer, gyroscope or magnetometer, which can detect and measure acceleration, angular velocity, magnetic fields, tilt, shock, vibration, rotation, and multiple degrees-of-freedom motions (Chernbumroong et al., 2014, Hassan et al., 2018). These observations vary sensitively along a wearer's movement or body postures, thereby delivering rich

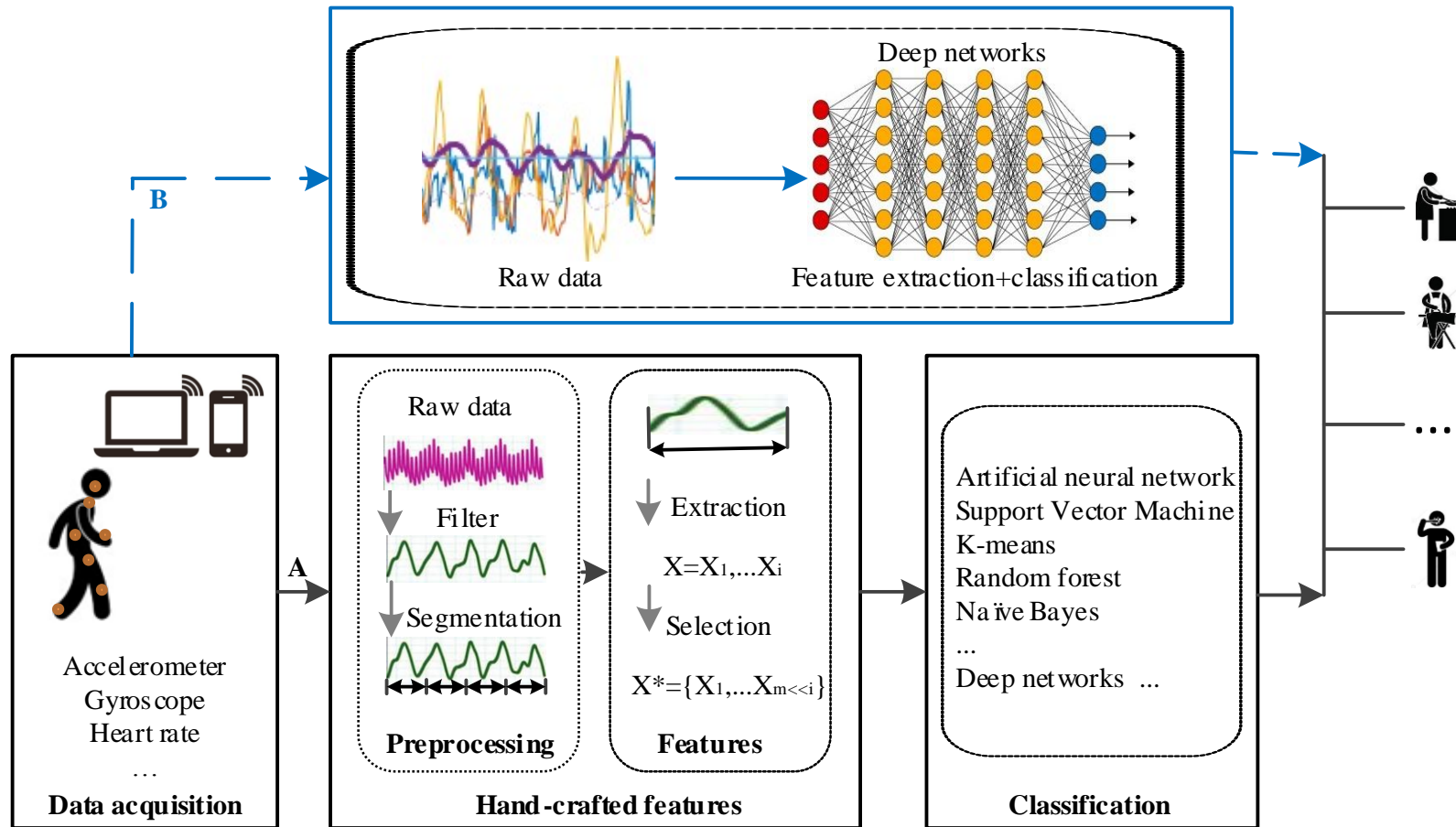


Figure 2. 2 Learning procedure of WSHAR

motion-caused information. Kwapisz et al., 2011 utilize phone-based accelerometers to identify five physical activities, i.e., walking, jogging, ascending/descending stairs, sitting and standing. Deng et al., 2014 develop a fast and robust activity recognition model based on Reduced Kernel Extreme Learning Machine to cope with varied device users. They use phone-embedded accelerometer and gyroscope. Guo et al., 2016 use an accelerometer, a magnetometer, and a gyroscope built in a smartphone for patients' activity recognition. Although inertial sensors have been widely applied in WSHAR systems, they still suffer from some limitations, e.g., the calibration for effective measurements, battery life due to continued logging, or arbitrary signals along with activity performing.

Physical health sensors, including heart rate (HR), oxygen saturation (SpO₂), blood pressure (BP), electrocardiogram (ECG), blood glucose (BG), respiratory rate (RR), etc., are used sometimes with inertial sensors to recognize the activities with rehabilitation purpose or capture vital signals for health condition evaluation. Chen et al., 2014 develop a framework to detect epileptic seizures using EEG sensors. Chernbumroong et al., 2014 propose a practical activity recognition system by combining a heart rate sensor attached to the chest with another six sensors worn on the wrists. Physical sensors have not been able to obtain a large-scale application in WSHAR due to the problems of size, precision, price, etc.

With respect to the environmental sensors, only the temperature sensor, barometer as well as the light sensor are used in HAR. For example, Maurer et al., 2006 implement a multi-sensor platform embedded with a light sensor. They attach the platform on five different positions to explore the best location on body achieving highest accuracy. A smartphone-based barometer in Khan et al., 2014 is used to help detect a total of 15 activities with other sensors inside.

2.3.2.2 Sensor platform

In WSHAR, the sensors (one or more) are typically integrated into one platform carried by users when they perform activities. To minimize the obtrusiveness, the sensor platforms are often shown in the following modes: smartphones, smartwatches, smart clothes, inertial units, specifically designed platforms, etc.

Today's smartphones are well equipped with a variety of sensors (such as accelerometers and gyroscopes) and are ubiquitously carried by people everywhere and every day. Using the data acquired from these sensors could enable applications to recognize a wide range of

Table 2. 1 Wearable sensors used in HAR

Wearable sensors	Examples	Pros	Cons
Inertial sensors	Accelerometer (Chernbumroong et al., 2014, Hassan et al., 2018) Gyroscope (Biswas et al., 2015) Magnetometer (Gjoreski and Gams, 2011)	Well applied, delivering rich motion information, small size, easy to use, etc.	Battery life limitation, arbitrary signals along with activities, etc.
Physical health sensors	Electrocardiogram (ECG) (Cook et al., 2015, Zhang and Wu, 2018) Skin temperature (Lara et al., 2012, Yoon et al., 2016) Heart rate (HR) (Tapia et al., 2007, Mehrang et al., 2017) Electroencephalograph (EEG) (Nakamura et al., 2010) Electromyogram (EMG), (Georgi et al., 2015, Lorussi et al., 2016) Force/pressor sensor (Lorussi et al., 2016, Kalantarian et al., 2016)	Delivering vital signals related to daily activities for rehabilitation and health condition detection, etc.	Unable to obtain large-scale application due to the issues of size, precision, price, etc.
Environmental sensors	Temperature (Chernbumroong et al., 2014) Humidity (Parkka et al., 2006) Light sensor (Bhattacharya and Lane, 2016) Barometer, etc. (Chernbumroong et al., 2013)	Delivering context information related to activities	Usually used with inertial sensors and producing noise signals, etc.
Others	Camera (Zhan et al., 2012) Microphone (Fontana et al., 2015) GPS, etc. (Reddy et al., 2010)	Complementary information with other sensors	Privacy concerns, complex algorithms applied, etc.

daily activities (Hassan et al., 2018, Kwon et al., 2014, Sun et al., 2010, Guo et al., 2016, Reddy et al., 2010). Also, smartphones are equipped with memory and battery, which provides a system for HAR without additional hardware requirements. The main problems when using smartphones for HAR involve the constraints of limited sensor types and locations (pockets or bags). Meanwhile, the smartphones' deployment locations on body might not be suitable for everyday use when the phone carrier performs daily activities at home. Furthermore, retraining procedures or transforms of coordinate is normally needed to achieve HAR due to the arbitrary orientations of the way carrying smartphones (Sun et al., 2010, Morales et al., 2014).

Smartwatches are designed with integrated sensors that enable a connection to a PC or a phone. The typical examples of using smartwatches to identify daily activities can refer to Filippoupolitis et al., 2017, Vepakomma et al., 2015, Chernbumroong et al., 2014, etc. A smartwatch is wrist-mounted, with a relatively standard and fixed body location, which is more convenient and less obtrusive for the user to wear compared to carrying a smartphone all the time. Nevertheless, smartphones and smartwatches share the same problem that the sensors inside are fixed and might not be the exact ones required for a specific task. In some cases, the data from the commercials might not be open-source to use.

Smart clothes can embed more sensors to achieve a diverse function compared with smartphones or smartwatches, especially for long-term monitoring applications (Adaskevicius, 2014). For instance, smart shirts are designed to monitor precise cardiac, respiratory, sleep and other daily activities, which incorporate heart rate and ECG sensors (Hexoshin, 2018). Lorussi et al., 2016 develop a smart textile platform, including sensing shirt, sensing trousers, sensing gloves and sensing shoes for the assessment of stroke patients. The platform embeds or knits inertial sensors, textile goniometers, piezoresistive sensors, EMG and goniometers. Zhou et al., 2016 present two types of textile-based sensors: a fabric pH sensor to collect and analyse sweat and piezoresistive textiles to capture body movements. Smart clothes are also designed to track babies' sleep, breathing, body position (Mimobaby, 2018). The abovementioned smart clothes are usually needed to wear tightly to ensure the quality contact of the sensors with the skin or other body parts, which may affect the comfort of the wearer for daily use. On the other hand, the relative movement between the body parts and the sensors due to the loose wear of smart clothes will give rise to motion artifacts.

An inertial measurement unit (IMU) is a special device that measures and reports a craft's





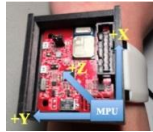
velocity and orientation, using a combination of an accelerometer, a gyroscope, a magnetometer and sometimes with a barometer. One or some combinations of IMU sensors are often employed to detect human gestures or activities in different applications (Georgi et al., 2015, Montalto et al., 2015, Bulling et al., 2014, Su et al., 2014).

Specifically designed platforms are built for one specific research or common research purposes in HAR, in which the sensors required for a specific task are integrated. Burns et al., 2010 design a flexible sensing device with multiple built-in sensors. Their device contains the capabilities of kinematic sensing, physiological sensing, ambient sensing, and external hardware integration. Uddin et al., 2015 present a framework with a wrist-worn-9-axis-sensors device. They verify the feasibility of the device based on two activities: hands washing and drinking. Cook et al., 2015 design an open-source, wearable, eight-channel bio-potential data collection platform integrated with an ECG and an accelerometer sensor, which can be used to record health-related information. Specifically, developed sensor devices can meet the sensor requirements for a specific task, while it may mean an extra cost in hardware and research period. The popular sensor platforms used in WSHAR are summarized in Table 2.2.

2.3.2.3 Sensor placement

Sensor placement refers to the body locations where the sensors are placed and how the sensors are attached to those locations, which is a research-worthy problem in WSHAR. Sensor placement may vary along different applications. For example, a foot-mounted accelerometer can well reflect the foot or leg involved motion, thereby for gait, step, distance or energy consumption detection (Bao and Intille, 2004, Mannini and Sabatini, 2010, Vepakomma et al., 2015, Chamroukhi et al., 2013, Moncada-Torres et al., 2014). The wrist-worn sensors can help recognise normal activities, such as ironing, brushing teeth and cooking (Mannini and Sabatini, 2010, Chernbumroong et al., 2013). The thigh-located sensors are sensitive to the leg-involved activities, like jogging, riding, walking, running, etc.(Wu et al., 2012, Moncada-Torres et al., 2014, Ronao and Cho, 2015). Most potential body locations have been explored to place sensor(s): hand (Bulling et al., 2014), arm (Bulling et al., 2014), wrist (Uddin et al., 2015), chest (Gao et al., 2014), pocket (Kwon et al., 2014), head (He and Bai, 2014), feet (Cleland et al., 2013), shank (Bahrepour et al., 2011),thigh (Banos et al., 2013), trunk (), vest (Bourke et al., 2008b), waist (Barreto et al., 2014), ankle (Suto et al., 2017), belt (Capela et al., 2015), pelvic (Ravi et al., 2005), hip (Banos et al., 2013), leg (Wang et al., 2013), abdomen (Zheng et al., 2013), back (

Table 2. 2 Sensor platforms in WSHAR

Platform	Case studies	Strengths	Weaknesses	Picture
Smartphones	Sun et al., 2010 Guo et al., 2016 Hassan et al., 2018	Ubiquitous, equipped with a variety of sensors, battery, and memory	Limited placing locations on body, arbitrary orientations in pockets, etc.	
Smart watches	Vepakomma et al., 2015 Chernbumroong et al., 2014 Uslu et al., 2013	Integrated sensors, a relatively standard and fixed body location	Limited sensor types for different applications	
Smart clothes	Adaskevicius, 2014 Hexoshin, 2018 Lorussi et al., 2016	More sensors embedded, long-term monitoring, the relative movement between the body parts and the sensors, etc.	Usually needed to wear tightly to ensure the quality contact of the sensors with the skin or other body parts	
Inertial measurement unit (IMU)	Georgi et al., 2015 Bulling et al., 2014, Su et al., 2014	A fixed combination of sensors, small, low power, can also provide the attitude angles of the device, etc.	Time-consuming alignment and calibration, etc.	
Specifically designed devices	Burns et al., 2010 Uddin et al., 2015 Cook et al., 2015	The sensors exactly required for a specific task or a common research purpose in HAR	An extra cost in hardware and research period	

He and Bai, 2014), knee (Atallah et al., 2010), ear (Pansiot et al., 2007), neck (Fontana et al., 2015), etc. Summarising the above discussion, we produce Figure 2.3 which presents the commonly explored sensor locations on body and the associated sensors in WSHAR.

In terms of sensor placement, we categorize WSHAR into four cases: the basic way is placing one single sensor on one single body part (One to One); the second one is attaching one single type of sensor on multiple body parts to gain complementary information from different body parts (One to Multi); the third one is placing a sensor device with two or more type of sensors built-in on only one body part, with the aim of capturing diverse-source information from different sensors (Multi to One); the last case is placing multiple devices, each embedded with two or more types of sensors, on multiple body parts (Multi to Multi) to take the advantages of the first three cases. The four types of sensor placement are presented in Figure 2.4.

One to One

One to One sensor placement aims to build a basic wearable network for HAR. In this scenario, the sensor's location may vary with tasks, from the head to the feet, but fixes on one body part. Rodriguez-Martin et al., 2013 investigate the recognition of transition-related postures for the patients with Parkinson or stroke by only using a single 3-axis accelerometer attached to users' waist (see Figure 2.5). The authors propose a hierarchical recognition algorithm to detect a total of 11 activities including lying from sitting, walking, sitting to standing, bending up/ down, etc. The evaluation data sets are gathered from 31 healthy volunteers and eight people with Parkinson's disease, respectively. The obtained results are with the sensitivity of 97% and specificity of 84% in posture recognition on the young volunteers' data, and sensitivity of 98% and specificity of 78% in the postural transition detection on the Parkinson people's data. Suto et al., 2017 investigate the efficiency of the popular machine learning strategies based on a right-ankle-mounted accelerometer, and their results suggest that one sensor is not enough for appropriate daily activity recognition due to the similar data generated from one sensor for different activities.

One to Multi

One to One sensor placement might deliver limited information for HAR; researchers then place the accelerometers to multiple body parts with the aim of capturing richer information

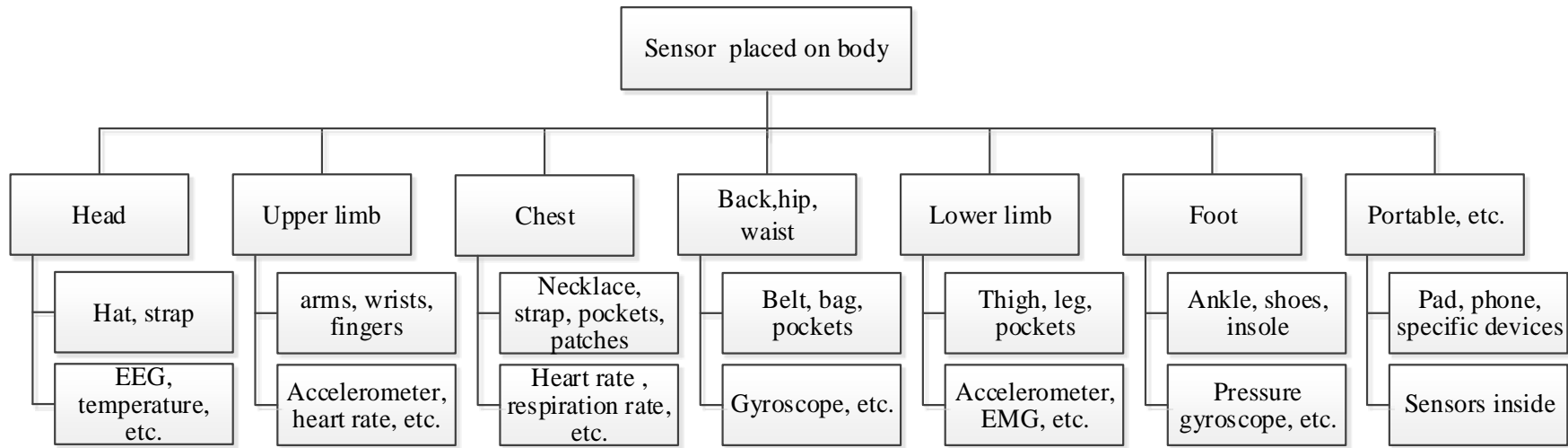


Figure 2. 3 Sensor placement on body and the associated sensors in WSHAR

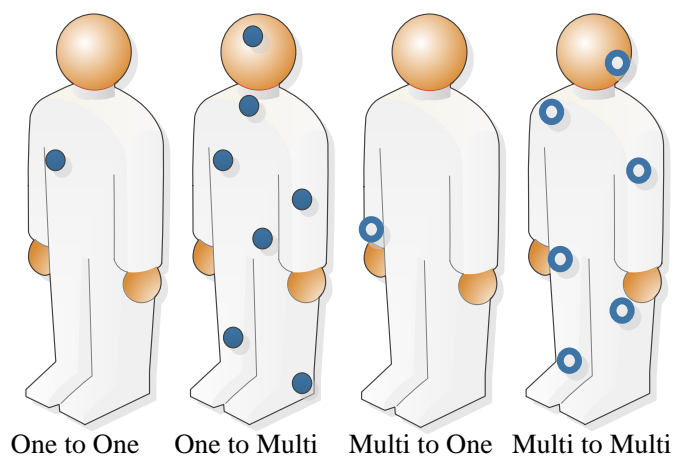


Figure 2. 4 Deployment of wearable sensors



Figure 2. 5 An accelerometer located at the waist (Rodriguez-Martin et al., 2013)

or evaluating the contributions of different sensor positions to recognition performance. Cleland et al., 2013 design an experiment system by deploying six wireless accelerometers on the participants' foot, thigh, hip, lower back, wrist and chest to collect the data from activities of walking, standing, walking up/down stairs, etc. Their experimental results indicate the hip was the best single location for their task and increasing sensing locations from one to two or more could achieve small but significantly better accuracy. Szt Tyler et al., 2017 develop a position-aware HAR system by placing seven accelerometers in different body positions. The sensor placement in Szt Tyler et al., 2017 is shown in Figure 2.6. Their real-world data set includes eight physical activities from 15 volunteers. They conduct comprehensive experiments, including cross-subjects and subject-specific approaches, to investigate the problem of recognizing the on-body position of the placed wearable sensor and impact of the body position on the activity recognition performance. The results suggest that their position-aware system consistently improves the recognition rate of the common activities and the waist is the best position for the same activity across different people.



Figure 2. 6 The accelerometer placed on multiple body parts (Sztyler et al., 2017)

Multi to One

An alternative strategy to acquire diverse-source data related to the activities is to integrate multiple types of sensors and place them on one body part (Multi to One) compared to One to One scenario. By doing this, combined information from different types of sensors will be obtained without increasing the obtrusiveness and complexity in sensor deployment. Mortazavi et al., 2014 propose a system to explore the only best single axis for each activity aiming at reducing computation load in repetition counting. They use a gyroscope and an accelerometer embedded in Samsung Galaxy Gear collecting five exercise routine activities (including bicep curls, crunches, and jumping) from 12 subjects (Figure 2.7). The authors try four data sets derived from different sensor combinations, with the corresponding average accuracies by the random forest of 92%, 85%, 93%, and 90%, respectively.



Figure 2. 7 Device worn on a wrist (Mortazavi et al., 2014)

Multi to Multi

Compared with the first three cases, Multi to Multi is expected to be the most comprehensive structure to achieve higher performance in WSHAR. Chernbumroong et al., 2014 propose a practical home-based HAR which use multiple types of sensors on multiple body positions. They investigate the contributions of seven sensors (an altimeter, an accelerometer, a heart rate monitor, a barometer, a gyroscope, a light, and a temperature sensor) towards activity classification. A ground-truth data set including 13 daily activities are acquired from a group of elderly participants. The heart rate sensor is attached to the chest using an elastic stretching band, and other sensors are distributed on two wrists, as shown in Figure 2.8. The experimental results show that their system is superior to the earlier studies, achieving the accuracy of 97%.

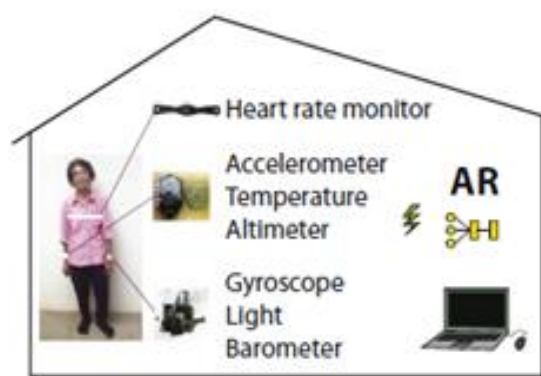


Figure 2. 8 Multiple sensors placed on body (Chernbumroong et al., 2014)

WSHAR systems deploy varied sensors on different body parts targeting different aims and applications. Generally, the case of One to One is the basic deployment and more suitable for those basic recognition tasks. Placing more sensors on more body parts is intuitively beneficial for improving the performance and robustness, whereas this also can increase complexity in deployment and computation cost of the system. Also, the sensors spread over a human body hinder the wearer doing everyday activities, this may cause the user rejecting to wear them. Consequently, exploring the way to implement WSHAR with less obtrusiveness, affordable cost, as well as higher accuracy, becomes more significant. The above discussed four sensor placements are summarised in Table 2.3.

2.3.3 Activities of daily living

HAR is an extensive research field of machine learning. Most studies in HAR focus on indoor activities of daily life (ADL) in assisted living applications, such as walking, running, exercise, lying, cooking, stairs using, falls, gaits, and so on (Hannink et al., 2017, Jung et

al., 2015, Zheng et al., 2014). These activities can reveal people's daily context and safety conditions. The recognition of ADL is helpful to understand, maintain and assist the daily life of the observed. For example, long-term sedentary activities may imply one person is suffering certain cognition problems or having early dementia symptoms; more sleep at daytime or less at night may reflect insomnia or other medical and psychiatric problems; frequent use of the toilet or frequent drinking are probably associated with diabetes or kidney diseases. And changes in routines prompt us some disorder may be happening compared with the normal patterns; on the other hand, regular eating, regular exercise, and other well-organized daily activities can reveal the subject is leading a healthy lifestyle. Also, older people living alone have a high risk of possible falls, which is the main concern for both themselves and their families. These conditions above all can be detected by HAR systems, and the corresponding decisions can be provided to assist older people living independently. Table 2.4 lists some case studies in HAR based on their defined activities in the application of safety and assisted living.

Real world data is the first material and important for the recognition tasks after determining sensor types and sensor deployment. While, data acquisition can be tedious and

Table 2. 3 Typical Sensor placement in WSHAR

Sensor placement	Examples	Strengths	Weaknesses
One to One	Bonomi et al., 2009 Rodriguez-Martin et al., 2013 Panwar et al., 2017	Less obtrusive, easy to deploy on body, low-cost, etc.	Limited information from one sensor and one body part, suitable for basic recognition tasks
One to Multi	Cleland et al., 2013 Xi et al., 2017 Szt Tyler et al., 2017	Rich information from different body parts	Obtrusive, increasing deployment complexity and computation cost
Multi to One	Mortazavi et al., 2014 Vepakomma et al., 2015 Shoab et al., 2014	Less obtrusive, complementary information from different sensors	A fixed body part might provide limited information for certain activities, such as the foot to cooking, etc.
Multi to Multi	Gjoreski and Gams, 2011 Chernbumroong et al., 2014	Rich information from different sensors and body parts	Reduce user's com-fort, high-cost, hindering the wearer performing activities, etc.

cumbersome work. Researchers may face a series of problems when collecting data, such as obtrusiveness, ease of using sensors, time arrangement, experiment environment, cost for participants, annotation, etc. the real-world data for a specific task in HAR should involve as more as possible target population with diverse age, gender, weight, height and health conditions. Whilst, due to the time cost and the subjects' will, the number of recruited volunteers are usually highly limited, varied from 1 (Alvarez-Alvarez et al., 2013), 12 (Bhattacharya and Lane, 2016), 30 (Fontana et al., 2015) to 45 (Hajihashemi and Popescu, 2013) apart from some benchmark datasets with larger population. As for the older participants, the number of participants is smaller (Bergmann et al., 2012, Chernbumroong et al., 2013, Wang et al., 2017d).

Table 2. 4 Case studies regarding activity types in assisted living

Application	Activity types	Reference
ADL	Brushing, Exercise, feeding, ironing, reading, sleeping, wiping, etc.	Chernbumroong et al., 2014
ADL and Falls	Walking, sitting, falls.	Rasheed et al., 2015
Gait analysis	Gait	Hannink et al., 2017
ADL and heart failure	Standing, walking, ascending/descending stairs, heart failure, etc.	Zheng et al., 2014
Physiatric rehabilitation	Joint dynamics, posture, head position	Hermanis et al., 2016
Assessment of stroke patients	Handshake, shoulder touch, etc.	Yu et al., 2016
Stroke patient treatment	Hand grips	Lorussi et al., 2016
Fall detection	Walking, sit down, stand up, stepping up/down, running, falling	Jung et al., 2015
Exercise motion detection	Hammer-curl with dumbbell, push-ups, etc.	Um et al., 2016
ADL and location	Location, sitting, standing, walking	Lee and Mase, 2002
Gesture during eating	Bite, drink, utensiling, etc.	Ramos-Garcia and Hoover, 2013
Lower limb motions	Gait circle, foot trajectory	Qiu et al., 2016

The protocol of data collection also affects the recognition performance, and the factors involve the number of activities, the number of participants, performing activities in a natural way or a constrained way, a controlled environment or a real-home setting, etc. Some studies collect their data based on the predefined activities under a controlled environment. E.g., the volunteers in Laudanski et al., 2015 perform the same activity in the approximate frequency and intensity, thereby achieving high accuracy due to the high intra-class similarity under the protocol. While data collection in Banos et al., 2014a is conducted in more natural settings. With respect to the data annotation, most studies supervise the data collection process. Deng et al., 2014 label the data by observers or record the process with a camera to avoid mislabelling. To provide a more natural environment for participants and minimize the burden of annotation, Adaskevicius, 2014 utilizes a semi-automatic approach for data collection. Bourke et al., 2008a label the activities using the developed application by themselves.

Researchers collect the data for their specific research purposes. They also can use the public datasets available for HAR to evaluate their proposed methods or compare their methods with other studies on the same datasets. The commonly used datasets are, 1:) *PAMAP2* (Reiss and Stricker, 2012) which comprises daily activities (sitting, watching TV, jogging, etc.) collected from 9 elderly subjects with three inertial sensors and heart rate placed on ankle, chest, and dominant arm; 2): *mHealth* (Banos et al., 2014b), which covers 12 daily activities for health monitoring using three inertial sensors and electrocardiogram sensor; 3): *WISDM* (Kwapisz et al., 2011), which is a dataset collected from 29 users with single accelerometer embedded in a mobile phone, including sitting, jogging, standing, working, etc.

2.3.4 Raw data pre-processing

The preprocessing of the wearable data in Figure 2.2 can involve filtering (noise elimination), nominalization, and segmentation, etc. This section only talks about data filtering and segmentation.

Filtering

In HAR, filtering is applied to the raw sensor signals to remove some unwanted components from a signal, since raw sensor data might be contaminated by electronic noise or other artefacts. Filtering is normally performed before the time series are split into time windows for feature extraction. Kalantarian et al., 2015 and Nam and Park, 2013 use low-pass filter to smooth or remove the outliers. Machado et al., 2015 apply a second-order Butterworth

High-Pass filter with cut-off frequency of 0.25 Hz to isolate the body acceleration component. Hu et al., 2014 exploit median filter for data pre-processing. N-point moving-average filters are adopted by Adaskevicius, 2014. Hassan et al., 2018 apply median and low-pass Butterworth filter to remove the noise from the acceleration signal. On the other hand, filtering is not always applied since some researchers state that filtering may cause the loss of relevant information (Atallah et al., 2007, Ord óñez et al., 2013, Fontana et al., 2015).

Window Segmentation

The time series data from wearable sensors are in the order of seconds or minutes, which is a relatively long period compared with the sensors' sampling rate (mostly varying from 20Hz to 100Hz). For facilitating the later learning, time series are often segmented into certain time windows. The sliding window is one of the most popular segmentation approaches due to its implementation simplicity. Sliding windows partition the time series into fixed-size windows.

Different window sizes have been employed in WSHAR, which are seen to vary from 0.08s (Berchtold et al., 2010), 0.1s (Murao and Terada, 2014), 0.2s (Zhang and Sawchuk, 2012), 0.5s (Chavarriaga et al., 2013a), 1s (Bulling et al., 2014), 1.6s (Suto et al., 2016), 2s (Laudanski et al., 2015), 2.56s (Hassan et al., 2018), 3.88s (Chernbumroong et al., 2014), 4s (Wang et al., 2013), 5s (Machado et al., 2015), 6.7s (Bao and Intille, 2004), 8.53s (Guo et al., 2012), 9s (Kalantarian et al., 2015), 10s (Zheng et al., 2013, Catal et al., 2015), to 30s (Tapia et al., 2007, Liu et al., 2012) and even higher. Usually, a window covers a few seconds long time interval. A small-size window allows for faster feature extraction in later steps but may not cover enough circles of one activity. A large-size window can cover more circles of one activity and contain the information from more than one activity; this may delay recognition. Some researchers determine the window size with empirical values or referring to other similar studies; others try a range of lengths on their data to find the optimal size. Finding the optimal window size is an application-dependent task. Hu et al. 2014 conclude that the length of the window should satisfy two conditions: first, at least one cycle of the activities is statistically included in one window and it has been proved that a window of several seconds can sufficiently capture circles of activities such as walking, running, using stairs, etc.; second, the size should better be set to the n th power of 2 thereby being easily employed in the Fast Fourier Transform (FFT) algorithm in one window. Therefore, a number of studies which use frequency-domain features set the samples in one

window as the n th power of 2 in each segment (Guo et al., 2012, Bayat et al., 2014).

We need to take the sampling rate of sensors into account with respect to the number of samples in one window since the sample number is determined by both the window size and the sampling rate. A wide range of sampling rates are used in WSHAR, varying from 1hz (Zhang et al., 2014), 5hz (Alshurafa et al., 2014), 6hz (Gjoreski and Gams, 2011), 10hz (Nam and Park, 2013), 20hz (Catal et al., 2015, Suto et al., 2016), 33hz (Chernbumroong et al., 2014), 50hz (Biswas et al., 2015, Hassan et al., 2018), 64Hz (Hammerla et al., 2016), 100hz (Sani et al., 2017), 120hz (Laudanski et al., 2015), 126hz (Gupta and Dallas, 2014), 135hz (Dalton and ÓLaighin, 2013), 200hz (Yao et al., 2017), 256hz (Chen et al., 2014), and up to 800hz (Montalto et al., 2015). Generally, higher sampling rates can catch more signal details but coupled with higher energy requirements and higher noise impact; lower sampling rates save considerable energy, which might omit certain relevant information, thus lower accuracy. Gao et al., 2014 find on their experimental results that the wearable systems adopting multiple sensors are less sensitive to the sampling rate than those only using a single sensor. Although the high sampling rate may help increase the recognition accuracy, it also leads to a several-fold increase in computing load. Therefore, they suggested 20 Hz to be the appropriate sampling rate for the wearable system using multiple sensors.

The number of samples in one window versus the window size based on the reviewed works is plotted in Figure 2.9, with several less commonly-used numbers being excluded (Machado et al., 2015). And we can see two obvious trends in Figure 2.9: one is that most sample numbers in one window fall into between 32 (Suto et al., 2016) and 256 (Hu et al., 2014); the other is that sample numbers of the n th power of 2 are often applied, such as 64 (Murao and Terada, 2014), and 128 (Ronao and Cho, 2016). The sampling rate, as well as the trade-off between recognition efficiency and performance, should be considered when manually determining the window size.

When applying window segmentations, the overlap between two consecutive windows is usually adopted to reduce information loss at the edges of the window. The most commonly used overlap rate is 50% (Laudanski et al., 2015, Kwon et al., 2014, Tapia et al., 2007, Suto et al., 2016, Davis et al., 2016). There are some other studies without performing overlap between windows (Davis et al., 2016, Banos et al., 2012).

2.3.5 Features for classification

Features are the inputs for most machine learning classifiers. In general, there are two

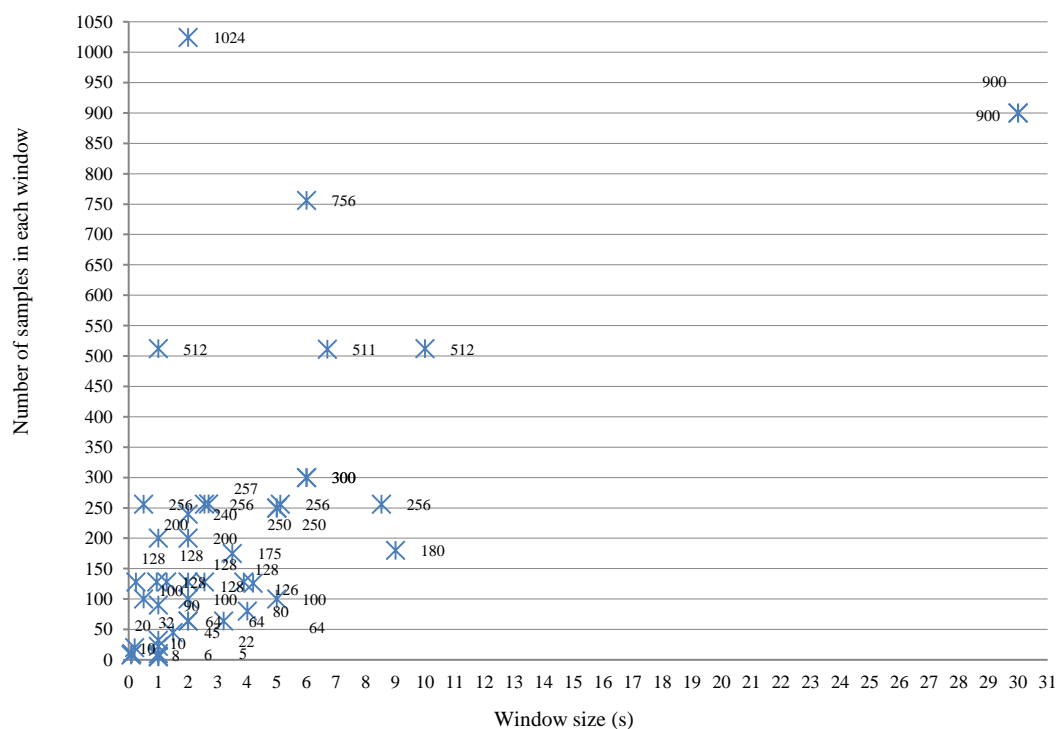


Figure 2. 9 Sample number of each window versus window size in publications

ways to extract features from raw sensor data, one is handcrafting features based on domain knowledge (Vepakomma et al., 2015) and the other is automatically learning features by deep networks (Ronao and Cho, 2016). Hand-crafted features are the measures computed from each window segmentation in the time domain or frequency domain, which are designed to capture the useful representation of the data for distinguishing different activities in HAR, such as mean, median and principal frequency (Hassan et al., 2018, Suto et al., 2016). Hand-crafted features have achieved great success in HAR applications (Li et al., 2009, Wang et al., 2016a, Hassan et al., 2018). The key advantage of using hand-crafted features is that the features are computationally lightweight to implement especially in ubiquitous devices (Morales and Akopian, 2017). These years, deep learning approaches have been applying in HAR to automatically learn features for HAR (Hammerla et al., 2015, Sani et al., 2017). The strengths of the automatically learned features by the deep networks are that the learning can be very deep, and the learning process does not rely on domain knowledge.

2.3.5.1 Hand-crafted features

In the raw data space, the specific value at a specific time instant of a sample (such as the

reading of 30°C from a temperature sensor) does not carry sufficient information to describe an activity that the reading originates from. Furthermore, when we compare two activities regarding two given time windows, it is nearly impossible that two-time series (i.e., segmented windows) contain identical signals even the two windows represent the same activity performed by the same person. Accordingly, quantitative and informative variables can be calculated based on each window from raw sensor data, these are hand-crafted features. Consequently, hand-crafted features are elaborately designed for comparing and differentiating different activities. A wide range of features have been explored to improve HAR performance (Heinz et al., 2006, Li et al., 2009, Wu et al., 2012, Attal et al., 2015, Wang et al., 2016a, Sani et al., 2017). We categorize the hand-crafted features as the following types, i.e., time-domain features, frequency-domain features, and other hybrid features.

Time-domain features are those features obtained directly from a window of sensor data and are typically statistical measures. They have been intensively investigated in different applications and proved to be effective and useful for HAR. These features are based on a comprehensive and intuitive understanding of how a specific activity or posture will produce a set of discriminative features from measured sensor signals. For instance, static and dynamic activities should produce different signal strengths. Take the acceleration signal as an example, the signal magnitude area (SMA) calculated by the acceleration magnitude summed over three axes within each window has been found especially effective to distinguish static activities from dynamic activities, such as sitting and walking. Machado et al., 2015 and Hassan et al., 2018 use SMA and other features to improve the recognition accuracy of dynamic activities. Studies also show that Standard deviation (Std) is helpful to achieve consistently high accuracy to differentiate activities such as walking, standing, and stairs using (Laudanski et al., 2015). Some other well-applied time-domain features are median (Murao and Terada, 2014), variance (Mortazavi et al., 2014), skewness (Zhang and Sawchuk, 2011, Hassan et al., 2018), zero crossing rate (Suto et al., 2016), Autoregressive coefficient (AR) (Hassan et al., 2018), peak-to-peak (Machado et al., 2015, Zheng et al., 2013) and so on.

Frequency-domain features are the features which are represented to describe the periodicity of signals. To produce frequency-domain features, a window of the sensor data should first be applied a transformation function, such as Fast Fourier Transform (FFT), Discrete Wavelet Transform (DWT), or Discrete Cosine Transform (DCT). The output of FFT giving is a set of basis coefficients which represent the amplitudes of the frequency

components of the signal and the distribution of the signal energy. Examples of frequency-domain features based on FFT include spectral energy (Hassan et al., 2018), entropy (Hassan et al., 2018), dominant frequency (Chernbumroong et al., 2013, Suto et al., 2016). These FFT-derived features are reported to be beneficial to improve the recognition performance in the above-mentioned applications. Ayachi et al., 2016 demonstrate the high efficiency of DWT in their detecting and segmenting tasks for older people's daily living activities based on multiple body-worn inertial sensors. Both Ocak, 2009 and Chen et al., 2017a develop their automated epileptic seizures detection schemes based on DWT and EEG to improve the accuracy. Alickovic et al., 2018 propose another automated seizure detection and prediction model based on EEG measurements. They employ wavelet packet decomposition (WPD), DWT and empirical mode decomposition (EMD) as feature extractors, and the WPD outperform other two methods. He and Jin, 2009 develop a human activity system based on DCT-extracted features from acceleration data, their experimental results achieve the accuracy of 97.51%. Desai et al., 2015 also apply DCT for feature extraction on their proposed automated cardiac arrhythmia detection framework.

Hybrid features

Most time-domain and frequency-domain features are generated from an individual channel (axis) of a sensor; such as mean and dominant frequency. On the contrary, the hybrid features are usually extracted from multiple sensory channels of a sensor or multiple sensors. By doing this, hybrid features implement sensor fusion through feature extraction. Take the inertial sensors as examples; there are several studies explore using hybrid features for HAR, e.g., the attitude angles of the wearable device, such as tilt, rotation, yaw and so on. These features are calculated by combining the values from multiple channels of an inertial sensor or multiple inertial sensors instead of a single inertial sensor, such as an accelerometer, a gyroscope or a magnetometer. Karantonis et al., 2006 and Suto et al., 2016 use the feature of tilt angle (Φ) to determine the postural orientation of the user in their studies. Other hybrid features, such as pitch and roll, can refer to the work in Gjoreski and Gams, 2011 and Kundu et al., 2017.

Extraction of hand-crafted features depends on domain knowledge. However, hand-crafted features are easy to understand and implement. We conclude the key hand-crafted features successfully exploited in different HAR applications in Table 2.5, which can give strong clues for HAR tasks.

2.3.5.2 Automatically learned features

The second feature representation technique in current HAR applications is using deep learning networks. Deep learning can automatically learn features from raw sensor data with less human effort, which optimizes parameters layer-by-layer following the principle that the decoded output should be equal to the input (Wang et al., 2017b). The automatically learned features from deep networks are developed and applied in recognition tasks to improve performance (Hammerla et al., 2015, Hammerla et al., 2016, Hannink et al., 2017). For example, Ronao and Cho, 2016 use a deep convolutional neural network (CNN) for human activity recognition. The network they propose automatically learns useful features from the raw data. They also investigate the effect of the performance of the extracted features from different layers on the increasing number of feature maps. The authors state their proposed network provides a way to automatically learn robust features without the requirements of preprocessing and time-consuming on feature hand-crafting. Zeng et al., 2014 propose a CNN-based feature extraction. Their experimental results indicate the extracted local dependency and scale invariant characteristics from the acceleration time series outperforms the state-of-the-art approaches.

Panwar et al., 2017 design a CNN-based framework for the recognition of three fundamental movements of the human forearm performed in daily life. Their framework learns features from the wrist-worn acceleration data. Their experimental results present the better performance of the proposed framework compared with other existing conventional methods. However, the authors do not give the details about what specific hand-crafted features they use for the conventional methods. Sani et al., 2017 also report that the automatically learned features perform better compared to hand-crafted features. They compare the automatically learned features with the hand-crafted features from the time domain, frequency domain, FFT and Discrete Cosine Transform (DCT) separately. DCT performs best on the thigh data and automatically learned features outperform DCT slightly on the wrist data. While, their experimental results do not answer a key question that whether the automatically learned features they used can beat the combination of all the hand-crafted feature sets they use instead of beating them separately.

Some other studies explore combining hand-crafted features and automatically learned features for HAR. Plötz et al., 2011 propose an RBM-based feature learning approach to discover universal features for activity recognition. Their experimental results based on four publicly available AR datasets indicate that combining the automatically learned

Table 2. 5 Typical hand-crafted features used in HAR

Item	Feature title	Description	Formula (if possible)
	Mean (Margarito et al., 2016)	The average value of the signal over the window	$\mu = \frac{1}{T} \sum_{i=1}^T s_i$
	Root Mean Square (Rms) (Sani et al., 2017)	The quadratic mean value of the signal over the window	$\sqrt{\frac{1}{T} \sum_{i=1}^T s_i^2}$
	Peak-to-peak amplitude (Ptp) (Machado et al., 2015)	The difference between the maximum and the minimum value over a window	$\max\{s_1, s_2, \dots, s_T\} - \min\{s_1, s_2, \dots, s_T\}$
	Zero crossing rate (Czr) (Machado et al., 2015)	Rates of time signal crossing the zero value, normalized by the window length	
	Mean crossing rate (Cmr) (Banos et al., 2014a)	Rates of time signal crossing the mean value, normalized by the window length	
Time-domain features	Signal magnitude area (SMA) (Hassan et al., 2018)	The acceleration magnitude summed over three axes within each window normalized by the window length	$\frac{1}{T} (\sum_{i=1}^T a_x(t) + \sum_{i=1}^T a_y(t) + \sum_{i=1}^T a_z(t))$
	Average of peak frequency (Apf) (Janidarmian et al., 2017)	The average number of signal peak appearances in each window	
	Log-energy (Sani et al., 2017)	Log of energy	$\sum_{i=1}^T \log(s_i^2)$
	Movement Intensity (MI) (Chernbumroong et al., 2014)	Mean of the total acceleration vector over the window	$\frac{1}{T} \sum_{i=1}^T \sqrt{a_{xi}^2 + a_{yi}^2 + a_{zi}^2}$
	The variance of MI (VI) (Zhang and Sawchuk, 2011)	The variance of Movement Intensity over the window	$VI = \frac{1}{T} (\sum_{i=1}^T MI(i) - VI)^2$
	Averaged derivatives (Ader) (Zhang and Sawchuk, 2011)	The mean value of the first order derivatives of the signal over the window	$\frac{1}{T} \sum_{i=2}^T \frac{s_i - s_{i-1}}{2}$

Chapter 2 Literature review

	Crest factor (Cftor) (Wang et al., 2016b)	The ratio of peak values to the effective value over the window	$\frac{0.5(S_{max} - S_{min})}{RMS}$
	Percentiles (King et al., 2017)	10 th , 25 th , 50 th , 75 th , 90 th	
	The interquartile range (Interq) (King et al., 2017)	Difference between the 75 th and 25 th percentile	
	Autocorrelation (Autoc) (Machado et al., 2015)	The correlation between the values of the process at different times	$\frac{\sum_{i=1}^{T-1}(s_i - \mu)(s_{i+1} - \mu)}{\sum_{i=1}^T(s_i - \mu)^2}$
	Pairwise correlation (Corrcoef) (Janidarmian et al., 2017)	The ratio of the covariance and the product of the standard deviations between each pair of axes	$corr_{XY} = \frac{\sum_{i=1}^T(X_i - \bar{X})(Y_i - \bar{Y})}{\sqrt{\sum_{i=1}^T(X_i - \bar{X})^2} \sqrt{\sum_{i=1}^T(Y_i - \bar{Y})^2}}$
	Standard deviation(Std) (Laudanski et al., 2015)	A measure of the spreads of the signal over the window	$\sigma = \sqrt{\frac{1}{T} \sum_{i=1}^T (s_i - \mu)^2}$
Time-domain features	The coefficient of variation(Cv) (Janidarmian et al., 2017)	The ratio of the standard deviation to the mean	σ/μ
	Kurtosis (Sztyler et al., 2017)	The degree of peakedness of the signal probability distribution	$\frac{\frac{1}{T} \sum_{i=1}^T (s_i - \mu)^4}{(\frac{1}{T} \sum_{i=1}^T (s_i - \mu)^2)^2} - 3$
	Skewness (Zhang and Sawchuk, 2011)	The degree of asymmetry of the sensor signal probability distribution	$\frac{\frac{1}{T} \sum_{i=1}^T (s_i - \mu)^3}{(\frac{1}{T} \sum_{i=1}^T (s_i - \mu)^2)^{\frac{3}{2}}}$
	Max (Hassan et al., 2018)	The largest value in a set of data	$\max\{s_1, s_2, \dots, s_T\}$
	Min (Chernbumroong et al., 2013)	The smallest value in a set of data	$\min\{s_1, s_2, \dots, s_T\}$
	Median (Murao and Terada, 2014)	The middle number in a group of ordering numbers	median (s_i)
	Mode (Chernbumroong et al., 2014)	The number that appears the most often within a set of numbers	mode (s_i)
	Variance (Mortazavi et al., 2014)	The average of the squared differences from the Mean	$\frac{1}{T} \sum_{i=1}^T (s_i - \mu)^2$

Chapter 2 Literature review

	Autoregressive coefficient(AR) (Hassan et al., 2018)	Coefficients of an IIR filter, α_i	$X(n)=\sum_{i=1}^p \alpha_i s(n-p) + e(n)$
	Median absolute deviation(MAD) (Suto et al., 2016)	The median of the absolute deviations from the data's median	$Median_i (s_i - median_j(s_j))$
Frequency-domain features	Dominant frequency (Domifq) (Suto et al., 2016)	The frequency corresponding to the maximum of the squared discrete FFT component magnitude of the signal from each sensor axis	
	Spectral energy (SpecEgy) (Hassan et al., 2018)	The sum of the squared discrete FFT component magnitude of the signal from each sensor axis, normalized by the window length	$\frac{\sum_{i=1}^{ \omega } x_i ^2}{ \omega }$
	Spectral entropy (SpecEnt) ()	A measure of the distribution of frequency components, normalized by the window size	$\sum_{i=1}^{T/2} [P(i) \cdot \lg(P(i))]$
	The spectral centroid frequency (SCF) (Sani et al., 2017)	The estimate of the “centre of mass “of the spectrum	
Other hybrid features	Eigenvalues of dominant directions (EVA) (Zhang and Sawchuk, 2011)	The relative motion magnitude along the vertical direction and the heading direction respectively	
	Averaged velocity along heading direction (AVH) Zhang and Sawchuk, 2011)	Firstly, calculating the averaged velocities along y and z-axes over the window, and then Computing the Euclidean norm of those two velocities	
	Pitch, yaw, roll features (Kundu et al., 2017)	The features extracted from the attitude values of an Inertial Measurement Unit	

Features with the hand-crafted features outperform other classical approaches. The results in Kashif et al., 2016 have shown that adding hand-crafted features to the raw data can help improve the detection accuracy of deep convolutional neural networks for tumour cells in histology images. Meanwhile, there are some other studies giving certain interesting findings in similar fields, e.g., the experimental results in Khan and Yong, 2016 indicate that the hand-crafted features outperform the automatically learned features in medical images. Song et al., 2016 use both video and wearable sensor data to tackle the egocentric activity recognition problem. They propose multi-stream CNN and Long short-term memory (LSTM) deep architectures to learn features from video and sensor data respectively. Experimental results indicate their proposed methods do not perform better than the hand-crafted features used in their work. They explained that this is due to that the amount of training data for their deep networks is small. Collectively, feature representation or extraction is a crucial step in HAR process. The problem of feature learning could depend on a task at hand. We produce Table 2.6 which summaries the advantages and disadvantages of hand-crafted features and automatically learned features based on the abovementioned studies in Section 2.3.5.

2.3.6 Feature dimensionality reduction and feature selection

More features carry richer information, which is beneficial for improving classification performance. Feature dimension, especially for the hand-crafted features, extracted from the time, frequency or hybrid domains, becomes very high in most HAR tasks. The initial set of features can be redundant or too large to be manipulated; this could cause higher computation cost, low learning efficiency, and overfitting on unseen data (Li et al., 2017a). Proper feature dimensionality reduction and feature selection can be applied in this regard to facilitate more accurate and faster learning, improving generalization and interpretability.

2.3.6.1 Feature dimensionality reduction

Feature dimensionality reduction is one of the two methods to address the above-described issues, which reconstructs features to replace the original features by producing linear or nonlinear combinations of the input in an unsupervised way, such as Prominent Component Analysis (PCA) (He and Jin, 2009), Kernel PAC (kPCA) (Hassan et al., 2018), Autoencoder (Wang, 2016), Sparse filtering (Ngiam et al., 2011) and so on.

PCA is one of the well-known dimensionality reduction methods. The basic idea behind PCA is to find the optimal projection that linearly transforms the original features into a

Table 2. 6 Comparison between hand-crafted features and automatically learned features

Feature type	Advantages	Disadvantages
Hand-crafted Features	Easy to understand the physical meanings of the features; Extraction is efficient and easy to deploy; Work well for many AR problems.	Domain knowledge is needed; Sensor-type specific; Need further feature selection.
Automatically learned features	No domain knowledge needed; Automatically learning features from raw data; Features are more robust and generalized.	Additional computing resources are needed; Parameters are difficult to adjust; Features are less interpretable.

new feature space in the variance sense (Yang et al., 2012). The variables, which are ranked according to their variance (from largest to lowest) in the new feature space, are called principal components. The principal components that contribute to very high variance are preserved. kPCA finds the optimal nonlinear transformation of data, which maps the input features into a higher-dimensional feature space through a kernel function (e.g., radial basis function (RBF) kernel); followed by a typical PCA (Wu et al., 2007). PCA family are good at seeking the best representative data projection. However, it may not work well since PCA does not consider any difference in classes. Unlike PCA, Linear Discriminant Analysis (LDA) projects the original features into a new space of lower dimension by maximizing the between-class separability while minimizing their within-class variability (Uray et al., 2007). The nonlinear extension of LDA is Kernel LDA (kLDA) which performs LDA in the feature space mapped by a nonlinear kernel function (Schölkopf et al., 1998). Hassan et al., 2018 propose a smartphone inertial sensor-based system for human activity recognition. The hand-crafted features, including mean, median, coefficients, etc., are further processed by kPCA and LDA for dimension reduction. The comparison studies show the superiority of their proposed approach.

An autoencoder network can learn a lower-dimensional representation of input data by minimizing the mean squared error between the input and the output (ideally, the input and the output are equal) (Van Der Maaten et al., 2009). An autoencoder consists of two parts, namely encoder, and decoder. The encoder aims to compress the original input data into a low-dimensional representation; the decoder tries to reconstruct the original input data based on the low-dimension representation generated by the encoder. As a result, the

autoencoder is widely used to reduce the data dimension. These years, the autoencoder and its extensions demonstrate a promising ability to learn meaningful features from data for activity recognition (Chen et al., 2017b, Gu et al., 2015, Chikhaoui and Gouineau, 2017). Sparse filtering is an unsupervised feature learning algorithm designed to learn features which are sparsely activated without needing to model the data's distribution (Ngiam et al., 2011). For each sample in feature space, only a small subset of features is activated to achieve population sparsity; each feature is only activated on a small subset of the samples to reach lifetime sparsity, and features are roughly activated equally often to attain high dispersal. Hahn et al., 2015 present a new neural network framework by combining sparse filtering model and locally competitive algorithms to demonstrate their network's ability to classify human actions from the video. Raja et al., 2015 propose a new feature extraction method based on deep sparse filtering to obtain robust features for unconstrained iris images. Other dimensionality reduction methods in HAR can be found from Álvarez-Meza et al., 2017, Peng et al., 2017, and Biagetti et al., 2017.

2.3.6.2 Feature selection

Feature selection (FS) techniques, different to normal dimensionality reduction techniques (such as PCA) described in Section 2.3.6.1, select a subset from a feature set without altering the original representation of the features (Guyon and Elisseeff, 2003). Thus, the selected features preserve the original semantics of the original features. An efficient feature selection can eliminate redundant features, simplify the model construction, provide the advantage of interpretability and enhance generation performance. A wide variety of feature selection approaches have been proposed and applied in HAR. These methods can be classified into three groups based on their relationship with the inductive learning method for model construction, i.e., filter, wrapper and embedded.

The filter methods, as the name suggests, are those FS algorithms which filter out irrelevant features by evaluating the relevance of a feature to the output using certain criteria, such as correlation, distance, information, consistency, similarity and statistical measures (Gheid and Challal, 2016, Dessì and Pes, 2015, Li et al., 2017a). A filter algorithm first ranks the original features based on its criteria, then selects the features with higher rankings. Filter methods are independent of any classifiers, thereby being more efficient. The typical examples of filter methods are Relief (Gupta and Dallas, 2014), Correlation-based Feature Selection (CFS) (Hemalatha and Vaidehi, 2013), Minimum-Redundancy-Maximum-Relevance (mRMR) (Peng et al., 2005), Canonical Correlation Analysis (CCA) (Kaya et al.,

2014), etc. Mutual information (MI)-based feature selection methods are a big family in filter methods, the algorithms in this family exploit the filter criteria based on MI which carries correlation between features. MI and its extensions include mRMR (Peng et al., 2005), Joint Mutual Information (JMI) (Bennasar et al., 2015), Conditional Mutual Information Maximum (CMIM) (Gao et al., 2016), Double Input Symmetrical Relevance (DISR) (Meyer and Bontempi, 2006) and so on. While, MI-based feature selection (FS) methods share a common problem, i.e., it does not fully consider the complementarity within a feature set or between features and the label since MI considers the correlation in pairs. Unlike MI, CCA measures the linear relationship between two multidimensional by maximizing the correlation coefficients between them. CCA can be used as a feature selector. CCA and its extended FS algorithms include LSCCA (Kursun et al., 2011), DCCA (Andrew et al., 2013), MCR-CCA (Kaya et al., 2014), etc.

The wrapper methods select a subset of features with the most discriminating properties by using certain classifiers to evaluate the quality of a candidate feature, like SVM (Bolón-Canedo et al., 2013) and neural networks (NNs) (Kabir et al., 2010). Given a predefined classifier, a typical wrapper goes through the following process: first it searches a subset of features; second, it evaluates the selected feature set by the performance of the predefined classifier; finally, the process repeats until when the estimated accuracy of adding any feature is less than the estimated accuracy of the feature set already selected. The wrapper methods consider the features dependency and the interaction with a classifier, thereby tending to offer a better result. While, the wrapper methods are very computationally expensive since performance assessments with a classifier are generally done using cross-validation (Wang et al., 2005). As a result, the wrapper methods are rarely used.

The embedded methods tend to take advantage of the merits of filter and wrapper methods by integrating feature selection into model learning (Li et al., 2017a). This can be implemented by regularization techniques which introduce additional constraints (feature coefficients) into the optimization (minimizing fitting errors) simultaneously. The most widely used embedded methods are Lasso (Li et al., 2017b) and Ridge regression (Liu et al., 2015). LASSO, i.e., ℓ_1 -norm regularization, has the property for feature selection, which can force a number of feature coefficients to become smaller or exactly zero. And the features with large feature weights can be selected. Li et al., 2017b introduce group Lasso into their proposed distributed feature selection method to reduce the high dimensionality of data in the genetic study of Alzheimer's disease. Similarly, Ridge performs ℓ_2 -norm regularization for feature selection (Huang et al., 2015).

Other feature selection methods, such as sparse representation, can refer to the works in Subrahmanya and Shin, 2010, Liu and Zhang, 2016 and Chu et al., 2013. There is no rigorous boundary between feature dimensionality reduction and feature selection; research continues to support the claim that there is not a “best method” for all tasks (Gui et al., 2017). The choice of the best feature set is usually with the aid of feature selection techniques or empirical evaluation of different combinations of features (Sani et al., 2017).

2.3.7 Classification algorithms

Classification process must be done to recognize human activities. The role of classification is to interpret the input features and give a prediction of the observations (the activity) (Alpaydin, 2014). Regarding classification algorithms used for HAR, current techniques can be categorized into two types: conventional classification algorithms and deep learning algorithms. The conventional classification algorithms attempt to build a complete description of the input with a probabilistic model such as a Bayesian network or model the mapping from inputs (features) to outputs (activity labels) such as SVM (Chen et al., 2012). The features used by conventional classification algorithms can be the hand-crafted or automatically learned features. Deep learning algorithms are the representation-learning methods with multiple layers of representation starting from the raw data (LeCun et al., 2015). Thereby, the features can be learned automatically through the network simultaneously with the process of modeling. The features used by deep learning algorithms can also be hand-crafted features.

2.3.7.1 Conventional classification algorithms

Following flowchart A shown in Figure 2.2, the features derived from raw sensor data are then fed to different classification algorithms for models constructing to analyse and classify data (e.g., the activities under consideration regarding HAR). The conventional classification algorithms in Figure 2.2 can be generally categorized into two types: supervised and unsupervised. Supervised classification algorithms deal with labeled data, and unsupervised algorithms draw inferences from datasets consisting of unlabelled input data. Supervised algorithms use training datasets to build models and test datasets to validate the models. Supervised classification is a very productive field, and a large number of efficient and well-known algorithms come under this category. Some well-performed and well-known supervised algorithms are like Support Vector Machines (SVMs) (Mehrang et al., 2017), Artificial Neural Network (ANN) (Khan et al., 2014), Naïve Bayes (NB) (Wu et al., 2018), Decision trees (DT) (Kumar et al., 2017), k-Nearest Neighbours (kNN)

(Adaskevicius, 2014), Multiplayer Perceptron (MLP) (Bayat et al., 2014), Random forest (RF) (Pavey et al., 2017), etc. Atallah et al., 2011 present a framework investigating the sensor placement and the corresponding relevance for activity recognition. The authors use kNN with different values of k to assess the effect of outlier points and a Bayesian classifier to model the data. Janidarmian et al., 2017 conduct a comprehensive comparison of 293 different classifiers, including DT, SVM, kNN, NB, etc., to find the best predictive model for diverse human activities. They first create the complete dataset focusing on acceleration data and do an extensive feature extraction on data. PCA is then used for feature dimensionality reduction. The averaged accuracy achieves $96.44 \pm 1.62\%$ with k-fold cross-validation and $79.92\% \pm 9.68\%$ with subject-independent cross-validation. Comprehensive experiment results demonstrate that kNN and its ensemble methods show stale results over different situations, followed by ANN and SVM. The authors conclude that the determination of parameters values in each classifier can have a significant impact on the classifier's performance. They also state that certain factors, such as sensor position on body, clothing, body shape and accidental misplacements, hinder building a solid model for different activities. Mehrang et al., 2017 investigate activity monitoring using a single wrist-worn device that is equipped with an optical heart rate sensor and a triaxial accelerometer. The authors apply RF and SVM to classify a variety of home-specific activities (sitting, standing, household, and stationary cycling) performed by 20 male participants. Results of leave-one-subject-out cross-validation show 89.2% and 85.6% average accuracies from RF and SVM, respectively.

In unsupervised learning, all the sensor data are passed to the algorithm which automatically identifies a certain number of states or data clusters, each of which may correspond to a specific activity. The most common unsupervised learning method is cluster analysis, which is used for exploratory data analysis to find hidden patterns or grouping of data. The clusters are modeled using a measure of similarity which is defined upon metrics such as Euclidean or probabilistic distance. Typical unsupervised learning algorithms include k-Means (Kwon et al., 2014), Gaussian mixture models (GMM) (Kwon et al., 2014), Hidden Markov models (HMM) (Uslu et al., 2013). Mannini and Sabatini, 2011 propose a cHMM-based sequential classifier for physical activity recognition, which is indicated to outperform the GMM classifier they use for the same data (99.1% vs. 92.2%). Kwon et al., 2014 present unsupervised learning using smartphone sensor to overcome the needs of generating training dataset and a number of activities extending in previous studies. Experimental results demonstrate the hierarchical clustering attains above 90% accuracy

when k is unknown. Their proposed approach provides a new way of automatically selecting an appropriate value of k without the generating training datasets by hand.

Some other studies combine different classification algorithms to cope with the limitations of them. Chernbumroong et al., 2015 explore combining MLP, RBF and SVM classifiers and use GA to find the optimal combination between classifiers. Reiss et al., 2015 propose a confidence-based boosting algorithm. Experimental results indicate their proposed method significantly outperforms other boosting algorithms on most of the benchmark datasets they used and especially for larger and complex classification tasks.

2.3.7.2 Deep learning algorithms

The majority of the abovementioned classification algorithms rely on hand-crafted features as input (Flowchart A in Figure 2.2). Recent years have witnessed a new area of machine learning techniques for HAR, e.g., deep learning-based networks, including CNN (Panwar et al., 2017), RNN (Hammerla et al., 2016), DBN (Hassan et al., 2018), RBM (Plötz et al., 2011), etc. Deep networks can both learn automatically learned features from raw sensor data and perform classification simultaneously (Wang et al., 2017a), as shown in Flowchart B in Figure 2.2. Many case studies have showed the superior performance of deep learning in HAR. Lane and Georgiev, 2015 investigate the question of whether deep learning techniques can address the accuracy, robustness, and efficiency on mobile sensing. The authors apply DNN, DT and GMM on activity, emotion and speaker recognition sensing tasks. Experiment setup considers the aspects of feasibility, scalability, cloud partitioning and so on, and their results provide some critical needs of the widespread adoption of sensing. Panwar et al., 2017 present a CNN-based generalized model for the recognition of three fundamental movements collected from a single wrist-worn accelerometer sensor. The comparison study among their presented method and SVM, K-means, LDA demonstrate the former outperforms with an average recognition rate of 99.8%. Also, their CNN-based method can handle both the feature engineering and classifying. But the authors do not give a clue whether they use delicate hand-crafted features on the latter classifiers or only pick some hand-crafted features at random. Um et al., 2017 propose a 7-layer CNN structure for augmentation of wearable data for Parkinson's disease monitoring. Ignatov, 2018 present a CNN-based deep network for online human activity recognition, their experimental results show the CNN augmented with statistical features produce a significantly-improved performance. They also demonstrate their proposed shallow architecture can be executed on mobile phones in real time. Ravi et al., 2016 also present an efficient implementation of

mobile phones, and the network they used is a shallow CNN structure. Suto et al., 2017 mention in their other study that a simple ANN can perform better than complex CNNs in HAR since they believe CNN can conduct feature extraction itself whereas the CNN may not substitute the feature extraction stage in conventional techniques. Collectively, how to effectively combine hand-crafted features, automatically learned features, conventional classification algorithms, and deep learning algorithms are still worth investigations. Based on the above discussion, we summarise the characteristics of conventional and deep learning classification algorithms shown in Table 2.7.

Table 2. 7 Comparison of conventional and deep learning classification algorithms

	Conventional	Deep learning
Features	Hand-crafted Dependent on domain knowledge	Automatically learned Independent on domain knowledge
Feature selection	Needed	No need Data pre-processing for deep networks are challenging
Model building	Model structure of a specific classifier is relatively fixed	No universal deep networks for the tasks at hand
Parameters setting and time cost	Parameters are easy to determine, comparatively takes much less time to train	A high number of hyperparameters are needed to tune, that training them takes longer

2.4 Ambient-sensor-based HAR (ASHAR)

Wearable-sensor-based systems described in Section 2.2 have achieved wide-spread use in HAR with different applications due to the ease of deployment and use, low-cost and satisfied performance (Lara and Labrador, 2013, Cornacchia et al., 2017). While WSHAR can only provide the recognition of specific activities without the ambient context. Ambient sensors can provide rich contextual information relating to human daily activities, and ambient-sensor-based HAR (ASHAR) systems have also been found widely used in HAR (Wilson and Atkeson, 2005, Tunca et al., 2014, Luo et al., 2017). This thesis pays more attention to WSHAR. Therefore, the review on ASHAR systems in this section will be more compact compared to WSHAR. ASHAR systems identify human activities from the environment which is augmented with a variety of sensors, such as a door with a switch sensor, a kettle with object tags, a fridge with contact sensors, a floor with pressure sensors,

a room mounted with motion sensors, etc., these sensors provide the user's contextual information where they perform activities (Tunca et al., 2014, Debes et al., 2016, Mehr et al., 2016). A wide range of ambient sensors are available and have been exploring for HAR, including cameras, light sensor, reed switch sensor, RFID, PIR, temperature, flow sensor, pressure sensor, etc. We summarise the most widely used ambient sensors in Table 2.8. These sensors have enabled monitoring of the daily life with somewhat general tasks. Here, we classify camera-based HAR (CHAR) into ASHAR.

2.4.1 Camera-based HAR (CHAR)

The camera-based HAR (CHAR) is an active field in computer vision. There are many research works on activity recognition by cameras, in which visual information acquired from the cameras mounted in fixed locations inside the building is utilized to match with the features extracted from action labels for activity recognition (Jalal et al., 2014, Jalal et al., 2017). Bian et al., 2015 propose a robust fall detection approach by analysing the key joints tracked from a single depth camera. Khan and Sohn, 2011 use one single camera to recognize six different abnormal activities (a headache, chest pain, forward fall, faint,

Table 2. 8 Ambient sensors used in HAR

Sensor	Function	Location	Target activity	Reference
Cameras, Kinect	Images or videos	In rooms	Multiple activities	Jalal et al., 2014, Phillips et al., 2017
Audio, sound, microphone	sound	In rooms	Communication falls, cries, etc.	Maekawa et al., 2010, Vacher et al., 2010, Fleury et al., 2010
PIR	Presence or motion	Ceilings, walls, etc.	Leaving/entering/passing a place, speed, etc.	Wilson and Atkeson, 2005, Luo et al., 2017
RFID	Objects information	Cupboard, kettle, etc.	Taking medicine, using belongings, etc.	Wilson and Atkeson, 2005, Fang and Hu, 2014
Light	Light intensity	In rooms	Sleeping,	Hristova et al., 2008
Pressure	Force on the sensor	Beds, floors, chairs, etc.	Lying, sleeping, sitting, etc.	Tunca et al., 2014
Contact switches	Contact information identifying	Doors, drawers, etc.	Leaving/entering room, etc.	Van Kasteren et al., 2008, Tunca et al., 2014
Temperature	Contextual temperature	Bathroom, kitchen, etc.	Room-related activities	Fleury et al., 2010, Kushwah et al., 2015

backward fall and vomit). Binary silhouettes instead of depth silhouettes are extracted to minimize the privacy at the price of failing to distinguish different body parts. Jalal et al., 2014 develop a life-logging HAR system using magnitude and directional angular features from the skeleton joints extracted from depth video sensors. Their system shows the potential to be applied in many applications to monitor and generate life logs of human activities or behaviours. The skeleton representation of certain activities in Jalal et al., 2014 is shown in Figure 2.10. Jalal et al., 2017 present a depth video-based novel method using robust multi-features and embedded Hidden Markov Models (HMMs), with the aim of providing a healthcare monitoring system to support independently living for older people. The multi-features are extracted from human depth silhouettes and joint body parts information. Experimental results demonstrate the significant recognition performance and potential applications for older and sick people. The activity silhouette presentation in Jalal et al., 2017 can refer to Figure 2.11.

Thanks to the advances in 3D depth cameras, Kinect sensors (typically including an infrared camera, infrared projector and microphone array) are deployed to detect the person's full-body motion, facial recognition, voice recognition and so on. Mohamed et al., 2012 develop a wireless sensor-based smart home, they explore Kinect sensors monitoring an older person or ill person. Stone and Skubic, 2015 propose a two-step approach to detect falls for older people living at home by utilizing the Microsoft Kinect sensors. Phillips et al., 2017 use Kinect sensors not only for gait change prediction but also the occurrence of future falls. They also process the Kinect depth images as silhouettes to protect privacy and embed the Kinect sensor on a small shelf above the front door to maximize the camera's view of activity.

Collectively, the significant advantage of camera-based monitoring systems is the contactless observation. And the rich information from images and videos is capable to detect verified activities (Mabrouk and Zagrouba, 2017). While, sophisticated algorithms are normally needed to cope with arbitrary views of the pictures captured from cameras or complex contexts. It may cause huge time consumption. Meanwhile, it is both difficult and too expensive to install cameras in all the places where older people are active. Also, the recognition accuracy of such systems decreases because of variable lighting and other disturbances (Wang et al., 2017d). The privacy concerns cannot also be avoided, although the researchers have been trying to minimize privacy by using the mini-dome and integrated cameras or exploring silhouettes instead of real pictures for activity recognition. CHAR

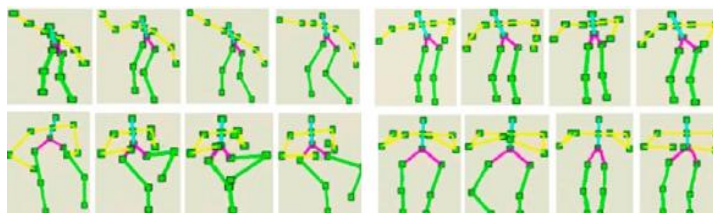


Figure 2. 10 Skeleton representations of some specific activities (Jalal et al., 2014)

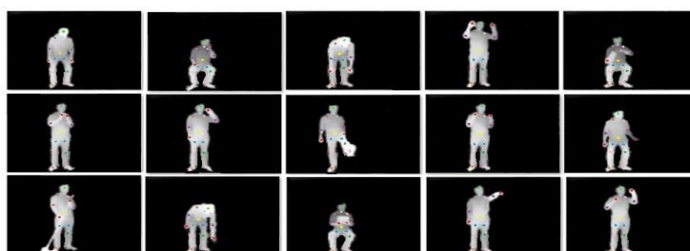


Figure 2. 11 Samples of human depth silhouettes (Jalal et al., 2017)

systems are therefore more suitable for an emergency, public safety surveillance, or scheduled meetings, instead of home-based daily monitoring. Kinect sensor systems hold promise for unobtrusively monitoring while maintaining privacy and eliminating the burden of additional monitoring procedures. Deploying a Kinect sensor set in each room at home for daily activity recognition is also less affordable.

2.4.2 Normal ambient-sensor-based HAR

Typical ASHAR systems here refer to other ASHAR systems excluding CHAR systems, which detect users' activities by detecting if the user contacts the object attached with ambient sensors or by identifying whether the user enters the viewing range of one specific ambient sensor. One of the typical examples can refer to Tunca et al., 2014. The authors develop an Ambient Assisted Living (AAL) system to infer the users' health and wellbeing status. A high number of sensors, including contact sensors, IR (infrared) receivers, sonar sensors, etc., are deployed in real environment settings. The layout and sensor deployment are shown in Figure 2.12.

Kushwah et al., 2015 present a multi-ambient-sensor framework for indoor activity recognition. Their work focuses on dealing with the difficulty of identifying the events that occur in the same context where the same set of sensors are activated during the occurrence. The authors use two smart home datasets in their experiments; one house is equipped with

14 digital sensors, such as toilet flush sensors, doors, refrigerator, and cupboards location sensors, with five different activities collected, including Drink, Dinner, Breakfast and so on; the other house is equipped with 21 sensors, with 15 activities recorded including Toileting, Showering, Drink, Brush teeth and so on.

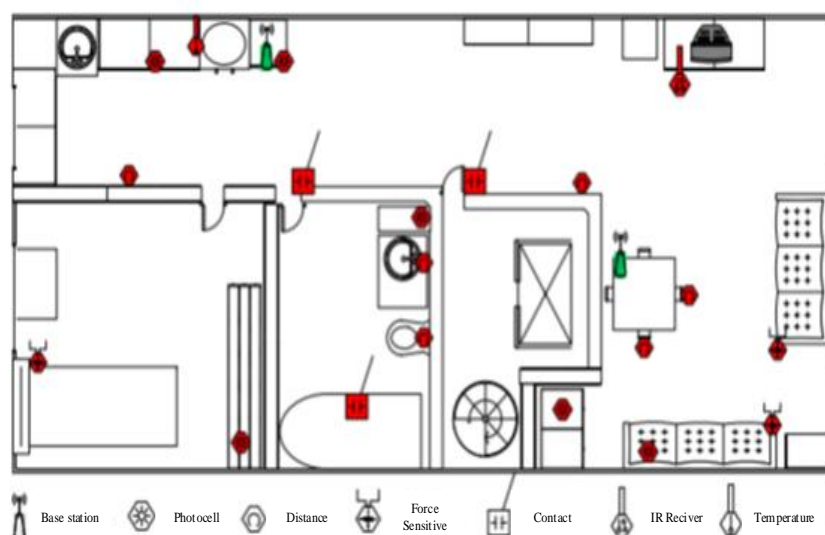


Figure 2. 12 A study of the ambient-sensors based smart home (Tunca et al., 2014)

Wilson and Atkeson, 2005 introduce the simultaneous tracking and activity recognition (STAR) problem for multiple people in a home setting. The instrumented home contains three stories with 20 separate rooms. One RFID reader is deployed in the front doorway. Each room has at least one motion detector located. Eight wireless keypads are placed on the front door, the study, the kitchen, the living room, upstairs bathroom, the downstairs bathroom, and each of the two bedrooms, which can identify which occupant enters a room after he/she pushes the button with the corresponding name gathered before. 24 contact switches are distributed in each doorway, the kitchen cabinets, the fridge, and the drawers. The proposed approach is evaluated with the following functions, like identifying which rooms are occupied, counting the occupants in a room, identifying the occupants, tracking occupant movements, and recognizing whether the occupants are moving or not. This identified information shows the potential of using simple ambient sensors for automatic health monitoring. Luo et al., 2017 propose another framework to solve the problem of STAR. They deploy the ceiling-mounted PIR sensor array in a room. The captured information, including location, speed, and duration is fed to the proposed two-layer RF (Random Forest) algorithm for activity recognition. The experimental results are encouraging, with the recognition accuracy of above 92% for five daily activities, i.e.,

walking, lying, sitting, standing and transitional activities. Yasmin van Kasteren et al., 2017 explore a routine-based approach for the interpretation of smart home sensor data, they only exploit PIR sensors and power use sensors located in the participants' bathroom, lounge, bedroom, and kitchen. They successfully record 180 days of sensor data coupled with the corresponding interview data from five participants' instrumented homes. The findings from the longitudinal data demonstrate the potential of using the routines and the variation in routine to make a real-time monitoring, reliable alerts and the satisfaction of the persons being monitored. PIR sensors are also used for gait assessment in Kaye et al., 2012, the authors use a line of ceiling-attached passive infrared motion sensors for gait speed estimation and walking speed assessment from the pattern and time intervals of sensor firings. Castro et al., 2017 present a system based on the Internet of Things (IoT) to HAR by monitoring vital signs remotely. The system is successfully implemented with a 95.83% success ratio for four pre-established categories (lie, sit, walk and jog).

From the above mentioned studies in ASHAR, we can see that HAR systems deployed with typical ambient sensors are less obtrusive because the user does not need to wear any sensors. Whilst, these systems normally deploy a high number of ambient sensors at fixed locations in the environment, this will cause poor flexibility and complex sensor deployment. Also, ASHAR works in a limited area (Tunca et al., 2014, Debes et al., 2016, Mehr et al., 2016).

2.5 Hybrid-sensory-based HAR (HSHAR)

A HAR system normally uses a single modality sensor, i.e. wearable or ambient alone. Each sensor modality has its own strengths and limitations (as discussed in Section 2.3 and Section 2.4) and single sensor modalities sometimes cannot well cope with complex situations in practice. This lays the foundation for exploring hybrid sensory systems in HAR. Different sensor modalities offer diverse information and varied performance for specific tasks. E.g., cameras deliver precise and direct information while coupled with privacy issues or working in a constrained space defined by the camera position and settings; ambient sensors (such as the temperature or light sensor) can provide important contextual information, whilst this can only give limited information for activity detection; door switches and other binary sensors are inexpensive and easy to install, but the captured ambient information by them is simple and limited to detect high-level activities; accelerometer, gyroscope, and other wearable sensors are miniature-sized and can be

flexibly worn on body to capture sufficient motion-related information, however, they cannot provide the contextual information and suffer the problem of arbitrary data caused by activities. Consequently, it is inappropriate to say which sensor modality is the best in an oversimplified way since different systems carry varied strengths and technologies targeting different applications unless we limit the task in a very specific range. Nevertheless, it is obvious that the combination of sensor modalities can capture rich information of human activities. This section looks into certain studies which combine different sensor modalities for HAR.

2.5.1 CHAR/Audio plus WSHAR

Liu et al., 2014a propose a hybrid sensor modality framework based on the probabilistic HMM classification for hand gesture recognition. Their framework fuses the data from an inertial sensor and a Kinect depth sensor. Their experimental results show that the accuracy can reach 93% after the data fusion while the performances of using the inertial sensor and the vision depth sensor individually are only 88% and 84%, respectively. The corresponding experimental set in Liu et al., 2014a is shown in Figure 2.13. Pansiot et al., 2007 present a sensor-fusion-based framework, in which an ear-worn accelerometer and a vision sensor



Figure 2. 13 The Experimental setup (Liu et al., 2014a)

installed in the environment are combined to improve classification accuracy. Hayashi et al., 2015 investigate the combination of environmental sound and acceleration data using DNN for HAR. Experimental results demonstrate the effectiveness of their proposed methods with an accuracy rate of 91.7% for nine different daily activities.

2.5.2 ASHAR plus WSHAR

Stikic et al., 2008 explore semi-supervised and active learning for human activity based on

acceleration and infra-red data. They utilize the number of activations from infrared sensors plus features extracted from the acceleration data as the input of the classifiers when combining the two-source data. Take active learning with 12.5% labeled data as examples in the study, the corresponding results are $60.6\% \pm 2.3\%$, $42.3\% \pm 2.1\%$ and $64.2 \pm 1.9\%$, respectively, for acceleration, infra-red data and the combined data. Pham et al., 2018 propose a hybrid sensory system for the localization of a resident in indoor environments. The authors deploy eight environmental PIR sensors distributed in a mock apartment and a wearable sensor device (i.e., IMU). The acceleration and angular rate data from the IMU are used for body activity recognition. The PIR sensors provide rough external tracking of the human location. By recognizing human activity and integrating with a known map of furniture in a testing environment, the accuracy of localization and tracking is greatly improved. Figure 2.14 presents the sensor deployment in Pham et al., 2018.

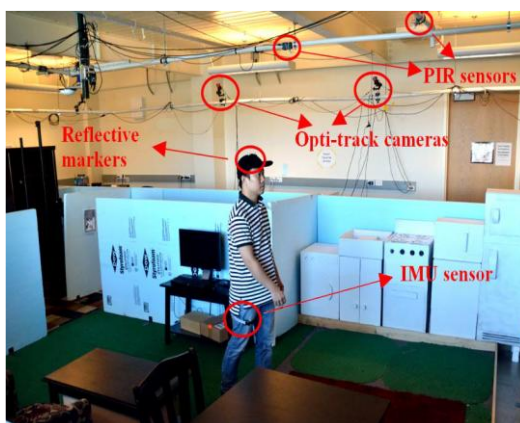


Figure 2. 14 Experiment setup in Pham et al., 2018

2.5.3 CHAR plus ASHAR plus WSHAR

Diethe et al., 2017 introduce using Bayesian models to tackle the challenges of fusion of heterogeneous sensor modalities. The multiple-sensor-modality data, including environmental data from PIR sensors, accelerometer data, and video data, are collected in the HealthCare in the Residential Environment SPHERE house (Diethe et al., 2014). The authors summarize that their proposed approach can identify the modalities for each particular activity and the features relevant to the activity simultaneously. Also, the results show how the approach fuses and separates the tasks of activity recognition and location prediction. Nakamura et al., 2010 present a collective framework which can monitor a user's location and vitals (heart rate or blood pressure) by synchronizing wearable and ambient

sensors.

Following the above discussions, we summarise the three sensor modalities in Table 2.9.

2.5.4 Data fusion algorithms among different sensor modalities

In hybrid sensory HAR systems, data fusion is a key question when combining multiple sensor modalities. Data fusion among different sensor modalities is seen in different ways.

Raw Data level: Liu et al., 2014a propose a data fusion method from inertial and depth sensor data for hand gesture recognition. They use the 3-axis accelerometer, and the 3-axis gyroscope signals from the inertial sensors and the 3-axis coordinate signals from the Kinect sensor to form the observation sequence of the HMM classifier after the synchronization. It is the raw data-level fusion. After merging the data from the inertial sensors and a visual depth sensor, the overall recognition rate for five motional hand gestures under realistic conditions is improved to 93% which is higher than when using each sensor modality individually on its own.

Feature level: In the work by Pansiot et al., 2007, the data independently obtained from the ear-worn accelerometer and the wall-mounted camera are pre-processed as features before they are fed to a Bayesian classifier. It is the feature level fusion. Significant improvements in the recognition rates of all activities are achieved when compared to using wearable or ambient sensors alone. Similarly, Stikic et al., 2008 use the number of activations of infrared sensors plus features extracted from the acceleration data as the input of the classifiers when combining the two-source data.

Decision level: In the work by Liu et al., 2014b, data from differing modality sensors are fed to a multi-HMM classification framework for hand gesture recognition. Each classifier generates its own likelihood probability and the maximum of which is considered to be the recognized gesture. It is the decision level fusion. Pham et al., 2018 deploy wearable sensors to derive the human location/activity and the PIR sensors to provide the location information. To improve the localization accuracy, the authors propose a particle filter-based sensor fusion algorithm that takes advantage of the correlation between human activity and the location in an indoor environment. By fusing the two channels of information: PIR data and IMU data, the more accurate location estimation is achieved than using only one of them. Li et al., 2015b propose a sensor fusion algorithm to improve tracking accuracy and estimate the individual's state. Firstly, they use the PIR sensor network to detect the rough area where the individual may be in and use the distribution of the furniture to improve the

Table 2. 9 Summary of sensor modalities in HAR systems

Sensor modality	Description	Sensor examples	Case study	Advantages	Disadvantages
WSHAR	Recognizing human activities by mining the informative data from wearable sensors	Accelerometer, gyroscope, heart rate, etc., built in a smartphone, band, watch, garment or other devices	Chernbumroong et al., 2014 Laudanski et al., 2015 Sztylek et al., 2017	Miniature-sized, low-cost, flexibly worn on body, capture motion-related information	Cannot provide the contextual information, suffer the problem of arbitrary data caused by activities
ASHAR	Inferring human activities from the sensors that are normally fixed in the environment	Surveillance camera	Phillips et al., 2017 Jalal et al., 2017	The camera can give precise and direct information	Privacy issues, expensive, working in a constrained space
		PIR, RFID, contact sensor, temperature sensor, humidity sensor etc.	Luo et al., 2017 Tunca et al., 2014 Mehr et al., 2016	provide important contextual information, less obtrusive	Limited information and working space, complex sensor deployment
HSHAR	Combining WSHAR and ASHAR for HAR	Combination of vision and accelerometers, a fusion of PIR sensors and accelerometers, etc.	Hayashi et al., 2015 Diethe et al., 2017 Nakamura et al., 2010	Capture rich information and use the strengths of different sensor modalities	Complex system structure and high cost, data fusion, and synchronization

accuracy of the estimation simultaneously. Secondly, they use the acceleration sensor placed on the foot to determine whether the individual stands still or walks out.

From the discussions above, it is found that different hybrid sensory systems deploy specific data fusion algorithms for their specific applications and research purposes. How to fuse the data from multi-sensor modalities depends on the task at hand.

2.6 Performance evaluation and criteria

2.6.1 Performance evaluation

Evaluation of recognition performance of a HAR system is also crucial. Two typical approaches are normally found applied in HAR applications through literature review, i.e. k-fold-cross-validation and leave-one-subject-out. The k-fold cross validation is a procedure used to estimate the performance of the model on unknown data (James et al., 2013). The procedure 1): shuffles the dataset available randomly, 2): then splits the dataset into k folds of approximately equal size; 3): for each unique fold, take the fold as a hold out as the test data set; take one fold from the k-1 folds as the validation data set and the remaining k-2 folds as the training data set; 4:) fit the model on the training set and evaluate it on the valuation set; 5:) test the model with the highest evaluation score and discard the other models; and the test conducts k times. The results of a k-fold cross-validation run are often summarized with the mean of the k times' test (Kuhn and Johnson, 2013). In practice, the k value must be chosen, for example, k is set as two in Hu et al., 2014, three in Chavarriaga et al., 2013a, five in Hemalatha and Vaidehi, 2013, eight in Kreil et al., 2014, and 10 in Nam and Park, 2013. The value for k is common to fix to 5 or 10, since these values have been shown empirically yielding a model performance estimate with low bias and a modest variance (James et al., 2013, Biswas et al., 2014, Ignatov, 2018). When k equals the number of subjects, the k-fold cross-validation is exactly the leave-one-subject-out cross-validation (Liu et al., 2012), which means the models are trained on the data for all subjects except one in one round, and the data from the left-out subject is used for testing. This process is repeated for each subject and the averaged result across all the subjects is the final result (Biswas et al., 2014, Gupta and Dallas, 2014).

2.6.2 Performance criteria

Classification accuracy is the most commonly adopted performance criterion in HAR, meanwhile, there exist other measures providing different views to understand a

classification model especially for unbalanced data (Patil and Sherekar, 2013). And these criteria can be calculated from a confusion matrix. Confusion matrix, also known as an error matrix, is a specific matrix that allows visualization of the performance of a classification (James et al., 2013). Each row in a confusion matrix represents the instances in an actual class while each column of the matrix represents the instances in a predicted class. The element M_{ij} in a $M_{n \times n}$ matrix is the number of instances from class i that is recognized as class j actually. M_{ii} represents the number of instances from class i that is actually classified as class i . Therefore, some particular values or performance indexes can be calculated easily from the confusion matrix including TP (true positives), TN (true negatives), FP (false positives), FN (false negatives), accuracy, precision, F-score and so on (Nweke et al., 2018). Table 2.10 shows a basic two-class confusion matrix.

Table 2. 10 Confusion matrix

Actual class	Classified as	
	c1	c2
c1	TP	FN
c2	FP	TN

TP: true positives, the number of actually positive instances that are correctly classified as positive. TN: true negatives, the number of actual negative instances that are correctly classified as negative. FP: false positives, the number of actual negative instances that are incorrectly classified as positive FN: false negatives, the number of actually positive instances that are incorrectly classified as negative.

The accuracy is widely used as a statistical measure of how well a classification test correctly identifies a condition (Kwon et al., 2014). It is the proportion of true results (both true positives and true negatives) among the total number of cases examined, which is defined as:

$$Accuracy = \frac{TP + TN}{TP + TN + FP + FN}$$

The precision, on the other hand, is defined as the proportion of the true positives against all the positive results (both true positives and false positives), which is also used as the metrics in many applications (Murao and Terada, 2014).

$$Precision = \frac{TP}{TP + FP}$$

The recall, also called true positive rate, is the ratio of correctly classified positive instances to the total number of positive instances. In simple terms, high precision means that a classifier returns substantially more relevant results than irrelevant, while high recall means that a classifier returns most of the relevant results (Muraio and Terada, 2014).

$$Recall = \frac{TP}{TP + FN}$$

F-measure, also called F-score, is a more comprehensive measure (Gjoreski and Gams, 2011) compared to the aforementioned three ones, which combines the precision with the recall to compute the score and can be interpreted as a weighted average of the precision and recall, where an F score reaches its best value at 1 and worst score at 0.

$$F - measure = \frac{2 * Precision * Recall}{Precision + Recall}$$

Other performance indexes, including receiver Operating Characteristic Curve, i.e., ROC curve, and Area Under Curve, i.e., AUC, can also be seen in associated studies. A ROC represents a relation between Recall and false positive rate (specificity). AUC refers to the area under the ROC curve. Both ROC and AUC are insensitive to imbalanced classes. The studies use AUC and ROC for their performance assessment can refer to Chavarriaga et al., 2013b, Cheng et al., 2010, and Catal et al., 2015.

2.7 Applications of HAR in assisted living

The recognition of human activity is not always the final goal. It is usually adopted as a paramount step for a wide range of potential applications that can cover fitness systems, e-healthcare, interactive games, sports performance surveillance, social physical interaction, factory workers monitoring, etc. (Kon et al., 2017). The applications of HAR in assisted living mainly involve medical purposes and security concerns; the former focuses on monitoring patients with dementia, diabetes, obesity, arthritis or rehabilitation as an assistance diagnosis or treatment, and the latter highlights dealing with sports, entertainment, ADL, abnormal activities or safety. Figure 2.15 presents the most popular applications in healthcare, especially for WSHAR.

Certain typical WSHAR applications in Figure 2.15 are as follows: Rodriguez-Martin et al., 2013 utilize a waist-attached accelerometer to identify the posture and posture transitions on healthy and Parkinson's Disease (PD) volunteers. Hammerla et al., 2015

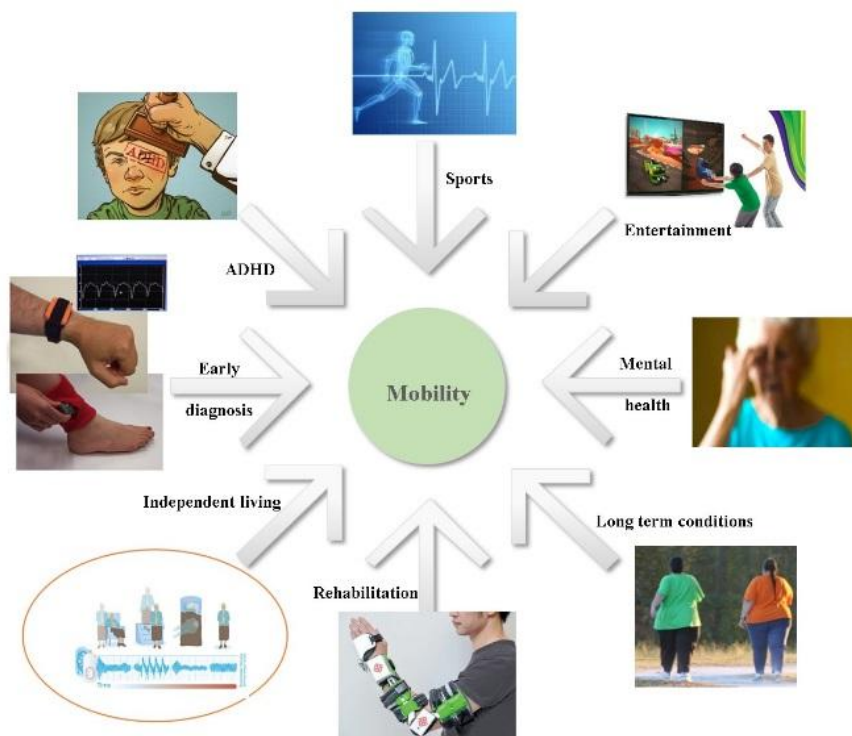


Figure 2. 15 Applications of HAR for daily life in healthcare
(ADHD: Attention deficit hyperactivity disorder)

propose an assessment system, which can predict the disease state in PD patients by deploying a tri-axial accelerometer on each wrist of the participants. Khan et al., 2017 use passive Wi-Fi sensing for respiration-related activity monitoring by detecting breath rate, with the potential application of stress levels and psychological states assessment. Pourbabaee et al., 2017 focus on monitoring the patients with paroxysmal atrial fibrillation based on ECG time-series data from patient screening. Sathyanarayana et al., 2016a and Sathyanarayana et al., 2016b investigate the prediction of sleep quality by using deep learning methods based on a wrist-worn actigraphy, with the aim of exploring and improving eHealth solutions.

We summarise other populous applications in ASHAR, WSHAR and HSHAR systems in Table 2.11 in terms of sensor modality, sensor type, sensor placement, features extracted, classification algorithms, performance, etc.

2.8 Research gaps

Research on HAR using different sensor modalities has made significant progress in continuous monitoring, performance improvement, computation cost reduction, practicability enhancement and so on (Chernbumroong et al., 2014, Jalal et al., 2017, Diethel et al., 2017). Due to the progress achieved in HAR-based assistive technologies, people's quality of life is enhanced, especially those who may be physically or cognitively challenged. Nevertheless, concerns about HAR systems, including accuracy, robustness, user compliance, cost, intrusiveness, privacy and so on, make HAR share many challenges. This research attempts to focus and address the following research gaps:

1) Determination of wearable sensor types, number, and placement

Taking WSHAR as an example, inertial sensors, physical sensors, and environmental sensors are explored in different applications. Different sensors deliver diverse information and act their roles with advantages and disadvantages, as shown in Table 2.1. In some cases, only one sensor is placed on one body part (Rodriguez-Martin et al., 2013), and other situations may deploy multiple sensors on multiple body parts (Chernbumroong et al., 2014). Each sensor placement case has its own strengths and weaknesses (see Table 2.3), which can cause different obtrusiveness levels, cost as well as performance. Consequently, how to determine the sensor types, sensor number and sensor placement for a specific task is needed to consider carefully.

2) Challenges of wrist-worn sensors

It is less feasible to wear sensors on multiple body parts for daily use outside of a laboratory setting. On the contrary, a wrist-worn watch-like device with embedded sensors is more convenient and less obtrusive for daily wearing, as shown in Table 2.2. Also, the wrist is a promising position to produce high accuracy as most activities are associated with wrist movements (Mannini et al., 2013, Chernbumroong et al., 2014, Biswas et al., 2015, Mortazavi et al., 2015). Whilst, one of the most significant challenges for wrist-worn sensors is the sensor signals (especially acceleration) suffer high within-class variance due to the similar attributes regarding wrist movements (Chernbumroong et al., 2013,

Table 2. 11 Review of existing works in HAR based on sensor modality

Sensor modality	Sensor placement	Sensor type	Sampling rate (Hz)	Window size	Feature	Activities (#)	# Subject (age)	Classifier	Performance	Target & Ref.	
ASHAR	Ceiling	PIR arrays	15	1s	Hand-crafted	Walking, lying, sitting, standing, transitional (5)	3 (23 to 37)	RF	Accuracy:92%	Location & ADL [1]	
	In-room	Camera	NA ^a	NA ^a	Hand-crafted	Faint, backward fall, chest pain, headache, etc. (6)	6	HMM	Accuracy:95.8%	Abnormal activities [2]	
WSHAR	One to One	Waist	Acc. ¹	40	3.2s	Hand-crafted	Walking, bending, lying, etc. (11)	31 healthy people, 8 patients	SVM-based	Sensitivity: 97% (healthy) Sensitivity: 98% (patients)	ADL & PD patients [3]
		Wrist	Acc.	50	1.28s	Automatically learned features	Lift cup to mouth, perform pouring, etc. (3)	4 (20 to 40)	CNN, K-means, LDA, SVM	Accuracy:99.8%(CNN)	Arm movements [4]
		Lower back	Acc.	20	6.4s /12.8 s	Hand-crafted	Walking, running, and cycling, etc. (20)	20(29 ±6)	DT	Accuracy:93%	Indoor & outdoor activities [5]
	Multi to One	Wrist	Acc., Gyro. ² , Tem. ³ , GPS, Humi. ⁴ , Pressure	100 (Acc., Gyro) 5(Pressure) 1(others)	2s	Hand-crafted	Indoor to outdoor, lying on the bed, Walking just, etc. (22)	2	DNN	Accuracy:90%	ADL [6]
		Wrist	Acc., Gyro.	50	2.56s	Deep & hand-crafted	Standing, sitting, laying down, walking, etc. (6)	30 (19 to 48)	CNN, NB, J48, SVM, ANN	Accuracy:95.75%	ADL [7]
	One to Multi	Lower limbs, ankle	EMG	1024	1.5s	Hand-crafted	Trip falls, stand-to-squat, stand-to-sit, walking, etc. (8)	3(24 to 26)	FDA ⁵ , FMMNN ⁶ , GK-FDA ⁷ , FCM ⁸ , GK-SVM ⁹	Accuracy:97.35% (GK-SVM8) Sensitivity:98.70% (GK-FDA)	ADL and falls [8]
		Wrist, thigh	Acc.	100	NA ^b	Deep & hand-crafted	Walking, jogging, sitting, etc. (6)	34 (18 to 54)	SVM, CNN, CNN-SVM, CNN-kNN	F1 score:0.85 (CNN-SVM, wrist) F1 score:0.967 (SVM, thigh)	ADL [9]
Multi to Multi	Chest, thigh, ankle	Acc., Gyro., Mag. ¹⁰	6	1s	Hand-crafted	Lying down, sitting, etc. (8)	11	RF, SVM, J48 ¹²	Accuracy:96.6%	ADL [10]	
	Wrists, chest	Acc., Gyro., Tem., light, Baro. ¹¹ , HR ¹³ , altimeter,	33 (Acc., Gyro) 1 (others)	3.88 s	Hand-crafted	Brushing teeth, feeding, wiping etc. (13)	12(73±4.41)	SVM, MLP, RBF	Accuracy:97%	ADL [11]	
HSHAR	Thigh, room	PIR, Acc., Gyro.	20	2s	Hand-crafted	Tracking human indoor location	6	K-NN, DT, boosting, particle filtering	Mean of distance Error:0.137 m	Indoor localization [12]	
	Room, pant pockets	PIR, Acc., Gyro.	80	5s	Hand-crafted	6: micro-activities 6: macro-activities	10	HMM	Accuracy: ~70 %	Smart environments [13]	

Ref: Reference ^aNA: Not Applicable ^bNA: Not available ¹Acc.: Accelerometer ²Gyro.: Gyroscope ³Tem.: Temperature ⁴Humi.: Humidity ⁵FDA: Fisher Linear Discriminant Analysis ⁶FMMNN: Fuzzy Min-Max Neural Network ⁷GK-FDA: Gaussian Kernel Fisher Linear Discriminant Analysis ⁸FCM: Fuzzy C-means algorithms ⁹GK-SVM: Gaussian Kernel Support Vector Machine ¹⁰Mag.: magnetometer ¹¹Baro.: Barometer ¹²J48: the implementation of decision tree algorithm in WEKA (a suite of machine learning software written at the University of Waikato) ¹³HR: Heart rate [1] Luo et al., 2017 [2] Khan and Sohn, 2011 [3] Rodriguez-Martin et al., 2013 [4] Panwar et al., 2017 [5] Bonomi et al., 2009 [6] Vepakomma et al., 2015 [7] Ronao and Cho, 2016 [8] Xi et al., 2017 [9] Sani et al., 2017 [10] Gjoreski and Gams, 2011 [11] Chernbumroong et al., 2014 [12] Pham et al., 2018 [13] Roy et al., 2016

Mortazavi et al., 2015), which will lower recognition accuracy caused by some easily misclassified activities, such as brushing teeth and eating (feeding), wiping and ironing (Chernbumroong et al., 2013). This imposes a challenge to activity monitoring using wrist-worn sensors. One way to overcome this challenge can be adding additional sensors to provide more sufficient information, the second can rely on feature learning from limited sensors, and another option can consider merging other sensor modality to relieve the requirements for wrist-worn sensors.

3) Less fully using sensors

It is common in WSHAR to use from one to seven and even more types of sensors for a specific task (See Table 2.11). Researchers prefer to acquire more diverse information through adding sensor types or sensor placing positions on body, thereby improving performance (Cleland et al., 2013, Sztylek et al., 2017). These sensors are less fully used in some cases. For instance, a large number of studies exploit inertial sensors, i.e. accelerometer, gyroscope and magnetometer, but most of them only extract features from an individual sensor or multiple channels of a sensor, e.g., the mean of the acceleration readings along the x -axis, or the correlation between the x -axis and y -axis of the acceleration readings (Chernbumroong et al., 2014, Mortazavi et al., 2014). The studies above all employ limited feature sets from the sensors they choose. Only a handful of studies try few roll, yaw or pitch-related features (Montalto et al., 2015, Gjoreski and Gams, 2011) derived from multiple inertial sensors as features for activity recognition, as shown in Table 2.5. This research explores the contribution of a new feature set to HAR, and the features are derived from limited wearable sensors and can help improve performance without additional sensors used.

4) Improving feature selection in HAR

Supervised feature selection methods, typically designed for classification or regression tasks, are commonly seen as a filter, wrapper, and embedded approaches (Li et al., 2017a). Filter methods filter out irrelevant features by evaluating the relevance of a feature to the class label using a specific selection criterion (Gheid and Challal, 2016, Dessì and Pes, 2015). Selection criteria play a critical role in filter-based FS methods. A variety of measures have been applied in filter methods, such as mutual information, correlation, Canonical Correlation Analysis (CCA) (Li et al., 2017a). MI-based feature selection methods are a big family in filter methods, including mRMR, JMI, CMIM, DISR (Brown et al., 2012). MI-based FS shares a common problem, i.e. it does not fully consider the complementarity within a feature set or between features and the label, since MI considers the correlation in pairs and then uses a simple

approximation strategy, such as the sum or the average, to approximate the relation between one feature (or the label) and a feature set. Different to MI, CCA measures the linear relationship between two multidimensional variables by maximizing the correlation coefficients between them. This is particularly useful to determine the relationship between the criterion and the set of their explanatory factors; it is easily employed as a feature selector. Inspired by the MI-based FS methods, this research proposes a feature selection method which uses the correlation derived from Kernel CCA as the selector to maximize the joint relevance between the feature candidate and the selected features with the label and minimize the redundancy between the selected features and the label.

5) Data fusion from multiple sensor modalities

Data fusion of information from multiple (usually two) sensor modalities can be done in three different ways: a) data -level, b) feature-level and c) decision-level, as discussed in Section 2.4.4. Raw data level fusion occurs at the raw data level where incoming raw data from different sensor modalities s are combined (Liu et al., 2014a). Feature-level fusion involves carrying out data fusion after features are extracted from individual sensor modalities (Pansiot et al., 2007). Decision-level fusion involves fusing the decisions made by individual classifiers from the corresponding sensor modalities (Liu et al., 2014b). Fusion of information from two sensor modalities still need to be investigated, and this thesis proposes an effective and practical fusion mechanism between ambient and wearable sensor modalities.

6) Hand-crafted features, automatically learned features, or both

Hand-crafted features have been successfully applying in HAR applications (Li et al., 2009, Wang et al., 2016a, Hassan et al., 2018). These years, deep learning approaches have been showing their superiority in automatically feature learning for HAR (Hammerla et al., 2015, Sani et al., 2017). The key advantages and disadvantages of hand-crafted features and automatically learned features are briefly summarized in Table 2.6. Studies by Panwar et al., 2017 and Sani et al., 2017 report automatically learned features which perform better than hand-crafted features in their tasks. Plötz et al., 2011 and Kashif et al., 2016 present that combining hand-crafted features to the automatically learned features from raw data can help improve the detection accuracy of deep networks. Meanwhile, Khan and Yong, 2016 and Song et al., 2016 indicate that the hand-crafted features outperform the automatically learned features in their studies. Therefore, how to effectively use features for a HAR task is still challenging. To the best of our knowledge, very few researchers have investigated the

performance of using automatically learned features and hand-crafted features together in HAR.

2.9 Summary

This chapter provides a state-of-art review of the sensor-based HAR systems, focusing on wearable sensor modality. The review has shown that sensor-based HAR systems have been achieving continuous progress in different applications for living assistance in terms of sensor modality combination, feature dimensionality reduction techniques, classification algorithms and so on. We identify certain research gaps in HAR, as shown in Table 2.12, and this thesis is focusing on the gaps 1-6, while the gap 7 is beyond the scope of this thesis and will be the future work. This research is interesting in combining wearable sensor modality and ambient sensor modality, with the aim of providing a more comprehensive and more accurate HAR system for older people to assist their daily life. Chapter 3 proceeds with our proposed hybrid-sensory HAR system with the associated approaches targeting the identified research gaps.

Table 2. 12 Identified research gaps in HAR by the review

1	Determination of wearable sensor types, number, and placement
2	Challenges of wrist-worn sensors
3	Less fully using sensors (feature extraction)
4	Improving feature selection in HAR
5	Data fusion from multiple sensor modalities
6	Hand-crafted features, automatically learned features, or both

Chapter 3

Methodology and system design

3.1 Introduction

Chapter 2 reviews the sensor-based human activity recognition systems and identifies certain research gaps, especially on the WSHAR (shown in Table 2.12). WSHAR has been receiving considerable attention in recent years due to its flexible applications in assisted living systems. However, the WSHAR has some intrinsic limitations that may enable less accurate recognition for certain activities and be unable to provide rich contextual information. Meanwhile, a HAR-based assisted living should also consider the practicability apart from the accuracy. This research aims to design and implement a more comprehensive hybrid-sensory HAR system for older people to assist them to live independently. The developed system combines the wearable sensors and the ambient sensors, with the aim of recognizing both a user's specific daily activities and the room-level daily routine. The system also increases the recognition accuracy by improving the feature extraction and utilizing the data fusion between multiple sensors. Chapter 3 presents the research methodology and the overview of the system design, sensor prototype development, sensor placement, research methods and the process to address the research problems.

3.2 Methodology

Research methodology discusses the advantages/disadvantages, feasibility, practicality, ethical issues, and parameters for the approaches to do the research; it investigates, compares, contrasts and explains the different ways that a research could be conducted (Hassani, 2017). Throughout the discussion, the methodology clarifies why a particular method is taken to address the research questions and how this method would be implemented. Different methods are normally included in these processes. The basic methodology can include descriptive/

analytical research, applied/fundamental research, theoretical/experimental research, quantitative /qualitative research, and so on (Nallaperumal, 2015). In computer science, there are two main research methods, i.e., theoretical and experimental research (Hassani, 2017). Theoretical methods are mainly based on mathematics and logic, and most research works in this field aim at forming a theorem or a formal model to lead to generalization of findings, or to improve the previous models and algorithms (Guha and Dukkupati, 2015). Experimental methods use empirical methods, such as best practices, procedures, and techniques to assist moving the computer science from its theoretical base towards an applied science (Easterbrook, 2007, Lockhart and Weiss, 2014). The process of experimental research can be divided into experimental/case study setting, data acquisition, and data analysis (Xu, 2017). Human activity recognition in machine learning has become mature as a field, and most WSHAR studies follow the procedure shown in Figure 2.2. This thesis has its specific research problems (presented in Section 2.8), the proposed hybrid system and the data fusion method formulate the corresponding research steps.

The methodology used in carrying out the research is shown in Figure 3.1, which includes three main blocks: data collection (wearable information and ambient information), data processing (feature extraction and selection) and data analysis (data fusion and classification). The wearable sensing in data collection involves a wrist-worn device with five initially selected sensors inside, delivering the user's motion-caused observations. Each ambient sensing set (with a PIR sensor inside) is mounted in one room, which provides the user's room-level location information. The system targets older people who live alone, which means, most of the time, only one ambient sensing set can capture "1" (presence) and others capture "0" (absence) at one specific moment. The recorded long-time "0" and "1" series can reveal the occupant's daily routine.

Meanwhile, most WSHAR studies using the hand-crafted features exploit the conventionally-used features (*CUFs*) (Sani et al., 2017, Wang et al., 2016a, Attal et al., 2015), i.e., the *CUFs* are extracted from an individual sensor or multiple channels of a sensor. E.g., the *maximum* of the acceleration readings along the y-axis, or the *correlation* between the x-axis and z-axis of the acceleration readings. While, the wearable sensor device used in this research can deliver not only the reading from each single sensor but the attitude values (*pitch*, *roll*, *yaw*) of the wearable device. The attitude-related features (*ARFs*), on the other hand, are derived from the multiple sensory channels or multiple sensors. The contribution of the attitude-related features (*ARFs*) has not been comprehensively explored in WSHAR, and the *ARFs* can be seen only in several related studies (Szytler et al., 2017, Kundu et al., 2017,

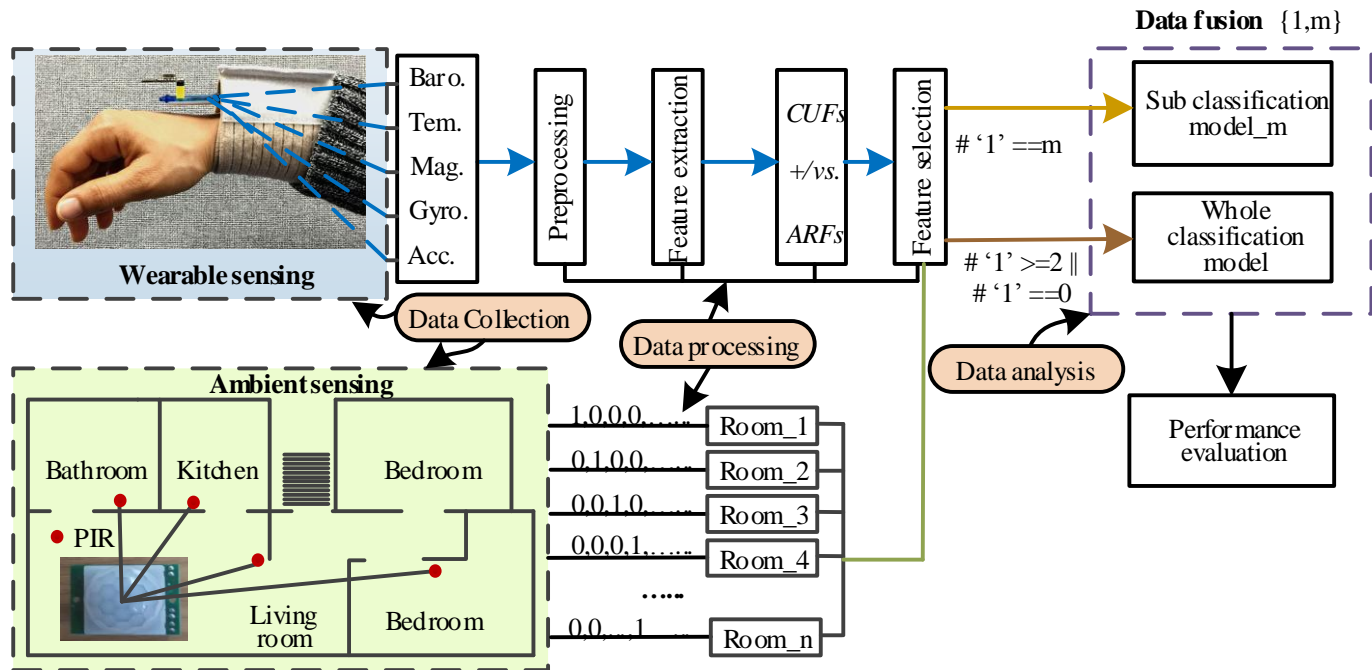


Figure 3. 1 The development steps of the research

(Acc.: accelerometer; Gyro.: gyroscope; Mag.: magnetometer; Baro.: barometer; Tem.: temperature)

Montalto et al., 2015). This thesis explores the functions of both the *CUFs* and *ARFs* on daily activity recognition in the data processing step. To select the optimal sub-feature set from the original feature set (*CUFs* and *ARFs*), this research also proposes an effective feature selection method, called mRMR-KCCA presented in Chapter 5. As presented in Figure 3.1, we first compare the individual performance of the attitude *ARFs*, and the *CUFs* extracted from the wearable data for all defined daily activities before applying data fusion; and the best-performed feature set is fed to later classification and data fusion. The following sub sections detail and discuss what materials and methods are used in Figure 3.1, and why they are adopted, including the system design, sensor prototype development, feature selection and classification algorithms, performance evaluation and so on.

3.2.1 System design

As presented in Section 2.8, the typical ASHAR systems are less obtrusive for HAR and can provide the contextual information of activities. A WSHAR system can be more flexible and function in a relatively large space for HAR. The WSHAR systems normally deploy multiple types of sensors on multiple body parts (head, wrists, waist, legs, feet, etc.) to improve the performance and robustness of WSHAR (Laudanski et al., 2015, Ian et al., 2013). However, WSHAR systems are either confronted with the problems of complex sensor deployment on body or the limited capacity of identifying certain elaborate motions. Hybrid sensory systems in HAR harness the strengths of each single sensor modalities, thereby benefiting improving accuracy or enhancing compliance (Atallah et al., 2007, Stikic et al., 2008, Roy et al., 2016, Pham et al., 2018). This thesis proposes a unique hybrid sensory system which combines the wrist-worn sensors and the ambient-mounted PIR sensors for older people's daily activity recognition. The system provides a more comprehensive monitoring by providing the recognition of not only room-level daily routine but also specific daily activities of the user.

In this research, we assume, for instance, that eating is less likely happening in a bathroom. Thus, if the ambient information can tell the classifier that the user is in the bathroom at a specific moment, it will be easier to differentiate brushing teeth from eating. Based on the assumptions, the proposed system skilfully splits the whole task of identifying all the defined activities into different room-level subtasks according to the generally occurring rooms of an activity. Meanwhile, an effective data fusion method is proposed to hybridize the ambient and wearable data.

Figure 3.2 illustrates the conceptual framework of the proposed monitoring system in this

thesis. The room-level location information of the user who lives alone in the home in Figure 3.2 can be captured by the room-mounted PIR sensors; at the same time, the observations from the wearable sensors on the wrist of the user can be logged at the same time. All the gathered data are wirelessly transmitted to the processing centre (e.g., a laptop) for further processing. The wearable data are used for recognition of specific daily activities. The location information captured by the room-mounted PIR sensors has two functions. Firstly, it is used for inference of a user's room-level daily routine. In data fusion, the location information is also used to trigger the sub models that are pre-trained by the corresponding wearable data. Since each sub-classification model for each subtask conducts recognition on a smaller number of activities, we can improve the efficiency and accuracy of the recognition compared with the scenario of recognizing all the defined activities using wearable data alone.

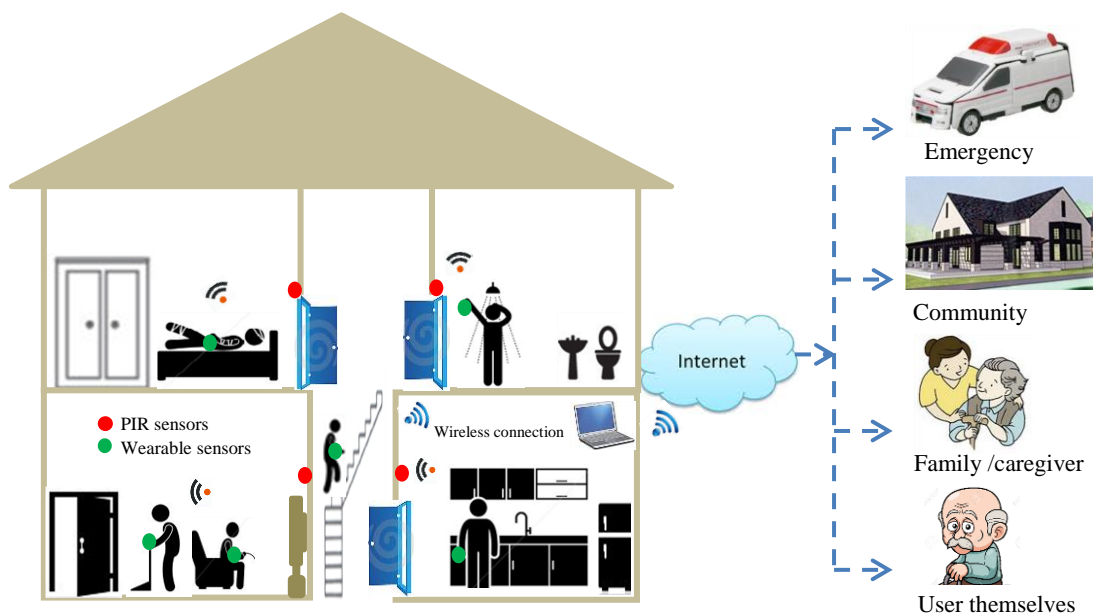


Figure 3. 2 Conceptual framework of the proposed system

Living in the proposed hybrid system, an older person can conduct the daily activities with minimal assistance from others, intervention from others, such as personal healthcare, would only be required if the system detects emergencies or anomalies in the user's behaviour. The final decisions derived from the system can be sent to the community centre, a caregiver or family members, users themselves, and even emergency centre ask for timely help, as shown in Figure 3.2. The community centre and the family members/caregiver can learn the daily activity routine and safety status of the user to see if the user is leading a healthy life; the user themselves also can enhance behaviours by adjusting their daily routine; the hospital can use the data processed from a long time or specific time to help diagnose; and the emergency

centre can provide timely assistance if the alarms are triggered by the decisions, such as falls or long-term sleep. The proposed system fusing the wearable and ambient sensors shown in Figure 3.1 and Figure 3.2 provides a more comprehensive and less obtrusive monitoring for older people's daily life.

3.2.2 Data fusion

Data fusion is the core of the hybrid sensory systems. Stikic et al., 2008 explore combining acceleration and infra-red data for human activity recognition. They calculate the number of the activations for each of the used ten infra-red sensors as features and feed them to the classifiers with the features extracted the wearable accelerometer. In our research, a PIR sensor installed in a specific room is used to detect the room-level location of the person under monitored, i.e., "1" represents the presence and "0" represents absence. The number of the activations of each PIR sensor in our research does not imply which can be connected to any specific daily activities, e.g., if the person enters the kitchen three times in a period, it is difficult to identify what the person is doing only by the times who activate the PIR sensor. Li et al., 2015b deploy a PIR sensor node and a wearable accelerometer to improve tracking accuracy and estimate the individual's state. They first use the PIR sensor network and furniture distribution to detect the individual's rough area and then use the acceleration sensor to determine whether the individual stands still or walks out. With their proposed data fusion method, the better tracking accuracy is achieved. Pham et al., 2018 also use PIR sensors and the wearable IMU for the indoor localization of a resident. The authors propose a particle filter-based sensor fusion algorithm that takes advantage of the correlation between human activity and the location in a mock indoor environment. The work in both Li et al., 2015b and Pham et al., 2018 deploy PIR sensors and wearable sensors, however, they use the sensors for indoor location tracking, and they also take advantage of the furniture distribution to improve the tracking performance. The data fusion algorithms they proposed are therefore less feasible for our system.

Considering our research aim and objectives, we propose and implement a different data fusion method, as shown in Figure 3.1, in which the "presence" information of "1" is used for triggering a sub-classification model that is trained by the wearable data from the activities limited in the corresponding room. For example, when room *n* is detected as occupied, only the sub model *n* is activated and works at this moment. Thus, each submodel is responsible for recognizing a smaller number of activities compared with the scenario of recognizing all the defined activities using wearable sensing alone (the whole model). By doing this, the overall

recognition accuracy can be improved without additional computation. The system switches to “the whole model” mode to deal with the situation when more than one occupant or no occupant is detected, i.e., two or more than two “1” or no “1” are captured at a specific time.

Collectively, the infrared sensors have a different role in our hybrid system. Instead of using it as the input of a classifier, we use the binary location information derived from infrared sensors to trigger sub classification models for data fusion. There are three function modes in our system: the whole classification model (the pure wearable sensing mode) identifying all the defined activities, the pure ambient sensing mode delivering the occupant’s room-level daily routine, and the room-based sub classification mode (data fusion applied) providing the spatio-temporal surveillance with the wearable sensors. The first mode can work alone when the ambient sensing fails, and the second mode can roughly identify the person’s daily routine without wearable sensing. The data fusion mode provides a more accurate and complementary HAR surveillance when both the wearable sensing and ambient sensing function properly. We evaluate the performance of the proposed system with the ground-truth data following the procedure in Figure 3.1.

3.2.3 Sensor prototype

We combine the ambient-mounted PIR sensors and the wrist-worn sensors, and these sensors have different functions in the proposed hybrid sensory system. The wearable data are used for recognition of specific daily activities. The location information captured by the PIR sensors has two functions. Firstly, it is used for the inference of a user’s daily routine. According to the normally occurring rooms of an activity, we skilfully divide the whole task of recognizing all the defined activities into several room-based subtasks. Since each sub-classification model for each subtask takes a smaller number of activities’ recognition, we can improve efficiency and accuracy. In data fusion, the location information is also used to trigger the submodels that are trained by the wearable data. This section presents the details of the sensor prototype developed in this research. The developed hybrid sensory prototype has the capacity of capturing the motion-caused wearable information and the room-based contextual information simultaneously.

Selected wearable sensors

Table 2.1 lists the popularly used wearable sensors in HAR. Considering the research aim and the target population and referring to related publications and some commercial wearable products, we select those sensors which are more objective and can capture the informative movement information caused by different activities. We try to avoid using the sensors which

are easy to be affected by the environmental or emotional factors. Firstly, a heart rate sensor and other related physical sensors which measure vital signals are eliminated since signals from these sensors are not only related to some activities but also are affected by emotional or physical factors. E.g., the findings from (Chernbumroong et al. 2014, Tapia et al. 2007, Fortino et al. 2015 and Chernbumroong et al. 2015a) indicate the contribution of a heart rate sensor to activity recognition, but it is very limited. People's heart rate or respiratory rate will speed when they are running or exercising compared with the situation when lying or sitting. It is well aware that the heart rate can also be faster when people are in excitement or anger. Meanwhile, the heart rate sensor and other physical sensors are needed to be fixed on some special body parts to properly function, such as head, chest, ear, and finger, which may cause obtrusiveness and discomfort for daily use. The optical sensing technology enables measuring heart rate on the wrist-placed sensor, whereas the reports suggest (Wang et al., 2017c, Wallen et al., 2016) that wrist-worn sensor may not provide satisfied accuracy due to the loose wearing, environmental variation, skin pigmentation and so on. Secondly, the light sensor and humidity sensor are also not selected. Although some studies (Chernbumroong et al. 2014) report light sensor can help recognize sleeping and stairs. Users may sleep with the sensor covered by some cover or not, in the daytime, night, dark or other complex environments. Therefore, the light sensor might not provide the key information as individuals can perform any activity under diverse contextual conditions regarding the weather or the illumination. More importantly, in our research, the sensors will be worn on the wrist, this means sometimes the sensor device may be covered by clothes sometimes not. Hence, the light intensity captured under an unknown wearing condition can be noisy and even the confused information for further learning.

We then select five wearable sensors from the list: a 3-axis accelerometer (MPU6050, range of $\pm 2g$), a 3-axis gyroscope (MPU6050, range of ± 1000 %s), a 3-axis magnetometer (HMC588, range of ± 4.07 Gauss), a barometer for height measurements (BMP180, with resolution of 0.5m for the height measuring) and a temperature sensor (BMP180, range of -10 - $60^{\circ}C$). The accelerometer measures linear motion. The gyroscope measures rotational motion. The magnetometer provides the direction of an ambient magnetic field. The three inertial sensors above enable the measurement of motion-caused variations and offer useful information for activity recognition (Gjoreski and Gams, 2011, Chernbumroong et al., 2013, Wu and Xue, 2008). Also, we derive the attitude-related features (*ARFs*) from the three inertial sensors in this work. The barometer and the temperature sensor are selected since the height variations are likely linked to certain activities, such as climbing stairs; and the temperature changes are

usually accompanied with some specific activities, such as cooking or eating. The five selected sensors are integrated into a specifically-customized module, as shown in Figure 3.3. The upper one in Figure 3.3 is the wearable device with five built-in sensors, and the lower one is the receiver. The wearable device has an on-board processing system that can deliver the device's attitude angles. Thus, the wearable module provides three attitude values (*yaw*, *pitch*, *roll*) of the wearable device and another 11 readings from the five individual sensors. All the readings are wirelessly recorded with a nearby laptop at the sampling rate of 20Hz. Eq. (3.1) presents data D_t series at time t from the wearable module.

$$D_t = \{Att_t, Acc_t, Gyro_t, Mag_t, Tem_t, Hei_t\}, t = 1, \dots, k \quad (3.1)$$

where k denotes the index of the data series regarding the sample rate; Tem_t and Hei_t are the temperature and the height measurements at time t , respectively, and



Figure 3. 3 Wearable sensors used in this research

(1) Wireless transceiver; (2) USB powered; (3) USB to PC

$$Att_t = \{Roll_t, Pitch_t, Yaw_t\};$$

$$Acc_t = \{Acc_x, Acc_y, Acc_z\};$$

$$Gyro_t = \{Gyro_x, Gyro_y, Gyro_z\};$$

$$Mag_t = \{Mag_x, Mag_y, Mag_z\}.$$

Exploited ambient sensors

The main function of the ambient sensors in this research is to detect the user's room-level location information. The PIR sensor is selected due to its utility, cost savings and energy savings in smart homes (Hajihashemi and Popescu 2013, Yun and Lee, 2014). PIR sensors,

as the name suggests, detect changes in infrared light, which is triggered by any hot moving body, such as human or any other warm-blooded animal movement. This means a PIR sensor does not actively radiate any energy for motion detection, thereby more energy efficient during real long-time operations, especially when there is less, or no movement detected. We can read the infrared variations to detect the human's activity, location or room-level daily routine from PIR sensors installed in rooms (Luo et al., 2017). The developed ambient sensor module consists of two parts (see Figure 3.4): the Receiving Terminal Unit (RTU) and the Centre Unit (CU). The components in the CU (lower part in Figure 3.4) involve a computer

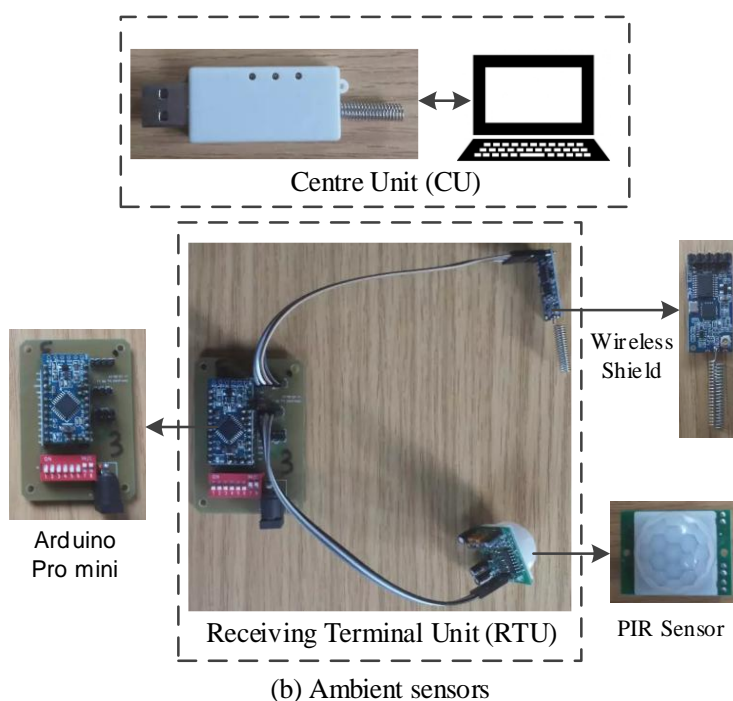


Figure 3. 4 Ambient sensors in this research

(not shown here), a USB-to-serial module and a wireless shield. The RTU comprises an Arduino® microprocessor, a PIR sensor, a wireless shield, and a DIP (Double In-line Package) switch. The DIP switch here is used to set and number the addresses of multiple PIR sensors; the Arduino processor detects the signal status and instructions from the wireless shields. An actual monitoring system can include a CU and a couple of RTU sets according to the home structures and specific tasks.

Figure 3.5 presents the flowchart of the software in the CU, the program running on the computer are responsible for data acquisition and Access® database development for data

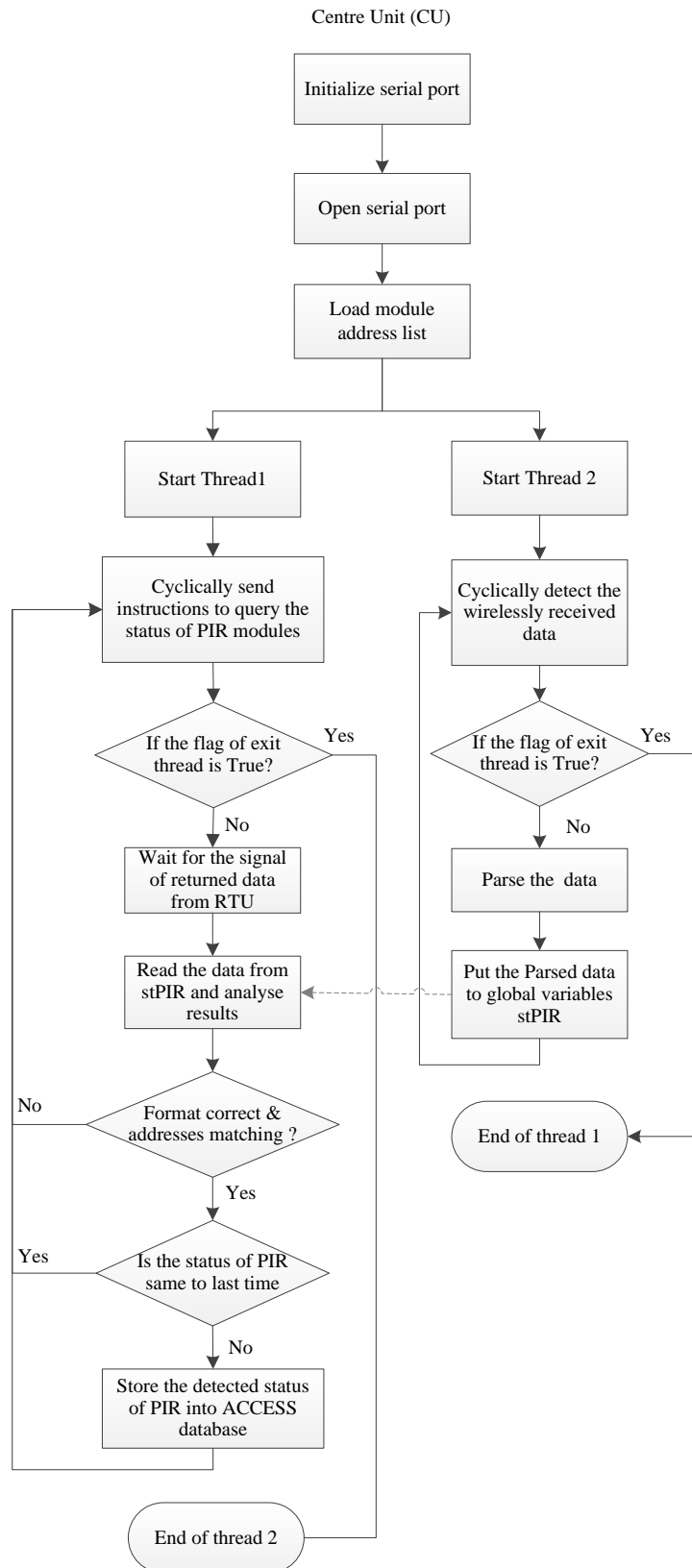


Figure 3. 5 Flowchart of the Centre Unit

storage. The CU continuously inquiries about the status of each PIR sensor and receives the data sent from the RTU whose address matches with the inquiry instruction. To reduce the burden of the processor and data storage, the status of a PIR sensor will be stored in the database only when changes comparing with its last instantaneous status are detected. In the ambient sensing network, all the wireless shields transmit and receive data on the same frequency band. Thus the polling mode is used in the CU to inquire about the status of each PIR sensor in an RTU. By doing this, the signal interference between different RTUs can be avoided. Any RTU responds to the CU only when it parses that the received address information sent from the CU matches its own address. The software flow chart of the RTU is shown in Figure 3.6.

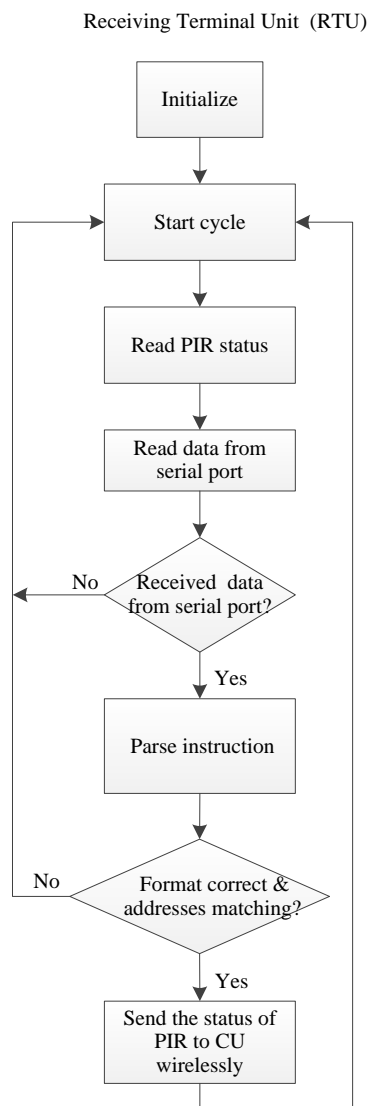


Figure 3. 6 Flowchart of the Receiving Terminal Unit

Sensor placement

Sensor placement is one of the important issues for WSHAR. Sensors placing on different body parts offer diverse information and lead to different recognition performances. It is less feasible to wear sensors on multiple body parts for daily use outside of a laboratory setting. On the contrary, a wrist-worn watch-like device with embedded sensors is more convenient and less obtrusive. Also, the wrist is a promising position to produce high accuracy as most activities are associated with wrist movements (Mannini et al., 2013, Chernbumroong et al., 2014, Biswas et al., 2015, Mortazavi et al., 2015). Additionally, according to the survey in Bergmann et al., 2012, 299 responders from four different countries give the answer that the wrist is the best-preferred placement when asked about where they would like to wear the sensors. We choose the dominant wrist as the on-body place for wearable sensors (Figure 3.7), taking both the recognition performance and the user acceptance into account.

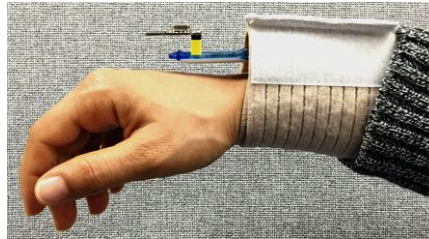


Figure 3. 7 Wearable sensor placement in this research

As mentioned above, PIR sensors are well used for occupancy detecting and motion tracking. Each PIR sensor has its sensing range and should be installed skilfully thereby meeting the requirements of a specific task. For example, a PIR sensor could be installed in the corner of a wall above the door in a room to detect whether a person enters or leave the room; also, a PIR sensor can be installed on the wall or the ceiling of a corridor to detect whether people pass by; and the ceiling-mounted PIR sensor array that is fixed within certain distance can be used to track people's movements. The optimal number of PIR sensors depends on specific tasks. Generally, one room or one area only needs one PIR sensor for the pure occupancy detection in HAR. While, more PIR sensors are needed for both the location and movement detection in HAR; and the sensor node design can refer to the related studies (Luo et al., 2017 and Kaye et al., 2012).

In our system, the ideal place for a PIR sensor in a room for occupancy detecting is suggested to be the corner of a wall above the door inside the room for achieving higher

accuracy, at the same time, the installation tilt angle can be adjusted to avoid the disturbances caused by pets. This research considers a room with one door only. We deploy a PIR sensor in each room and each sensor set is placed on the rear side behind the door on the floor in the room for simplicity and disturbances avoiding during data collection because 1) we may hammer nails into the wall to fix the sensors if attaching them on walls, which will damage the walls of the participants' homes; 2) putting them behind the door is a feasible way instead. The sensor deployment is shown in Figure 3.8, in which each PIR sensor set (i.e., RU) set on the rear side of the floor behind the door in the room for simplicity and disturbances avoiding. Considering the home structure where we collected data, we use four sets of RUs and a CU set in each home.

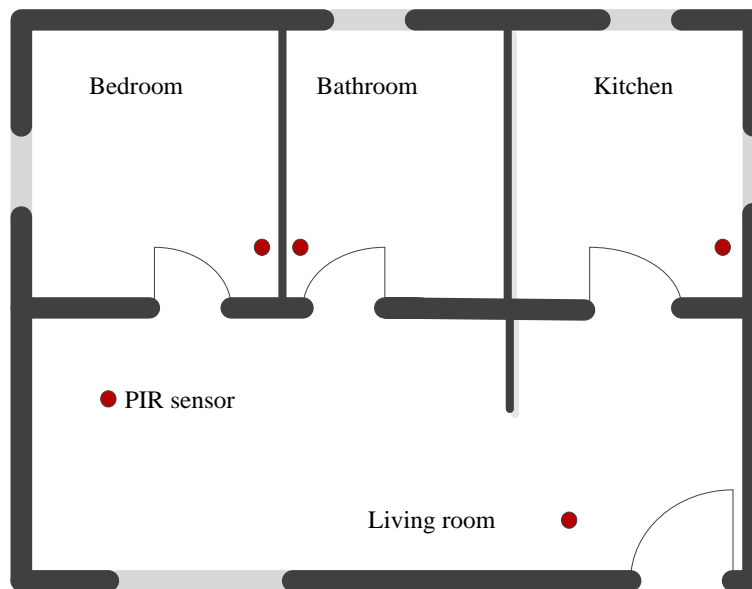


Figure 3. 8 Ambient sensor placement in this research

3.2.4 Data collection and feature extraction

Activity recognition research requires high quality and diverse activity data for specific application purposes. The data collection in this research involves the data collected from both the wearable sensors and the ambient sensors. We put the details of the data collection using the wearable sensors based on Figure 3.3 and the ambient sensors in Figure 3.4 as well as the feature extraction in Chapter 4, with the aim of clearly linking data collection with feature extraction.

3.2.5 Feature selection methods used in the system

Hand-crafted features, as the inputs for most machine learning methods, are the quantitative and informative variables generated from the original data. The created original features for this research are detailed in Chapter 4. The initial features are usually redundant or may be too large to be efficiently dealt with, resulting in several issues, like higher computation cost involved in learning, low learning efficiency, overfitting on unseen data, etc. (Chu et al., 2013, Gheid and Challal, 2016, Guyon and Elisseeff, 2003). Feature selection (FS) is one of the most commonly used dimensionality reduction strategies, which selects a smaller-size feature subset of the original feature set by removing the redundant and irrelevant features. The selected features are part of the original features without any feature transformation and maintain the physical meanings of the original features. In this way, FS helps users acquire a better understanding of their data by figuring out the most informative features, and hence to facilitate learning, enhance the generation performance and improve model interpretability (Tang et al., 2014).

Supervised FS methods, typically designed for classification or regression tasks, are commonly seen as the following types: filter (Gheid and Challal, 2016), wrapper (Bolón-Canedo et al., 2013), and embedded approaches (Li et al., 2017b). Filter methods filter out irrelevant features by evaluating the relevance of a feature to the class label using a specific selection criterion (Urbanowicz et al., 2017). A filter algorithm first ranks the original features based on the criterion, then selects the features with higher rankings. This process is independent of any classifier, computationally efficient and usually obtains a trade-off between performance and efficiency. As the largest family in filter-based FS methods, an MI-based FS algorithm measures the importance of a feature by its selection criterion with the class label, it assumes that the feature with a stronger correlation with the label will benefit improving classification performance. The popular algorithms in this family are like minimum Relevance Maximum Relevance (mRMR) (Peng et al., 2005), Joint Mutual Information (JMI) (Bennasar et al., 2015), Conditional Mutual Information Maximum (CMIM) (Gao et al., 2016), etc.

MI-based feature selection methods (Brown et al., 2012) are used in Chapter 5 and Chapter 6 for selecting optimal sub feature sets from different feature sets to 1) identify the contributions of the selected wearable sensors and the augmented features and 2) evaluate the data fusion. The MI is one of the most effective criteria to measure the correlation between variables. Supposing that x and y are two discrete random variables, the MI between x and y

is defined as

$$I(x; y) = H(x) - H(x | y) \quad (3.2)$$

where $H(x)$ represents the entropy of x which quantifies the degree of uncertainty in a discrete or discretized random variable X and $H(x | y)$ represents the conditional entropy of x given y . The MI signifies how much information x and y share, which is nonnegative and equals zero if x and y are independent. The minimum Redundancy Maximum Relevance (mRMR) algorithm, which directly uses MI to value the redundancy and relevance of involved variables, is one of the most popular FS methods. The ranking criterion of the mRMR is

$$J_{mRMR}(f_k) = \max_{f_l \in S, f_k \in F-S} [I(f_k; C) - \frac{1}{|S|} \sum I(f_k; f_l)] \quad (3.3)$$

where $I(\cdot)$ is given in Eq. (3.2), f_k is a feature candidate; F is the whole feature set; S is the already selected feature set; f_l can be any feature in S ; and C is the class labels. The second term in Eq. (3.3) considers the redundancy between the feature candidate and any already selected features concerning paired variables, which does not consider the joint relevance and the conditional redundancy given the third or more variables. The improved mutual information measures can deal with the MI between three variables, one of which is Conditional Mutual Information Maximization (CMIM). The corresponding criterion of the CMIM is

$$J_{cmim}(f_k) = I(f_k; C) - \max[I(f_k; f_l) - I(f_k; f_l | C)] \quad (3.4)$$

where the additional term $I(f_k; f_l | C)$ includes the redundancy given the class labels C compared with the mRMR criterion. The other two typical MI-based methods are Joint Mutual Information (JMI) that includes the complementary information that is shared between the feature candidate and the already selected features given the class labels. The criterion of JMI is given in Eq. (3.5) below. Double Input Symmetrical Relevance (DISR) is the modification of JMI by estimating the normalization $H(f_k, f_l; C)$.

$$J_{JMI}(f_k) = \max_{f_l \in S} \sum I(f_k, f_l; C) \quad (3.5)$$

Here, $H(f_k, f_l; C)$ is the joint entropy of variables f_k, f_l and C .

In Chapter 5, we propose a feature selection method, named mRMJR-KCCA, which combines the measurement of kernel canonical correlation analysis (KCCA) with the mutual information (MI) -based feature selection method. mRMJR-KCCA maximizes the relevance

between the feature candidate and the target class labels, and simultaneously minimize the joint redundancy between the feature candidate and the already selected features in the view of kernel canonical correlation analysis (KCCA). The mRMJR-KCCA omits the sum approximation \sum in mRMR and measure the nonlinear correlation between two multidimensional datasets. The feature selection method experimentally performs better compared with the mutual information-based, Autoencoder, Sparse filtering feature selection methods over the ground truth data and other 10 UCI classification-related benchmark datasets.

3.2.6 Classification algorithms and performance assessment

The classification is the key stage in Figure 3.1 after obtaining the optimal feature set, which identifies which of a set of categories a new observation belongs to, by a training set of data containing observations whose category membership is known (Alpaydin, 2014). As discussed in Section 2.3.7, there are many classification models applied in different applications for HAR. This research adopts SVM and RF as the classification algorithms for system evaluation due to both their excellent performance in HAR and very few parameters needed to be tuned in practice. Fernández-Delgado et al., 2014 present an exhaustive evaluation of 179 classifiers arising from 17 families, including random forest, support vector machines, Bayesian, boosting, principal component regression, neural networks, bagging, and other methods. They use 121 UCI machine learning classification data sets to evaluate the classifiers and achieve significant conclusions. Their experimental results indicate that the best family of classifiers is a random forest regarding the maximum accuracy and the rankings, followed by SVM. These years, deep learning has had many successes at different benchmarks and various commensal applications (LeCun et al., 2015, Nweke et al., 2018), for example, convolutional neural networks (CNN) on visual and image processing (Silver et al., 2016), Recurrent neural networks (RNNs) on speech and natural language processing (Cireşan and Meier, 2015). Nevertheless, looking at Kaggle machine learning competitions, the classifiers that perform best vary from case to case. In those questions that are not related to vision or sequential tasks, random forests, gradient boosting, or SVMs do better even when compared to deep learning methods. Rodriguez-Martin et al., 2013 present a novel postural detection algorithm based on SVM methods to detect Walking, Sit to Stand, Bending up/down, and other transitions with a sensitivity of 97% and specificity of 84% on the ground truth data. Chernbumroong et al., 2014 apply SVM, MLP and RBF network on their proposed multi-sensor activity recognition system and SVM performs best achieving 97% accuracy. Sani et al., 2017 explore the deep learning and hand-crafted features for HAR. CNN performs better on the wrist-worn data while SVM performs best on the thigh-attached data.

Support Vector Machines

SVM is one of the most robust and accurate methods among all well-known classification algorithms (Janidarmian et al., 2017, Mehrang et al., 2017). The goal of SVM modelling is to find the optimal hyperplane that separates clusters of a vector in such a way that cases with one category of the target variable are on one side of the plane and cases with the other category are on the other size of the plane. The vectors near the hyperplane are the support vectors. SVM intends to determine the minimizing training set error by maximizing the boundary among separating hyper-plane and the data. Figure 3.9 indicates a basic overview of the SVM solution. SVM inherently solves two-class problems. We use the libSVM package

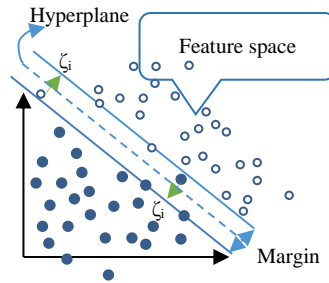


Figure 3. 9 Classification boundaries of SVM solution

in MATLAB (Chang and Lin, 2011). libSVM runs a ‘one versus one’ approach for multi-class classification. For k classes, $k*(k-1)/2$ classifiers are constructed and each one is trained with the data from two classes. Then each SVM votes for one class. The data point is assigned to the class with the highest number of votes after all classes. For a binary classification problem, given a training set $U = \{(x, y_i), i = 1, \dots, l\}$, where $x_i \in R^n$ and $y_i \in \{1, -1\}^l$, SVM is formulated as solving an optimization problem:

$$\min_{w, \omega_0, \zeta_i} \frac{1}{2} \|w\|^2 + C \sum \zeta_i \quad (3.6)$$

$$s. t. y_i(w^T \phi(x_i) + b) \geq 1 - \zeta_i$$

$$\zeta_i \geq 0$$

where ζ_i are slack variables, which are introduced to address the noise problems by allowing some points violate the margin constraints; C is the penalty factor of classifying a point into a class j while its true class is i , which is a tradeoff parameter for the points violation; It should be noted that the larger the C , the more the error is penalized. Thus, C should be chosen with care to avoid overfitting. The function $\phi(x_i)$ is used to map the samples x_i into a higher

dimensional space when data is not linearly separable in the original feature space. For calculation simplicity a kernel function $K(x_i, x_j) = \phi(x_i)^T \phi(x_j)$ is needed instead of exact $\phi(x_i)$ itself.

There are different kernel functions applied in SVM for calculation simplicity in a higher dimensional space, such as linear, polynomial, sigmoid, radial basis function (RBF), etc. As the most popular choice of kernel types used in SVM by far, the RBF is chosen as the kernel function when applying the SVM algorithm for classification modelling due to the following reasons. First, according to the SVM guide, the RBF kernel is a reasonable first choice. The RBF kernel nonlinearly maps samples into a higher dimensional space so it, unlike the linear kernel, can handle the case when the relation between class labels and attributes is nonlinear. Furthermore, the linear kernel is a special case of RBF (Hsu et al., 2003). Only when the number of features is much larger than the number of instances or both numbers of instances and features are large, the linear kernel is suggested. For our data, the number of instances is much greater than the number of features. Second, the sigmoid kernel behaves like RBF for certain parameters (Hsu et al., 2003). Third, the polynomial kernel has more hyperparameters than the RBF kernel, which is difficult to optimize in real use. Finally, we also refer to certain related papers (Fatima et al., 2013, Chernbumroong et al., 2013, Yekkehkhany et al., 2014) in which the RBF kernel shows more steady or higher performance compared with other kernels.

The RBF kernel is given:

$$K(x_i, x_j) = \exp\left(-\frac{\|x_i - x_j\|^2}{2\sigma^2}\right) \quad (3.7)$$

where $\|x_i - x_j\|^2$ may be recognized as the squared Euclidean distance between the two feature vectors x_i and x_j , for simplicity, $\gamma = \frac{1}{2\sigma^2}$ is sometimes involved in the definition. The 10-fold cross-validation is widely used to evaluate the result of classification and to avoid overfitting. In this research, the best combination of parameters C and γ is selected with grid-search method during 10-fold the cross-validation process (Hsu et al., 2003, Khan et al., 2013). We set the appropriate search values in the region of the grid for the upper and lower bounds as $C(2^{-12}, 2^{-11}, \dots, 2^0, 2^1, \dots, 2^{12})$, $\gamma(2^{-2}, 2^{-1}, \dots, 2^0, 2^1, \dots, 2^{10})$. We use a multiple-stage grid search during real searching; we first use a larger step set to search the relatively best parameters and followed by smaller steps within a narrower searching area based on the last stage. All results reported in this research are the average of the 10 test measures for each dataset. The 10-fold data split is shown in Figure 3.10. The available dataset from all subjects are split into 10 roughly equal-sized folds, and each fold has the roughly same number of

patterns from each activity of each subject. 8 folds are used as training data, one fold serves for validation, and one fold is for testing the model. Each of the 10 folds is used exactly once as test data and the test data is unseen for the classifier. The 10-fold cross-validation procedure is briefly shown in Table 3.1, which is conducted on each dataset in this thesis.

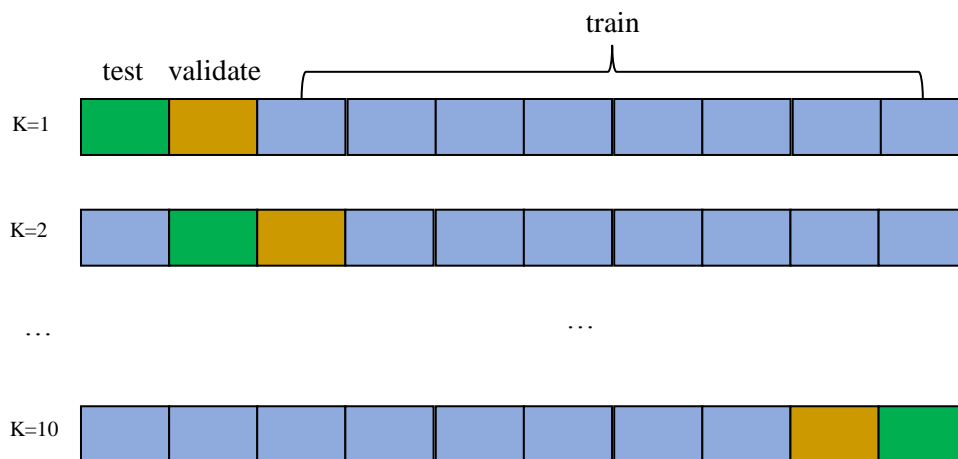


Figure 3. 10 10-fold data split

Table 3. 1 10-fold cross-validation procedure

Input: a feature set $F = \{f_1, f_2, \dots, f_N, C\}$ Hassan et al., 2018, C represents the class labels, f_1, f_2, \dots, f_N are the original features

Output: a measure of classification quality

$K=10$;

Split F into K folds, $K=10$

For fold=1: K

Put aside this fold for test

For fold=1: $K-1$

Put aside this fold from the $K-1$ folds for validation

Train the model on the other $K-2$ folds with parameters searching

Validate the model on validation fold

Save the model with the maximum accuracy

End

Test the model with the maximum validation result

Save the test result

End

Average the accuracy by K

Random Forest

As the name suggests, Random Forest creates the forest with a number of Decision trees. A simplified Random Forest is presented in Figure 3.11. To classify a new task from an input vector, the vector is put into each of the trees in the forest. Each tree gives a classification and “vote” for the class. The forest chooses the classification having the most votes over all the trees in the forest (Breiman, 2001). RF combines "bagging" idea and a random selection of features to construct a collection of decision trees with controlled variance (Ho, 1995, Amit and Geman, 1997). RF overcomes the decision tree’s overfitting to its training set and is a highly accurate, fast and noise resistant classification method (Friedman et al., 2001).

Gjoreski and Gams, 2011 apply SVM, J48, and RF on their activity/posture recognition, and RF achieves the best results. The authors decide to use RF also because RF is designed to operate quickly over large datasets. Mehrang et al., 2017 use RF and SVM on the heart rate and acceleration data for a variety of home-specific activities recognition. The two algorithms obtain 89.2% and 85.6% average accuracies, respectively. Alickovic et al., 2018 use RF and SVM since two classifiers result in high performance. The authors employ a Discrete wavelet transform (DWT), Empirical mode decomposition (EMD) and Wavelet packet decomposition

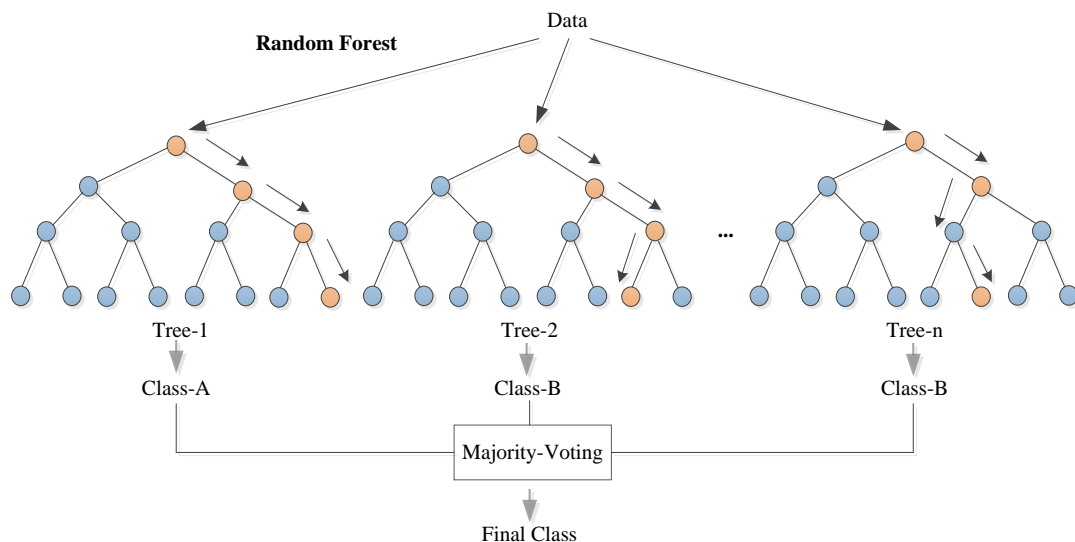


Figure 3. 11 The simplified Random Forest

(WPD) feature extraction based on two EEG datasets for seizure prediction. The experimental results suggest that the overall accuracy for WPD + RF on the adult's data and WPD + SVM on the children data is 99.5% and 99.7%, respectively. This research uses TreeBagger (MATLAB, 2015) to create an ensemble of bagged decision trees, and the determination of parameters in SVM and the number of trees in TreeBagger is conducted during the 10-fold cross-validation process.

Summarizing Section 3.2.1 to Section 3.2.6, Table 3.2 lists the materials using for HAR in the system.

3.3 Summary

This chapter presents the methodology adopted in the research, including the system design, the sensor prototype development, and the methods adopted to conduct the research, such as the feature selection methods and classification algorithms, etc. Specifically, the principles of choosing wearable sensors and ambient sensors for the system are discussed. The sensor network building and the respective functions of the wearable module and the ambient module are detailed. This chapter also discusses the placement of the wearable sensors on body and the ambient sensors in rooms. The feature selection is critical to obtain the relevant features from the original feature pool for further classification. Our research uses the MI-based methods and our proposed feature selection method (i.e., mRMJR-KCCA) described in Chapter 5 for feature selection. As two of the most robust and must-be classification algorithms, SVM and RF are chosen as the classifiers for this research. The next chapter details the data collection and the data pre-processing.

Table 3. 2 Materials and methods used in the research

	Type	Sensor placement	Output	
Sensors	3-axis accelerometer	Wrist	Accx, Accy, Accz	
	3-axis gyroscope		Gyrox, Gyroy, Gyroz	
	3-axis magnetometer		Magx, Magy, Magz	
	Barometer		Height	
	Temperature		Temperature	
			<i>Yaw, Pitch, Roll</i>	
	Ambient sensors	PIR sensors	Room	{0,1} absence/presence information
Feature selection (FS)	MI-based FS Proposed mRMJR-KCCA			
Classification	SVM and RF			

Chapter 4

Data collection and data preprocessing

The commonly defined daily activities for safety surveillance and health monitoring in HAR are shown in Table 2.4. These activities can reveal people's daily context and safety conditions. The recognition of daily activity is helpful to understand, maintain and assist the daily life of the observed. Activity recognition research usually requires high quality and diverse activity data. As discussed in Section 2.3.3, the data sets in most research studies have some limitations, such as few subjects, few activities, collected under laboratory settings, etc.(Bhattacharya and Lane, 2016, Laudanski et al., 2015). For this research and the corresponding experiment purposes, we collect the data using the developed wearable and ambient sensors in real home settings from the recruited participants. This chapter first details the daily activity definition and data collection. The data pre-processing on the wearable data and ambient data are then described, including window segmentation and feature extraction from wearable data, etc.

4.1 Data acquisition for the research

4.1.1 Activity definition and wearable data collection

This research focuses on indoor daily activity recognition for older people to observe their daily activities and daily routine. Based on the activities listed in Table 2.4 and considering the research aim of the thesis as well as the willing of the participants, we predefine 17 activities in Table 4.1 which could basically reveal independent life skills (Eldercare at Home, 2013), including basic survival tasks (walking, eating, cooking, dishes washing, stairs using, teeth brushing, etc.), the activities for maintaining an independent life at home (using phones,

mopping, washing, ironing, exercising, reading, etc.) and abnormal activities (Falls, long-term lying). Some activities, such as toilet use, dressing/undressing, and bathing, are not included due to the privacy concerns or the unavailability of data because of the limitation of the sensor modules. We do not directly monitor the toilet using or bathing, nevertheless, we can capture how often and how long the occupant uses the bathroom from the ambient sensors. It is worth noting that 17 is not a necessary number for activity types. We do not intend to define all the daily activities; however, we need a large dataset for our experimental purpose.

The data collection associated procedures are approved by Bournemouth University Research Ethics Committee. The data collection is carried using our developed hybrid sensory home environments in China. The activities except Falls are collected from 21 participants (aged from 60 to 74, 11 females and 10 males, all right-handed). ‘Fall detection’ is one of the important tasks in HAR Kau and Chen, 2015. Considering older participants’ safety, we

Table 4. 1 Daily activity defined in this research

Name	Description	Collected in
Brush	Brushing teeth on their own natural way	Bathroom
Clean	Cleaning the windows or cupboard doors with a cloth	Bathroom, K*
Cook	Making a meal on a fire	Kitchen
Eat	Having a meal using a spoon, a fork or a pair of chopsticks	Living room
Exercise	Waving or stretching arms in a wide range	Living room
Falls	Performing a natural fall from different directions onto a mattress on the floor	All rooms
Iron	Ironing a shirt, trousers, T-shirt, etc. on a table surface or flat board	Kitchen, L*
Lie	Lying down on a bed or sofa without frequent turns	Bedroom
Mop	Cleaning the floor with a mop	Bathroom, K*
Phone	Answering a call using a telephone or mobile phone when sitting or standing	Bedroom, L*
Read	Reading a book or newspaper when sitting	Living room
Stairs use	Walking down or up on the stairs	Living room
Stand	Still standing without continuous additional actions	All rooms
Walk	Walking around at home at a normal pace and turns are allowed	Bedroom, L*
Wash dishes	Cleaning bowls, plates, glasses, etc. in a sink	Kitchen
Watch	Sitting on a sofa with a remote in one hand for channels changing use when watching TV	Living room
Wipe	Clean a table or other flat surface with a cloth	Kitchen

L*: Living room, K*: Kitchen

recruit 21 young participants (aged from 25 to 35, 11 females, and 10 males) who take the older subjects' places and perform natural falls in different ways (forward, backward, left-side and right-side) onto a mattress. Table 4.2 shows the older and young participants' demographic information.

Table 4. 2 Participants' demographic information

	Gender	Age (year)			Height (cm)		Weight (kg)		BMI (kg/m ²)	
		Mean	Std.	Range	Mean	Std.	Mean	Std.	Mean	Std.
Older	Female	66.4	3.1	7	160.2	4.3	61.6	4.7	19.2	1.1
	Male	67.3	3.9	9	166.5	5	64.8	6.5	19.4	1.5
	All	66.8	3.5	13	163.2	5.6	63.1	5.7	19.3	1.3
	Gender	Age (year)			Height (cm)		Weight (kg)		BMI (kg/m ²)	
		Mean	Std.	Range	Mean	Std.	Mean	Std.	Mean	Std.
Young	Female	29.2	3.7	7	166.6	5.3	62.8	7.9	18.8	1.9
	Male	30.7	2.9	9	170.8	4.1	69.8	3.8	20.4	0.8
	All	29.9	3.3	10	162.8	2.9	56.5	4.5	17.3	1.3

Before data collection, we explain the research purpose and data collection procedure to each participant. The participants are encouraged to perform each activity in their own way independently. They can have any breaks during data collection. The valid data from the same activity are added up if the data collection is interrupted. We label the data manually and mark the start and end time for each activity. During data collection, the wearable device (in Figure 3.3) is tightly bound at the participant's dominant wrist for acquiring the movement-caused signals from the sensors inside.

Meanwhile, we deploy a PIR sensor set (the RTU in Figure 3.4) in each room (Figure 3.8) to capture the user's presence and absence information. Considering the layout of the homes we used for data collection, we assign our predefined activities to four groups (the last column in Table 4.1) according to the occurring places, i.e., five activities in the bathroom, eight in the kitchen, ten in the living room and five in the bedroom. It is worth noting that the activities assignment in Table 4.1 is not fixed, which is a case study for our proposed system. We prepare the activity list for each room for each participant. The raw data example collected from the five wearable sensors by one participant (Participant 1) is presented in Table 4.3. The raw data

Yaw	Pitch	Roll	hei[m]	tem[C]	Accx	Accy	Accz	Gyrox	Gyroy	Gyroz	Magx	Magy	Magz	Class label	Participant
206.5	36.9	21.2	0.8	37.3	0.371948	0.665649	0.590027	-5.34058	-25.0244	31.67725	-0.39547	-0.11328	-0.2504	0	1
206.5	36.9	22.6	0.8	37.3	0.403809	0.554443	0.715271	-0.36621	-18.8599	12.78687	-0.35175	-0.07154	-0.27027	0	1
211.1	20.9	34.9	0.4	35.8	0.563904	0.590576	0.709961	26.88599	12.8479	7.659912	-0.02583	-0.18879	-0.27027	1	1
209.9	21.4	35.1	0.4	35.8	0.641968	0.455994	0.669495	1.831055	13.5498	28.44238	-0.02186	-0.19277	-0.27027	1	1
185.9	9.8	-1.9	4.2	36	-0.35089	-0.00214	1.449463	103.5156	22.36938	-22.0642	0.043721	-0.01987	-0.23848	2	1
187	14.9	-1.8	4.2	36	-0.44653	0.652771	1.211792	86.9751	-30.5176	-5.79834	0.039746	-0.05167	-0.24643	2	1
235.1	53	19.5	4.4	37.7	0.335571	0.776123	0.564148	8.453369	6.774902	-2.89917	-0.10334	-0.2504	-0.28021	3	1
234.8	53.1	19.2	4.4	37.7	0.34082	0.745239	0.553589	0.12207	6.92749	-2.99072	-0.10334	-0.25239	-0.27822	3	1
249.7	34.7	-56.1	0.7	33.8	-1.0531	0.157104	0.241821	27.22168	-74.6155	27.46582	0.164946	-0.23053	-0.1411	4	1
253.7	35.3	-50.5	0.7	33.8	-1.24042	0.281067	0.317322	10.65063	-89.1418	37.56714	0.143086	-0.24245	-0.157	4	1
228.3	48.8	21.4	10.5	32.6	0.356201	0.607056	0.700562	-3.20435	-3.50952	6.256104	-0.30207	-0.15104	-0.21065	5	1
227.3	49.3	21.5	10.5	32.6	0.385986	0.638977	0.555054	9.521484	-0.39673	2.990723	-0.30207	-0.15302	-0.20867	5	1
271.1	30.7	-33.1	-0.1	35.2	-0.37781	0.489868	0.749939	-4.82178	18.67676	-23.6816	-0.0477	-0.3915	-0.11129	6	1
271.1	31.5	-33.6	-0.1	35.2	-0.35028	0.524597	0.711182	12.72583	24.9939	-23.5291	-0.03776	-0.3915	-0.11129	6	1
247.5	29.1	-4	6.3	36.4	-0.07983	0.503052	0.856934	-0.12207	0.427246	0.549316	0.07353	-0.19674	-0.20867	7	1
247.6	29.1	-4	6.3	36.4	-0.08118	0.503723	0.855713	-1.0376	0.427246	0.549316	0.075518	-0.19873	-0.20867	7	1
201.1	141.2	-45.3	0.7	36	-0.85962	0.533508	-0.36951	8.666992	10.31494	30.36499	0.071543	-0.40938	0.071543	8	1
202.7	140.6	-45.8	0.8	36	-0.80609	0.428955	-0.31372	16.54053	-3.66211	25.14648	0.063594	-0.41336	0.075518	8	1
165.4	-12.3	57	-0.6	35.6	0.870483	-0.11609	0.526306	-3.11279	-0.27466	2.716064	-0.36566	0.037759	-0.28021	9	1
165	-12.7	57.1	-0.6	35.6	0.865234	-0.13672	0.514709	-3.41797	0.244141	2.075195	-0.36169	0.037759	-0.28021	9	1
188.8	-8	-0.2	0	38.4	-0.01196	-0.14911	0.9823	4.089355	1.068115	-1.28174	-0.30803	-0.23251	-0.20271	10	1
188.7	-7.7	-0.3	0	38.4	-0.00702	-0.05798	0.97876	-0.15259	2.410889	0.488281	-0.30803	-0.2345	-0.20469	10	1
50	-57.5	-81.9	6.4	35.1	-0.88684	-0.18292	0.044983	39.52026	-18.9209	2.563477	0.07353	-0.25239	-0.16296	11	1
44.8	-50.6	-81.2	6.4	35.1	-0.89532	-0.11194	0.062195	45.71533	-18.7378	1.647949	0.067568	-0.25835	-0.157	11	1
344	12.7	-79	-0.3	37.5	-0.93176	0.03418	0.155151	0.396729	0.88501	0.671387	0.107314	-0.08347	-0.22258	12	1
344	12.6	-79	-0.3	37.5	-0.93396	0.040283	0.163208	0.183105	0.915527	0.457764	0.109302	-0.08347	-0.22258	12	1
47.8	-21.8	-76.3	-0.6	36.2	-0.89539	0.033691	0.273926	62.71362	-29.48	23.16284	0.133149	-0.1411	-0.20072	13	1
40.9	-15.2	-74.7	-0.6	36.2	-0.83057	0.02594	0.229858	50.44556	-27.4353	22.97974	0.123213	-0.15898	-0.20867	13	1
256.8	46.1	-30.7	1.7	38.3	-0.61011	0.688599	0.296509	274.2004	-17.3645	100.4639	-0.15501	-0.31598	-0.14309	14	1
258.3	40.8	-35	1.7	38.3	-0.875	-0.24182	0.491211	-66.1926	10.5896	-21.1182	-0.17687	-0.33585	-0.12321	14	1
238.1	2	-17.9	-0.3	38.4	-0.35327	0.070557	0.883911	0.518799	0.762939	-0.54932	-0.06558	-0.36368	-0.20668	15	1
238.3	2.1	-17.9	-0.3	38.4	-0.35382	0.07782	0.883484	0.549316	0.671387	-0.30518	-0.06558	-0.36368	-0.20271	15	1
307	9	-47.3	-0.5	37	-0.51575	-0.17505	1.060791	76.01929	-22.5525	-5.0354	-0.1093	-0.27425	-0.24841	16	1
314.5	9.5	-42.1	-0.5	37	-0.40936	-0.16083	1.068909	142.9138	-79.2847	-65.6128	-0.1093	-0.30207	-0.22854	16	1

Table 4. 3 Raw data examples collected from wearable sensors from the first participant

for each participant includes 14 readings, e.g., the attitude angles (yaw, pitch, roll), height (height [m]), acceleration along three axes (Accx, Accy, Accz), angular velocity along three axes (Gyrox, Gyroy, Gyroz), magnetic fields along three axes (Magx, Magy, Magz). The class labels in Table 4.3 are nominated as 0, 1...16 to denote the 17 defined activities. No personal information about the participant can be identified from the raw data in Table 4.3. The useful features will be extracted from the raw data to recognize the specific activities in Section 4.2.

The whole data collection lasts over twenty days. Each older participant completes 16 activities, and each young participant only performs Falls with wearable sensors on body. We use 17 activities after merging Falls to the 16 activities for each participant out of 21. The valid data from each activity is five minutes with the sampling rate of 20Hz. The total sample size for wearable data is therefore 2,142,000 from 17 activities and 21 participants. The data for each activity does not contain overlap and disturbances between activities. Figure 4.1 shows some data collection cases with the corresponding raw data, in which the y-axis shows the readings from different sensors and the x-axis represents the number of data points. The raw data over different activities present diverse values and variations. Using the attitude angles as an example, we can see from Figure 4.1 that the *yaw* angle fluctuates between 100 degrees and 150 degrees for Cook, waves between slightly under 250 degrees and over 300 for Mop, while keeps relatively steady just over 200 degrees then drops dramatically until a fall occurs for Falls. Mining useful information from the raw data can facilitate the later learning in HAR.

4.1.2 Ambient data

The status of a PIR sensor in this research is logged as “0” and “1”, “1” represents the user occupies the room where the PIR sensor is mounted at a specific moment, and vice versa. To reduce the burden of data storage, the status of a PIR sensor is stored when variations are detected compared with its last instantaneous status. Here we only store the status of “1” for each PIR sensor, an data example of the collected raw data is presented in Table 4.4. From Table 4.4, we can see that only the presence status is recorded on the sheet, this means the other times unrecorded imply absence of “0”. For example, room four was only occupied at the times of around 08:45 am and 08:59 am on the day.

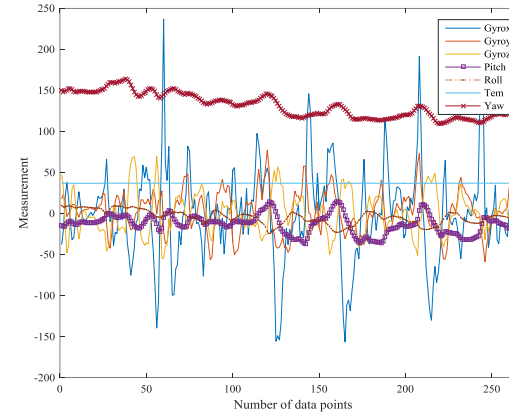
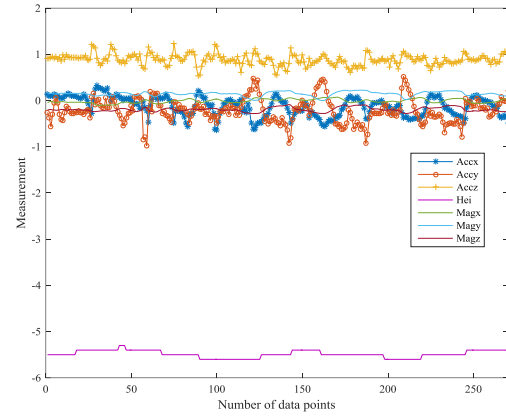
4.2 Feature pool generation for the system

Feature extraction plays a pivotal role in HAR, which typically transforms the original data

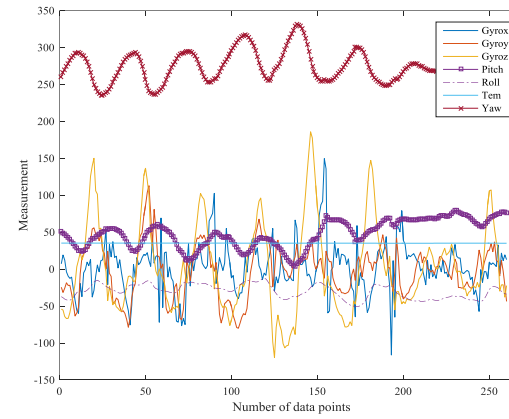
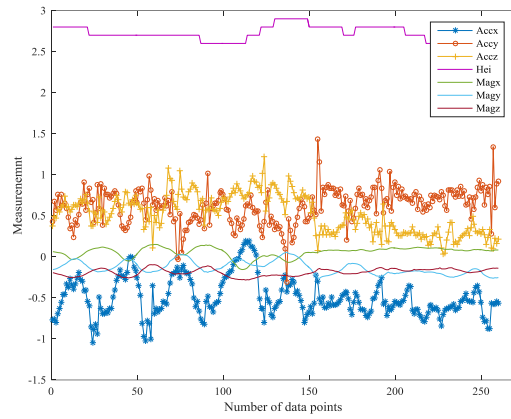
Chapter 4 Data collection and data preprocessing



Cook



Mop





Falls

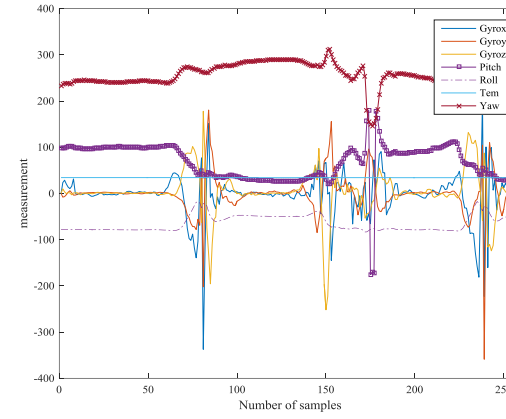
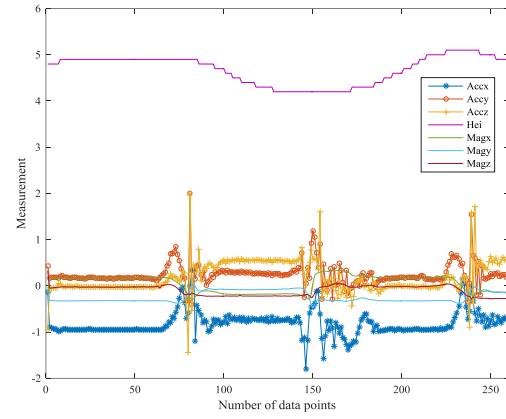


Figure 4. 1 Data collection examples and the recorded wearable raw data

R e c T i m e	2	2	2	2	2	2	2	2	2	2	2	2	2	2	2	2	2	2	2	2	2	2	2	2	2	2	2	2	2	2	2	2	2	2	2		
	0	0	0	0	0	0	0	0	0	0	0	0	0	0	0	0	0	0	0	0	0	0	0	0	0	0	0	0	0	0	0	0	0	0	0		
	1	1	1	1	1	1	1	1	1	1	1	1	1	1	1	1	1	1	1	1	1	1	1	1	1	1	1	1	1	1	1	1	1	1	1		
	5	5	5	5	5	5	5	5	5	5	5	5	5	5	5	5	5	5	5	5	5	5	5	5	5	5	5	5	5	5	5	5	5	5	5		
	-	-	-	-	-	-	-	-	-	-	-	-	-	-	-	-	-	-	-	-	-	-	-	-	-	-	-	-	-	-	-	-	-	-	-	-	
	0	0	0	0	0	0	0	0	0	0	0	0	0	0	0	0	0	0	0	0	0	0	0	0	0	0	0	0	0	0	0	0	0	0	0	0	
	8	8	8	8	8	8	8	8	8	8	8	8	8	8	8	8	8	8	8	8	8	8	8	8	8	8	8	8	8	8	8	8	8	8	8	8	
	-	-	-	-	-	-	-	-	-	-	-	-	-	-	-	-	-	-	-	-	-	-	-	-	-	-	-	-	-	-	-	-	-	-	-	-	-
	1	1	1	1	1	1	1	1	1	1	1	1	1	1	1	1	1	1	1	1	1	1	1	1	1	1	1	1	1	1	1	1	1	1	1	1	
	6	6	6	6	6	6	6	6	6	6	6	6	6	6	6	6	6	6	6	6	6	6	6	6	6	6	6	6	6	6	6	6	6	6	6	6	
	0	0	0	0	0	0	0	0	0	0	0	0	0	0	0	0	0	0	0	0	0	0	0	0	0	0	0	0	0	0	0	0	0	0	0	0	
	8	8	8	8	8	8	8	8	8	8	8	8	8	8	8	8	8	8	8	8	8	8	8	8	8	8	8	8	8	8	8	8	8	8	8	8	9
	:	:	:	:	:	:	:	:	:	:	:	:	:	:	:	:	:	:	:	:	:	:	:	:	:	:	:	:	:	:	:	:	:	:	:	:	:
	4	4	4	4	4	4	4	4	4	4	4	4	4	4	5	5	5	5	5	5	5	5	5	5	5	5	5	5	5	5	5	5	5	5	5	0	
	4	4	4	5	5	5	6	7	7	8	9	0	1	1	1	1	2	3	3	4	5	6	7	7	7	8	8	9	9	9	9	9	9	9	9	0	
	:	:	:	:	:	:	:	:	:	:	:	:	:	:	:	:	:	:	:	:	:	:	:	:	:	:	:	:	:	:	:	:	:	:	:	:	:
	1	1	5	1	1	4	1	0	5	2	0	3	1	4	4	3	4	5	2	5	2	1	4	5	1	5	1	2	1								
	2	4	1	6	9	3	9	0	9	1	5	1	3	1	3	9	8	9	7	3	2	9	8	1	5	8	7	1	0								
	Bedroom	1	1	1	1	1	1	1	1	1	1	1																									
	Bathroom					1							1	1	1	1	1	1	1	1	1	1	1	1	1	1	1	1	1	1							
Living room																																				1	
Kitchen																																			1		

Table 4. 4 Raw data captured by the PIR sensors

into the informative features for classification. As mentioned in Section 2.3.5, there are two ways to extract formative features from raw sensor data, i.e., hand-crafted features generated manually in each sliding window based on domain knowledge and automatically learned features with deep networks without any domain knowledge (automatically learned features). Research using hand-crafted features has been greatly successful (Lee and Cho, 2014, Wang et al., 2016a, Sani et al., 2017). One of the key advantages of using the hand-crafted features is that they are computationally lightweight to calculate, which enable them to be calculated on ubiquitous devices (Kwapisz et al., 2011, Kwapisz et al., 2011, Khan et al., 2013). This research focuses on the hand-crafted features on human activity recognition with the research objectives presented in Section 1.2.

Typical hand-crafted features for HAR include heuristic features (Machado et al., 2015), time-domain features (Mortazavi et al., 2014), frequency-domain features (Chernbumroong et al., 2013) as well as other hybrid features (Kundu et al., 2017). This thesis implements the hand-crafted features based on both *CUFs* and *ARFs* (refer to Section 3.1). As presented in Figure 4.2, the *roll* here is the sides of the device moving up/down; the *pitch* is the head of the device moving up and down, and the *yaw* is the head moving right and left. The attitude angles of the device on body vary when the wearer performs different activities. The attitude variations over different movements (see Figure 4.1) show the potential of the *ARFs* for activity recognition. Other systems only explored a handful of *ARFs* (Kundu et al., 2017,

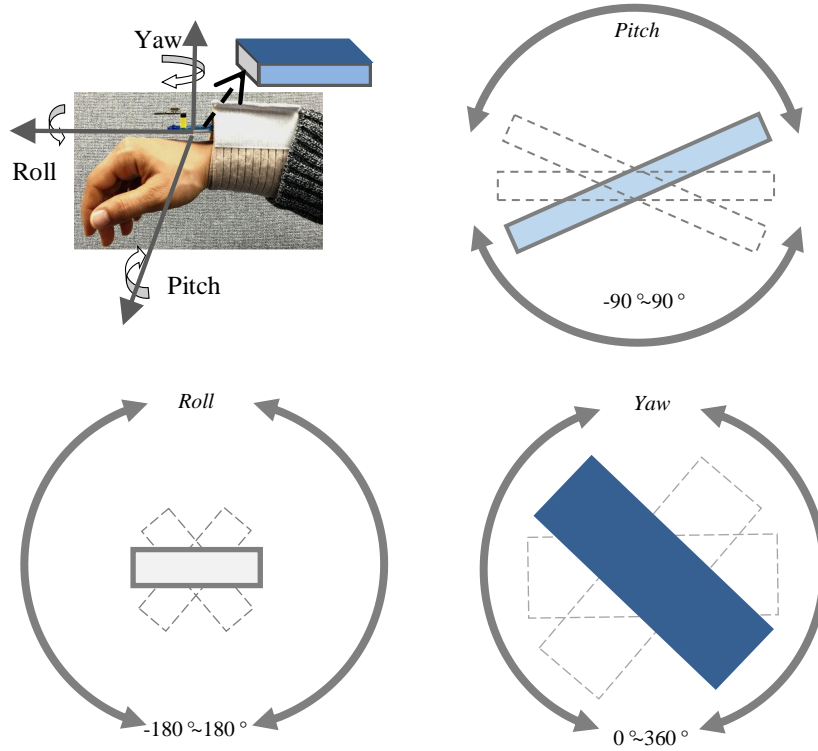


Figure 4. 2 The wearable device on the wrist and the corresponding attitude

Montalto et al., 2015). We apply the typical time-domain and frequency-domain features in the observations to produce *CUFs* and *ARFs* for later learning. The obtained feature space is presented as

$$v = \mathcal{F}\{D_t, w_i\} = \{ARFs, CUFs\} \quad (4.1)$$

where \mathcal{F} is the feature extraction function set, implementing the calculation of all the features used in the study; D_t in Eq. (4.1) is the data series obtained from the wearable device. We denote all the extracted features as *All* (*ARFs* + *CUFs*), the features related to the wearable device's attitude as *ARFs*, the remaining features (excluding *ARFs*) as *CUFs*. The feature extraction is conducted in each segmentation window w_N . The details of the specific features used in this work are given below.

List of features used in this research

1. Mean: The average value of the signal over the window
2. Root Mean Square (Rms): The quadratic mean value of the signal over the window
3. Peak-to-peak amplitude (Ptp): The difference between the maximum and the minimum value over a window

4. Mean crossing rate (Cmr): Rates of time signal crossing the mean value, normalized by the window length
5. Zero crossing rate (Czr): Rates of time signal crossing the zero value, normalized by the window length
6. Signal magnitude area (SMA): The acceleration magnitude summed over three axes within each window normalized by the window length
7. Average of Peak Frequency (Apf): The average number of signal peak appearances in each window
8. Movement Intensity (MI): Mean of the total acceleration vector over the window
9. Averaged derivatives (Ader): The mean value of the first order derivatives of the signal over the window
10. Crest factor (Cftor): The ratio of peak values to the effective value over the window
11. Autocorrelation (Autoc): The correlation between the values of the process at different times
12. Percentiles: 10th,25th,50th,75th,90th
13. Interquartile range (Interq): Difference between the 75th and 25th percentile
14. Pairwise correlation (Corrcoef): The ratio of the covariance and the product of the standard deviations between each pair of axes
15. Standard deviation (Std): Measure of the spreadness of the signal over the window
16. Standard deviation to the mean (Stdm): The ratio of the standard deviation to the mean
17. Kurtosis: The degree of peakedness of the signal probability distribution
18. Skewness: The degree of asymmetry of the sensor signal probability distribution
19. Max: The largest value in a set of data
20. Min: The smallest value in a set of data
21. Median: The middle number in a group of ordering numbers
22. Mode: The number that appears the most often within a set of numbers
23. Variance: The average of the squared differences from the Mean
24. Median Absolute Deviation (MAD): The median of the absolute deviations from the data's median
25. Dominant frequency (Domifq): The frequency corresponding to the maximum of the squared discrete FFT component magnitude of the signal from each sensor axis
26. Spectral energy (SpecEgy): The sum of the squared discrete FFT component magnitude of the signal from each sensor axis, normalized by the window length

27. Spectral entropy (SpecEnt): Measure of the distribution of frequency components, normalized by the window size
28. First five components (MFC): Magnitude of first five components of FFT analysis
29. Median Frequency (Medifq): The frequency corresponding to the median of the squared discrete FFT component magnitude of the signal from each sensor axis

Here, we give certain typical feature calculation examples from the feature extraction function set \mathcal{F} in Eq. (4.1). In the feature extraction definitions below, T is the length of the window segmentation, s, s_i or s_j is the readings in Eq. (3.1).

- a). Median Absolute Deviation (MAD): The median of the absolute deviations from the data's median.

$$MAD = Median_i(|s_i - median_j(s_j)|) \quad (4.2)$$

- b). Crest factor (Cftor): The ratio of peak values to the effective value over the window

$$Cftor = \frac{0.5(s_{max} - s_{min})}{Root\ Mean\ Square(RMS)} \quad (4.3)$$

- c). Spectral energy (SpecEgy): The sum of the squared discrete FFT component magnitude of the signal from each sensor axis, normalized by the window length

$$SpecEgy = \frac{\sum_{i=1}^T |s_i|^2}{T} \quad (4.4)$$

- d). Pairwise correlation (Corrcoef): The ratio of the covariance and the product of the standard deviations between each pair of axes (x, y)

$$Coorcoef = \frac{\sum_{i=1}^T (x_i - \bar{x})(y_i - \bar{y})}{\sqrt{\sum_{i=1}^T (x_i - \bar{x})} \sqrt{\sum_{i=1}^T (y_i - \bar{y})}} \quad (4.5)$$

To the *CUFs*, we do not apply all types of features on each of all five sensors evenly. This is because people live in varied floors, different weather conditions and changing room environments, which means some features (like the max, the mean of the height or the temperature) are less useful to distinguish activities. Only the features that can represent the variations of the observations instead of the absolute or specific values are applied to the measurements of the height and the temperature. Features with multiple null values or with similar or equal values for different activities are removed manually. Finally, the feature pool is constructed in Table 4.5 with the feature abbreviations. Table 4.5 includes the potential features for activity recognition and often contains many redundant and irrelevant features.

Applying the feature selection can select the optimal sub-feature set and reduce the dimensionality of the feature space.

Table 4. 5 The original feature pool created in this research

Sensor	Feature title	Feature count
<i>CUFs</i>	Accelerometer	296
	Gyroscope	
	Magnetometer	
	Barometer	
	Temperature	
<i>ARFs</i>	Attitude (Roll, Pitch, Yaw)	75
<i>All</i>	<i>CUFs+ARFs</i>	371

4.3 Data segmentation of wearable data

The data obtained from PIR sensors are processed as the format of $\{0,1\}$ digital series. The data pre-processing here refers to the wearable sensory data. For facilitating the later learning, time data series D in Eq. (3.1) are needed to segment into certain fixed sub windows. It is generally acknowledged that a window length of several seconds can sufficiently capture circles of activities (Deng et al., 2014, Hu et al., 2014), such as walking, running, using stairs, etc. Here, we follow the principles concluded in Hu et al., 2014 to set our segmentation length

initially as 12.8s (256 samples in each window) according to the circles variations of our collected activities, i.e., 0.5s (Wash), 6s (Eat), 13s (Falls), etc. Meanwhile, 50% overlap between consecutive windows is adopted to reduce possible information loss at the edges of a pair of adjacent sub windows. The total number of window segmentations N for a data series is then obtained in Eq. (4.6)

$$N = \frac{DL - OV}{SL - OV} \quad (4.6)$$

where DL is the data length, OV is the overlap size and, SL is the segmentation length. Eq. (3.2) rounds a number to the next lower integer. After segmentation, D is split into N sub windows $D = \{w_1, w_2, \dots, w_N\}$. For example, the data size of one activity from one subject is 6000 (5min); if we use the segmentation length (SL) of 256 (12.8s); the overlap size is 128 (6.4s); the data are consequently segmented into 46 sub windows according to Eq. (4.6). The feature extraction will be then applied in each sub window. No smoothing filtering or medium filtering is applied to the raw data before feature extraction in this research.

Following the principles concluded in Hu et al., 2014, we set our segmentation length initially as 12.8s. To further identify the best window segmentation, we compare five different segmentation lengths (3.2s, 6.4s, 12.8s, 25.6s, 51.2s) using half of the original dataset by applying SVM classification and mRMR feature selection. We first identify the optimal segmentation length for the *CUFs*. The results in Figure 4.3 illustrate that different window lengths have obvious impacts on the recognition performance of *CUFs*, and 12.8s presents the higher and more stable results. The size of 12.8s (256 samples in each window considering the sampling rate of 20Hz) is to be the appropriate window segmentation length for *CUFs*.

Similarly, the results in Figure 4.4 show that the best segmentation size for *ARFs* should better be set as 12.8s as well. Taking the process efficiency into account, 25.6s and 51.2s will result in longer delays for future online recognition, although they perform better on *ARFs*. Meanwhile, we can see from Figure 4.3 and Figure 4.4, the classification results only increase limitedly when the number of selected features is greater than 30, and fewer features are helpful to develop simpler, faster-response and more generalized models with lower computation cost and improved performance. Consequently, at most the top 30 features within each dataset are selected for classification afterward in this research.

The features examples extracted based on the window size of 12.8s are shown in Table 4.6, and the features listed in Table 4.6 are only a few examples out of 371 features shown in Table

4.5.

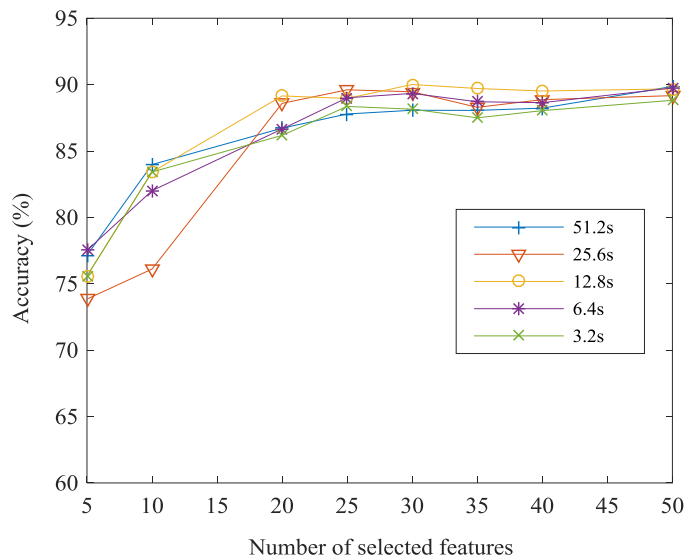


Figure 4. 3 Performance of different window lengths based on *CUFs* with SVM

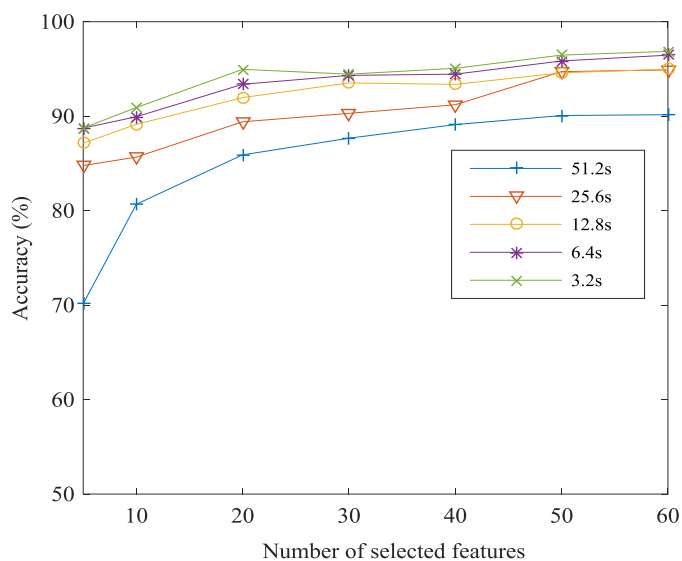


Figure 4. 4 Performance of different window lengths based on *ARFs* with SVM

mean_yaw	mean_pitch	rms_accz	rms_gyrox	cmr_hei	cmr_tem	entropy_magy	entropy_magz	class_label	participant
0.55388083	0.5828508	6.17E-05	0.00652201	0.007813	0	0.753147653	0.802755445	0	1
0.55155491	0.57931675	6.28E-05	0.00749014	0.015625	0	0.954568379	0.854058572	0	1
0.5559007	0.58391176	6.19E-05	0.00826812	0.015625	0.007813	0.935757022	0.785639364	0	1
0.56043449	0.58936848	6.07E-05	0.01078219	0.015625	0.007813	0.918842806	0.815379856	0	1
0.56344682	0.58696513	6.32E-05	0.0126775	0.015625	0	0.955297714	0.846067379	0	1
0.56075802	0.5794612	6.62E-05	0.00995305	0.007813	0	0.85741914	0.812288643	0	1
0.55916879	0.58139135	6.53E-05	0.00880801	0.015625	0	0.729894115	0.743029063	0	1
0.55114831	0.57388244	6.64E-05	0.01344432	0.015625	0.007813	0.859646603	0.615525365	0	1
0.54333113	0.56631376	6.78E-05	0.01423046	0.015625	0.007813	0.873635609	0.479079704	0	1
0.54577072	0.56905333	6.71E-05	0.01241759	0.007813	0.007813	0.795129466	0.534706058	0	1
0.54326992	0.56647813	6.7E-05	0.01451587	0.007813	0.023438	0.967664301	0.786930685	0	1
0.54071229	0.56563634	6.65E-05	0.0135592	0.007813	0.015625	0.94349171	0.749743084	0	1
0.54637625	0.57225364	6.45E-05	0.00805368	0.007813	0	0.950581654	0.66496635	0	1
0.54432577	0.56520797	6.58E-05	0.01431729	0.023438	0	0.668805062	0.811188741	0	1
0.51615244	0.53439031	7.08E-05	0.01969861	0.015625	0	0.757443471	0.801602375	0	1
0.49597555	0.51698159	7.36E-05	0.02127242	0.023438	0	0.909531533	0.869268105	0	1
0.50045906	0.52176837	7.35E-05	0.02398222	0.007813	0	0.913325522	0.807355291	0	1
0.49848072	0.51767894	7.42E-05	0.0273498	0.007813	0.007813	0.960445736	0.953372898	0	1
0.49196859	0.5127776	7.51E-05	0.02532242	0.007813	0.007813	0.906759796	0.927835509	0	1
0.49409558	0.51652085	7.48E-05	0.02032564	0.023438	0	0.944051723	0.842923822	0	1
0.5007651	0.52129517	7.41E-05	0.01832344	0.007813	0.007813	0.807944553	0.659530737	0	1

Table 4. 6 Feature examples from the raw data of the first participant

4.4 Summary

Data are the first material for activity recognition after determining sensor types and sensor deployment. Data acquisition can be tedious and cumbersome work. This chapter then describes the activity definition, the data collection process, the data segmentation and the feature preparing for later experiments. We define 17 daily activities, which is large enough for our experiments purpose, and assign the activities in different rooms targeting the research aim. The window segmentation size of 12.8s is further determined after experimentally compared to other window sizes. The followed section details the original feature pool created in this research, including the *CUFs*, *ARFs* and *All (CUFs + ARFs)*. The feature selection is critical to obtain the relevant features from the original feature pool for later classification. Chapter 5 proceeds with the identification of the contributions of the selected wearable sensors and the augmented features using the collected data and extracted features in Chapter 4.

Chapter 5

Identification of the contributions of the selected wearable sensors and the augmented features

We have initially selected five wearable sensors for the proposed system, i.e., the accelerometer for linear motion measurement, the gyroscope for rotational motion measurement, the magnetometer an ambient magnetic field measurement, the barometer for height measurement and the temperature sensor for ambient temperature measurement. All the five selected sensors have shown their contributions in related applications (Hassan et al., 2018, Chernbumroong et al., 2013, Wu and Xue, 2008). In this chapter, we identify the contribution of the selected wearable sensors to our system by comparing their performances on the defined daily activities. Additionally, features can not only be extracted from a single axis of a single or multiple axis from a single sensor, which can also be derived from multiple sensors. Extracting augmented features from multiple sensors can be a way to fully use the limited sensors. This research implements an augmented feature set presented in Chapter 4, called the attitude-related features (*ARFs*). *ARFs* are extracted from the accelerometer, the gyroscope, and the magnetometer. This chapter also explores the contribution of *ARFs* to HAR in our system, by comparing them with the conventionally-used features (*CUFs*).

This chapter first presents the proposed kernel canonical correlation analysis (KCCA)-based feature selection method (i.e., mRMJR-KCCA) and experimentally evaluates its performance on 10 UCI² benchmark datasets and our ground-truth datasets. The contribution identifications of the sensors and the augmented features are then conducted with the MI-based feature selection methods described in Chapter 3 and our proposed mRMJR-KCCA method respectively.

² <http://archive.ics.uci.edu/ml/>

5.1 Mutual information inspired feature selection using kernel canonical correlation analysis

Filter-based feature selection methods can usually obtain a trade-off between the performance and the efficiency since they are independent of any classifier during feature selection (Urbanowicz et al., 2017). A filter algorithm first ranks the original features based on the criterion, then selects the features with higher rankings. This process is independent of any classifier, computationally efficient and usually obtains a trade-off between performance and efficiency. Selection criteria play a critical role in filter-based FS methods. A range of criteria has been proposed in the past decades, such as distance measure, similarity, dependency, mutual information (MI), correlation measure, canonical correlation analysis (CCA) (Gheid and Challal, 2016, Dessì and Pes, 2015, Li et al., 2017a, etc.). As the largest family in filter-based FS methods, an MI-based FS algorithm measures the importance of a feature by its selection criterion with the class label, assuming that the feature with a stronger correlation with the label will improve classification performance. The popular algorithms in this family are minimum Relevance Maximum Relevance (mRMR) (Peng et al., 2005), Joint Mutual Information (JMI) (Bennasar et al., 2015), Conditional Mutual Information Maximum (CMIM) (Gao et al., 2016), etc. MI considers the correlation of variables in pairs and then uses a simple approximation strategy, i.e., the sum or the average, to approximate the relation between one feature (or the label) and a set of features (Brown et al., 2012). As a result, MI-based FS shares a common problem, i.e., it does not fully consider the complementarity within a set of features or between features and the label. Different to MI, CCA measures the linear relationship between two multidimensional variables by maximizing the correlation coefficients between them. CCA may not extract a useful description of the data due to its linearity. Kernel CCA is a nonlinear correlation measurement by mapping the data into a higher-dimensional feature space with kernel tricks (Hardoon et al., 2004). CCA or KCCA are easily employed as a feature selector (Sakar et al., 2012, Arora and Livescu, 2012).

Inspired by MI-based FS methods and CCA-based measurements, this thesis proposes and implements an FS method, named mRMJR-KCCA. mRMJR-KCCA uses the correlation derived from KCCA to maximize the relevance between the feature candidate and the class labels and simultaneously minimizes the joint redundancy between the feature candidate and the already selected features. The proposed mRMJR-KCCA is experimentally evaluated over 10 UCI benchmark datasets and three ground-truth datasets. We also conduct comparison studies with other available popular feature selection methods, including MCR-CCA and

mRMR-CCA (Kaya et al., 2014), Autoencoder (Wang, 2016), Sparse Filtering (Ngiam et al., 2011), four MI-based methods in Brown et al., 2012.

mRMR uses the approximation of sum operation \sum when measuring the redundancy between the feature candidate and the already selected features in pairs, as shown in Eq. (3.3), which somehow does not fully consider the complementarity within the already selected features. mRMJR-KCCA introduces the measurement of Kernel CCA into mRMR, which replaces the approximation of sum in mRMR with the KCCA analysis to measure the joint redundancy between the feature candidate and the already selected features. We apply Incomplete Cholesky Decomposition (ICD) (Li et al., 2015a) to reduce the dimensionality of the kernel matrix in the implementation of mRMJR-KCCA on the large-size ground truth datasets. We also investigate the impact of the kernel parameter and the number of components decomposed from the kernel matrix by ICD on the classification accuracies.

5.1.1 KCCA and the proposed feature selection method mRMJR-KCCA

The MI in Eq. (3.3) is one of the most effective criteria to measure the correlation between variables. Let x and y are two discrete random variables, both x and y have N observations, the MI between x and y is defined as

$$I(x; y) = H(y) - H(y|x) = \sum_{x,y} p(x, y) \frac{p(x, y)}{p(x)p(y)} \quad (5.1)$$

where $H(y)$ represents the entropy of y which quantifies the degree of uncertainty in a discrete or discretized random variable y and $H(x|y)$ represents the conditional entropy of x given y ; $p(\cdot)$ is the probability mass function (Bennasar et al., 2015).

CCA (Hotelling, 1936) statistically finds the relationship between two sets of random variables X and Y . Denote $X = (x_1, \dots, x_p) \in R^{n \times p}$, $Y = (y_1, \dots, y_q) \in R^{n \times q}$. X and Y can be two feature spaces or a feature space and a label space. To obtain the correlation between the two sets of variables, CCA finds a projection direction u in the space of X , and a projection direction v in the space of Y , so that the projected data onto u and v have maximum correlation. This is formulated as

$$\rho_{CCA} = \operatorname{argmax}_{u \in R^p, v \in R^q} \frac{u'X'Yv}{\sqrt{(u'X'Xu)(v'Y'Yv)}} \quad (5.2)$$

Solving Eq. (5.2) can be reduced to a generalized eigenvalue problem (Hardoon et al., 2004). CCA-based filter FS methods intend to use the relationship (measured by the correlation coefficient in Eq. (5.2)) between the two projections of the variables to figure out the most important original features. Kaya et al., 2014 propose two CCA-based FS methods. The first method is called mRMR-CCA, which replaces the MI indicator with the CCA coefficient, as presented in Eq. (5.3). The second term in Eq. (5.3) is changed from a sum of paired redundancy in Eq. (5.1) to the redundancy which is handled once from multidimensional variables.

$$J_{mRMR-CCA}(f_k) = \max[\rho_{CCA}(f_k; C) - \rho_{CCA}(f_k; S)] \quad (5.3)$$

where ρ_{CCA} is given in Eq (5.3). The second method in Kaya et al., 2014 is the Maximum Collective Relevance (MCR-CCA), similar to the JMI, which maximizes the collective correlation of the feature candidate and the already selected features against the class labels. The criterion of the MCR-CCA is

$$J_{MCR-CCA}(f_k) = \max[\rho_{CCA}(f_k \cup S; C)] \quad (5.4)$$

CCA describes the linear relation between two sets of variables, which are often insufficient to reveal the highly nonlinear relationship with many real-world data (Wang and Livescu, 2015). KCCA, on the other hand, catches nonlinear relation that corresponds to influential hidden factors responsible for the correlations by mapping the data into a higher-dimensional feature space before performing CCA (Sakar et al., 2012). The KCCA-applied correlation between two sets of random variables X and Y is thus to identify the weights α, β that maximize

$$\rho_{KCCA} = \operatorname{argmax}_{\alpha, \beta} \frac{\alpha' K_X K_Y \beta}{\sqrt{(\alpha' K_X K_X \alpha)(\beta' K_Y K_Y \beta)}} \quad (5.5)$$

where $K_X = XX'$ and $K_Y = YY'$ are the kernel matrices corresponding to the variable sets X and Y . N equals to the size of the sample. However, the kernelized CCA problem in Eq. (5.5) causes an ill-posed inverse problem, and thus a regularization approach is needed to construct a meaningful estimator of the canonical correlation (Bach and Jordan, 2002, Ashad Alam and Fukumizu, 2015). The objective function for regularized kernel CCA becomes

$$\rho_{KCCA} = \operatorname{argmax}_{\alpha, \beta} \frac{\alpha' K_X K_Y \beta}{\sqrt{(\alpha' K_X K_X \alpha + \epsilon \alpha' K_X \alpha) \cdot (\beta' K_Y K_Y \beta + \epsilon \beta' K_Y \beta)}} \quad (5.6)$$

where ϵ is a regularization parameter that should be a small and positive value and approaches zero with an increasing sample size N (Lisanti et al., 2014).

In KCCA, the inputs $X = \{x_p\}_1^N$ and $Y = \{y_q\}_1^N$ caused kernel matrix K_X and K_Y are both with the size of $N \times N$. Thus, solving Eq. (5.6) involves an eigenvalue problem of size $N \times N$, which is expensive both in memory (storing the kernel matrices) and in time with naively costs $\mathcal{O}(N^3)$ (Wang and Livescu, 2015). To overcome this issue, a range of kernel approximation techniques have been proposed to scale up KCCA, including singular value decomposition (SVD) (Arora and Livescu, 2012), Nyström method (Patel et al., 2016), Incomplete Cholesky decomposition (ICD) (Li et al., 2015a), and so on. After applying these approximation methods, the efficiency of calculating KCCA can be much improved (Wang and Livescu, 2015).

Over the last two decades, KCCA has been used for various purposes in statistic and machine learning, such as feature learning (Sakar et al., 2012), computational vision (Bilenko and Gallant, 2016), statistical independence measurement (Lopez-Paz et al., 2013) and so on. Lisanti et al., 2014 investigate matching people across cameras views by applying a learning method based on KCCA to find a common substance between their proposed descriptors extracted from two disjoint cameras, their experimental results demonstrate the superiority of the proposed method. Sakar et al., 2012 proposes a filter method for feature selection with the aim to find the unique information, which exploits correlated functions explored by KCCA as the inputs to mRMR. They demonstrate the usefulness of the method on benchmark datasets. Considering Eq. (5.4) to Eq. (5.6), we propose a new kernel version FS method, i.e., mRMJR-KCCA, by applying KCCA in Eq. (5.6) to Eq. (5.3). The criterion of mRMJR-KCCA is

$$J_{mRMJR-KCCA}(f_k) = \max_{f_k \in F-S} [\rho_{KCCA}(f_k; C) - \rho_{KCCA}(S; f_k)] \quad (5.7)$$

where ρ_{KCCA} is the correlation coefficient calculated by KCCA between two sets of variables, given in Eq. (5.6). mRMJR-KCCA combines mRMR and KCCA to maximize the relevance between the feature candidate and the target class labels, and simultaneously minimize the joint redundancy between the already selected features and the feature candidate.

To implement mRMJR-KCCA especially for our large-size ground-truth datasets, we apply Incomplete Cholesky Decomposition (ICD) for kernel matrix approximation to improve the computation efficiency due to its accurate matrix approximation with far fewer samples (Patel et al., 2016). ICD generates a low-rank matrix $N \times M$ ($M \ll N$) by performing a standard Cholesky decomposition but terminating the decomposition considering a small number of columns (M) (Hardoon et al., 2004). So that the complexity to the eigenvalue problem of size $N \times N$ in Eq. (5.6) turns to $\mathcal{O}(M^2N)$. The procedure to implement mRMJR-KCCA is presented in Table 5.1.

5.1.2 Experimentations and results based on the mRMJR-KCCA

5.1.2.1 Benchmark datasets and learning algorithms

We employ 10 UCI benchmark datasets and three ground-truth datasets, as shown in Table

Table 5. 1 Pseudocode of the mRMJR-KCCA

Algorithm mRMJR-KCCA: Maximum Relevance and Minimum Joint Redundancy Kernel CCA

Input: an original feature set F , the number of features to be selected U

Output: a selected feature set S

Initialize $F = \{f_1, f_2, \dots, f_l, \dots, f_n\}, S = \{ \}, U$

Normalize features to $[0,1]$

Calculate $\rho_{KCCA}(f_n, C)$ using Eq. (5.6) for each f_n with the class labels C

Select the first feature f_s with maximum $\rho_{KCCA}(f_n, C)$

Update $S = S \cup \{f_s\}, F = F \setminus \{f_s\}$

If $U < \text{desired numbers}$

Calculate mRMJR-KCCA: $\rho_{KCCA}(f_k; C) - \rho_{CCA}(S; C)$ by Eq. (5.7)

Select the next feature maximizing mRMJR-KCCA

Update S, F

End

Write S to an excel file

5.2, to experimentally evaluate the performance of mRMJR-KCCA. The datasets are all related to classification problems, covering both binary-class and multi-class; the data type includes real, integer and categorical; the number of original features ranges from 4 to 371; the sample number of each dataset varies from 150 to 16065. The ground truth datasets 10, 11 and 12 in Table 5.2 are the data collected for this research using the five selected wearable sensors. The datasets 10, 11 and 12 include 17 activities. Referring to Table 4.5, the *ARFs* represent the feature set extracted from the wearable device's attitude (*roll*, *pitch*, and *yaw*) and *CUFs* are the features generated from the sensor readings of an accelerometer, a gyroscope, and a magnetometer, a barometer, and a temperature individually. *All* is the combination of *ARFs* and *CUFs*.

We experimentally evaluate mRMJR-KCCA using two learning algorithms on the selected

subset of features, i.e., SVM and RF due to their excellent performance in classification applications (Chernbumroong et al., 2014, Alickovic et al., 2018, Sani et al., 2017). The pair of parameters γ and c in SVM, and the number of trees in RF are determined in 10-fold cross validation process individually. The results report the average accuracy and the deviation from 10 times test. At the same time, we compare mRMJR-KCCA with some popular FS methods presented in Section 5.1.

Table 5. 2 Descriptions of UCI datasets and ground-truth datasets used in the experiments

Dataset	Data type	#Feature	# Class	# Instance	Year
1 Blood	Real	4	2	748	2008
2 Diabetes	Integer, Real	8	2	768	1990
3 Heart	Categorical, Real	13	2	270	N/A
4 Iris	Real	4	3	150	1988
5 Parkinsons	Real	22	2	195	2008
6 Seeds	Real	7	3	210	2012
7 Wdbc	Real	30	2	569	1995
8 Wine	Integer, Real	13	3	178	1991
9 Wine_red	Real	11	6	1599	2009
10 Wdbc	Real	33	2	198	1995
11 ARFs	Real	75	17	16065	2015
12 CUFs	Real	296	17	16065	2015
13 All	Real	371	17	16065	2015

5.1.2.2 Experimental results on the used datasets

The classification accuracies with SVM and RF are shown in Table 5.3 and Table 5.4, respectively. Based on the SVM-based classification results in Table 5.3, mRMJR-KCCA comes with the highest average accuracy (rank) of 89.33% on the 13 datasets, followed by MCR-CCA with the performance of 89.08%. mRMJR-KCCA exhibits the best performance on datasets Wdbc, Wine, CUFs, All, etc. CCA-based methods show better performances than the MI-based methods regarding the overall average classification accuracy on the datasets in Table 5.3. The accuracies of MI-based methods on datasets CUFs and All are much lower, which lowers down the average and rank of MI-based methods. However, mRMR produces

Table 5. 3 Classification accuracy (%) with SVM plus mRMJR-KCCA on the used data sets

Dataset	mRMJR-KCCA (Proposed)	mRMR- CCA(Kaya et al., 2014)	MCR-CCA (Kaya et al., 2014)	Sparse Filtering (Ngiam et al., 2011)	Autoencoder (Wang, 2016)	mRMR (Brown et al., 2012)	JMI (Brown et al., 2012)	CMIM (Brown et al., 2012)	DISR (Brown et al., 2012)
Blood	77.94±2.33	77.94±2.33	77.94±2.33	77.94±2.33	77.94±2.33	77.94±2.33	77.94±2.33	77.94±2.33	77.94±2.33
Diabetes	77.98±4.91	77.98±4.91	78.12±4.51	72.26±3.70	70.18±8.06	77.98±4.91	77.79±4.26	77.99±5.04	77.79±4.20
Heart	84.07±6.77	84.93±6.49	84.81±5.64	71.48±6.77	80.37±8.56	83.33±6.11	83.85±8.81	83.33±6.60	83.70±7.24
Iris	96.67±4.71	96.67±4.71	96.67±4.71	96.67±4.71	96.67±4.71	96.67±4.71	96.67±4.71	96.67±4.71	96.67±4.71
Parkinsons	92.21±8.19	91.74±7.88	91.24±7.52	91.26±4.18	92.76±7.15	92.21±8.32	90.74±5.89	89.58±10.2	90.21±7.97
Seeds	93.81±6.37	91.43±5.85	93.81±6.37	94.76±4.17	96.19±4.92	94.29±3.76	92.86±7.19	93.81±5.52	93.81±5.52
Wdbc	97.71±2.04	97.01±2.35	97.07±1.54	95.25±2.50	95.78±2.89	96.31±2.41	96.31±2.41	96.32±2.84	96.52±2.76
Wine	99.44±1.76	97.78±3.88	99.44±1.76	97.78±3.88	96.22±5.97	96.11±3.75	99.44±1.76	99.44±1.76	99.44±1.76
Wine_red	68.35±2.56	68.98±2.06	68.29±2.05	70.1±2.18	66.48±3.80	68.17±2.61	68.04±2.42	68.04±2.42	68.05±2.93
Wpbc	80.82±7.90	79.26±6.33	80.37±5.83	76.82±8.18	78.82±7.67	81.37±8.09	78.26±6.29	78.82±4.74	78.79±2.82
ARFs	96.51±0.22	94.90±0.35	96.10±0.28	95.75±0.30	94.61±3.13	93.46±0.17	96.82±0.21	96.82±0.15	96.78±0.20
CUFs	97.29±0.22	96.14±0.24	96.01±0.35	95.92±0.41	94.3±3.47	89.81±0.54	86.83±0.43	88.26±0.54	86.98±0.49
All	98.50±0.24	97.75±0.28	97.75±0.28	98.04±0.21	97.51±3.25	91.19±0.34	90.61±0.36	91.74±0.35	90.63±0.37
Average (rank)	89.33 (1)	88.65 (3)	89.05 (2)	87.23 (8)	87.53 (5)	87.6 (4)	87.4 (7)	87.6 (4)	87.49 (6)

Table 5. 4 Classification accuracy (%) with RF plus mRMJR-KCCA on the used data sets

Dataset	mRMJR-KCCA (Proposed)	mRMR-CCA (Kaya et al., 2014)	MCR-CCA (Kaya et al., 2014)	Sparse Filtering (Ngiam et al., 2011)	Autoencoder (Wang, 2016)	mRMR (Brown et al., 2012)	JMI (Brown et al., 2012)	CMIM (Brown et al., 2012)	DISR (Brown et al., 2012)
Blood	75.94 ±2.94	75.94 ±2.94	75.94 ±2.94	75.94±2.94	75.94±2.94	75.94 ±2.94	75.94 ±2.94	75.94 ±2.94	75.94 ±2.94
Diabetes	76.29±4.26	77.47±3.97	77.07±5.67	71.62±3.60	68.22±2.03	77.46±5.36	76.68±6.42	77.46±4.76	76.51±5.32
Heart	84.44±6.00	82.22±7.57	83.33±6.82	71.11±5.60	80.74±7.57	82.22±6.94	82.22±7.57	82.22±7.57	81.48±7.81
Iris	96.67±3.51	96.67±3.51	96.67±3.51	96.67±3.51	96.67±3.51	96.67±3.51	96.67±3.51	96.67±3.51	96.67±3.51
Parkinsons	94.34±5.65	92.26±6.62	92.79±8.17	90.26±3.77	89.18±9.03	90.13±10.0	90.66±7.81	92.26±7.37	91.68±7.16
Seeds	92.86±4.05	90.48±6.55	94.29±5.70	93.81±2.30	95.24±5.02	94.76±3.42	94.29±5.26	94.29±5.26	94.29±3.66
Wdbc	96.84±1.99	96.08±4.68	96.08±2.96	94.02±2.92	96.14±2.15	96.39±3.57	96.19±3.54	96.05±4.63	95.93±2.34
Wine	97.75±3.92	95.57±4.75	97.78±3.88	96.6±3.93	96.86±9.42	96.29±7.24	97.78±3.88	97.78±3.88	97.78±3.88
Wine_red	64.29±3.56	64.29±3.56	63.66±4.89	60.91±2.56	70.98±1.57	64.60±2.59	62.23±2.93	63.29±5.04	62.23±2.93
Wpbc	76.87±8.40	76.76±8.36	76.79±8.37	76.76±5.98	81.79±4.42	76.76±12.2	76.32±6.18	77.29±2.10	76.29±2.10
ARFs	96.62±0.19	95.63±0.31	96.65±0.14	93.55±0.36	92.74±3.04	94.28±0.42	96.55±0.36	96.63±0.25	96.57±0.27
CUFs	97.80±0.31	95.79±0.46	95.79±0.37	94.17±0.15	93.39±3.17	96.25±0.31	96.52±0.30	96.69±0.35	96.80±0.41
All	98.80±0.14	97.88±0.25	97.87±0.26	95.81±0.23	95.67±4.38	96.71±0.30	95.88±0.34	96.86±0.29	95.92±0.23
Average (rank)	88.42 (1)	87.46 (7)	88.05 (2)	85.48 (9)	87.2 (8)	87.57 (4)	87.53 (6)	87.96 (3)	87.55 (5)

the highest accuracy of $81.37\% \pm 8.09$ on dataset Wpbc. For datasets Blood and Iris, all the nine feature selection methods present the same performances since the size of the original feature set on the two datasets is small (i.e., 4) and all the four features are used for classification. Autoencoder presents the highest accuracies of $92.76\% \pm 7.15$ and $96.19\% \pm 4.92$ on datasets Parkinsons and Seeds respectively. Sparse Filtering performs best on dataset Wine_red (70.1 ± 2.18).

Considering RF-based classification results in Table 5.4, mRMJR-KCCA and MCR-CCA still rank the first two on the 13 datasets with the average accuracy of 88.42% and 88.05% respectively, followed by CMIM and mRMR. mRMR produces the highest accuracy of $70.98\% \pm 1.57$ on dataset Wine_red. JMI, CMIM, DISR, and MCR-CCA performs best on dataset Wine with RF classification. Autoencoder and Sparse Filtering obtains much lower results on datasets of Heart and Diabetes with both SVM and RF; this brings down the average performance of Autoencoder on the datasets. Autoencoder and Sparse Filtering fail to show their superiority in this research, which could be attributed to the fact that most of the datasets we used are low-dimensional and small-size and the superiority of these two feature methods is the dimension reduction to high-dimensional or sparse data. Comparing the results in Table 5.3 and Table 5.4, the performance of mRMJR-KCCA and MCR-KCCA is very consistent, which ranks the first two with both SVM and RF.

5.1.2.3 Impact of kernel parameter of γ on the performance of KCCA

To produce kernel matrices in KCCA in this research, we use a Gaussian RBF kernel, given in Eq. (5.8). Note that the parameter γ in Eq. (5.8) differs from the choice of kernel bandwidth, which affects the shape of the distribution of canonical features. We explore the impact of

$$k(\mathbf{x}_i, \mathbf{x}_j) = e^{-\gamma \|\mathbf{x}_i - \mathbf{x}_j\|^2} \quad (5.8)$$

kernel parameter γ on different datasets. Figure 5.1 shows the variations of classification accuracy with different kernel parameter γ in mRMJR-KCCA on datasets of Seeds and Parkinsons. γ varies from 0.1 to 100 with different steps. Figure 1 only presents part of results based on the γ values since certain γ values yield similar results, e.g., 80-100. We can see that γ has different impacts on different datasets. The values of $\gamma = 0.9, 1$ and 2 produce better performance on dataset Seeds with both SVM and RF classification, and the values of $\gamma = 0.1$ and 1 perform better on dataset Parkinsons. $\gamma = 1$ exhibits robust and steady performance on both datasets. We set γ as 1 for most datasets in Table 5.3 and Table 5.4.

Figure 5.2 presents the impact of γ on the accuracies of dataset *ARFs* when we fix the

number of selected features as 30, from which we can see that when $\gamma = 0.3, 0.5, 0.9, 1$ and 2 , better and similar results with both SVM and RF are achieved. This further demonstrates that $\gamma=1$ exhibits better results for most of the datasets used in this section.

5.1.2.4 Impact of the number of Components decomposed in ICD from kernel matrices on the performance

The sample sizes of the first 10 datasets in Table 5.2 are small and the full kernel matrix in KCCA can be easily complemented on them. However, for datasets of *ARFs*, *CUFs* and *All*, the sample size is much larger ($N=16065$), which is memory intensive and computation expensive to realize a $\mathcal{O}(N^3)$ kernel matrix solution. A positive semi-definite matrix K can be decomposed as LL^* , where L is an $N \times N$ matrix, the decomposition in Incomplete Cholesky Decomposition (ICD) is to find a matrix \tilde{L} of size $N \times M$, for a small M , such that the difference $K - \tilde{L}\tilde{L}^T$ has norm less than a given value Bach and Jordan, 2002. This research applies ICD on the KCCA for kernel matrix approximation, which reduces the computation complexity of KCCA to $\mathcal{O}(M^2N)$, here, M is the maximal rank of the solution. We set the range of M from 1 to 100 to investigate the impact of number of the components in ICD on our ground-truth data using the top 30 selected features. Figure 5.3 presents the effect of the increasing number of components decomposed in ICD on the performance of mRMJR-KCCA evaluated by SVM and RF. As can be seen in Figure 5.3, the number of components in ICD has a slight impact on datasets of *ARFs*, *CUFs* and *All* with RF classification, whilst, it has a bigger impact when using SVM classification. This may be attributed to that the optimal parameters in RF models are easier to obtain than in SVM models.

From Figure 5.3, we also observe that increasing the number of components decomposed in ICD from kernel matrices does not necessarily increase in performance. When $M= 1, 20$ and 50 , the better performances are achieved on mRMJR-KCCA and RF; when $M= 20$, the best performance is achieved with mRMJR-KCCA and SVM.

5.1.3 Remarked conclusion

The proposed mRMJR-KCCA replaces the correlation measurement of MI in mRMR with KCCA. mRMR gives an entropy-based score between two variables and utilizes a sum approximation to measure the relationship between a variable and a set of variables. While KCCA searches for the nonlinear relationship between two sets of variables in mRMJR-KCCA, mRMJR-KCCA can avoid the approximation in mRMR when measuring the joint redundancy between the feature candidate and the already selected features, which considers

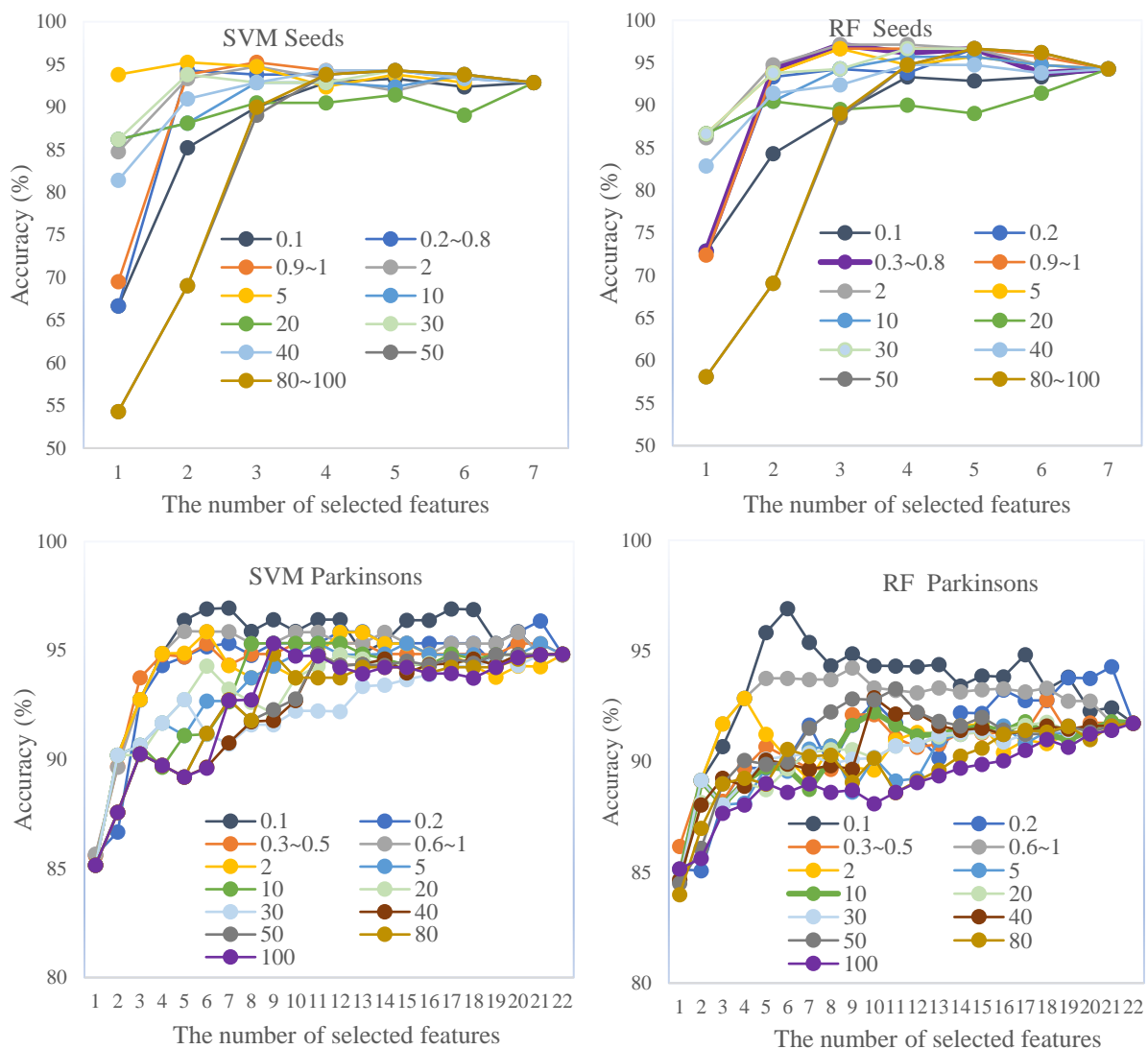


Figure 5. 1 Classification accuracies versus increasing γ (0.1~100) on Seeds and Parkinsons

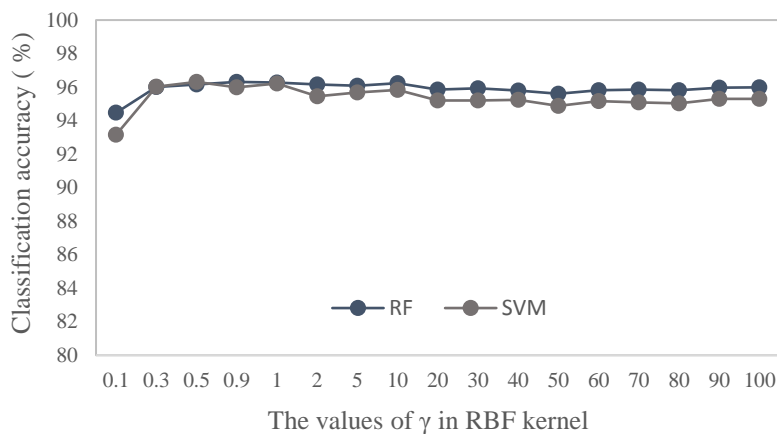


Figure 5. 2 Classification accuracies versus varied γ values in the RBF kernel on ARFs

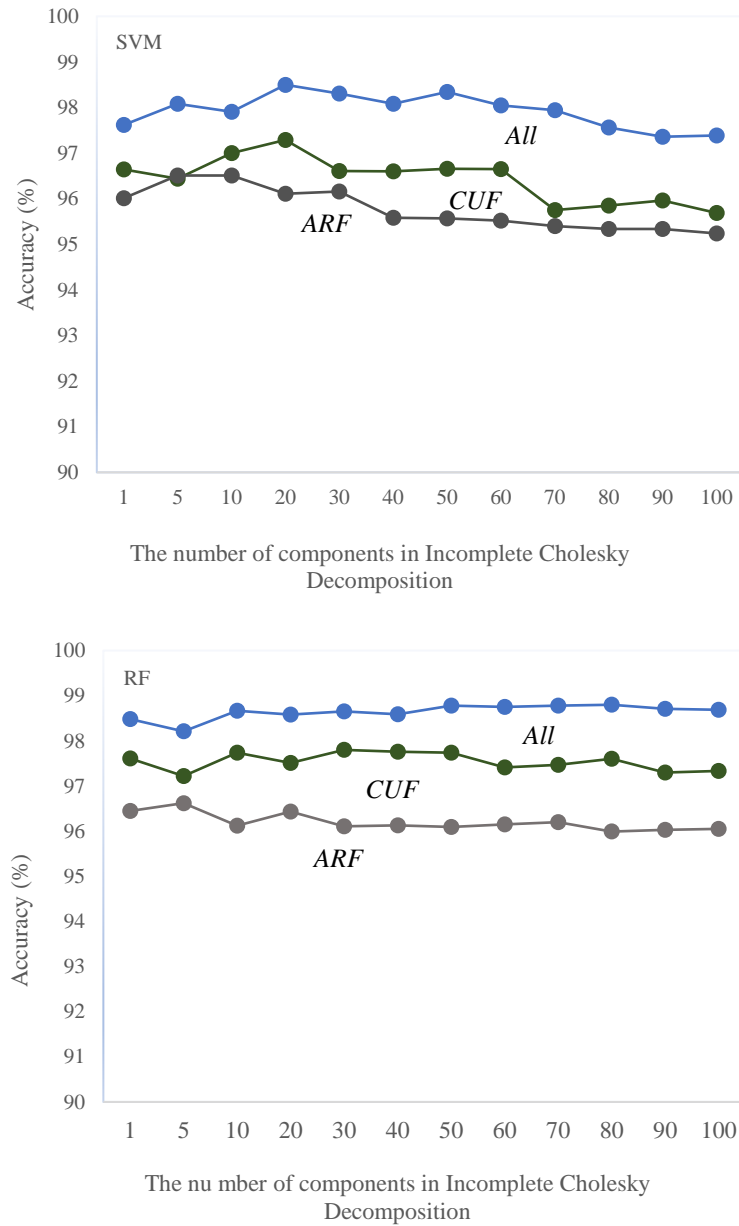


Figure 5. 3 Classification accuracies versus the number of components in ICD on *ARFs*, *CUFs*, and *All* with SVM and RF classification

the complementarity between the already selected features in some way. Experimental results demonstrate the superior performance of mRMJR-KCCA on 13 classification associated datasets compared with other eight benchmark feature selection methods. mRMJR-KCCA ranks first regarding the average classification accuracy of 89.33% and 88.42% with both SVM and RF respectively. mRMJR-KCCA also presents better performance on the ground-truth datasets *ARFs*, *CUFs* and *All*. Referring to the results from Figure 5.1 to Figure 5.3, we set $\gamma = 1$ and $M = 20$ when implementing mRMJR-KCCA on the datasets *ARFs*, *CUFs* and *All* afterwards in this thesis.

5.2 Identification of the contribution of the selected wearable sensors

5.2.1 Sensor contribution identification with the MI-based feature selection methods

We initially selected five types of sensors which are integrated into a wrist-worn device, as mentioned in Section 3.3.1. In this section, we use MI-based feature selection methods identifying the contribution of the five sensors. It is less practical to show the performance of all possible combinations of the five sensors. We divide the five sensors into the following groups (see the first column in Table 5.5) according to their performance in other related studies (Choudhury et al., 2008, Gjoreski and Gams, 2011, Chernbumroong et al., 2014, Roy et al., 2016) to identify the sensors' contributions in this research. Each sensor combination dataset in Table 5.5 contains all the 17 defined activities and different original features accordingly. Each original feature set corresponding to each sensor combination in Table 5.5 contains the same number of samples (all the 17 activities from all participants) and different feature dimension accordingly. The mRMR, JMI, CMIM, and DISR are individually applied to select the best sub-feature set only based on the *CUFs* for each sensor group. The *CUFs* are the features extracted from each sensor (Table 4.5), this is therefore beneficial to the identification of the contribution of each sensor. The selected feature set is fed into the SVM and RF classifiers for classification with 10- fold-cross validation.

For the performance based on SVM classification shown in Table 5.5, the accelerometer and the gyroscope together achieve the better average accuracy of 83.62% and 82.18% respectively, when only using one single sensor; and the magnetometer gives a lower average classification accuracy of 74.25%; the temperature and the barometer seem unlikely useful on their own from the experimental results, giving the lowest average results of only 24.28% and 19.32% respectively. When deploying any two sensors among the accelerometer, the gyroscope, and the magnetometer, the classification accuracies are improved to a range of accuracies, between 84.26% and 86.35%. The combination of the accelerometer, the gyroscope and the magnetometer (AGM) gives the highest average accuracy of 87.97%, and the best accuracy of 89.81% among all the groups is achieved by using the mRMR plus the SVM. When the barometer or/and the temperature sensor is utilized together with the AGM, the accuracies remain unchanged at 89.81%. The experimental results indicate that the temperature and the barometer fail in improving the recognition accuracy, which could be

attributed to the assumption that the features extracted from these two sensors might be less discriminating or overwhelmed by the features extracted from other sensors.

Table 5.5 Classification Accuracy (%) of different sensor combinations with SVM plus MI-based feature selection

Sensor group	Feature selection methods				Average
	mRMR	JMI	CMIM	DISR	
Acc.	83.2±0.65	83.59±0.43	83.94±0.62	83.76±0.45	83.62
Gyro.	82.48±0.46	80.25±0.70	83.85±0.69	82.12±0.43	82.18
Mag.	72.89±0.66	74.28±0.66	75.55±0.46	74.28±0.66	74.25
Baro.	19.32±0.49	19.32±0.49	19.32±0.49	19.32±0.49	19.32
Tem.	24.28±0.57	24.28±0.57	24.28±0.57	24.28±0.57	24.28
Acc.Gyro.	83.84±0.58	85.29±0.49	84.71±0.50	84.59±0.64	84.61
Acc.Mag.	84.41±0.33	84.13±0.45	83.97±0.41	84.53±0.30	84.26
Gyro.Mag.	85.73±0.59	87.88±0.53	85.47±0.64	86.32±0.35	86.35
Acc.Gyro.Mag.	89.81±0.54	86.83±0.43	88.26±0.54	86.98±0.49	87.97
Acc.Baro.	83.2±0.65	83.59±0.43	83.94±0.62	83.76±0.45	83.62
Acc.Gyro.Baro.	83.84±0.58	85.29±0.49	84.71±0.50	84.59±0.64	84.61
Acc.Mag.Baro.	84.41±0.33	84.13±0.45	83.97±0.41	84.53±0.30	84.26
Gyro.Mag.Baro.	85.73±0.59	87.88±0.53	85.47±0.64	86.32±0.35	86.35
Acc.Gyro.Mag.Baro.	89.81±0.54	86.83±0.43	88.26±0.54	86.98±0.49	87.97
Acc.Gyro.Mag.Tem.	89.81±0.54	86.83±0.43	88.26±0.54	86.98±0.49	87.97
Acc.Gyro.Baro.Tem.	83.84±0.58	85.29±0.49	84.71±0.50	84.59±0.64	84.61
Acc.Mag.Baro.Tem.	84.41±0.33	84.13±0.45	83.97±0.41	84.53±0.30	84.26
Gyro.Mag.Baro.Tem.	85.73±0.59	87.88±0.53	85.47±0.64	86.32±0.35	86.35
Acc.Gyro.Mag.Baro.Tem.	89.81±0.54	86.83±0.43	88.26±0.54	86.98±0.49	87.97

Acc.: accelerometer; Gyro.: gyroscope; Mag.: magnetometer; Baro.: barometer; Tem.: temperature

For the performance of RF classification as shown in Table 5.6, the sensor contributions exhibit generally similar trends with SVM-based results, for example: the accelerometer performs best among each sensor; the combination of the accelerometer and the gyro meter perform better among any combination of using two sensors among AGM; the AGM performs best among all sensor combinations in Table 5.6; the temperature and the barometer individually present the much lower performance. On the other hand, RF with MI-Based feature selection methods generally produce higher accuracies compared with the SVM models, for example, the accelerometer, the gyroscope and the magnetometer yield the average accuracy of 89.23%, 85.36%, and 87.54%, respectively; the AGM gives the average

accuracy of 91.53%, and RF with mRMR presents the highest performance of $91.78 \pm 0.43\%$.

The experimental results in Table 5.5 and Table 5.6, on the other hand, imply that none of the features relating to the temperature and the barometer is selected by MI-based FS methods when the barometer and the temperature are used with any other sensor candidates in Table 5.5. It could be likely that the height and the temperature-related features are overwhelmed by the more informative features from other sensors. As a result, the temperature sensor and the barometer do not contribute to the improvement of the recognition accuracy with MI-based FS methods. Concerning the mRMJR-KCCA FS selection, only few barometer and temperature-related features are selected, and the experimental results show the very limited

5.2.2 Sensor contribution identification with the proposed mRMJR-KCCA feature selection method

The AGM combination shows the best performance among all the sensor combinations in Table 5.5 and Table 5.6, and there is no contribution presented from the barometer and the temperature with MI-based feature selection. The top 30 features from all the five wearable sensors (AGMBT) selected by mRMR are shown in the left part of Table 5.7. We observe that no features extracted from the barometer and the temperature, which can explain why accuracies remain unchanged when the barometer or/and the temperature sensor work together with the AGM in Table 5.5 and Table 5.6.

To further identify the contribution of the barometer and the temperature, this section uses the proposed mRMJR-KCCA to select features from the sensor group AGM (the accelerometer, the gyroscope, and the magnetometer) and the AGMBT (AGM plus the barometer plus the temperature) and then compare their performance. As previously mentioned in this chapter, we set $\gamma = 1$ in RBF kernel and $M = 20$ when applying mRMJR-KCCA for feature selection. The dimension of the original feature set from AGMBT in Table 5.4 is 296, and the counterpart from AGM is 276 (excluding 20 features relating to the barometer and the temperature sensor). The classification results on AGMBT and AGM with mRMJR-KCCA plus RF is shown in Figure 5.4, from which we can see that AGM performs slightly better than AGMBT when the number of selected features is below around 15 then AGM and AGMBT reach similar results with the increase of the number of selected features. SVM plus mRMJR-KCCA gives similar results on AGM and AGMBT, as presented in Figure 5.5. With the top 30 selected features in both Figure 5.4 and Figure 5.5, AGMBT performs slightly better than AGM, i.e., 96.57% (SVM+AGM), 96.96% (SVM+AGMBT), 97.65% (RF+AGM), 98%

(RF+AGMBT), respectively. There is a slight difference of 0.35% between RF+AGM and RF+AGMBT. The accuracy does not rise when the number of the selected features varies from five to six in Figure 5.5; it could be because the parameters of the SVM models are not optimized. The top 30 selected features by mRMJR-KCCA from AGMBT are shown in the right part in Table 5.7, from which we observe that mRMR and mRMJR-KCCA select different features from the same original feature set. mRMJR-KCCA selects two barometer-related features (the 4th and the 18th underlined in Table 5.7) and one temperature-related feature (the 11th). No barometer and temperature-related features are selected by mRMR in Table 5.7; this can explain that why the barometer and the temperature sensor fail in contributing to the performance improvement in Table 5.5 and Table 5.6.

Table 5.6 Classification accuracy (%) of different sensor combinations with RF plus MI-based feature selection

Sensor group	Feature selection methods				Average
	mRMR	JMI	CMIM	DISR	
Acc.	89.99±0.32	89.03±0.75	89.99±0.51	87.91±0.50	89.23
Gyro.	86.4±0.45	84.97±0.46	85.35±0.42	84.71±0.43	85.36
Mag.	87.97±0.59	87.49±0.53	87.54±0.31	87.17±0.43	87.54
Baro.	28.91±0.48	28.91±0.48	28.91±0.48	28.91±0.48	28.89
Tem.	21.19±0.96	21.19±0.96	21.19±0.96	21.19±0.96	21.19
Acc.Gyro.	91.61±0.46	90.95±0.51	91.51±0.30	90.04±0.39	91.03
Acc.Mag.	91.55±0.40	91.16±0.36	91.2±0.61	89.73±0.50	90.91
Gyro.Mag.	90.67±0.52	89.19±0.25	89.59±0.29	88.17±0.32	89.41
Acc.Gyro.Mag.	91.78±0.43	91.59±0.54	91.52±0.46	91.23±0.84	91.53
Acc.Baro.	89.99±0.32	89.03±0.75	89.99±0.51	87.91±0.50	89.23
Acc.Gyro.Baro.	91.61±0.46	90.95±0.51	91.51±0.30	90.04±0.39	91.03
Acc.Mag.Baro.	91.55±0.40	91.16±0.36	91.2±0.61	89.73±0.50	90.91
Gyro.Mag.Baro.	90.67±0.52	89.19±0.25	89.59±0.29	88.17±0.32	89.41
Acc.Gyro.Mag.Baro.	91.78±0.43	91.59±0.54	91.52±0.46	91.23±0.84	91.53
Acc.Gyro.Mag.Tem.	91.78±0.43	91.59±0.54	91.52±0.46	91.23±0.84	91.53
Acc.Gyro.Baro.Tem.	91.61±0.46	90.95±0.51	91.51±0.30	90.04±0.39	91.03
Acc.Mag.Baro.Tem.	91.55±0.40	91.16±0.36	91.2±0.61	89.73±0.50	91.53
Gyro.Mag.Baro.Tem.	90.67±0.52	89.19±0.25	89.59±0.29	88.17±0.32	89.41
Acc.Gyro.Mag.Baro.Tem.	91.78±0.43	91.59±0.54	91.52±0.46	91.23±0.84	91.53

Acc.: accelerometer; Gyro.: gyroscope; Mag.: magnetometer; Baro.: barometer; Tem.: temperature

Table 5. 7 The top 30 features selected by mRMR and mRMJR-KCCA from CUFs with all five wearable sensors (AGMBT)

Features selected by mRMR		Features selected by mRMJR-KCCA	
Order	Name of features	Order	Name of features
1	Per10_accx	1	MI_gyro
2	Max_accx	2	SpecEnt_accz
3	SMA_gyro	3	Coorcoef_Axz
4	Min_accx	4	<u>SpecEnt hei</u>
5	Per90_accx	5	Cmr_gyro
6	Per25_accx	6	Coorcoef_Gxy
7	Std_accy	7	Cftor_accx
8	Per75_accx	8	Cftor_accz
9	Rms_accx	9	SpecEnt_magx
10	MAD_gyrox	10	Skewness_accx
11	Per50_accx	11	<u>SpecEgy tem</u>
12	Mean_accx	12	Apf_accy
13	Rms_gyro	13	Coorcoef_Ayz
14	Mode_accx	14	Coorcoef_Myz
15	Std_magx	15	Skewness_magx
16	Median_accx	16	Apf_magx
17	SpecEgy_accx	17	MFC_gyrox
18	Std_accz	18	<u>Cmr hei</u>
19	MAD_gyroz	19	Cftor_magz
20	Stdm_accx	20	Domifq_gyro
21	Interq_gyrox	21	Autoc_accx
22	Variance_accy	22	Coorcoef_Gyz
23	Std_accx	23	Cftor_magy
24	Interq_gyro	24	Domifq_gyrox
25	Stdm_accz	25	Cftor_gyro
26	Per25_magx	26	Apf_magz
27	MI_gyro	27	MFC_gyroz
28	Interq_gyroz	28	Per90_magx
29	Ptp_accy	29	Per90_gyrox
30	Per10_magx	30	Apf_accz

The number of the original features is 296 shown in Table 4.5

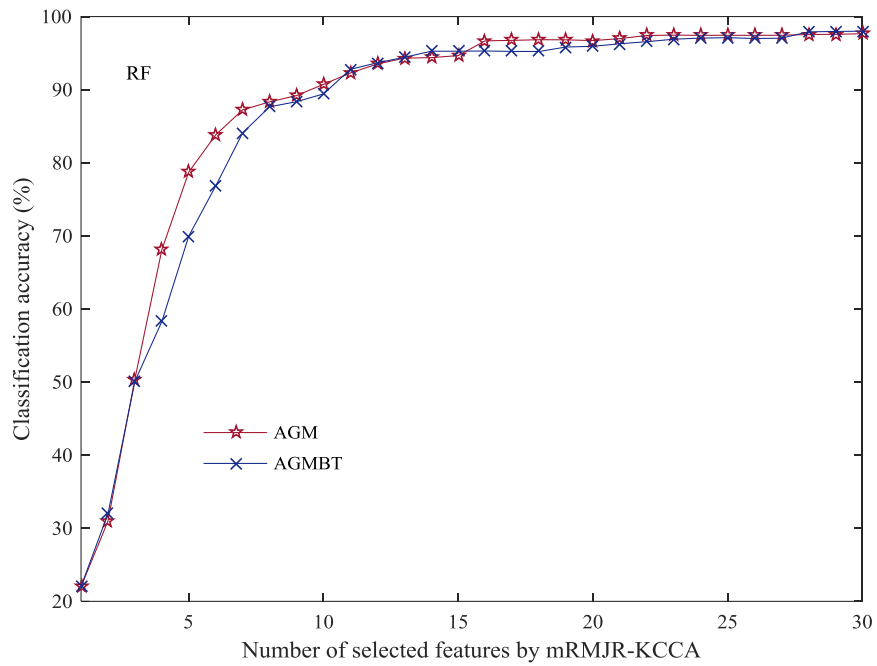


Figure 5. 4 Performance of AGM and AGMBT with RF for 17 defined activities

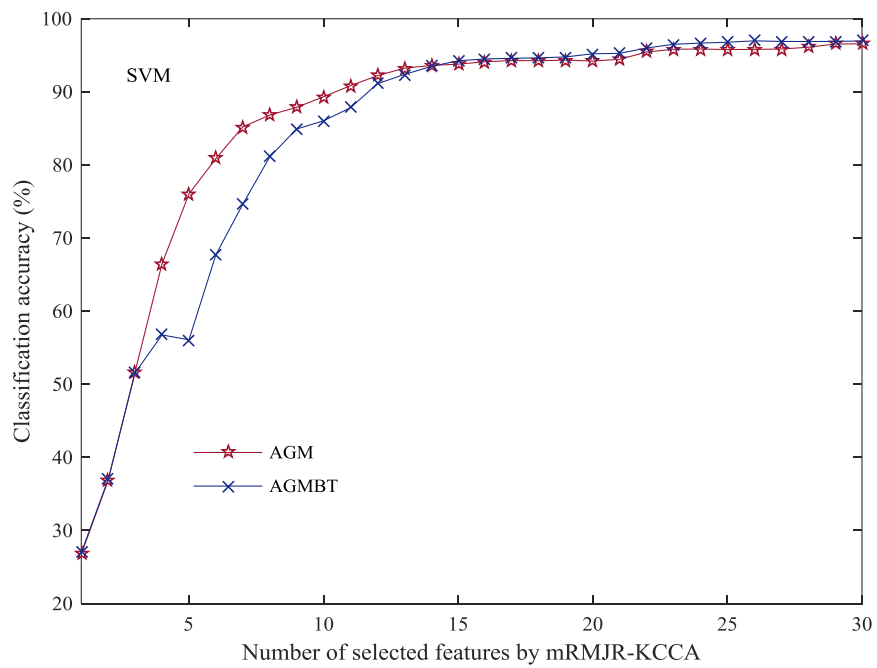


Figure 5. 5 Performance of AGM and AGMBT with SVM for 17 defined activities

5.2.3 Remarkd conclusion

Collectively, the barometer and the temperature sensor show no obvious contribution to the HAR in the research with the MI-based feature selection methods from Table 5.5 and Table 5.6, since on related features from the barometer and the temperature sensor are selected from AGMBT. While, in Figure 5.4 and Figure 5.5, the barometer and the temperature sensor present very limited contribution to the defined 17 daily activities with the mRMJR-KCCA feature selection, and only three features relating to the barometer and the temperature are selected in Table 5.7. Nevertheless, the related studies illustrated that the barometer (for the height measurement) (Chernbumroong et al., 2014, Lester et al., 2006, Mass éet al., 2015) and the temperature sensor (Chernbumroong et al., 2014) could contribute HAR when being combined with other wearable sensors. This research finds that the function of a sensor not only depends on the sensor's intrinsic characteristic but on what specific information extracted from the sensor when the sensor is used. For example, the *mean*, the max or other absolute values extracted from the barometer contribute the activity recognition (Chernbumroong et al., 2014, Lester et al., 2006, Mass éet al., 2015). These features abovementioned showed the importance to the classification only in the specific environment, e.g., on the same floor or over a short time. The problem could be that it might be less useful for detecting Activity A on the ground floor if the max of the height value is useful for detecting activity A on the fifth floor. The similar issues can also be applied to the temperature sensor. For instance, if the mean of the temperature is useful for differentiating Activity B in winter, it might be invalid for the same activity in summer or a different temperature environment. This research holds that people live in varied floors, different weather conditions and changing room environments, which means the features (like the *max/min* of the height, the *mean* of the temperature, etc.) are less beneficial to distinguish different activities in varied living environments. Therefore, only the features that can represent the relative variations of the height and the temperature, such as the *peak-to-peak amplitude* or the *standard deviation*, *to-peak amplitude* or the *standard deviation*, are used for the two sensors (Table 4.5).

The experimental results in Table 5.5 and Table 5.6, on the other hand, imply that none of the features relating to the temperature and the barometer is selected by MI-based FS methods when the barometer and the temperature are used with any other sensor candidates in Table 5.5. It could be likely that the height and the temperature-related features are overwhelmed by the more informative features from other sensors. As a result, the temperature sensor and the barometer do not contribute to the improvement of the recognition accuracy with MI-based FS methods. Concerning the mRMJR-KCCA FS selection, only few barometer and

temperature-related features are selected, and the experimental results show the very limited contribution of the two sensors in Figure 5.4 and Figure 5.5. The barometer and the temperature sensor have no obvious contribution to our research, whereas they might be useful for other tasks in assisted living systems, such as people's vital signal detection or the ambient-sensor-based systems.

5.3 Identification of the augmented features from wearable sensors

5.3.1 Experimental results with the MI-based feature selection methods

In Section 5.2, we identify the contribution of the selected wearable sensors to the defined 17 activities using the *CUFs* which are extracted from the individual sensors. This research also extracts augmented *ARFs* from the AGM. In this section, we apply the mRMR, JMI, CMIM, DISR, and mRMJR-KCCA on the *ARFs* and *All (CUFs + ARFs)* feature sets to identify the contribution of the feature set *ARFs* on the defined 17 activities. We still use SVM and RF as classifiers. Figure 5.6 shows the classification results on the three feature sets of *ARFs*, *CUFs* and *All (CUFs + ARFs)* using MI-based FS methods and SVM classification. We can see that in Figure 5.6 the *ARFs* (the curve group in red) present the highest accuracy with respect to the used FS methods, followed by the feature set of *ARFs+CUFs* (the curves in blue) and the *CUFs* (the curves in green). The *ARFs* produce higher accuracies only using 5 to 20 features selected by the JMI, CMIM, and DISR. The *ARFs+CUFs* perform better than the *CUFs*, with the best accuracy of around 92% and 90%, respectively. When applying the FS on the *ARFs+CUFs*, taking the mRMR as an example, nearly half of the selected features are from the *CUFs* and the other half from the *ARFs*. Figure 5.7 shows the accuracies of the *ARFs*, the *CUFs*, and *All (ARFs+CUFs)* with RF classification. We can also see that the *ARFs* (the curve group in red) present the best results, followed by the feature set of *ARFs+CUFs* (the curves in blue) and the *CUFs* (the curves in green). The *ARFs+CUFs* perform better than the *CUFs*, with the best accuracy of around 94% and 92%, respectively. The *ARFs* can reach higher accuracies using 10 to 20 features selected by the JMI, CMIM, and DISR, with the best accuracy of $96.68\% \pm 0.28$ with CMIM and RF.

The detailed results for each activity from Figure 5.6 are shown in Table 5.8, in which all the results are obtained with 30 selected features. Specifically, the mRMR produces the

highest accuracy of 89.8% based on the feature set of *CUFs*; the CMIM achieves the highest accuracy of 91.74% on the *CUFs+ARFs*; and the JMI, CMIM, and DISR present a much higher accuracy of over 96% on *ARFs*. The highest accuracy of $96.82\% \pm 0.15$ is produced by CMIM and SVM on *ARFs*. Table 5.9 details the classification accuracy for each activity in accordance with the three best cases in bold based on RF classification, in which the mRMR produces the highest accuracy of 91.79% based on the feature set of *CUFs*; the CMIM achieves the highest accuracy of 94.24% on the *CUFs+ARFs*; and the CMIM presents the best performance of 96.68% on *ARFs*. The last column in Table 5.8 and Table 5.9 shows the accuracy for each activity between the *ARFs* and the *CUFs*. We can see that the accuracy increases at different degrees for the majority of the activities. Take the results in Table 5.8 as examples; the Read presents the largest increase by 20.45% on *ARFs*, which is somehow misclassified as Lie on *CUFs*. Next is the Mop with a rise of 12.69%, which is incorrectly classified as Walk or Stairs on *CUFs*; followed by the Wipe with an increase of 12.16%, which is easily misclassified as Iron when using *CUFs*. The Exercise and the Phone only see a slightly increased accuracy; a dropped accuracy only occurs with the Stand. It is also found that the Falls and the Walk achieve their highest accuracies when using the feature set of *CUFs + ARFs*. Also, the Read, Watch, Walk, and Stairs rank the most difficult activities to recognize. The *ARFs* plus the CMIM performs best with an overall difference of 7.01% in accuracy to the *CUFs* with mRMR.

5.3.2 Experimental results with mRMJR-KCCA feature selection

In Section 5.2, experimental results show the very limited contribution of the barometer and the temperature sensor to HAR in this research. This section then uses the mRMJR-KCCA to explore the contribution of feature sets *CUFs*, *ARFs* and *All (CUFs+ARFs)* from only the sensor group AGM instead of AGMBT. Therefore, the number of the original features for *CUFs*, *ARFs* and *All* are 276, 75 and 351 respectively (Table 4.5), here, 20 features originated from the barometer and the temperature sensor are eliminated from Table 4.5. Figure 5.8 and Figure 5.9 present the performance of the three feature sets from AGM with RF and SVM respectively, from which we can see that feature sets *All*, *CUFs* and *ARFs* exhibit different results on all the 17 activities. Overall, with the first top 30 selected features, the feature set *All* performs best with both RF and SVM classification; *CUFs* produce better results than *ARFs* with RF, and the two feature sets give similar performances with SVM after the number of the selected features is greater than 23 in Figure 5.9. Specifically, the classification accuracies with RF+mRMJR-KCCA in Figure 5.8 for *All (CUFs+ARFs)*, *CUFs* and *ARFs* are

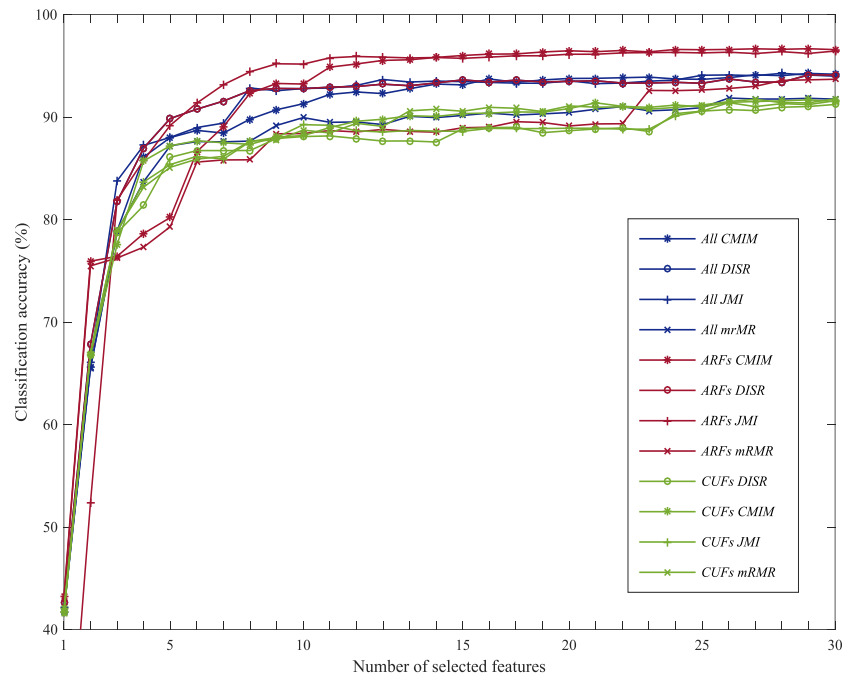


Figure 5. 6 Classification accuracy versus the number of selected features from different feature sets with SVM plus MI-based FS methods (“All” represents “CUFs+ARFs”)

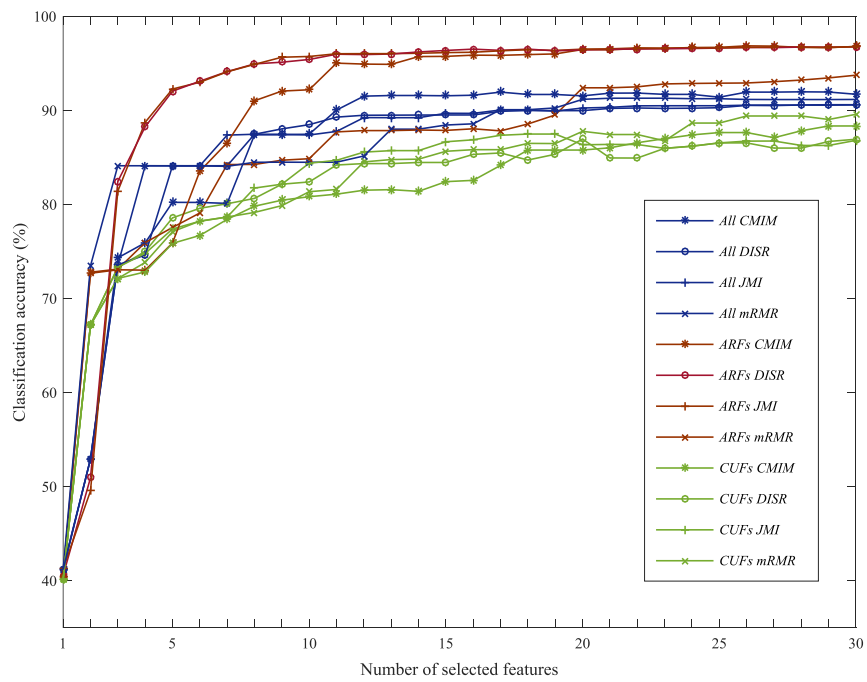


Figure 5. 7 Classification accuracy versus the number of selected features from different feature sets with RF plus MI-based FS methods (“All” represents “CUFs+ARFs”)

Table 5. 8 Classification results with SVM for each activity (%) on different feature sets

Classification accuracy (%) based on the wearable information					
	FS methods	<i>CUFs</i>	<i>CUFs +ARFs</i>	<i>ARFs</i>	
Activity	mRMR	89.81±0.54	91.19±0.34	93.46±0.17	Difference (<i>ARFs</i> vs. <i>CUFs</i>)
	JMI	86.83±0.43	90.61±0.36	96.82±0.21	
	CMIM	88.26±0.54	91.74±0.35	96.82±0.15	
	DISR	86.98±0.49	90.63±0.37	96.78±0.20	
Brush		93.38	90.58	99.74	6.36
Clean		90.06	95.13	99.69	9.63
Cook		91.82	94.82	98.96	7.14
Eat		91.41	94.51	98.71	7.30
Exercise		97.83	91.77	99.74	1.91
Falls		93.17	98.96	97.31	4.14
Iron		94.57	94.25	97.15	2.58
Lie		94.41	88.05	98.45	4.04
Mop		84.57	89.18	97.26	12.69
Phone		98.76	93.79	99.74	0.98
Read		75.88	83.64	96.33	20.45
Stairs		79.14	86.8	86.39	7.24
Stand		99.95	91.98	97.46	-2.49
Walk		78.47	88.3	88.04	9.57
Wash		90.01	94.41	98.86	8.85
Watch		89.39	90.73	96.07	6.68
Wipe		83.96	92.65	96.12	12.16
Overall		89.81	91.74	96.82	7.01

98.48% ±0.22, 97.65% ±0.21, 96.28% ±0.22, respectively; the counterparts with SVM in Figure 5.9 are 98.32% ±0.27, 96.57% ±0.3 and 96.16±0.36%, respectively.

5.3.3 Remarked conclusion

For the identification of the contribution of the augmented feature set *ARFs*, the MI-based

Table 5. 9 Classification results with RF for each activity (%) on different feature sets

Classification accuracy (%) based on the wearable information					
Activity	FS methods	$CUFs$	$CUFs + ARFs$	$ARFs$	Difference ($ARFs$ vs. $CUFs$)
	mRMR		91.78 ± 0.63	92.10 ± 0.32	
JMI		91.58 ± 0.43	94.04 ± 0.37	96.48 ± 0.37	
CMIM		91.54 ± 0.46	94.24 ± 0.38	96.68 ± 0.28	
DISR		91.25 ± 0.46	94.14 ± 0.17	96.41 ± 0.29	
Brush		90.53	97.36	99.33	8.80
Clean		92.96	97.36	99.17	6.21
Cook		91.61	94.10	98.19	6.58
Eat		90.01	94.72	98.50	8.49
Exercise		98.81	98.86	99.74	0.93
Falls		92.08	91.25	96.64	4.56
Iron		88.56	92.39	97.26	8.70
Lie		94.25	97.20	99.02	4.77
Mop		89.54	91.36	94.93	5.39
Phone		98.65	99.28	99.48	0.83
Read		88.10	92.75	97.88	9.78
Stairs		85.61	88.72	87.58	1.97
Stand		97.00	96.38	97.15	0.15
Walk		87.73	89.39	89.03	1.30
Wash		94.20	94.41	99.48	5.28
Watch		93.37	94.15	95.76	2.39
Wipe		87.32	92.39	94.36	7.04
Overall		91.78	94.24	96.68	4.89

feature selection methods, and the proposed mRMJR-KCCA give different results, i.e., in Section 5.3.1, $Accuracy_{ARFs} > Accuracy_{All} > Accuracy_{CUFs}$ (Figure 5.6 and Figure 5.7), whereas, in Section 5.3.2, the mRMJR-KCCA gives the performance of $Accuracy_{All} > Accuracy_{CUFs} > Accuracy_{ARFs}$. The different results, on the one hand, can be partially explained that the features selected from *All* ($ARFs + CUFs$) by MI-based FS methods carry more redundancy between features; on the other hand, the parameters optimization of different

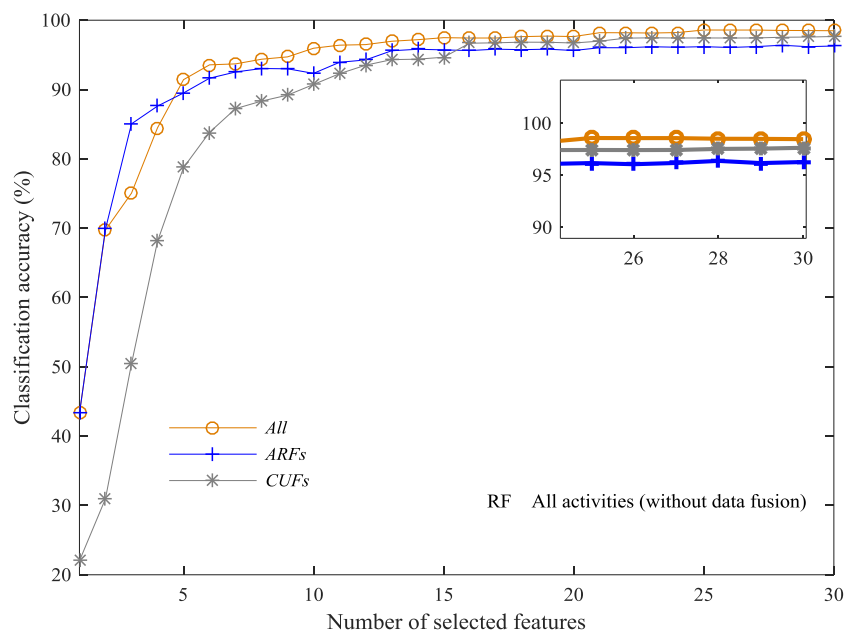


Figure 5. 8 Classification accuracies of *CUFs*, *ARFs* and *All* on all 17 activities with RF+mRMJR-KCCA

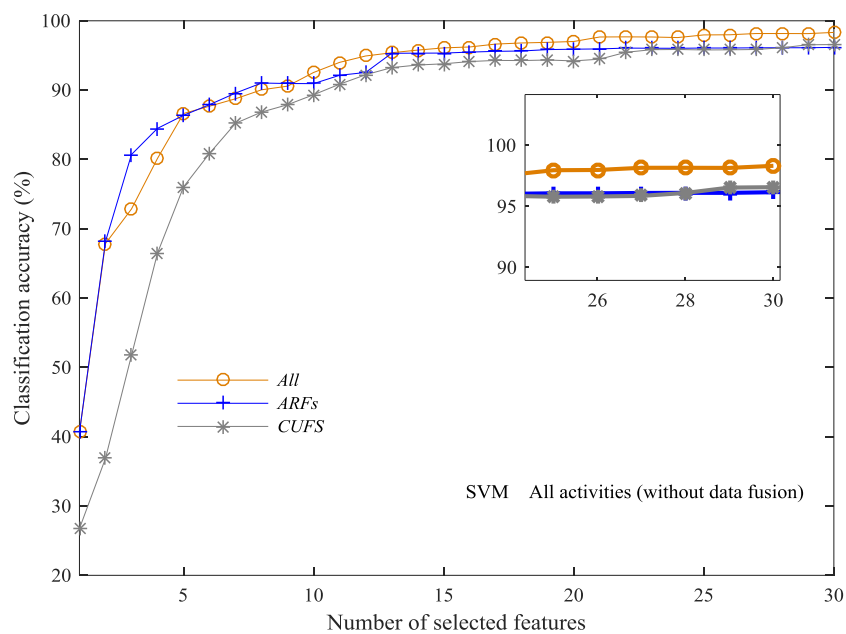


Figure 5. 9 Classification accuracies of *CUFs*, *ARFs* and *All* on all 17 activities with SVM+mRMJR-KCCA

Table 5. 10 The top 30 features selected by mRMR and mRMJR-KCCA from *All* (*ARFs* + *CUFs*) with three sensors (AGM)

Features selected by mRMR		Features selected by mRMJR-KCCA	
Order	Name of features	Order	Name of features
1	Min_roll	1	Min_roll
2	Max_roll	2	Variance_roll
3	SMA_gyro	3	SpecEnt_magx
4	Per10_accx	4	Variance_gyrox
5	Max_accx	5	SpecEgy_pitch
6	Min_accx	6	Skewness_accx
7	Stdm_roll	7	Cmr_yaw
8	Per10_roll	8	SpecEnt_accz
9	Per90_accx	9	Corrcoef_Ayz
10	Std_accy	10	SpecEgy_roll
11	Per25_accx	11	Autoc_gyroy
12	Per90_roll	12	Corrcoef_Axz
13	MAD_gyrox	13	Per75_gyroz
14	Rms_accx	14	Domifq_gyroy
15	Mean_roll	15	Cftor_magy
16	Per25_roll	16	Skewness_magx
17	Rms_gyroy	17	Max_gyrox
18	Per75_accx	18	Cftor_magz
19	Per50_roll	19	Mean_yaw
20	MAD_gyroz	20	Apf_magx
21	Per75_roll	21	Corrcoef_Gxy
22	Std_accz	22	Cftor_accx
23	SpecEgy_accx	23	SpecEgy_gyroz
24	Median_roll	24	Ader_yaw
25	Stdm_magx	25	Apf_accy
26	Interq_gyrox	26	MFC_gyrox
27	Mode_accx	27	Min_gyrox
28	Per50_accx	28	MFC_yaw
29	Variance_accy	29	Variance_pitch
30	Rms_roll	30	Ader_roll

classifiers also affects the performance of a same selected feature set. Nevertheless, the *ARFs* feature set presents similar accuracies of around 96% with different FS methods. Table 5.10 lists the first 30 features selected by mRMR and the mRMJR-KCCA from *All* with AGM. In the left part of Table 5.10, mRMR selects 13 features from the accelerometer, 11 from the Roll angle, five from the gyroscope and one from the magnetometer out of the 30 selected features. The mRMJR-KCCA in the right part of Table 5.10 selects nine features from the gyroscope, six from the accelerometer, five from the magnetometer, four from the Roll angle, four from the Yaw angle and two from the Pitch angle out of the top 30 selected features.

5.4 Summary

This chapter uses the existing MI-based FS methods and the proposed mRMJR-KCCA FS method identifying the contributions of the selected wearable sensors and the augmented features which are extracted the attitude angles of the wearable device. Experimental results show the very limited contribution of the barometer and the temperature sensor to recognizing the defined 17 daily activities in this research. Regarding the contribution of the augmented features (*ARFs*), the CMIM plus SVM present the highest accuracy of $96.82\% \pm 0.15$ from the feature set *ARFs* when using the MI-based FS methods. mRMJR-KCCA plus RF give the best performance of $98.48\% \pm 0.22$ from the feature set *All* (*ARFs+CUFs*). Based on the results above achieved only with the wearable sensors, Chapter 6 will investigate the data fusion of the wearable information with the ambient information using the proposed data fusion method.

Chapter 6

Data fusion of the wearable information and the ambient information

Figure 3.1 presents the diagram of the proposed system. Chapter 4 presents the activity definition and the original feature creation. Chapter 5 investigates the contributions of the selected five wearable sensors and the augmented features from the wearable sensors. The best performance based on the MI-based feature selection methods is obtained by the SVM+CMIM on the *ARFs* feature set, and the counterpart with the mRMJR-KCCA feature selection is from the RF+mRMJR-KCCA on the feature set *All (ARFs +CUFs)*. This chapter, therefore, uses both SVM+CMIM and RF+mRMJR-KCCA for data fusion evaluation.

The ambient information from PIR sensors are processed as $\{0,1\}$ digital series, in which “1” represents the room with a PIR sensor installed is occupied by a user at a specific moment, and “0” means the room is not taken by a user. For the data fusion referring to Figure 3.1, the “presence” information of “1” is used for triggering a sub-classification model that is trained by the wearable data from the activities limited in the corresponding room. After applying data fusion, each room-based submodel is only responsible for a smaller number of activities compared with the scenario of recognizing all the 17 defined activities with the wearable data alone. Thus, the overall recognition accuracy is expected to be improved without additional computation and also with smaller numbers of features. Additionally, the system after applying data fusion can deliver more comprehensive surveillance for older people for their daily life, i.e., both the specific daily activities and the room-based daily routine only using three wrist-worn sensors and the ambient PIR sensors.

6.1 Daily routine derived from the PIR sensors

The digital series $\{0, 1\}$ represents the status of a room with a PIR sensor set mounted in is occupied or not by the subject at a specific moment. With these $\{0,1\}$ series, the room-level occupation routine can be derived. The original data acquired from ambient sensors in a home is shown in Table 4.4, in which the status of a PIR sensor is stored only when variations are detected compared with its last instantaneous status. We thereby only store the status of “1” for each PIR sensor to save storage. Considering the home structure where we collected data, we use four sets of RUs and a CU set in each home, as shown in Figure 3.8. We collect ambient data when we collect wearable data. However, those ambient data are only the tiny part of a day, which cannot reveal a long-term daily routine. The data collection for ambient information for a whole day is very difficult since we require no other people and pets living with the participant during ambient data collection to avoid interference for PIR sensors. We also need to consider the older participant’s feeling of living alone in a home for one day. Consequently, we only pick two people from the older participants (one male, one female) completed a continuous 24-hour data collection separately in their own homes. During data collection, they did not need to wear any other technologies and just lived in an obtrusive environment with PIR sensors mounted as they performed the daily routine. The only constraint is that the participant only could stay at home without going outside during the 24 hours only if some emergency circumstances happen. We prepare enough food materials, drinks and other necessities for each participant and keep in touch with them every few hours to make sure they are well. The raw data from the ambient sensors about the participant’s room-level location information for a whole day can be recorded, and the data samples are shown in Table 6.1.

Figure 6.1 presents the partisan’s daily routine inferred from the data in Table 6.1, which can generally reveal when, how long, and how often (WHH) the participant takes a specific room. Figure 6.1 also gives specific details about the routine. For example, the participant under monitored in Figure 6.1 got up in the bedroom at around 6.30 am, went to bed at about 9.30 pm and used the toilet once at night, etc. Furthermore, the room-level daily routine over a long time can reveal whether the user could actively organize daily life, or whether the user is leading an abnormal routine compared with the normal routines. Accordingly, combining the room-level daily routine derived from the ambient information with the recognized daily activities from the wearable sensors in Chapter 5 can deliver a more comprehensive surveillance, i.e., we can answer the questions of WWHH from the proposed system, including what the user is doing in the WHH.

6.2 Data fusion between the wearable sensors and the ambient sensors

To fuse the data from the wearable and ambient sensors, we propose a simple and effective method shown in Figure 3.1, which is different from any other published methods reviewed in Chapter 2. The proposed data fusion method is based on the following assumptions: some activities can be limited in a specific room based on their occurring places, for instance, cooking is highly impossible taking place in a bedroom and teeth brushing might not be done in a bedroom, etc. Hence, we can assign different activities in different rooms and first



Figure 6. 1 One subject's room-level routine over a whole day

train the room-based sub classification models with the corresponding wearable data. Each of the sub-models is only responsible for the recognition of a smaller number of room-assigned activities compared with the scenario of recognising all the defined activities together only using the wearable data. The captured ambient information “1” (presence) is then used to trigger a sub model. As a result, after fusing the ambient data with the wearable data, the whole classification model turns into the parallel-working sub classification models (see Figure 3.1). To unify the home structures where we collect data, for instance, Eat is collected at a living room since there are no dining rooms in some homes; the 17 activities are assigned to four groups shown in Table 6.2, i.e., five activities in Bathroom, eight in Kitchen, ten in Living room and five in Bedroom. The activity types in each room decrease, thereby reducing recognition requirements and simplifying the classification models. To facilitate the later

comparisons, the sample size used for each activity remains unchanged before and after data fusion. Note that our case study is to assign the activities into a different room (which room an activity should be assigned to). The activity assignment can change for different applications and purposes.

Table 6. 2 Activity assignment in rooms for data fusion

	All activities (before data fusion)	After data fusion				
		Bathroom	Kitchen	Living room	Bedroom	
1	Brush teeth	√				
2	Clean	√	√			
3	Eat			√		
4	Cook		√			
5	Exercise			√		
6	Falls	√	√	√	√	
7	Iron		√	√		
8	Lie				√	
9	Mop	√	√			
10	Phone			√	√	
11	Read			√		
12	Stairs use			√		
13	Stand	√	√	√	√	
14	Walk			√	√	
15	Wash		√			
16	Watch TV			√		
17	Wipe		√			
Activity count		17	5	8	10	5

6.2.1 Experiments of the data fusion based on MI-based feature selection

In Chapter 5, the *ARFs* perform better when we apply the MI-based FS methods. The data fusion in this section then first uses the MI-based methods for feature selection and the SVM for classification based on the *ARFs* (Table 5.8). The data fusion procedure can refer to Figure 3.1. Figure 6.2 compares the performances of before and after data fusion based on the *ARFs*. The four FS methods all produce a consistent performance, i.e., $Accuracy_{Fusion} > Accuracy_{ARFs}$. Experimental results, including the scenarios of before data fusion (the whole model) and after

data fusion (room-based sub-models), are detailed in Table 6.3. The Accuracy, Precision, Recall and F-score present similar performance trends for each model in Table 6.3. The experimental results are then reported only with the index of accuracy for highlights and simplicity afterward.

Table 6.3 shows that the CMIM plus SVM achieves the highest accuracy of 98.32% after data fusion, followed by the JMI and DISR with the accuracy of 97.89% and 97.66% respectively. The mRMR produces the largest increase by around 3.35% (from 3.46% to 96.81% before and after data fusion). Combined with the PIR-sensor-captured location information, the submodels for the corresponding rooms are assigned with smaller numbers

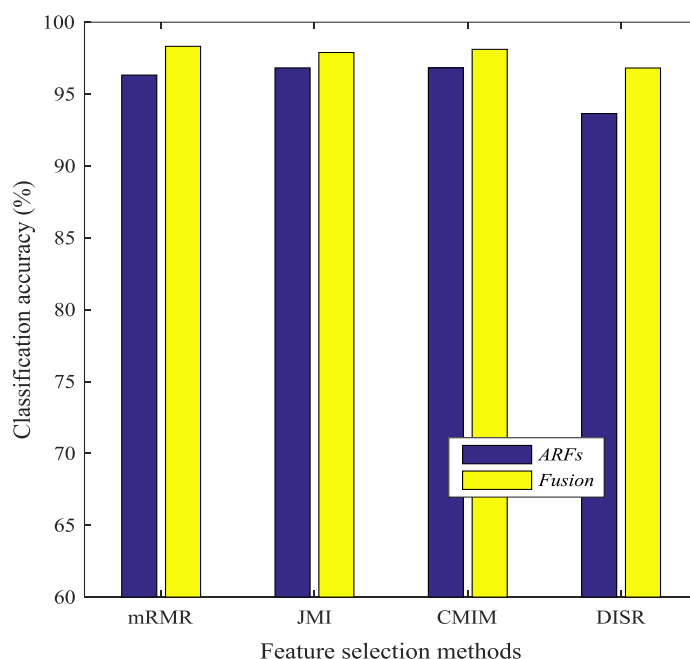


Figure 6. 2 Classification accuracy before and after data fusion using different feature selection methods with SVM based on ARFs

(Fusion: Based on the feature set *ARFs* and the ambient information)

of activities and hence most submodels obtain their improved performance. From Table 6.3, we can see that the accuracy for Bathroom, Kitchen, and Bedroom all greatly increases after data fusion; only Living room obtains a slightly higher or lower accuracy. More importantly, the improved accuracies are achieved with a smaller number of features compared with the 30 features used for dealing with all the activities together. Taking mRMR and CMIM as examples, we list the selected optimal feature sets for the corresponding models in Table 6.4, in which the features are selected from the original 75 *ARFs* presented in Table 4.5. Only two

Table 6. 3 Classification accuracy (%) with SVM before and after applying data fusion based on *ARFs*

FS method	Performance index (%)	Model for (# of activities)					Overall accuracy (%)
		Whole model (17)	Fusion (sub models)				
			Bathroom (5)	Kitchen (8)	Living room (10)	Bedroom (5)	
mRMR	A1	93.46 ±0.17	98.61 ±0.65	98.12 ±0.39	94.32 ±0.56	99.34 ±0.3	96.81
	P1	93.58 ±0.38	98.08 ±0.95	98.14 ±0.43	93.92 ±0.57	99.03 ±0.51	
	R1	93.46 ±0.38	97.93 ±0.98	98.11 ±0.43	93.48 ±0.58	98.88 ±0.51	
	F1	93.45 ±0.37	98.00 ±0.93	98.12 ±0.44	94.48 ±0.62	98.95 ±0.54	
JMI	A1	96.82 ±0.21	99.23 ±0.60	98.87 ±0.28	96.21 ±0.44	99.36 ±0.37	97.89
	P1	96.84 ±0.21	98.98 ±0.78	98.87 ±0.32	95.89 ±0.53	98.95 ±0.59	
	R1	96.82 ±0.21	99.04 ±0.79	98.83 ±0.26	95.85 ±0.55	99.09 ±0.46	
	F1	96.82 ±0.21	99.01 ±0.78	98.84 ±0.27	95.85 ±0.49	99.01 ±0.52	
CMIM	A1	96.82 ±0.15	99.42 ±0.39	98.95 ±0.29	96.80 ±0.49	99.36 ±0.37	98.32
	P1	96.83 ±0.21	99.25 ±0.51	98.95 ±0.37	96.60 ±0.55	98.95 ±0.59	
	R1	96.82 ±0.15	99.18 ±0.48	98.91 ±0.29	96.62 ±0.51	99.09 ±0.46	
	F1	96.82 ±0.15	99.21 ±0.48	98.92 ±0.31	96.60 ±0.51	99.01 ±0.52	
DISR	A1	96.78 ±0.20	98.47 ±0.63	97.89 ±0.51	96.60 ±0.34	99.36 ±0.32	97.66
	P1	96.80 ±0.22	98.14 ±0.82	97.79 ±0.53	96.28 ±0.42	98.91 ±0.60	
	R1	96.78 ±0.23	97.76 ±0.80	97.92 ±0.54	96.31 ±0.33	99.08 ±0.46	
	F1	96.78 ±0.23	97.93 ±0.80	97.85 ±0.52	96.28 ±0.34	98.99 ±0.52	

A1: Accuracy, P1: Precision, R1: Recall, F1: F-score

or three features can produce the accuracy of over 99.3% in Bedroom; both Kitchen and Bathroom achieve their increased accuracy of over 98% using no more than 20 features. To the mRMR, it is found that f_{40} , i.e., the 90th percentile of the *roll*, ranks top 10 selected features for all models, top three in Bedroom and Kitchen, top five for the case of all activities. Also, eight out of top ten selected features are related to the *roll* according to the number of occurrences of each selected feature. To the CMIM, f_{40} also ranks the top selected features for all room-based submodels. The last column in Table 6.4 gives the computation time of the feature selection with the same computer configuration and the time drops for each room-level task compared to the task of recognizing all the activities together using mRMR and CMIM.

To study the performance of each activity before and after data fusion, we look into the results from the mRMR and keep an eye on the CMIM. Table A.1 and Table A.2 present the correct and incorrect classifications of before and after data fusion. When using mRMR for

Table 6. 4 Features selected by mRMR and CMIM before and after data fusion

FS	Model for	# Selected features	Feature ranking	Computation consuming (s)
mRMR	All activities	30	$f_{52} f_{49} f_{28} f_3 \mathbf{f_{40}} f_{46} f_9 f_{37} f_{31} f_6 f_8 f_{34} f_{55} f_{58} f_{69} f_7 f_{43} f_{64} f_{42} f_{47} f_{59} f_{25} f_{63} f_{41} f_{61} f_{38} f_{62} f_{60} f_{35} f_{21}$	1.765455
	Bathroom	20	$f_{46} f_{49} f_9 f_{16} f_{37} f_{47} f_7 f_{52} \mathbf{f_{40}} f_{43} f_{55} f_{64} f_{28} f_{41} f_{34} f_{14} f_{59} f_3 f_{58} f_{61}$	0.138422
	Kitchen	20	$f_{28} f_8 \mathbf{f_{40}} f_{52} f_{46} f_7 f_{31} f_{49} f_3 f_{37} f_{33} f_{34} f_{59} f_{58} f_{55} f_{21} f_{47} f_{42} f_{48} f_{41}$	0.346742
	Living room	25	$f_{28} f_9 f_{49} f_6 f_{59} f_{37} f_8 f_{31} f_7 \mathbf{f_{40}} f_{52} f_{43} f_{69} f_{21} f_{34} f_{60} f_{55} f_{25} f_3 f_{41} f_{58} f_{64} f_{44} f_{42} f_{61}$	0.566477
	Bedroom	3	$\mathbf{f_{40}} f_6 f_{21}$	0.023285
CMIM	All activities	30	$f_{52} f_9 f_{49} f_{46} f_6 f_{14} f_7 f_{50} f_{35} f_{55} f_2 f_{66} f_{45} f_{47} f_8 f_{16} f_{48} f_{51} f_{31} f_{29} f_{70} f_{13} f_3 f_{12} f_{17} f_5 f_{32} f_{26} f_{22} f_{30}$	2.715012
	Bathroom	16	$f_{46} f_{49} f_9 \mathbf{f_{40}} f_{16} f_{52} f_{43} f_{37} f_{64} f_{34} f_{58} f_{28} f_7 f_3 f_{55} f_{41}$	0.175898
	Kitchen	16	$f_{28} f_8 \mathbf{f_{40}} f_{52} f_7 f_{31} f_{37} f_3 f_{46} f_{49} f_{34} f_{58} f_{33} f_{41} f_{55} f_{42}$	0.405028
	Living room	24	$f_{28} f_9 f_{49} f_6 f_{59} f_{37} f_8 f_{69} \mathbf{f_{40}} f_{52} f_{43} f_{31} f_7 f_{34} f_{64} f_3 f_{21} f_{58} f_{41} f_{55} f_{62} f_{25} f_{60} f_{46}$	0.440814
	Bedroom	2	$\mathbf{f_{40}} f_{21}$	0.036533

feature selection, Table A.2 indicates that the vast majority of activities achieve an increased accuracy after applying the data fusion. For instance, the Read obtains the largest increase by 10.09%, next is the Stairs with a rise of 8.49% and followed by the Mop with an improvement of 5.28%. Only the Falls and the Stand have a little drop in accuracy. The improved recognition results can be attributed to the assumption that some confusing activities are separated into different room groups to avoid misclassification. In Table A.1, 1.92% of patterns from the Phone are incorrectly classified as the Brush when using the wearable sensors alone. While, when the Brush is limited in Bathroom after applying data fusion, the accuracy of the Phone rises to 99.95% in Table A.2 from 97.77% in Table A.1. Similarly, 13.1% of the Read are misclassified as the Lie before data fusion in Table A.1, while only 5.38% of the Read are misclassified as the Watch after data fusion in Table A.2; this can help partially explain why the Read obtains greatly increased accuracy. Collectively, the Read and the Watch, the Walk and the Stairs, rank the most two confusing pairs of activities, although

the recognition accuracies are improved after data fusion. The Clean, the Cook, the Exercise, the Phone, the Stand, and Wash seem to be easily distinguished from other activities regardless of combining ambient information or not. For the results from the CMIM in Table A.3 and Table A.4, the experimental results exhibit certain different findings. The activities that already have high accuracies of over 99% before data fusion, such as the Clean, the Exercise and the Phone, only have a slight increase or remain unchanged in accuracy after data fusion. The Stairs and the Walk, on the other hand, present a further increase of 4.97% and 3.66%, respectively. Also, the great improvements can be found to the Read, the Watch, the Stand, and the Mop.

6.2.2 Data fusion of the hybrid sensory system using mRMJR-KCCA feature selection

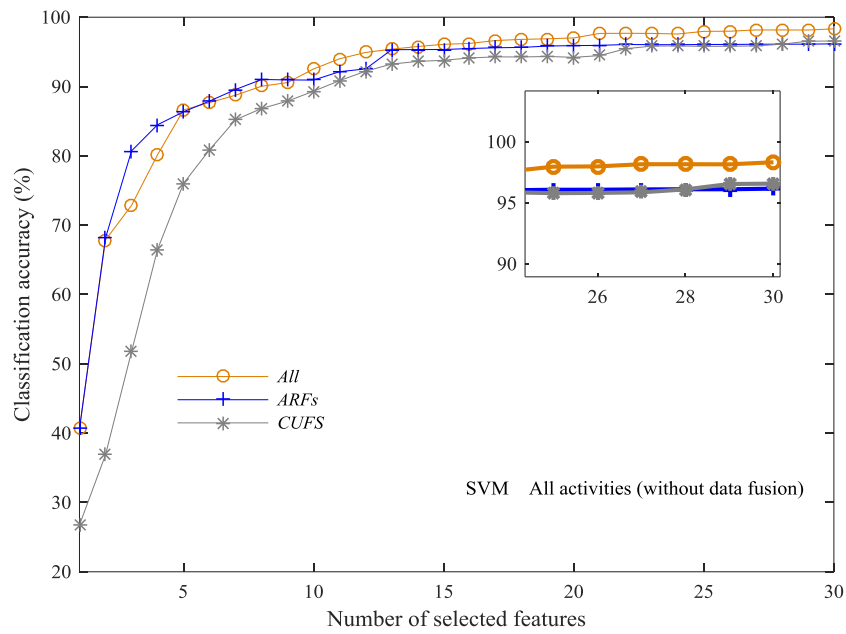
In Section 5.2, experimental results using mRMJR-KCCA and other four MI-based feature selection methods all suggest the very limited contribution of the barometer and the temperature sensor to HAR in this research. Section 5.3.2 identifies the contribution of the different feature sets (presented in Table 4.5). The SVM and RF classification plus the mRMJR-KCCA feature selection give the consistent performance of $Accuracy_{All} > Accuracy_{CUFs} > Accuracy_{ARFs}$. Referring to Figure 5.8 using RF+mRMJR-KCCA, the accuracy with the top 30 selected features for feature set *All* ($CUFs+ARFs$), *CUFs* and *ARFs* are $98.48\% \pm 0.22$, $97.65\% \pm 0.21$, and $96.28\% \pm 0.22$, respectively; and the counterparts in Figure 5.9 using SVM+mRMJR-KCCA are $98.32\% \pm 0.27$, $96.57\% \pm 0.3$ and $96.16 \pm 0.36\%$, respectively. The feature set *All* ($ARFs + CUFs$) performs best with both RF and SVM; *ARFs* and *CUFs* also give satisfactory results. This section, therefore, uses the mRMJR-KCCA feature selection with SVM and RF classification evaluating the data fusion. The data fusion experiments are first conducted based on feature set *All* ($CUFs+ARFs$), *CUFs* and *ARFs* from the three sensors (AGM) and the detailed results before and after data fusion are then reported. Note that the number of the original features for *CUFs*, *ARFs* and *All* are 276, 75 and 351 respectively, with 20 features originated from the barometer and the temperature being excluded from *CUFs* and *All* in Table 4.5.

Figure 6.3 and Figure 6.4 shows the classification accuracy based on the three feature sets (*All*, *CUFs* and *ARFs*) from AGM using mRMJR-KCCA plus SVM and RF respectively. The results from Figure 6.3 (b) to (e) and Figure 6.4 (b) to (e) show that the classification accuracy for each room-based model after data fusion increases to some extent using a much smaller number of selected features. For example, Bedroom uses three features; Bathroom uses around

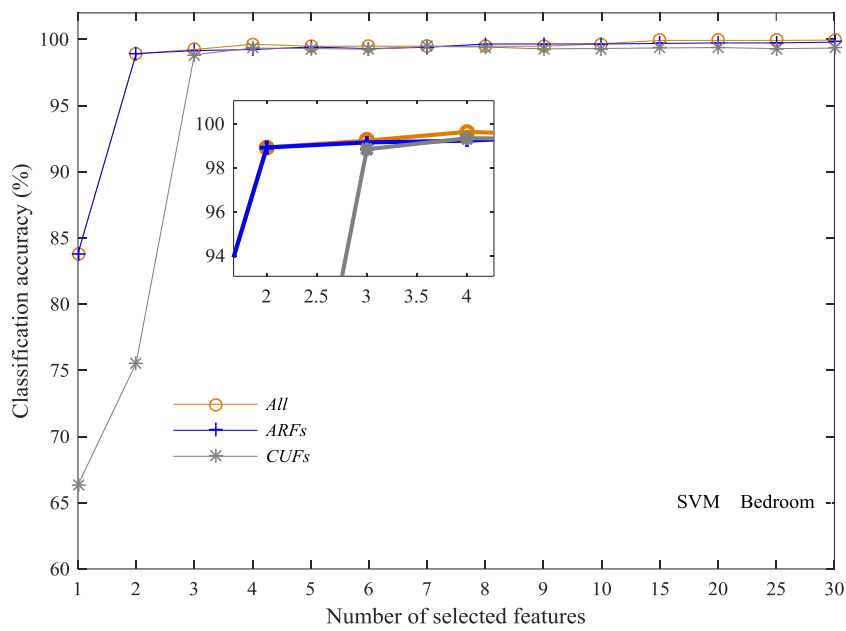
15 features, Kitchen and Living room use approximate 20 features achieving higher accuracies. The classification before data fusion in Figure 6.3 (a) and Figure 6.4 (a) use 25 to 30 selected features. Feature sets *All*, *CUFs* and *ARFs* exhibit different contributions on different models. For example, from Figure 6.3 (a) and Figure 6.4, we can see that the feature set *All* performs best, followed by *CUFs* and *ARFs* with both SVM and RF classification. After being applied data fusion in Figure 6.3 (b) to (e) and Figure 6.4 (b) to (e), the feature set *All* performs best on most room-based models, especially those with larger number of activities to recognize, such as living room and the whole model; *ARFs* give best results on Kitchen with SVM, *CUFs* perform best on Bedroom with RF and produce lower accuracy on Kitchen with both RF and SVM.

Table 6.5 details the results from Figure 6.4 with fixed number of selected features, from which we can see that the overall accuracy after data fusion is greater than the accuracy of the whole model which deals with all the activities together using wearable data, e.g., the overall accuracy before and after data fusion is 96.31% and 97.94% respectively on *ARFs*; 97.42% and 98.85% respectively on *CUFs*; 98.96% and 98.56% respectively on *All*. The best performance is obtained by RF+mRMJR-KCCA on the feature set of *All* (*CUFs* +*ARFs*). The feature set *CUFs* produces similar overall accuracy after data fusion with the feature set *All*, nevertheless, its performance of $97.42\% \pm 0.32$ before data fusion is lower than the performance of *All* ($98.56\% \pm 0.23$). Based on the results from RF+mRMJR-KCCA in Table 6.5, the accuracy distribution of all the 17 activities before and after data fusion on each feature set is plotted in Figure 6.5, in which the bottom and top edges of the box indicate the 25th and 75th percentiles on each box and the whiskers extend to the most extreme data points without considering outliers. Figure 6.5 also tells us that the maximum and median (the red central mark) rise after data fusion on each feature set; and the outlier ('+' symbol on each box) approaches closer to the rest of the data on *ARFs* and disappears on *All* and *CUFs* after data fusion.

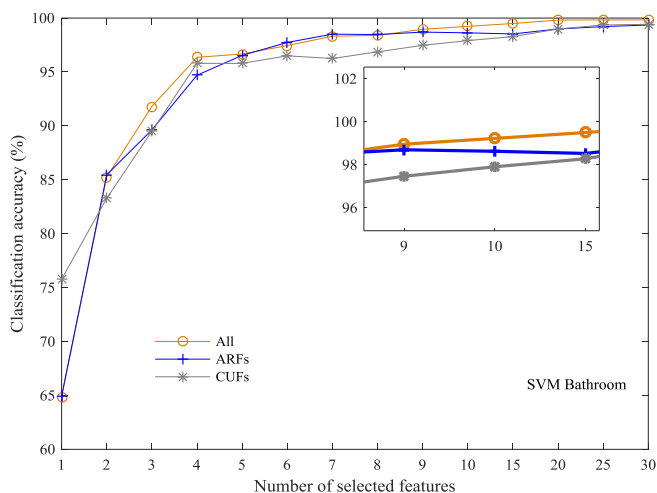
Take the results from the feature set *All* as an example in Table 6.5, Table A.5 and Table A.6 detail the correct and incorrect classifications for each activity before and after data fusion respectively. Comparing the two tables, the activity of Watch obtains the biggest improvement from 97.72% to 99.84%. Eat, Lie and Stand also achieve higher performance after data fusion with more than 1% improvement. Brush, Clean, Cook, Exercise, Phone, Wash, Wipe and other activities already acquire high accuracies before data fusion, and their corresponding performance remains almost unchanged after data fusion. While, Iron, Walk, and Falls see an



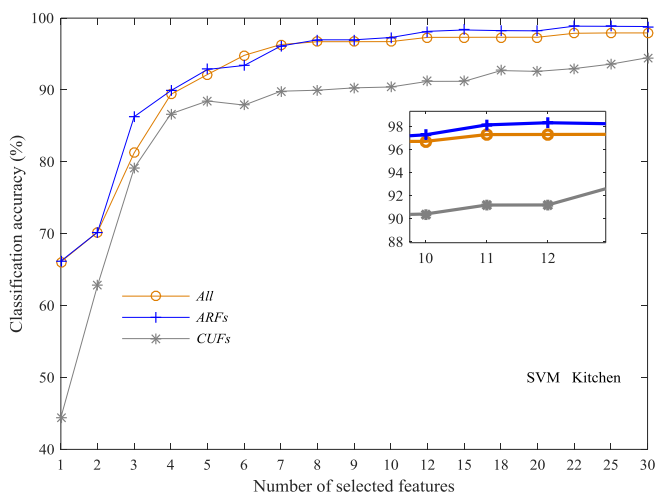
6.3 (a)



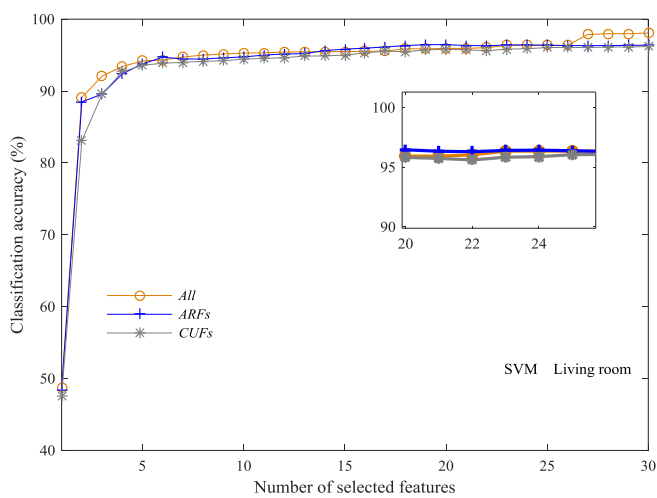
6.3 (b)



6.3 (c)

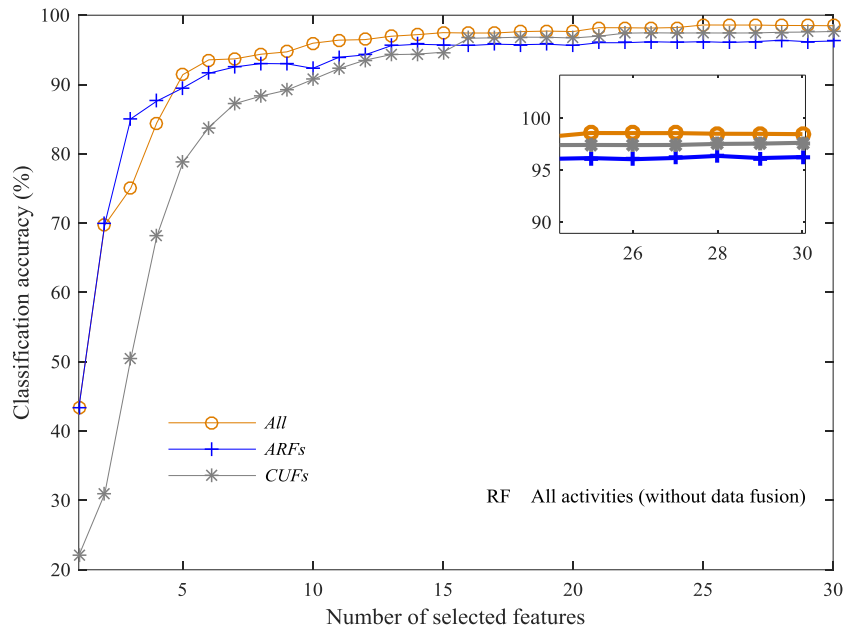


6.3 (d)

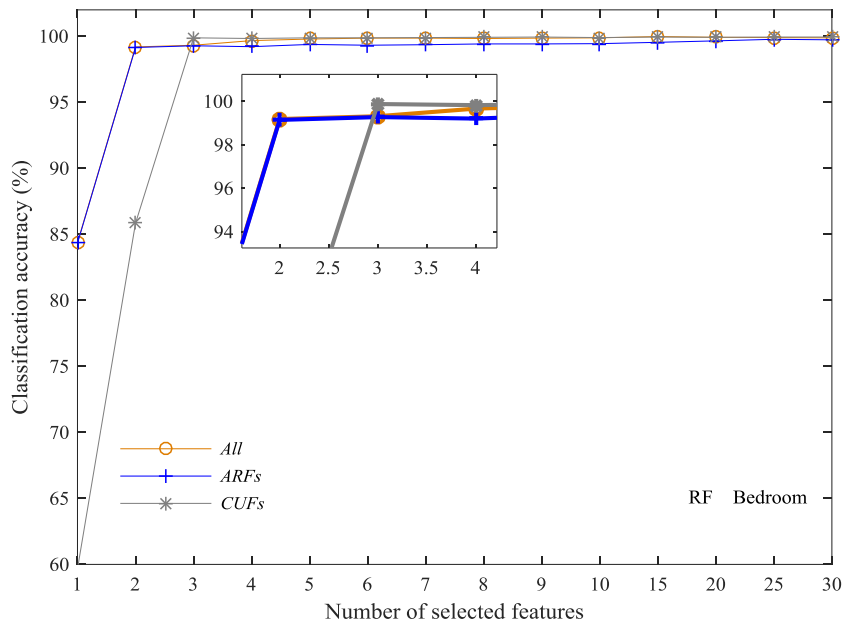


6.3 (e)

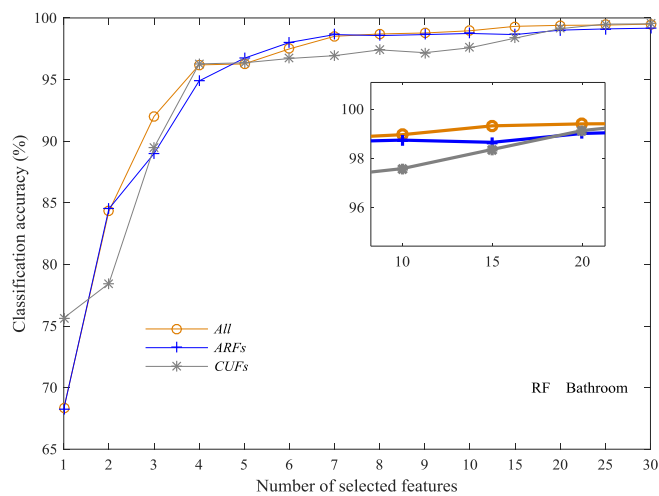
Figure 6. 3 Classification accuracy of before and after data fusion with SVM+mRMJR-KCCA



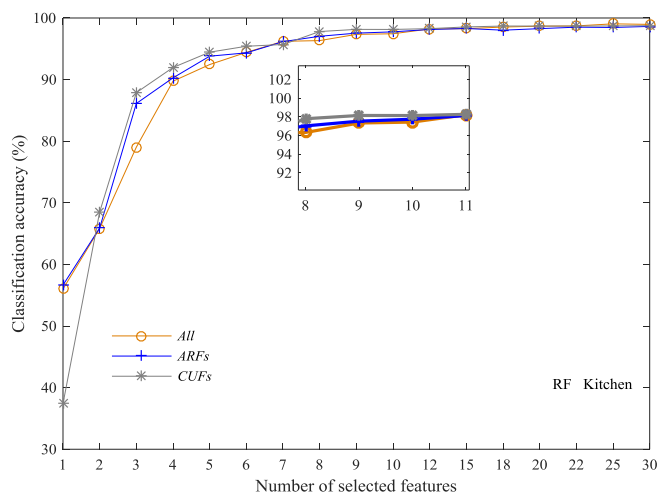
6.4 (a)



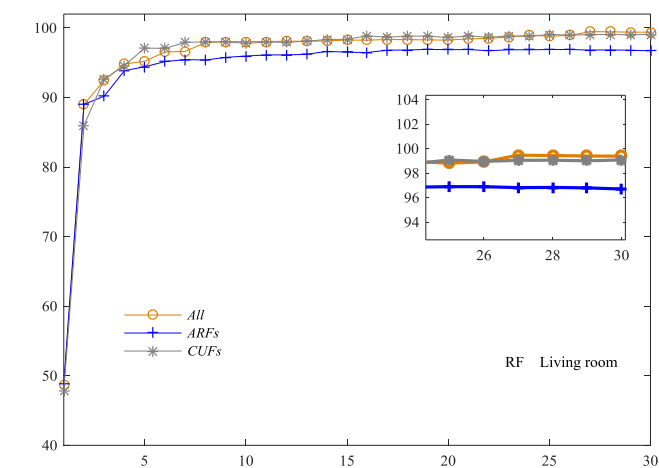
6.4 (b)



6.4 (c)



6.4 (d)



6.4 (e)

Figure 6. 4 Classification accuracy of before and after data fusion with RF+mRMJR-KCCA

obvious decrease in accuracy. To explain the dropped accuracy of Iron after data fusion, there are two possible reasons, one could be attributed to that the optimal number of trees in RF failed to be searched; the other explanation could be that the selected features are less helpful to differentiate Iron from Wipe in Kitchen, as 2.8% of Iron misclassified as Wipe.

6.3 Summary

This chapter presents the experimental results on data fusion. First, the daily routine derived from the PIR sensors are discussed. The example shown in Figure 6.2 can monitor a user's room-level daily routine and answer the questions of when, how long, and how often (WHH) the user takes in a specific room. Additionally, the logged $\{0,1\}$ digital series from PIR sensors have another role in the system, i.e., instead of extracting features from the room location information as the input of a classifier, we use the binary location information to trigger sub classification models in data fusion. In other words, the whole task of recognizing all defined 17 activities are skilfully separated into several subtasks according to the room-level location information captured by infrared sensors. By doing this, we improve the overall accuracy practically. Next, to fuse the ambient data with the wearable data, we use four MI-based methods for feature selection, SVM and RF for classification. The CMIM plus SVM achieves the highest accuracy of 98.32% after data fusion on the feature set *ARFs*, with the accuracy of 96.82% before data fusion, shown in Table 6.3. With data fusion, the room-based submodels are assigned with smaller numbers of activities, and most submodels obtain their improved performance. Bathroom, Kitchen, and Bedroom all greatly increase after data fusion with a smaller number of features; and experimental results show that the vast majority of activities achieve an increased accuracy after applying the data fusion.

Finally, we use our proposed feature selection method mRMJR-KCCA for data fusion evaluation on three feature sets *All*, *CUFs* and *ARFs*. Similarly, the overall accuracy after data fusion is greater than the accuracy of the whole model which deals with all the activities together using wearable data. The best performance is obtained by RF+mRMJR-KCCA on the feature set of *All* (*CUFs* +*ARFs*) with a smaller number of used features for each sub-model, with the accuracy of 98.96% after data fusion and 98.56% before data fusion respectively, as shown in Table 6.5.

Table 6. 5 Classification accuracy with RF before and after data fusion on different feature sets from AGM

	Model (# activity)	Accuracy (%)	# features used	Model (# activity)	Accuracy (%)	# features used	Model (# activity)	Accuracy (%)	# features used
After data fusion	Bed (5)	99.88±0.17	3	Bed (5)	99.30±0.26	3	Bed (5)	99.28±0.34	3
	Bath (5)	98.43±0.54	15	Bath (5)	99.32±0.37	15	Bath (5)	98.61±0.85	15
	Kitchen (8)	98.69±0.31	20	Kitchen (8)	98.73±0.59	18	Kitchen (8)	98.35±0.48	20
	Living room (10)	98.90±0.35	20	Living room (10)	98.88±0.30	20	Living room (10)	96.92±0.35	18
	Overall accuracy	98.85		Overall accuracy	98.96		Overall accuracy	97.94	
Before data fusion	Whole model (17)	97.42±0.32	25	Whole model (17)	98.56±0.23	25	Whole model (17)	96.31±0.38	25
Feature set	<i>CUFs</i>			<i>All (CUFs +ARFs)</i>			<i>ARFs</i>		

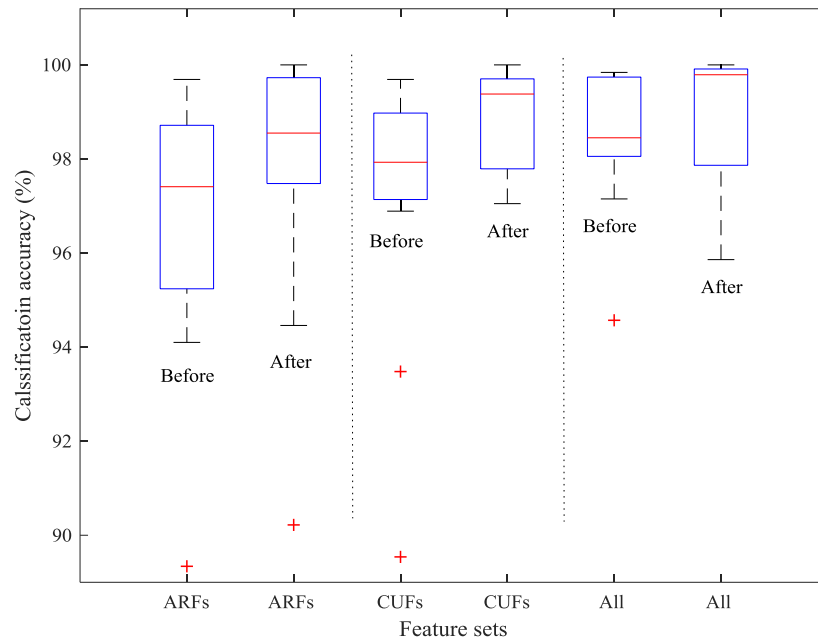


Figure 6. 5 Classification accuracy of all 17 activities with RF on different feature sets before and after data fusion

Chapter 7

Conclusions and future works

7.1 Thesis summary

The ageing population has caused many potential impacts on families, communities as well as societies, e.g., the increasing expenditure on healthcare. Older people need more options to organize their healthcare to enhance confidence in living independently and improve the quality of living. Human Activity Recognition (HAR) is one of the most important assisted technologies, with the aim of recognizing the user's activities from a series of observations on the user's behaviour in real life settings. HAR enables not only personalized supporting for maximizing independence, home rehabilitation as well as early diagnosis of certain diseases, but connecting to other associated applications, such as sports, entertainment or sociology. A typical HAR normally exploits a single modality sensor, i.e., wearable or ambient alone. Each sensor modality has its limitations, and single sensor modalities sometimes cannot cope well with complex situations in practice, which lays the foundation for exploring hybrid sensory systems in HAR.

The proposed system aims to simultaneously monitor older people's specific daily activity, and daily routine, which is designed to answer the questions of WWHH in a HAR assisted living system, i.e., what the user is doing, when, how long, and how often the user stays in specific rooms at home. The final decisions from the system can be sent to the community, caregiver, family members, users themselves, the hospital and the emergency center to ask for further help or other applications.

The initial results are promising. The best wearable sensor combination of sensor candidates is the accelerator, the gyroscope, and the magnetometer; the temperature sensor and the barometer show very limited contribution to the improvement of the recognition accuracy with MI-based and KCCA-based feature selection methods. The ambient sensor network can work

alone for room-level daily routine inferring and the location information from which is also used as the trigger signal in data fusion to activate the room-based submodels. Our proposed feature selection method (mRMJR-KCCA) experimentally outperforms compared with the mutual information-based, Autoencoder, and Sparse Filtering feature selection methods over the ground truth data and other 10 UCI classification-related benchmark datasets. The *ARFs* perform better than the *CUFs* based on the applied four MI-based feature selection methods plus SVM classifiers over the ground truth data; however, the feature set *All (CUFs+ARFs)* perform best on the 17 activities before data fusion with mRMJR-KCCA plus RF. The system uses a unique data fusion approach to hybridize the wearable information and the ambient information. The data fusion improves the accuracy with smaller sizes of features compared with the scenario of recognising all the activities only using the wearable sensors. We evaluate the system based on the data from all the subjects to obtain a model for generic users. Meanwhile, we can also train and test the models subject-dependently to meet specific requirements. Additionally, the wearable network and the ambient network can function as a stand-alone network when any of the other fails to function. The former can work alone for distinguishing the specific activities of the wearer, and the latter can work for monitoring a person's room-level daily routine on its own.

7.2 Main findings

The thesis aims to provide a more accurate and more comprehensive HAR system for older people to assist them living independently, with the objectives of identifying practical ways to improve the recognition accuracy of human activity recognition. The proposed system leverages the advantages of wearable-sensor-based systems and ambient-sensor-based systems to improve recognition accuracy and mitigate obtrusiveness. This chapter presents the reflections of the thesis in responding to the eight objectives set in Chapter 1.

1. Identifying the related research gaps through literature review

We review a large number of papers involving different HAR systems with their applications and the used techniques. The review looks into different sensor modalities, then focuses on wearable-sensor-related methods. Certain key research questions are identified, which include the issues of Determination of the sensor modality for a specific task, Less fully using sensors, Improving feature selection, Data fusion from multiple sensor modalities, Hand-crafted features, and automatically learned features, and so on, shown in Table 2.12.

2. Designing a practical and hybrid sensory system

We develop a practical hybrid human activity recognition system shown in Figure 3.1, in which the wrist-worn device takes the main responsibility to capture the user's data of daily activities and the PIR sensors installed in each room at home to deliver the user's location information. The fusion of data from wearable sensing and ambient sensing is proved to have improved the accuracy significantly with fewer features. We are not the first to propose a hybrid system for HAR. However, our system only uses a wearable device, and one single type of ambient sensor (i.e., PIR sensor) installed at home, which has been preliminarily evaluated to be a practical, simple and compact, more accurate and less obtrusive HAR structure.

3. Building the hybrid sensor network

Based on the proposed system framework, we have initially selected a total of five wearable sensors that are integrated into a small and light device (shown in Figure 3.3). The wearable device delivers not only the variations from each sensor inside but the attitude angles derived from multiple sensors. All the recorded data is wirelessly transported to a processing centre with the sampling rate of 20Hz. The ambient sensor network consists of the Receiving Terminal Unit (RTU) and the Centre Unit (CU) in Figure 3.4. The RTU detects the status of the PIR sensor associated with it. The CU regularly inquires the status of each RTU and receives the data sent from the RTU. The whole sensor network delivers both specific-activity-caused motion information of the wearer and the room-level location information.

4. Collecting multi-activity data in real home settings from older participants

We collect 16 defined daily activities from 21 older participants (aged between 60 and 74, female and male) and Falls from the same number of younger volunteers in real home settings. The demographic information of the participants is shown in Table 4.2. Each activity lasts at least five minutes. A total of 2,142,000 patterns from wearable sensors are obtained taking the sampling rate of 20Hz into account.

5. Identifying the contributions of selected sensors

To identify the contributions of the selected wearable sensors, we combine the sensors in different groups and compare their performances accordingly. For each combination, we first use MI-based feature selection methods selecting the relevant features and then classify them using the SVM and RF classifiers. The test results suggest that using the accelerometer, the gyroscope and the magnetometer together can achieve the highest classification accuracy without the temperature sensor and the barometer included (refer to Table 5.5). We also use the proposed mRMJR-KCCA as the feature selection method, and the results also show the

temperature sensor and the barometer have a very limited contribution to the improvement of activity recognition in our system, since there are very few features related to the barometer and the temperature sensor are selected by different feature selection methods.

6. Extracting augmented features to improve the recognition accuracy and fully use the selected sensors

To evaluate the contributions of the new feature set of *ARFs*, we separate them from the commonly used features (*CUFs*). Although the *ARFs* of the wearable device is not the first time to be used in HAR, other studies only used single or a handful of them for activity recognition without a comprehensive comparison on the contributions of this group of features. We introduce and implement *ARFs* in our HAR system. The experimental results demonstrate the great contribution of *ARFs* to activity recognition with the MI-based feature selection methods (see Figure 5.6). With the proposed mRMJR-KCCA feature selection, the *ARFs* perform better combining with the *CUFs*, especially on before data fusion for all the 17 activities (Figure 5.9). Furthermore, the *ARFs* are related to the attitude angles which are still stemmed from sensors of accelerometer, gyroscope magnetometer. By mining new features, we have fully used the current sensors and obtain the improved performance.

7. Proposing and implementing a new feature selection method

Mutual information (MI)-based feature selection methods explore an entropy-based score between two or three variables when measuring the importance of a feature candidate. Kernel canonical correlation analysis (KCCA), on the other hand, searches for the nonlinear relationship between two sets of variables. We introduce the measurement of KCCA into an MI-based feature selection method (mRMR) to produce the feature selection method, i.e., mRMJR-KCCA. Calculating KCCA directly to implement mRMJR-KCCA on our ground truth data is memory costly, we, therefore, apply Incomplete Cholesky Decomposition to approximate kernel matrix with the aim of improving calculation efficiency. The experimental results demonstrate the better performance of mRMJR-KCCA on 10 UCI classification associated datasets and our system. And the proposed mRMJR-KCCA works better in the identification of the contributions of the selected wearable sensors and the augmented features and the data fusion, referring to Table 5.6, Figure 5.9 and Table 6.5.

8. Proposing a unique and practical data fusion method in hybrid sensor modalities

Our proposed hybrid system is simple and practical, which finally only needs three wrist-worn wearable sensors and one type of ambient sensor (i.e., PIR sensor) installed in each room. The ambient information is fused with the wearable information in a unique way based on the best-

performed feature sets extracted from wearable data. The binary ambient information triggering the room-based-sub-models provides a unique way to combine the ambient information and the wearable information. The improved performance after data fusion can be attributed to two factors: 1) the decrease of activity types reduces the requirements for each room-based model; 2) the confusing activities separated into different rooms can avoid the misclassification between them to some extent. After data fusion, the HAR system is extended to be more comprehensive which monitors the specific activities and the daily routine in the spatiotemporal environment simultaneously. According to the structure of homes where we collect data from participants, four new data sets are obtained, i.e., Bathroom (including five activities), Kitchen (eight activities), Bedroom (five activities) as well as Living room (ten activities). Table 6.3 and Table 6.5 give the experimental results before and after applying data fusion in the system with different feature selection methods on different feature sets. The whole recognition performance is improved after data fusion with a much smaller number of selected features compared with the scenario of recognizing all the activities together using wearable data alone.

7.3 Limitations and future direction

The promising results are achieved based on the case study in the designed HAR system, which provides rich insight into how specific daily activities and daily routines can be identified in the assisted living system. The research has, however, a few limitations. And the followed future work after each limitation can highlight the directions.

1. Hardware network

The wearable and the ambient network are separated in the current prototype; the data analysis apart from testing are all offline. Also, the impact of the pets or other visitors on the PIR sensors should be further studied and evaluated. We considered a room with only one door in this thesis; we will explore more PIR sensors to handle a room with multiple doors in our future work. The next version prototype can consider synchronizing two sensor networks into one after further evaluation of other associated problems, like wearable sensor displacement and comparisons between hand-crafted features and automatically learned features by deep networks. The current system targets older people who live alone. If the application is scaled up to a multi-person system, the future work should realize the identification of each specific user to activate sub classification models regarding the hardware part.

2. Data collection and activity assignment in rooms

It is worth noting that a larger data set is beneficial for evaluating our proposed system. Therefore, our data set has 17 activities, which is large enough for our experimental purpose. The limitation is that the types of the defined activities and activity assignment in each room are fixed. As a case study, we generally define the activities which most likely take place in different rooms to verify our system. In real use, since house structures and people habits vary, we cannot say hundred percent that what activities must occur in one specific room or not, for example, the Read can take place anywhere. The activity assignment in each room can refer to the research interests in different targeting applications, for instance, a doctor cares about whether a patient sleeps or lies in the bedroom instead of reading or not. Also, the data are collected only from Chinese, a larger population from different groups should be included in data collection.

We do not intend to identify all possible daily activities due to the uncertainty of daily activity types, privacy concerns as well as technical limitations; we predefine and detect a set of limited activities. While in real use, the classifier cannot avoid encountering the unknown or untrained activities. An extension of our work could thus explore semi-supervised methods based on feature mapping and feature similarity to learn unseen activities, in which we will regard part of the activities we defined in this research as unlabeled or unseen in both the home-level and the room level to address the limitation. We also plan to apply transfer learning to share the trained models and parameters on the known activities to learn new or unseen activities to reduce training time and provide versatile HAR system.

3. Fixed sensor attachment on the wrist

The wearable device in this research is tightly attached to the wrist of the wearer. Nevertheless, a user's self-placement or loose wearing in real use usually causes sensor displacement. The classification models trained to take no account of sensor displacement might fail to accurately recognize the activities when sensor displacement occurs. The impact of the sensor displacement on the recognition performance and the corresponding compensations can be further studied in the future work.

The current results are achieved without considering the sensor displacement of the wearable device. Sensor displace can happen in real use due to the user's self-placement and loose wearing. The goal of our future work is to investigate the impact of the sensor displacement on the daily activity recognition accuracy and compensate the displacement by featuring learning. The data regarding sensor displacement is already collected in Italy, from 12 local older people (seven male and five female). Two out of 12 data collections are carried

out in the participant's home, and the rest is done in a bar where local people get together for relaxing. We define four basic daily activities, i.e., standing, walking, lying and stairs using. We use the same wearable sensors used in the thesis acquiring the movement-caused signals. During data collection, the wearable device is still tightly bound at the user's dominant wrist in four predefined positions: top, left, right and bottom of the wrist. The four positions are to mimic the sensor displacement during real use. The participants are encouraged to perform each defined activity at each sensor placement, and each participant finishes each of four activities for four rounds accordingly.

4. Hand-crafted features and automatically learned features

Extracting effective features for identifying activities is a critical and challenging task. This research explores the useful hand-crafted features and proposes an effective feature selection method on the ground truth data. Nevertheless, there are no universal procedures for selecting appropriate features from hand-crafted features for a given human activity recognition system, referring to the experimental results in Table 5.3 and Table 5.4. These years see another way to automatically learned features from the raw data based on deep learning methods. Deep learning is about automatic extraction of features from raw data without any domain knowledge. Deep learning techniques have been developed and successfully applied in recognition tasks. Meanwhile, some other studies give certain interesting findings, e.g., the experimental results in Khan and Yong, 2016 indicate that the hand-crafted features outperform the automatically learned features in the medical image field. Kashif et al., 2016 conclude that the combination of hand-crafted features with raw data produces better detection results than the results of raw intensities with a similar kind of CNN architecture. Consequently, the feature learning could depend on a task at hand. This thesis focuses on using some typical algorithms evaluating our proposed method to provide a practical way for accuracy improving. Our future work will focus on using deep learning to automatically learn the features from the raw data for comparison and combination study with the hand-crafted features based on our system.

5. Data fusion in combined sensor modalities

The system proposed in this thesis combines the wearable sensor modality and ambient sensor modality, which provides a more comprehensive and more accurate HAR monitoring for older people. The ambient information is used as the trigger signal in the current data fusion mechanism. The future work can consider using more PIR sensors and the associated ambient information to explore other data fusion methods in the new system.

Appendix A Experimental results

Table A. 1 Confusion matrix based on mRMR plus SVM before data fusion (wearable sensing alone)

Actual	Classified as (%)																
	Brush	Clean	Cook	Eat	Exer.	Falls	Iron	Lie	Mop	Phone	Read	Stairs	Stand	Walk	Wash	Watch	Wipe
Brush	95.13	1.19	0.16	2.07	0.00	0.05	0.00	0.00	0.00	1.04	0.36	0.00	0.00	0.00	0.00	0.00	0.00
Clean	0.83	98.45	0.26	0.10	0.00	0.21	0.05	0.00	0.00	0.05	0.00	0.00	0.00	0.00	0.00	0.00	0.05
Cook	0.16	0.16	97.05	0.52	0.00	0.10	0.36	0.00	0.26	0.00	0.36	0.00	0.00	0.00	0.98	0.00	0.05
Eat	1.71	0.10	0.88	94.67	0.00	0.16	0.00	0.05	0.00	0.05	2.38	0.00	0.00	0.00	0.00	0.00	0.00
Exer.	0.00	0.16	0.00	0.00	98.55	1.29	0.00	0.00	0.00	0.00	0.00	0.00	0.00	0.00	0.00	0.00	0.00
Falls	0.00	0.00	0.16	0.05	0.16	95.86	0.26	0.00	1.71	0.00	0.00	0.78	0.16	0.67	0.00	0.10	0.10
Iron	0.00	0.10	0.21	0.00	0.00	0.05	93.48	0.00	0.36	0.00	0.00	0.00	0.00	0.00	0.52	0.00	5.28
Lie	0.00	0.00	0.05	0.00	0.00	0.00	0.00	96.79	0.00	0.00	3.00	0.00	0.00	0.00	0.00	0.16	0.00
Mop	0.00	0.05	0.16	0.00	0.00	2.74	0.41	0.00	92.91	0.00	0.00	0.83	0.00	0.62	0.21	0.00	2.07
Phone	1.92	0.31	0.00	0.00	0.00	0.00	0.00	0.00	0.00	97.77	0.00	0.00	0.00	0.00	0.00	0.00	0.00
Read	0.47	0.00	1.19	1.50	0.00	0.00	0.00	13.10	0.00	0.00	82.66	0.00	0.00	0.00	0.36	0.72	0.00
Stairs	0.00	0.00	0.00	0.00	0.00	1.50	0.00	0.00	1.09	0.00	0.00	82.09	0.00	15.32	0.00	0.00	0.00
Stand	0.00	0.00	0.00	0.00	0.00	0.16	0.00	0.00	0.05	0.00	0.00	0.05	99.64	0.10	0.00	0.00	0.00
Walk	0.00	0.00	0.00	0.00	0.05	0.98	0.00	0.00	0.83	0.00	0.00	13.35	0.05	84.73	0.00	0.00	0.00
Wash	0.00	0.05	1.14	0.00	0.00	0.05	0.67	0.00	0.05	0.00	0.16	0.00	0.00	0.00	97.77	0.10	0.00
Watch	0.00	0.00	0.10	0.00	0.00	0.21	0.36	4.76	0.05	0.00	0.52	0.00	4.76	0.00	0.10	89.08	0.05

Wipe	0.00	0.00	0.05	0.00	0.00	0.16	6.11	0.00	1.35	0.00	0.05	0.00	0.00	0.00	0.10	0.00	92.18
------	------	------	------	------	------	------	------	------	------	------	------	------	------	------	------	------	--------------

Exer. denotes Exercise from Table A.1 to Table A.6

Table A. 2 Confusion matrix based on mRMR plus SVM after data fusion (combined sensing)

Actual	Classified as (%)																
	Brush	Clean	Cook	Eat	Exer.	Falls	Iron	Lie	Mop	Phone	Read	Stairs	Stand	Walk	Wash	Watch	Wipe
Brush	100.00	0.00	0.00	0.00	0.00	0.00	0.00	0.00	0.00	0.00	0.00	0.00	0.00	0.00	0.00	0.00	0.00
Clean	0.10	99.38	0.05	0.00	0.00	0.10	0.00	0.00	0.36	0.00	0.00	0.00	0.00	0.00	0.00	0.00	0.00
Cook	0.00	0.00	99.95	0.00	0.00	0.00	0.00	0.00	0.00	0.00	0.00	0.00	0.00	0.00	0.05	0.00	0.00
Eat	0.00	0.00	0.00	98.24	0.00	0.16	0.88	0.00	0.00	0.00	0.72	0.00	0.00	0.00	0.00	0.00	0.00
Exer.	0.00	0.00	0.00	0.00	99.90	0.05	0.00	0.00	0.00	0.05	0.00	0.00	0.00	0.00	0.00	0.00	0.00
Falls	0.00	0.00	0.00	0.21	0.05	95.70	0.05	0.00	1.97	0.05	0.00	0.52	0.31	1.09	0.00	0.00	0.05
Iron	0.00	0.00	0.00	0.67	0.00	0.10	95.39	0.00	0.00	0.00	0.00	0.00	0.00	0.05	0.10	0.16	3.52
Lie	0.00	0.00	0.00	0.00	0.00	0.00	0.00	100.00	0.00	0.00	0.00	0.00	0.00	0.00	0.00	0.00	0.00
Mop	0.00	0.05	0.00	0.00	0.00	1.35	0.00	0.00	98.19	0.00	0.00	0.00	0.00	0.00	0.00	0.00	0.41
Phone	0.00	0.00	0.00	0.00	0.05	0.00	0.00	0.00	0.00	99.95	0.00	0.00	0.00	0.00	0.00	0.00	0.00
Read	0.00	0.00	0.00	1.71	0.00	0.05	0.05	0.00	0.00	0.05	92.75	0.00	0.00	0.00	0.00	5.38	0.00
Stairs	0.00	0.00	0.00	0.00	0.00	0.41	0.00	0.00	0.00	0.00	0.00	90.58	0.10	8.90	0.00	0.00	0.00
Stand	0.00	0.00	0.00	0.00	0.00	0.21	0.00	0.00	0.00	0.00	0.00	0.21	99.38	0.05	0.00	0.16	0.00
Walk	0.00	0.00	0.00	0.00	0.00	0.98	0.00	0.00	0.00	0.00	0.00	9.06	0.05	89.91	0.00	0.00	0.00
Wash	0.00	0.00	0.05	0.00	0.00	0.00	0.21	0.00	0.00	0.00	0.00	0.00	0.00	0.00	99.69	0.00	0.05
Watch	0.00	0.00	0.00	0.16	0.00	0.21	0.78	0.00	0.00	0.00	4.19	0.00	3.67	0.00	0.00	90.99	0.00

Wipe	0.00	0.00	0.00	0.00	0.00	0.05	3.99	0.00	0.21	0.00	0.00	0.00	0.00	0.00	0.05	0.00	95.70
------	------	------	------	------	------	------	------	------	------	------	------	------	------	------	------	------	--------------

Table A. 3 Confusion matrix based on CMIM plus SVM before data fusion (wearable sensing alone)

Actual	Classified as (%)																
	Brush	Clean	Cook	Eat	Exer.	Falls	Iron	Lie	Mop	Phone	Read	Stairs	Stand	Walk	Wash	Watch	Wipe
Brush	99.74	0.05	0.00	0.10	0.00	0.05	0.00	0.00	0.00	0.00	0.00	0.00	0.00	0.00	0.05	0.00	0.00
Clean	0.16	99.69	0.10	0.00	0.00	0.00	0.00	0.00	0.00	0.05	0.00	0.00	0.00	0.00	0.00	0.00	0.00
Cook	0.00	0.00	98.96	0.21	0.00	0.05	0.10	0.05	0.10	0.00	0.00	0.00	0.00	0.00	0.41	0.00	0.10
Eat	0.10	0.00	0.16	98.71	0.00	0.05	0.00	0.05	0.00	0.00	0.93	0.00	0.00	0.00	0.00	0.00	0.00
Exer.	0.00	0.16	0.00	0.00	99.74	0.10	0.00	0.00	0.00	0.00	0.00	0.00	0.00	0.00	0.00	0.00	0.00
Falls	0.00	0.00	0.16	0.05	0.21	97.31	0.16	0.00	0.88	0.00	0.00	0.52	0.16	0.52	0.00	0.05	0.00
Iron	0.00	0.00	0.05	0.00	0.00	0.05	97.15	0.00	0.05	0.00	0.00	0.00	0.00	0.05	0.10	0.00	2.54
Lie	0.00	0.00	0.00	0.10	0.00	0.00	0.00	98.45	0.00	0.00	1.24	0.00	0.00	0.00	0.00	0.21	0.00
Mop	0.00	0.00	0.05	0.00	0.00	1.14	0.16	0.00	97.26	0.00	0.00	0.41	0.00	0.21	0.00	0.00	0.78
Phone	0.16	0.10	0.00	0.00	0.00	0.00	0.00	0.00	0.00	99.74	0.00	0.00	0.00	0.00	0.00	0.00	0.00
Read	0.00	0.00	0.26	0.88	0.00	0.05	0.00	1.81	0.00	0.00	96.33	0.00	0.00	0.00	0.10	0.57	0.00
Stairs	0.00	0.00	0.00	0.00	0.00	0.72	0.00	0.00	0.57	0.00	0.00	86.39	0.00	12.32	0.00	0.00	0.00
Stand	0.00	0.00	0.00	0.00	0.00	0.05	0.00	0.00	0.00	0.00	0.00	0.00	97.46	0.00	0.00	2.48	0.00
Walk	0.00	0.00	0.00	0.00	0.00	0.47	0.00	0.00	0.47	0.00	0.00	11.02	0.00	88.04	0.00	0.00	0.00
Wash	0.00	0.00	0.78	0.00	0.00	0.05	0.21	0.00	0.00	0.00	0.05	0.00	0.00	0.00	98.86	0.00	0.05
Watch	0.00	0.00	0.00	0.10	0.00	0.31	0.00	0.21	0.00	0.00	0.62	0.00	2.59	0.00	0.10	96.07	0.00
Wipe	0.00	0.00	0.00	0.00	0.00	0.00	3.11	0.00	0.52	0.00	0.05	0.00	0.00	0.05	0.16	0.00	96.12

Table A. 4 Confusion matrix based on CMIM plus SVM after data fusion (combined sensing)

Actual	Classified as (%)																
	Brush	Clean	Cook	Eat	Exer.	Falls	Iron	Lie	Mop	Phone	Read	Stairs	Stand	Walk	Wash	Watch	Wipe
Brush	99.95	0.05	0.00	0.00	0.00	0.00	0.00	0.00	0.00	0.00	0.00	0.00	0.00	0.00	0.00	0.00	0.00
Clean	0.26	99.69	0.05	0.00	0.00	0.00	0.00	0.00	0.00	0.00	0.00	0.00	0.00	0.00	0.00	0.00	0.00
Cook	0.00	0.00	99.90	0.00	0.00	0.05	0.00	0.00	0.00	0.00	0.00	0.00	0.00	0.00	0.05	0.00	0.00
Eat	0.00	0.00	0.00	99.69	0.00	0.10	0.21	0.00	0.00	0.00	0.00	0.00	0.00	0.00	0.00	0.00	0.00
Exer.	0.00	0.00	0.00	0.00	99.95	0.00	0.00	0.00	0.00	0.05	0.00	0.00	0.00	0.00	0.00	0.00	0.00
Falls	0.00	0.00	0.00	0.10	0.00	97.77	0.05	0.00	0.72	0.00	0.05	0.26	0.31	0.67	0.00	0.05	0.00
Iron	0.00	0.00	0.00	0.10	0.00	0.00	97.67	0.00	0.00	0.00	0.00	0.00	0.00	0.05	0.10	0.00	2.07
Lie	0.00	0.00	0.00	0.00	0.00	0.00	0.00	100.00	0.00	0.00	0.00	0.00	0.00	0.00	0.00	0.00	0.00
Mop	0.00	0.05	0.00	0.00	0.00	0.52	0.00	0.00	99.12	0.00	0.00	0.00	0.05	0.00	0.00	0.00	0.26
Phone	0.00	0.00	0.00	0.00	0.00	0.16	0.00	0.00	0.00	99.84	0.00	0.00	0.00	0.00	0.00	0.00	0.00
Read	0.00	0.00	0.00	0.31	0.00	0.00	0.00	0.00	0.00	0.00	98.86	0.00	0.00	0.00	0.00	0.83	0.00
Stairs	0.00	0.00	0.00	0.00	0.00	0.31	0.00	0.00	0.00	0.00	0.00	91.36	0.05	8.28	0.00	0.00	0.00
Stand	0.00	0.00	0.00	0.00	0.00	0.16	0.00	0.00	0.00	0.00	0.00	0.16	99.59	0.05	0.00	0.05	0.00
Walk	0.00	0.00	0.00	0.05	0.00	0.98	0.00	0.00	0.00	0.00	0.00	8.13	0.05	90.79	0.00	0.00	0.00
Wash	0.00	0.00	0.00	0.00	0.00	0.00	0.16	0.00	0.00	0.00	0.00	0.00	0.00	0.00	99.79	0.00	0.05
Watch	0.00	0.00	0.00	0.05	0.00	0.16	0.21	0.00	0.00	0.00	1.71	0.10	0.05	0.00	0.00	97.72	0.00
Wipe	0.00	0.00	0.00	0.00	0.00	0.10	1.60	0.00	0.21	0.00	0.00	0.00	0.00	0.00	0.10	0.00	97.98

Table A. 5 Confusion matrix based on mRMJR-KCCA plus RF before data fusion

Actually classified as (%)																	
	Brush	Clean	Cook	Eat	Exer	Falls	Iron	Lie	Mop	Phone	Read	Stairs	Stand	Walk	Wash	Watch	Wipe
Brush	99.74	0.00	0.00	0.10	0.00	0.00	0.00	0.00	0.00	0.00	0.00	0.00	0.00	0.00	0.16	0.00	0.00
Clean	0.05	99.79	0.05	0.00	0.00	0.00	0.00	0.00	0.10	0.00	0.00	0.00	0.00	0.00	0.00	0.00	0.00
Cook	0.00	0.00	99.74	0.10	0.00	0.00	0.00	0.00	0.00	0.00	0.05	0.00	0.00	0.00	0.00	0.05	0.05
Eat	0.10	0.00	0.16	98.29	0.00	0.00	0.00	0.05	0.00	0.10	1.29	0.00	0.00	0.00	0.00	0.00	0.00
Exer	0.00	0.16	0.00	0.05	99.74	0.05	0.00	0.00	0.00	0.00	0.00	0.00	0.00	0.00	0.00	0.00	0.00
Falls	0.00	0.00	0.00	0.21	0.16	98.45	0.05	0.00	0.41	0.00	0.05	0.05	0.16	0.21	0.00	0.26	0.00
Iron	0.00	0.00	0.16	0.00	0.00	0.00	99.28	0.00	0.05	0.00	0.00	0.00	0.00	0.00	0.00	0.00	0.52
Lie	0.00	0.00	0.00	0.00	0.00	0.00	0.00	98.45	0.00	0.00	1.50	0.00	0.00	0.00	0.00	0.05	0.00
Mop	0.00	0.00	0.05	0.00	0.00	0.67	0.00	0.00	98.76	0.00	0.00	0.05	0.00	0.10	0.00	0.00	0.36
Phone	0.05	0.10	0.00	0.00	0.00	0.00	0.00	0.00	0.00	99.84	0.00	0.00	0.00	0.00	0.00	0.00	0.00
Read	0.00	0.00	0.16	1.35	0.00	0.00	0.00	0.67	0.00	0.00	97.72	0.00	0.00	0.00	0.10	0.00	0.00
Stairs	0.00	0.00	0.00	0.00	0.00	0.31	0.00	0.00	0.10	0.00	0.00	97.98	0.00	1.60	0.00	0.00	0.00
Stand	0.00	0.00	0.00	0.00	0.00	0.05	0.00	0.00	0.00	0.00	0.00	0.00	98.14	0.00	0.00	1.81	0.00
Walk	0.00	0.00	0.00	0.00	0.00	0.10	0.00	0.00	0.05	0.00	0.00	2.64	0.00	97.15	0.00	0.00	0.05
Wash	0.00	0.00	0.00	0.00	0.00	0.00	0.05	0.00	0.05	0.00	0.00	0.00	0.00	0.00	99.84	0.00	0.05
Watch	0.00	0.00	0.00	0.00	0.00	0.00	0.05	0.05	0.00	0.00	1.04	0.00	4.19	0.00	0.10	94.57	0.00
Wipe	0.00	0.00	0.05	0.00	0.00	0.05	1.60	0.00	0.10	0.00	0.00	0.00	0.00	0.00	0.10	0.00	98.08

Table A. 6 Confusion matrix based on mRMJR-KCCA plus RF after data fusion

Actually classified as (%)																	
	Brush	Clean	Cook	Eat	Exer	Falls	Iron	Lie	Mop	Phone	Read	Stairs	Stand	Walk	Wash	Watch	Wipe
Brush	99.95	0.05	0.00	0.00	0.00	0.00	0.00	0.00	0.00	0.00	0.00	0.00	0.00	0.00	0.00	0.00	0.00
Clean	0.31	99.02	0.21	0.00	0.00	0.00	0.00	0.00	0.36	0.00	0.00	0.00	0.00	0.00	0.10	0.00	0.00
Cook	0.00	0.00	100.00	0.00	0.00	0.00	0.00	0.00	0.00	0.00	0.00	0.00	0.00	0.00	0.00	0.00	0.00
Eat	0.00	0.00	0.00	99.90	0.00	0.05	0.00	0.00	0.00	0.00	0.05	0.00	0.00	0.00	0.00	0.00	0.00
Exer.	0.00	0.00	0.00	0.00	99.90	0.00	0.00	0.00	0.00	0.10	0.00	0.00	0.00	0.00	0.00	0.00	0.00
Falls	0.05	0.00	0.00	0.05	0.16	97.15	0.16	0.05	0.36	0.05	0.16	0.41	0.26	0.98	0.10	0.00	0.05
Iron	0.00	0.00	0.00	0.00	0.00	0.05	97.00	0.00	0.00	0.00	0.00	0.00	0.00	0.00	0.10	0.05	2.80
Lie	0.00	0.00	0.00	0.00	0.00	0.00	0.00	100.00	0.00	0.00	0.00	0.00	0.00	0.00	0.00	0.00	0.00
Mop	0.00	0.05	0.00	0.00	0.00	0.72	0.00	0.00	98.91	0.00	0.00	0.00	0.05	0.00	0.00	0.00	0.26
Phone	0.00	0.00	0.00	0.00	0.00	0.00	0.00	0.00	0.00	100.00	0.00	0.00	0.00	0.00	0.00	0.00	0.00
Read	0.00	0.00	0.00	0.10	0.00	0.00	0.00	0.00	0.00	0.00	99.84	0.00	0.00	0.00	0.00	0.05	0.00
Stairs	0.00	0.00	0.00	0.00	0.00	0.26	0.00	0.00	0.00	0.00	0.00	97.52	0.00	2.23	0.00	0.00	0.00
Stand	0.00	0.00	0.00	0.00	0.00	0.16	0.00	0.00	0.00	0.00	0.00	0.00	99.79	0.05	0.00	0.00	0.00
Walk	0.00	0.00	0.00	0.00	0.00	0.72	0.00	0.00	0.00	0.00	0.00	3.42	0.00	95.86	0.00	0.00	0.00
Wash	0.00	0.00	0.05	0.00	0.00	0.00	0.05	0.00	0.10	0.00	0.00	0.00	0.00	0.00	99.79	0.00	0.00
Watch	0.00	0.00	0.00	0.00	0.00	0.05	0.05	0.00	0.0	0.00	0.16	0.00	0.00	0.00	0.00	99.74	0.00
Wipe	0.00	0.00	0.05	0.00	0.00	0.00	1.66	0.00	0.16	0.00	0.00	0.00	0.00	0.00	0.16	0.00	97.98

Appendix B Participant Information Sheet

The title of the research project

An Activity Recognition System for Elderly People in Assisted Living

Invitation paragraph

You are being invited to take part in a research project. Before you make your decision, it is important for you to understand why the research is being done. Please take time to read the following information carefully and discuss it with others if you wish. Ask us if there is anything that is not clear.

What is the purpose of the project?

In this research, we propose an activity recognition-based assist living system which can identify what activity one person is doing by analyzing the collected data. The results from the research can be used in many potential fields, such as safety monitoring for older adults, home rehabilitation for patients, etc. To develop this system, now we need to collect the daily activity data in China by targeting two different age groups.

What are the requirements for the participants?

We will recruit two groups of participants.

Group1: 20 participants (aged from 60 to 75) who are in good health condition and have the life-care ability.

Group2: 20 participants (aged from 25 to 35).

What do I need to do?

To collect your data, we will use two kinds of sensor devices in the project.

Sensor 1: a watch-like device that will be placed on your wrist (see figure A (a)) to record the signal variations of the sensors, e.g., acceleration and height, when you do the activities.

Sensor 2: a sensor box that will be put on the corner of each room in your house (see Figure A (b)) to record your location information, e.g., the time when you are in your kitchen.

We have prepared the activity list for each group, and you only need to do these activities as how you do them in your daily life.

The activities that you will be doing are:

Group1: watching TV, reading, standing, wiping the table, mopping the floor, walking, washing dishes, brushing teeth, etc.

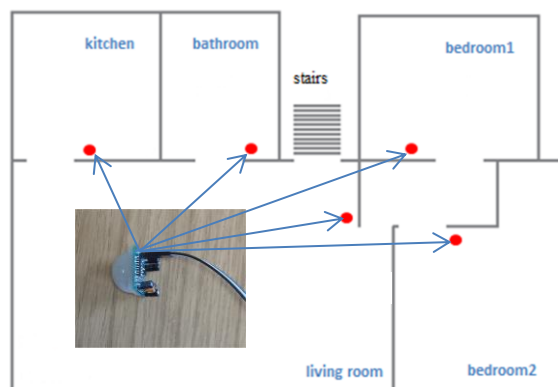
The data collection will be done in your own home since this would help you feel ease and natural. You will complete the listed activities in your way. We will not set any limitations on doing the activities. You can do the activities in any order and have breaks at any time. Each activity is expected to last 5 minutes. Data collection process will take approximately 2 hours.

Group 2: simulating natural falls.

‘Falls detection’ is one of the important tasks in this research. Considering the safety of elderly participants, you will take the place of them to simulate natural falls onto a thick and soft mattress (size: 150 x 200cms, depth: 25cms) on the ground.



(a) Sensor 1 on the wrist



(b) Sensor 2 in the rooms

Figure A The deployment of sensors during data collection

Do I have to take part?

Your decision to participate in this study is entirely voluntary. You will be able to withdraw up to the point of anonymization of the data. You do not need to explain your decision. If you do decide to take part, you will be given this information sheet to keep and be asked to sign a consent form.

What are the possible disadvantages and risks of taking part?

The sensors are completely safe to the human body. Doing daily activities are safe to older participants. Simulating natural falls onto a mattress is also safe for younger participants. So, in this way there is no direct risk to participants, the only thing to be considered is that they may get tired after doing a few activities, but to mitigate this risk, we can collect data in small durations with multiple breaks.

What are the possible benefits of taking part?

Your participation will help us proceed with the research. In the future, such assisted living systems may help improve the quality of life and independence of older adults.

Will my taking part in this project be kept confidential? / What will happen to the results of the research project?

Your responses and any personal data will remain confidential, and your data will be anonymized. Only researchers associated with this project will have access to the data. The data will be securely stored and only be used for the research purpose. The data from the study is expected to produce a variety of academic outputs (e.g., Journal paper and other publications).

What type of information will be sought from me and why is the collection of this information relevant for achieving the research project's objectives?

The raw data collected from you will be stored anonymously in digital files. Only my supervisors and I can access it. Useful features will be extracted to recognize your specific activities.

Who is organizing/funding the research? (If applicable)

This Research Project is funded by the Erasmus Mundus FUSION project.

www.fusion-edu.eu.

Contact for further information

You can contact me through the ways below for further information,

Email: i7646388@bournemouth.ac.uk

Phone: 07404766844

If you need to make some complaints, you can contact my supervisor whose email account is yuh@bournemouth.ac.uk.

You also can contact Professor Matt Bentley, who is the Deputy Dean of Research and Professional Practice and independent of this study. His email account is mbentley@bournemouth.ac.uk

Finally

If you decide to participate in this project you will be given a copy of the information sheet and, and you also will keep a signed consent form.

Additional question to include in an information sheet if the research involves producing recorded media:

Will I be recorded, and how will the recorded media be used?

No recording media will be used.

Appendix C Consent Form

The full title of the project:

An Activity Recognition System for Elderly People in Assisted Living

Name, position and contact details of the researcher:

Yan Wang, Ph.D. Candidate, Email: i7646388@bournemouth.ac.uk

Name, position and contact details of supervisor (if the researcher is a student):

Hongnian Yu, Professor, Email: yuh@bournemouth.ac.uk

Participants Please Initial Here

I confirm that I have read and understood the participant information sheet for the above research project and have had the opportunity to ask questions.	
I understand that my participation is voluntary. Participants will be able to withdraw up to the point of anonymisation of the data. Also, should I not wish to answer any particular question(s), complete a test or give a sample, I am free to decline.	
I give permission for members of the research team to have access to my anonymised responses. I understand that my name will not be linked with the research materials, and I will not be identified or identifiable in the report or reports that result from the research.	
I agree to take part in the above research project.	

If you need to make some complaints you can also contact Professor Matt Bentley, who is the Deputy Dean of Research and Professional Practice at Bournemouth University. He is independent of this study.

His email account is mbentley@bournemouth.ac.uk

Name of Participant	Date	Signature
---------------------	------	-----------

Name of Researcher	Date	Signature
--------------------	------	-----------

Once this has been signed by all parties, the participant should receive a copy of the signed and dated participant consent form, the participant information sheet and any other written information provided to the participants. A copy of the signed and dated consent form should be kept with the project's main documents which must be kept in a secure location.

Bibliography

2013. Eldercare at Home: Problems of Daily Living [Online]. Available: <http://www.healthinaging.org/resources/resource:eldercare-at-home-problems-of-daily-living/> [Accessed 02 2015].
- ABOWD, D., DEY, A. K., ORR, R. & BROTHERTON, J. 1998. Context-awareness in wearable and ubiquitous computing. *Virtual Reality*, 3, 200-211.
- ADASKEVICIUS, R. 2014. Method for recognition of the physical activity of human being using a wearable accelerometer. *Elektronika ir Elektrotechnika*, 20, 127-131.
- ALICKOVIC, E., KEVRIC, J. & SUBASI, A. 2018. Performance evaluation of empirical mode decomposition, discrete wavelet transform, and wavelet packed decomposition for automated epileptic seizure detection and prediction. *Biomedical Signal Processing and Control*, 39, 94-102.
- ALPAYDIN, E. 2014. Introduction to machine learning, MIT press.
- ALSHURAF, N., EASTWOOD, J.-A., POURHOMAYOUN, M., NYAMATHI, S., BAO, L., MORTAZAVI, B. & SARRAFZADEH, M. Anti-cheating: Detecting self-inflicted and impersonator cheaters for remote health monitoring systems with wearable sensors. *Wearable and Implantable Body Sensor Networks (BSN), 2014 11th International Conference on, 2014. IEEE, 92-97.*
- ALVAREZ-ALVAREZ, A., ALONSO, J. M. & TRIVINO, G. 2013. Human activity recognition in indoor environments by means of fusing information extracted from intensity of WiFi signal and accelerations. *Information Sciences*, 233, 162-182.
- ÁLVAREZ-MEZA, A. M., LEE, J. A., VERLEYSEN, M. & CASTELLANOS-DOMINGUEZ, G. 2017. Kernel-based dimensionality reduction using Renyi's α -entropy measures of similarity. *Neurocomputing*, 222, 36-46.
- AMIT, Y. & GEMAN, D. 1997. Shape quantization and recognition with randomized trees. *Neural computation*, 9, 1545-1588.
- ANDREW, G., ARORA, R., BILMES, J. & LIVESCU, K. Deep canonical correlation analysis. *International Conference on Machine Learning, 2013. 1247-1255.*
- ARORA, R. & LIVESCU, K. Kernel CCA for multi-view learning of acoustic features using articulatory measurements. *Symposium on Machine Learning in Speech and Language Processing, 2012.*
- ASHAD ALAM, M. & FUKUMIZU, K. 2015. Higher-order regularized kernel canonical correlation analysis. *International Journal of Pattern Recognition and Artificial Intelligence*, 29, 1551005.
- ATALLAH, L., ELHELW, M., PANSIOT, J., STOYANOV, D., WANG, L., LO, B. & YANG, G.-Z. 2007. Behaviour profiling with ambient and wearable sensing. *4th International Workshop on Wearable and Implantable Body Sensor Networks (BSN 2007). Springer.*
- ATALLAH, L., LO, B., KING, R. & YANG, G.-Z. Sensor placement for activity detection using wearable accelerometers. *Body Sensor Networks (BSN), 2010 International Conference on, 2010. IEEE, 24-29.*
- ATALLAH, L., LO, B., KING, R. & YANG, G.-Z. 2011. Sensor positioning for activity recognition using wearable accelerometers. *IEEE transactions on biomedical circuits and systems*, 5, 320-329.
- ATTAL, F., MOHAMMED, S., DEDABRISHVILI, M., CHAMROUKHI, F., OUKHELLOU, L. & AMIRAT, Y. 2015. Physical human activity recognition using wearable sensors. *Sensors*, 15, 31314-31338.

- AUGIMERI, A., FORTINO, G., REGE, M. R., HANDZISKI, V. & WOLISZ, A. A cooperative approach for handshake detection based on body sensor networks. *Systems Man and Cybernetics (SMC)*, 2010 IEEE International Conference on, 2010. IEEE, 281-288.
- AYACHI, F. S., NGUYEN, H. P., LAVIGNE-PELLETIER, C., GOUBAULT, E., BOISSY, P. & DUVAL, C. 2016. Wavelet-based algorithm for auto-detection of daily living activities of older adults captured by multiple inertial measurement units (IMUs). *Physiological measurement*, 37, 442.
- BACH, F. R. & JORDAN, M. I. 2002. Kernel independent component analysis. *Journal of machine learning research*, 3, 1-48.
- BAHREPOUR, M., MERATNIA, N., TAGHIKHAKI, Z. & HAVINGA, P. J. 2011. Sensor fusion-based activity recognition for Parkinson patients. *Sensor Fusion-Foundation and Applications*. InTech.
- BANOS, O., DAMAS, M., POMARES, H., PRIETO, A. & ROJAS, I. 2012. Daily living activity recognition based on statistical feature quality group selection. *Expert Systems with Applications*, 39, 8013-8021.
- BANOS, O., DAMAS, M., POMARES, H., ROJAS, F., DELGADO-MARQUEZ, B. & VALENZUELA, O. 2013. Human activity recognition based on a sensor weighting hierarchical classifier. *Soft Computing*, 17, 333-343.
- BANOS, O., GALVEZ, J.-M., DAMAS, M., POMARES, H. & ROJAS, I. 2014a. Window size impact in human activity recognition. *Sensors*, 14, 6474-6499.
- BANOS, O., GARCIA, R., HOLGADO-TERRIZA, J. A., DAMAS, M., POMARES, H., ROJAS, I., SAEZ, A. & VILLALONGA, C. mHealthDroid: a novel framework for agile development of mobile health applications. *International Workshop on Ambient Assisted Living*, 2014b. Springer, 91-98.
- BAO, L. & INTILLE, S. 2004. Activity recognition from user-annotated acceleration data. *Pervasive computing*, 1-17.
- BARRETO, A., OLIVEIRA, R., SOUSA, F., CARDOSO, A. & DUARTE, C. Environment-aware system for Alzheimer's patients. *Wireless Mobile Communication and Healthcare (Mobihealth)*, 2014 EAI 4th International Conference on, 2014. IEEE, 300-303.
- BAYAT, A., POMPLUN, M. & TRAN, D. A. 2014. A study on human activity recognition using accelerometer data from smartphones. *Procedia Computer Science*, 34, 450-457.
- BENNASAR, M., HICKS, Y. & SETCHI, R. 2015. Feature selection using joint mutual information maximisation. *Expert Systems with Applications*, 42, 8520-8532.
- BERCHTOLD, M., BUDDE, M., SCHMIDTKE, H. R. & BEIGL, M. An extensible modular recognition concept that makes activity recognition practical. *Annual Conference on Artificial Intelligence*, 2010. Springer, 400-409.
- BERGMANN, J. H., CHANDARIA, V. & MCGREGOR, A. 2012. Wearable and implantable sensors: the patient's perspective. *Sensors*, 12, 16695-16709.
- BHATTACHARYA, S. & LANE, N. D. From smart to deep: Robust activity recognition on smartwatches using deep learning. *Pervasive Computing and Communication Workshops (PerCom Workshops)*, 2016 IEEE International Conference on, 2016. IEEE, 1-6.
- BIAGETTI, G., CRIPPA, P., FALASCETTI, L., ORCIONI, S. & TURCHETTI, C. Human Activity Recognition Using Accelerometer and Photoplethysmographic Signals. *International Conference on Intelligent Decision Technologies*, 2017. Springer, 53-62.
- BIAN, Z.-P., HOU, J., CHAU, L.-P. & MAGNENAT-THALMANN, N. 2015. Fall detection based on body part tracking using a depth camera. *IEEE journal of biomedical and health informatics*, 19, 430-439.

- BILENKO, N. Y. & GALLANT, J. L. 2016. Pyrrca: regularized kernel canonical correlation analysis in python and its applications to neuroimaging. *Frontiers in neuroinformatics*, 10, 49.
- BISWAS, D., CRANNY, A., GUPTA, N., MAHARATNA, K., ACHNER, J., KLEMKE, J., JÖBGES, M. & ORTMANN, S. 2015. Recognizing upper limb movements with wrist worn inertial sensors using k-means clustering classification. *Human movement science*, 40, 59-76.
- BISWAS, D., CRANNY, A., RAHIM, A. F., GUPTA, N., MAHARATNA, K., HARRIS, N. R. & ORTMANN, S. 2014. On the data analysis for classification of elementary upper limb movements. *Biomedical Engineering Letters*, 4, 403-413.
- BOLÓN-CANEDO, V., SÁNCHEZ-MAROÑO, N. & ALONSO-BETANZOS, A. 2013. A review of feature selection methods on synthetic data. *Knowledge and information systems*, 34, 483-519.
- BONOMI, A. G., GORIS, A. H., YIN, B. & WESTERTERP, K. R. 2009. Detection of type, duration, and intensity of physical activity using an accelerometer. *Medicine & Science in Sports & Exercise*, 41, 1770-1777.
- BOURKE, A. K., VAN DE VEN, P. W., CHAYA, A., ÓLAIGHIN, G. & NELSON, J. 2008a. Design and test of a long-term fall detection system incorporated into a custom vest for the elderly.
- BOURKE, A. K., VAN DE VEN, P. W., CHAYA, A. E., OLAIGHIN, G. M. & NELSON, J. Testing of a long-term fall detection system incorporated into a custom vest for the elderly. *Engineering in Medicine and Biology Society*, 2008. EMBS 2008. 30th Annual International Conference of the IEEE, 2008b. IEEE, 2844-2847.
- BREIMAN, L. 2001. Random forests. *Machine learning*, 45, 5-32.
- BROWN, G., POCOCK, A., ZHAO, M.-J. & LUJÁN, M. 2012. Conditional likelihood maximisation: a unifying framework for information theoretic feature selection. *Journal of machine learning research*, 13, 27-66.
- BULLING, A., BLANKE, U. & SCHIELE, B. 2014. A tutorial on human activity recognition using body-worn inertial sensors. *ACM Computing Surveys (CSUR)*, 46, 33.
- BURNS, A., GREENE, B. R., MCGRATH, M. J., O'SHEA, T. J., KURIS, B., AYER, S. M., STROIESCU, F. & CIONCA, V. 2010. SHIMMER™—A wireless sensor platform for noninvasive biomedical research. *IEEE Sensors Journal*, 10, 1527-1534.
- CAPELA, N. A., LEMAIRE, E. D. & BADDOUR, N. 2015. Novel algorithm for a smartphone-based 6-minute walk test application: algorithm, application development, and evaluation. *Journal of neuroengineering and rehabilitation*, 12, 19.
- CARMELI, E., IMAM, B. & MERRICK, J. 2016. *Assistive Technology and Older Adults. Health Care for People with Intellectual and Developmental Disabilities across the Lifespan*. Springer.
- CASTRO, D., CORAL, W., RODRIGUEZ, C., CABRA, J. & COLORADO, J. 2017. Wearable-Based Human Activity Recognition Using and IoT Approach. *Journal of Sensor and Actuator Networks*, 6, 28.
- CATAL, C., TUFEKCI, S., PIRMIT, E. & KOCABAG, G. 2015. On the use of ensemble of classifiers for accelerometer-based activity recognition. *Applied Soft Computing*, 37, 1018-1022.
- CHAMROUKHI, F., MOHAMMED, S., TRABELSI, D., OUKHELLOU, L. & AMIRAT, Y. 2013. Joint segmentation of multivariate time series with hidden process regression for human activity recognition. *Neurocomputing*, 120, 633-644.

- CHANG, C.-C. & LIN, C.-J. 2011. LIBSVM: a library for support vector machines. *ACM transactions on intelligent systems and technology (TIST)*, 2, 27.
- CHAVARRIAGA, R., BAYATI, H. & MILLÁN, J. D. R. 2013a. Unsupervised adaptation for acceleration-based activity recognition: robustness to sensor displacement and rotation. *Personal and Ubiquitous Computing*, 17, 479-490.
- CHAVARRIAGA, R., SAGHA, H., CALATRONI, A., DIGUMARTI, S. T., TRÖSTER, G., MILLÁN, J. D. R. & ROGGEN, D. 2013b. The Opportunity challenge: A benchmark database for on-body sensor-based activity recognition. *Pattern Recognition Letters*, 34, 2033-2042.
- CHEN, D., WAN, S., XIANG, J. & BAO, F. S. 2017a. A high-performance seizure detection algorithm based on Discrete Wavelet Transform (DWT) and EEG. *PloS one*, 12, e0173138.
- CHEN, G., WANG, A., ZHAO, S., LIU, L. & CHANG, C.-Y. 2017b. Latent feature learning for activity recognition using simple sensors in smart homes. *Multimedia Tools and Applications*, 1-19.
- CHEN, L.-L., ZHANG, J., ZOU, J.-Z., ZHAO, C.-J. & WANG, G.-S. 2014. A framework on wavelet-based nonlinear features and extreme learning machine for epileptic seizure detection. *Biomedical Signal Processing and Control*, 10, 1-10.
- CHEN, L., HOEY, J., NUGENT, C. D., COOK, D. J. & YU, Z. 2012. Sensor-based activity recognition. *IEEE Transactions on Systems, Man, and Cybernetics, Part C (Applications and Reviews)*, 42, 790-808.
- CHENG, J., AMFT, O. & LUKOWICZ, P. Active capacitive sensing: Exploring a new wearable sensing modality for activity recognition. *International Conference on Pervasive Computing*, 2010. Springer, 319-336.
- CHERNBUMROONG, S., CANG, S., ATKINS, A. & YU, H. 2013. Elderly activities recognition and classification for applications in assisted living. *Expert Systems with Applications*, 40, 1662-1674.
- CHERNBUMROONG, S., CANG, S. & YU, H. 2014. A practical multi-sensor activity recognition system for home-based care. *decision support systems*, 66, 61-70.
- CHERNBUMROONG, S., CANG, S. & YU, H. 2015. Genetic algorithm-based classifiers fusion for multisensor activity recognition of elderly people. *IEEE journal of biomedical and health informatics*, 19, 282-289.
- CHIKHAOUI, B. & GOUINEAU, F. Towards Automatic Feature Extraction for Activity Recognition from Wearable Sensors: A Deep Learning Approach. *2017 IEEE International Conference on Data Mining Workshops (ICDMW)*, 2017. IEEE, 693-702.
- CHOUDHURY, T., CONSOLVO, S., HARRISON, B., HIGHTOWER, J., LAMARCA, A., LEGRAND, L., RAHIMI, A., REA, A., BORDELLO, G. & HEMINGWAY, B. 2008. The mobile sensing platform: An embedded activity recognition system. *IEEE Pervasive Computing*, 7.
- CHU, D., LIAO, L., NG, M. & ZHANG, X. Sparse kernel canonical correlation analysis. *Proceedings of International Multiconference of Engineers and Computer Scientists*, 2013.
- CIREŞAN, D. & MEIER, U. Multi-column deep neural networks for offline handwritten Chinese character classification. *Neural Networks (IJCNN)*, 2015 International Joint Conference on, 2015. IEEE, 1-6.
- CLELAND, I., KIKHIA, B., NUGENT, C., BOYTSOV, A., HALLBERG, J., SYNNESE, K., MCCLEAN, S. & FINLAY, D. 2013. Optimal placement of accelerometers for the detection of everyday activities. *Sensors*, 13, 9183-9200.

- COOK, A. J., GARGIULO, G., LEHMANN, T. & HAMILTON, T. J. 2015. Open platform, eight-channel, portable bio-potential and activity data logger for wearable medical device development. *Electronics Letters*, 51, 1641-1643.
- CORNACCHIA, M., OZCAN, K., ZHENG, Y. & VELIPASALAR, S. 2017. A survey on activity detection and classification using wearable sensors. *IEEE Sensors Journal*, 17, 386-403.
- DALTON, A. & ÓLAIGHIN, G. 2013. Comparing supervised learning techniques on the task of physical activity recognition. *IEEE journal of biomedical and health informatics*, 17, 46-52.
- DAO, M.-S., NGUYEN-GIA, T.-A. & MAI, V.-C. 2017. Daily Human Activities Recognition Using Heterogeneous Sensors from Smartphones. *Procedia Computer Science*, 111, 323-328.
- DAVIS, K., OWUSU, E., BASTANI, V., MARCENARO, L., HU, J., REGAZZONI, C. & FEIJS, L. Activity recognition based on inertial sensors for ambient assisted living. *Information Fusion (FUSION)*, 2016 19th International Conference on, 2016. IEEE, 371-378.
- DEBES, C., MERENTITIS, A., SUKHANOV, S., NIESSEN, M., FRANGIADAKIS, N. & BAUER, A. 2016. Monitoring activities of daily living in smart homes: Understanding human behavior. *IEEE Signal Processing Magazine*, 33, 81-94.
- DENG, W.-Y., ZHENG, Q.-H. & WANG, Z.-M. 2014. Cross-person activity recognition using reduced kernel extreme learning machine. *Neural Networks*, 53, 1-7.
- DESAI, U., MARTIS, R. J., NAYAK, C. G., SARIKA, K., NAYAK, S. G., SHIRVA, A., NAYAK, V. & MUDASSIR, S. 2015. Discrete cosine transform features in automated classification of cardiac arrhythmia beats. *Emerging research in computing, information, communication and applications*. Springer.
- DESSI, N. & PES, B. 2015. Similarity of feature selection methods: An empirical study across data intensive classification tasks. *Expert Systems with Applications*, 42, 4632-4642.
- DIETHE, T., TWOMEY, N., KULL, M., FLACH, P. & CRADDOCK, I. 2017. Probabilistic sensor fusion for ambient assisted living. *Information Fusion*.
- DIETHE, T. R., TWOMEY, N. & FLACH, P. SPHERE: A sensor platform for healthcare in a residential environment. *Proceedings of Large-scale Online Learning and Decision Making Workshop*, 2014.
- EASTERBROOK, S. M. Empirical research methods for software engineering. *Ieee/acm International Conference on Automated Software Engineering*, 2007. 574-574.
- FANG, H. & HU, C. Recognizing human activity in smart home using deep learning algorithm. *Control Conference (CCC), 2014 33rd Chinese*, 2014. IEEE, 4716-4720.
- FATIMA, I., FAHIM, M., LEE, Y.-K. & LEE, S. 2013. A unified framework for activity recognition-based behavior analysis and action prediction in smart homes. *Sensors*, 13, 2682-2699.
- FERNÁNDEZ-DELGADO, M., CERNADAS, E., BARRO, S. & AMORIM, D. 2014. Do we need hundreds of classifiers to solve real world classification problems. *J. Mach. Learn. Res.*, 15, 3133-3181.
- FILIPPOPOLITIS, A., OLIFF, W., TAKAND, B. & LOUKAS, G. 2017. Location-Enhanced Activity Recognition in Indoor Environments Using Off the Shelf Smart Watch Technology and BLE Beacons. *Sensors*, 17, 1230.
- FLEURY, A., VACHER, M. & NOURY, N. 2010. SVM-based multimodal classification of activities of daily living in health smart homes: sensors, algorithms, and first experimental results. *IEEE transactions on information technology in biomedicine*, 14, 274-283.

- FOERSTER, F., SMEJA, M. & FAHRENBERG, J. 1999. Detection of posture and motion by accelerometry: a validation study in ambulatory monitoring. *Computers in Human Behavior*, 15, 571-583.
- FONTANA, J. M., HIGGINS, J. A., SCHUCKERS, S. C., BELLISLE, F., PAN, Z., MELANSON, E. L., NEUMAN, M. R. & SAZONOV, E. 2015. Energy intake estimation from counts of chews and swallows. *Appetite*, 85, 14-21.
- FRIEDMAN, J., HASTIE, T. & TIBSHIRANI, R. 2001. *The elements of statistical learning*, Springer series in statistics New York.
- GAO, L., BOURKE, A. & NELSON, J. 2014. Evaluation of accelerometer based multi-sensor versus single-sensor activity recognition systems. *Medical engineering & physics*, 36, 779-785.
- GAO, S., VER STEEG, G. & GALSTYAN, A. Variational information maximization for feature selection. *Advances in Neural Information Processing Systems*, 2016. 487-495.
- GEORGI, M., AMMA, C. & SCHULTZ, T. Recognizing Hand and Finger Gestures with IMU based Motion and EMG based Muscle Activity Sensing. *BIOSIGNALS*, 2015. 99-108.
- GHEID, Z. & CHALLAL, Y. Novel Efficient and Privacy-Preserving Protocols For Sensor-Based Human Activity Recognition. *Ubiquitous Intelligence & Computing, Advanced and Trusted Computing, Scalable Computing and Communications, Cloud and Big Data Computing, Internet of People, and Smart World Congress (UIC/ATC/ScalCom/CBDCOM/IoP/SmartWorld)*, 2016 Intl IEEE Conferences, 2016. IEEE, 301-308.
- GJORESKE, H. & GAMS, M. 2011. Activity/Posture recognition using wearable sensors placed on different body locations. *The Fourteenth International Conference on Artificial Intelligence and Soft Computing*.
- GORDON, D., SCHMIDTKE, H. & BEIGL, M. Introducing new sensors for activity recognition. *How To Do Good Research In Activity Recognition: Experimental methodology, performance evaluation and reproducibility. Workshop in conjunction with Pervasive*, 2010.
- GRAVINA, R., ALESSANDRO, A., SALMERI, A., BUONDONNO, L., RAVEENDRANATHAN, N., LOSEU, V., GIANNANTONIO, R., SETO, E. & FORTINO, G. Enabling multiple BSN applications using the SPINE framework. *Body Sensor Networks (BSN)*, 2010 International Conference on, 2010. IEEE, 228-233.
- GU, F., FLÓREZ-REVUELTA, F., MONEKOSSO, D. & REMAGNINO, P. 2015. Marginalised stacked denoising autoencoders for robust representation of real-time multi-view action recognition. *Sensors*, 15, 17209-17231.
- GUHA, A. & DUKKIPATI, A. 2015. A faster algorithm for testing polynomial representability of functions over finite integer rings. *Theoretical Computer Science*, 579, 88-99.
- GUI, J., SUN, Z., JI, S., TAO, D. & TAN, T. 2017. Feature selection based on structured sparsity: A comprehensive study. *IEEE transactions on neural networks and learning systems*, 28, 1490-1507.
- GUO, J., ZHOU, X., SUN, Y., PING, G., ZHAO, G. & LI, Z. 2016. Smartphone-Based Patients' activity recognition by using a self-learning scheme for medical monitoring. *Journal of medical systems*, 40, 140.
- GUO, Y., HE, W. & GAO, C. 2012. Human activity recognition by fusing multiple sensor nodes in the wearable sensor systems. *Journal of Mechanics in Medicine and Biology*, 12, 1250084.
- GUPTA, P. & DALLAS, T. 2014. Feature selection and activity recognition system using a single triaxial accelerometer. *IEEE Transactions on Biomedical Engineering*, 61, 1780-1786.

- GUYON, I. & ELISSEFF, A. 2003. An introduction to variable and feature selection. *Journal of machine learning research*, 3, 1157-1182.
- HAHN, W. E., LEWKOWITZ, S., LACOMBE, D. C. & BARENHOLTZ, E. 2015. Deep learning human actions from video via sparse filtering and locally competitive algorithms. *Multimedia Tools and Applications*, 74, 10097-10110.
- HAIJHASHEMI, Z. & POPESCU, M. 2013. Detection of abnormal sensor patterns in eldercare. *E-Health and Bioengineering Conference (EHB)*, 2013, 1-4.
- HAMMERLA, N. Y., FISHER, J., ANDRAS, P., ROCHESTER, L., WALKER, R. & PLÖTZ, T. PD Disease State Assessment in Naturalistic Environments Using Deep Learning. *AAAI*, 2015. 1742-1748.
- HAMMERLA, N. Y., HALLORAN, S. & PLOETZ, T. 2016. Deep, convolutional, and recurrent models for human activity recognition using wearables. *arXiv preprint arXiv:1604.08880*.
- HANNINK, J., KAUTZ, T., PASLUOSTA, C. F., GAßMANN, K.-G., KLUCKEN, J. & ESKOFIER, B. M. 2017. Sensor-based gait parameter extraction with deep convolutional neural networks. *IEEE journal of biomedical and health informatics*, 21, 85-93.
- HARDOON, D. R., SZEDMAK, S. & SHAW-TAYLOR, J. 2004. Canonical correlation analysis: An overview with application to learning methods. *Neural computation*, 16, 2639-2664.
- HASSAN, M. M., UDDIN, M. Z., MOHAMED, A. & ALMOGREN, A. 2018. A robust human activity recognition system using smartphone sensors and deep learning. *Future Generation Computer Systems*, 81, 307-313.
- HASSANI, H. 2017. *Research Methods in Computer Science: The Challenges and Issues*.
- HAYASHI, T., NISHIDA, M., KITAOKA, N. & TAKEDA, K. Daily activity recognition based on DNN using environmental sound and acceleration signals. *Signal Processing Conference (EUSIPCO), 2015 23rd European, 2015. IEEE*, 2306-2310.
- HE, Z. & BAI, X. A wearable wireless body area network for human activity recognition. *Ubiquitous and Future Networks (ICUFN), 2014 Sixth International Conf on, 2014. IEEE*, 115-119.
- HE, Z. & JIN, L. Activity recognition from acceleration data based on discrete cosine transform and SVM. *Systems, Man and Cybernetics, 2009. SMC 2009. IEEE International Conference on, 2009. IEEE*, 5041-5044.
- HEINZ, E. A., KUNZE, K. S., GRUBER, M., BANNACH, D. & LUKOWICZ, P. Using wearable sensors for real-time recognition tasks in games of martial arts-an initial experiment. *Computational Intelligence and Games, 2006 IEEE Symposium on, 2006. IEEE*, 98-102.
- HEMALATHA, C. S. & VAIDEHI, V. 2013. Frequent bit pattern mining over tri-axial accelerometer data streams for recognizing human activities and detecting fall. *Procedia Computer Science*, 19, 56-63.
- HERMANIS, A., CACURS, R., NESENBERGS, K., GREITANS, M., SYUNDYUKOV, E. & SELAVO, L. Wearable Sensor System for Human Biomechanics Monitoring. *EWSN, 2016. 247-248*.
- HEXOSHIN. 2018. Hexoshin Smart Shirts Specifications [Online]. Available: <https://www.hexoskin.com> [Accessed 18 January 2018].
- HO, T. K. Random decision forests. *Document analysis and recognition, 1995., proceedings of the third international conference on, 1995. IEEE*, 278-282.
- HOTELLING, H. 1936. Relations between two sets of variates. *Biometrika*, 28, 321-377.
- HRISTOVA, A., BERNARDOS, A. M. & CASAR, J. R. Context-aware services for ambient assisted living: A case-study. *Applied Sciences on Biomedical and Communication Technologies, 2008. ISABEL'08. First International Symposium on, 2008. IEEE*, 1-5.

- HSU, C.-W., CHANG, C.-C. & LIN, C.-J. 2003. A practical guide to support vector classification.
- HU, L., CHEN, Y., WANG, S. & CHEN, Z. 2014. b-COELM: A fast, lightweight and accurate activity recognition model for mini-wearable devices. *Pervasive and Mobile Computing*, 15, 200-214.
- HUANG, H., YOO, S. & KASIVISWANATHAN, S. P. Unsupervised feature selection on data streams. *Proceedings of the 24th ACM International on Conference on Information and Knowledge Management*, 2015. ACM, 1031-1040.
- HUANG, J.-Y. & TSAI, C.-H. A wearable computing environment for the security of a large-scale factory. *International Conference on Human-Computer Interaction*, 2007. Springer, 1113-1122.
- HUYNH, T., FRITZ, M. & SCHIELE, B. Discovery of activity patterns using topic models. *Proceedings of the 10th international conference on Ubiquitous computing*, 2008. ACM, 10-19.
- IAN, C., BASEL, K., CHRIS, N., ANDREY, B., JOSEF, H., KÅRE, S., SALLY, M. C. & DEWAR, F. 2013. Optimal Placement of Accelerometers for the Detection of Everyday Activities. *Sensors*, 13, 9183.
- IGNATOV, A. 2018. Real-time human activity recognition from accelerometer data using Convolutional Neural Networks. *Applied Soft Computing*, 62, 915-922.
- JALAL, A., KAMAL, S. & KIM, D. 2014. A depth video sensor-based life-logging human activity recognition system for elderly care in smart indoor environments. *Sensors*, 14, 11735-11759.
- JALAL, A., KAMAL, S. & KIM, D. 2017. A Depth Video-based Human Detection and Activity Recognition using Multi-features and Embedded Hidden Markov Models for Health Care Monitoring Systems. *International Journal of Interactive Multimedia & Artificial Intelligence*, 4.
- JAMES, G., WITTEN, D., HASTIE, T. & TIBSHIRANI, R. 2013. *An introduction to statistical learning*, Springer.
- JANIDARMIAN, M., ROSHAN FEKR, A., RADECKA, K. & ZILIC, Z. 2017. A Comprehensive Analysis on Wearable Acceleration Sensors in Human Activity Recognition. *Sensors*, 17, 529.
- JUNG, S., HONG, S., KIM, J., LEE, S., HYEON, T., LEE, M. & KIM, D.-H. 2015. Wearable fall detector using integrated sensors and energy devices. *Scientific reports*, 5, 17081.
- JUSTCHECKING. 2014. Online activity monitoring system [Online]. Available: <https://www.justchecking.co.uk/> [Accessed 12 December 2014].
- KABIR, M. M., ISLAM, M. M. & MURASE, K. 2010. A new wrapper feature selection approach using neural network. *Neurocomputing*, 73, 3273-3283.
- KALANTARIAN, H., ALSHURAF, N., LE, T. & SARRAFZADEH, M. 2015. Monitoring eating habits using a piezoelectric sensor-based necklace. *Computers in biology and medicine*, 58, 46-55.
- KALANTARIAN, H., MOTAMED, B., ALSHURAF, N. & SARRAFZADEH, M. 2016. A wearable sensor system for medication adherence prediction. *Artificial intelligence in medicine*, 69, 43-52.
- KARANTONIS, D. M., NARAYANAN, M. R., MATHIE, M., LOVELL, N. H. & CELLER, B. G. 2006. Implementation of a real-time human movement classifier using a triaxial accelerometer for ambulatory monitoring. *IEEE transactions on information technology in biomedicine*, 10, 156-167.
- KASHIF, M. N., RAZA, S. E. A., SIRINUKUNWATTANA, K., ARIF, M. & RAJPOOT, N. Handcrafted features with convolutional neural networks for detection of tumor cells in histology

- images. Biomedical Imaging (ISBI), 2016 IEEE 13th International Symposium on, 2016. IEEE, 1029-1032.
- KAU, L.-J. & CHEN, C.-S. 2015. A smart phone-based pocket fall accident detection, positioning, and rescue system. *IEEE journal of biomedical and health informatics*, 19, 44-56.
- KAYA, H., EYBEN, F., SALAH, A. A. & SCHULLER, B. CCA based feature selection with application to continuous depression recognition from acoustic speech features. *Acoustics, Speech and Signal Processing (ICASSP), 2014 IEEE International Conference on, 2014. IEEE, 3729-3733.*
- KAYE, J., MATTEK, N., DODGE, H., BURACCHIO, T., AUSTIN, D., HAGLER, S., PAVEL, M. & HAYES, T. 2012. One walk a year to 1000 within a year: Continuous in-home unobtrusive gait assessment of older adults. *Gait & posture*, 35, 197-202.
- KE, S.-R., THUC, H. L. U., LEE, Y.-J., HWANG, J.-N., YOO, J.-H. & CHOI, K.-H. 2013. A review on video-based human activity recognition. *Computers*, 2, 88-131.
- KHAN, A. M., SIDDIQI, M. H. & LEE, S.-W. 2013. Exploratory data analysis of acceleration signals to select light-weight and accurate features for real-time activity recognition on smartphones. *Sensors*, 13, 13099-13122.
- KHAN, A. M., TUFAIL, A., KHATTAK, A. M. & LAINE, T. H. 2014. Activity recognition on smartphones via sensor-fusion and kda-based svms. *International Journal of Distributed Sensor Networks*, 10, 503291.
- KHAN, S. & YONG, S.-P. A comparison of deep learning and hand crafted features in medical image modality classification. *Computer and Information Sciences (ICCOINS), 2016 3rd International Conference on, 2016. IEEE, 633-638.*
- KHAN, U. M., KABIR, Z., HASSAN, S. A. & AHMED, S. H. 2017. A Deep Learning Framework using Passive WiFi Sensing for Respiration Monitoring. *arXiv preprint arXiv:1704.05708.*
- KHAN, Z. A. & SOHN, W. 2011. Abnormal human activity recognition system based on R-transform and kernel discriminant technique for elderly home care. *IEEE Transactions on Consumer Electronics*, 57.
- KING, R. C., VILLENEUVE, E., WHITE, R. J., SHERRATT, R. S., HOLDERBAUM, W. & HARWIN, W. S. 2017. Application of data fusion techniques and technologies for wearable health monitoring. *Medical Engineering and Physics*, 42, 1-12.
- KON, B., LAM, A. & CHAN, J. Evolution of Smart Homes for the Elderly. *Proceedings of the 26th International Conference on World Wide Web Companion, 2017. International World Wide Web Conferences Steering Committee, 1095-1101.*
- KREIL, M., SICK, B. & LUKOWICZ, P. Dealing with human variability in motion based, wearable activity recognition. *Pervasive Computing and Communications Workshops (PERCOM Workshops), 2014 IEEE International Conference on, 2014. IEEE, 36-40.*
- KUERBIS, A., MULLIKEN, A., MUENCH, F., MOORE, A. A. & GARDNER, D. 2017. Older adults and mobile technology: Factors that enhance and inhibit utilization in the context of behavioral health.
- KUHN, M. & JOHNSON, K. 2013. *Applied predictive modeling*, Springer.
- KUMAR, P. J., YUNG, Y. & HUAN, T. L. 2017. Neural Network Based Decision Trees using Machine Learning for Alzheimer's Diagnosis. *International Journal of Computer and Information Sciences*, 4, 63-72.
- KUNDU, A. S., MAZUMDER, O., LENKA, P. K. & BHAUMIK, S. 2017. Hand Gesture Recognition Based Omnidirectional Wheelchair Control Using IMU and EMG Sensors. *Journal of Intelligent & Robotic Systems*, 1-13.

- KURSUN, O., ALPAYDIN, E. & FAVOROV, O. V. 2011. Canonical correlation analysis using within-class coupling. *Pattern Recognition Letters*, 32, 134-144.
- KUSHWAH, A., KUMAR, S. & HEGDE, R. M. 2015. Multi-sensor data fusion methods for indoor activity recognition using temporal evidence theory. *Pervasive and Mobile Computing*, 21, 19-29.
- KWAPISZ, J. R., WEISS, G. M. & MOORE, S. A. 2011. Activity recognition using cell phone accelerometers. *ACM SigKDD Explorations Newsletter*, 12, 74-82.
- KWON, Y., KANG, K. & BAE, C. 2014. Unsupervised learning for human activity recognition using smartphone sensors. *Expert Systems with Applications*, 41, 6067-6074.
- LANE, N. D. & GEORGIEV, P. Can deep learning revolutionize mobile sensing? *Proceedings of the 16th International Workshop on Mobile Computing Systems and Applications*, 2015. ACM, 117-122.
- LARA, O. D. & LABRADOR, M. A. 2013. A survey on human activity recognition using wearable sensors. *IEEE Communications Surveys and Tutorials*, 15, 1192-1209.
- LARA, O. D., PÉREZ, A. J., LABRADOR, M. A. & POSADA, J. D. 2012. Centinela: A human activity recognition system based on acceleration and vital sign data. *Pervasive and mobile computing*, 8, 717-729.
- LAUDANSKI, A., BROUWER, B. & LI, Q. 2015. Activity classification in persons with stroke based on frequency features. *Medical engineering & physics*, 37, 180-186.
- LECUN, Y., BENGIO, Y. & HINTON, G. 2015. Deep learning. *nature*, 521, 436.
- LEE, S.-M., YOON, S. M. & CHO, H. Human activity recognition from accelerometer data using Convolutional Neural Network. *Big Data and Smart Computing (BigComp)*, 2017 IEEE International Conference on, 2017. IEEE, 131-134.
- LEE, S.-W. & MASE, K. 2002. Activity and location recognition using wearable sensors. *IEEE pervasive computing*, 1, 24-32.
- LEE, Y.-S. & CHO, S.-B. 2014. Activity recognition with android phone using mixture-of-experts co-trained with labeled and unlabeled data. *Neurocomputing*, 126, 106-115.
- LESTER, J., CHOUDHURY, T. & BORRIELLO, G. 2006. A practical approach to recognizing physical activities. *Pervasive computing*, 1-16.
- LI, J., CHENG, K., WANG, S., MORSTATTER, F., TREVINO, R. P., TANG, J. & LIU, H. 2017a. Feature selection: A data perspective. *ACM Computing Surveys (CSUR)*, 50, 94.
- LI, M., BI, W., KWOK, J. T. & LU, B.-L. 2015a. Large-scale Nyström kernel matrix approximation using randomized SVD. *IEEE transactions on neural networks and learning systems*, 26, 152-164.
- LI, Q., STANKOVIC, J. A., HANSON, M. A., BARTH, A. T., LACH, J. & ZHOU, G. Accurate, fast fall detection using gyroscopes and accelerometer-derived posture information. *Wearable and Implantable Body Sensor Networks*, 2009. BSN 2009. Sixth International Workshop on, 2009. IEEE, 138-143.
- LI, Q., ZHU, D., ZHANG, J., HIBAR, D. P., JAHANSHAD, N., WANG, Y., YE, J., THOMPSON, P. M. & WANG, J. 2017b. Large-scale Feature Selection of Risk Genetic Factors for Alzheimer's Disease via Distributed Group Lasso Regression. *arXiv preprint arXiv:1704.08383*.
- LI, Y., LIU, M. & SHENG, W. Indoor human tracking and state estimation by fusing environmental sensors and wearable sensors. *Cyber Technology in Automation, Control, and Intelligent Systems (CYBER)*, 2015 IEEE International Conference on, 2015b. IEEE, 1468-1473.

- LISANTI, G., MASI, I. & DEL BIMBO, A. Matching people across camera views using kernel canonical correlation analysis. *Proceedings of the International Conference on Distributed Smart Cameras*, 2014. ACM, 10.
- LIU, K., CHEN, C., JAFARI, R. & KEHTARNAVAZ, N. 2014a. Fusion of inertial and depth sensor data for robust hand gesture recognition. *IEEE Sensors Journal*, 14, 1898-1903.
- LIU, K., CHEN, C., JAFARI, R. & KEHTARNAVAZ, N. Multi-HMM classification for hand gesture recognition using two differing modality sensors. *Circuits and Systems Conference (DCAS)*, 2014 IEEE Dallas, 2014b. IEEE, 1-4.
- LIU, M. & ZHANG, D. 2016. Pairwise constraint-guided sparse learning for feature selection. *IEEE transactions on cybernetics*, 46, 298-310.
- LIU, S., GAO, R. X., JOHN, D., STAUDENMAYER, J. W. & FREEDSON, P. S. 2012. Multisensor data fusion for physical activity assessment. *IEEE Transactions on Biomedical Engineering*, 59, 687-696.
- LIU, Y., NIE, L., HAN, L., ZHANG, L. & ROSENBLUM, D. S. Action2Activity: Recognizing Complex Activities from Sensor Data. *IJCAI*, 2015. 1617-1623.
- LOCKHART, J. W. & WEISS, G. M. Limitations with activity recognition methodology & data sets. *Acm International Joint Conference on Pervasive & Ubiquitous Computing: Adjunct Publication*, 2014.
- LOGAN, B., HEALEY, J., PHILIPOSE, M., TAPIA, E. M. & INTILLE, S. 2007. A long-term evaluation of sensing modalities for activity recognition. *International conference on Ubiquitous computing*, 483-500.
- LOKAVEE, S., PUNTHEERANURAK, T., KERDCHAROEN, T., WATTANWISUTH, N. & TUANTRANONT, A. Sensor pillow and bed sheet system: Unconstrained monitoring of respiration rate and posture movements during sleep. *Systems, Man, and Cybernetics (SMC)*, 2012 IEEE International Conference on, 2012. IEEE, 1564-1568.
- LOPEZ-PAZ, D., HENNIG, P. & SCHÖLKOPF, B. The randomized dependence coefficient. *Advances in neural information processing systems*, 2013. 1-9.
- LORUSSI, F., CARBONARO, N., DE ROSSI, D., PARADISO, R., VELTINK, P. & TOGNETTI, A. 2016. Wearable textile platform for assessing stroke patient treatment in daily life conditions. *Frontiers in bioengineering and biotechnology*, 4, 28.
- LUO, X., GUAN, Q., TAN, H., GAO, L., WANG, Z. & LUO, X. 2017. Simultaneous Indoor Tracking and Activity Recognition Using Pyroelectric Infrared Sensors. *Sensors*, 17, 1738.
- MABROUK, A. B. & ZAGROUBA, E. 2017. Abnormal behavior recognition for intelligent video surveillance systems: A review. *Expert Systems with Applications*.
- MACHADO, I. P., GOMES, A. L., GAMBOA, H., PAIXÃO, V. & COSTA, R. M. 2015. Human activity data discovery from triaxial accelerometer sensor: Non-supervised learning sensitivity to feature extraction parametrization. *Information Processing & Management*, 51, 204-214.
- MAEKAWA, T., YANAGISAWA, Y., KISHINO, Y., ISHIGURO, K., KAMEI, K., SAKURAI, Y. & OKADOME, T. Object-Based Activity Recognition with Heterogeneous Sensors on Wrist. *Pervasive*, 2010. Springer, 246-264.
- MAINETTI, L., PATRONO, L., SECCO, A. & SERGI, I. 2017. An IoT-aware AAL System to Capture Behavioral Changes of Elderly People.
- MANNINI, A., INTILLE, S. S., ROSENBERGER, M., SABATINI, A. M. & HASKELL, W. 2013. Activity recognition using a single accelerometer placed at the wrist or ankle. *Medicine and science in sports and exercise*, 45, 2193.
- MANNINI, A. & SABATINI, A. M. 2010. Machine learning methods for classifying human physical activity from on-body accelerometers. *Sensors*, 10, 1154-1175.

- MANNINI, A. & SABATINI, A. M. 2011. Accelerometry-based classification of human activities using Markov modeling. *Computational intelligence and neuroscience*, 2011, 4.
- MARGARITO, J., HELAOUI, R., BIANCHI, A. M., SARTOR, F. & BONOMI, A. G. 2016. User-independent recognition of sports activities from a single wrist-worn accelerometer: A template-matching-based approach. *IEEE Transactions on Biomedical Engineering*, 63, 788-796.
- MASSÉ, F., GONZENBACH, R. R., ARAMI, A., PARASCHIV-IONESCU, A., LUFT, A. R. & AMINIAN, K. 2015. Improving activity recognition using a wearable barometric pressure sensor in mobility-impaired stroke patients. *Journal of neuroengineering and rehabilitation*, 12, 72.
- MATLAB. 2015. TreeBagger [Online]. Available: https://uk.mathworks.com/help/stats/treebagger-class.html_2015].
- MAURER, U., SMAILAGIC, A., SIEWIOREK, D. P. & DEISHER, M. Activity recognition and monitoring using multiple sensors on different body positions. *Wearable and Implantable Body Sensor Networks*, 2006. BSN 2006. International Workshop on, 2006. IEEE, 4 pp.-116.
- MEHR, H. D., POLAT, H. & CETIN, A. Resident activity recognition in smart homes by using artificial neural networks. *Smart Grid Congress and Fair (ICSG)*, 2016 4th International Istanbul, 2016. IEEE, 1-5.
- MEHRANG, S., PIETILA, J., TOLONEN, J., HELANDER, E., JIMISON, H., PAVEL, M. & KORHONEN, I. 2017. Human Activity Recognition Using A Single Optical Heart Rate Monitoring Wristband Equipped with Triaxial Accelerometer. *EMBE & NBC 2017*. Springer.
- MEYER, P. E. & BONTEMPI, G. On the use of variable complementarity for feature selection in cancer classification. *Workshops on Applications of Evolutionary Computation*, 2006. Springer, 91-102.
- MIMOBABY. 2018. Sleep trackers for little ones [Online]. Available: <https://www.minobaby.com> [Accessed 18 Jan 2018].
- MOHAMED, A. B. H., VAL, T., ANDRIEUX, L. & KACHOURI, A. Using a Kinect WSN for home monitoring: principle, network and application evaluation. *Wireless Communications in Unusual and Confined Areas (ICWCUCA)*, 2012 International Conference on, 2012. IEEE, 1-5.
- MONCADA-TORRES, A., LEUENBERGER, K., GONZENBACH, R., LUFT, A. & GASSERT, R. 2014. Activity classification based on inertial and barometric pressure sensors at different anatomical locations. *Physiological measurement*, 35, 1245.
- MONTALTO, F., GUERRA, C., BIANCHI, V., DE MUNARI, I. & CIAMPOLINI, P. 2015. MuSA: Wearable Multi Sensor Assistant for Human Activity Recognition and Indoor Localization. *Ambient Assisted Living*. Springer.
- MORALES, J. & AKOPIAN, D. 2017. Physical activity recognition by smartphones, a survey. *Biocybernetics and Biomedical Engineering*, 37, 388-400.
- MORALES, J., AKOPIAN, D. & AGAIAN, S. Human activity recognition by smartphones regardless of device orientation. *IS&T/SPIE Electronic Imaging*, International Society for Optics and Photonics, 2014. 90300I-90300I.
- MORTAZAVI, B., NEMATI, E., VANDERWALL, K., FLORES-RODRIGUEZ, H. G., CAI, J. Y. J., LUCIER, J., NAEIM, A. & SARRAFZADEH, M. 2015. Can smartwatches replace smartphones for posture tracking? *Sensors*, 15, 26783-26800.
- MORTAZAVI, B. J., POURHOMAYOUN, M., ALSHEIKH, G., ALSHURAF, N., LEE, S. I. & SARRAFZADEH, M. Determining the single best axis for exercise repetition

- recognition and counting on smartwatches. *Wearable and Implantable Body Sensor Networks (BSN)*, 2014 11th International Conference on, 2014. IEEE, 33-38.
- MURAO, K. & TERADA, T. A recognition method for combined activities with accelerometers. *Proceedings of the 2014 ACM International Joint Conference on Pervasive and Ubiquitous Computing: Adjunct Publication*, 2014. ACM, 787-796.
- NAKAMURA, M., NAKAMURA, J., SHUZO, M., WARISAWA, S. & YAMADA, I. Collaborative processing of wearable and ambient sensor system for health monitoring application. *Applied Sciences in Biomedical and Communication Technologies (ISABEL)*, 2010 3rd International Symposium on, 2010. IEEE, 1-5.
- NALLAPERUMAL, K. 2015. *Engineering Research Methodology A Computer Science and Engineering and Information and Communication Technologies Perspective*, New Delhi, India, PHI Learning Private Limited.
- NAM, Y. & PARK, J. W. 2013. Child activity recognition based on cooperative fusion model of a triaxial accelerometer and a barometric pressure sensor. *IEEE journal of biomedical and health informatics*, 17, 420-426.
- NGIAM, J., CHEN, Z., BHASKAR, S. A., KOH, P. W. & NG, A. Y. Sparse filtering. *Advances in neural information processing systems*, 2011. 1125-1133.
- NWEKE, H. F., TEH, Y. W., AL-GARADI, M. A. & ALO, U. R. 2018. *Deep Learning Algorithms for Human Activity Recognition using Mobile and Wearable Sensor Networks: State of the Art and Research Challenges*. *Expert Systems with Applications*.
- OBR. 2017. *Fiscal sustainability report* [Online]. Available: https://assets.publishing.service.gov.uk/government/uploads/system/uploads/attachment_data/file/583956/OBR_fiscal_sustainability_report_print.PDF.
- OCAK, H. 2009. Automatic detection of epileptic seizures in EEG using discrete wavelet transform and approximate entropy. *Expert Systems with Applications*, 36, 2027-2036.
- OGAWA, M., SUZUKI, R., OTAKE, S., IZUTSU, T., IWAYA, T. & TOGAWA, T. Long-term remote behavioral monitoring of the elderly using sensors installed in domestic houses. *Engineering in Medicine and Biology*, 2002. 24th Annual Conference and the Annual Fall Meeting of the Biomedical Engineering Society EMBS/BMES Conference, 2002. *Proceedings of the Second Joint*, 2002. IEEE, 1853-1854.
- ORDÓÑEZ, F. J., IGLESIAS, J. A., DE TOLEDO, P., LEDEZMA, A. & SANCHIS, A. 2013. Online activity recognition using evolving classifiers. *Expert Systems with Applications*, 40, 1248-1255.
- PANSIOT, J., STOYANOV, D., MCILWRAITH, D., LO, B. & YANG, G. Ambient and wearable sensor fusion for activity recognition in healthcare monitoring systems. *4th international workshop on wearable and implantable body sensor networks (BSN 2007)*, 2007. Springer, 208-212.
- PANWAR, M., DYUTHI, S. R., PRAKASH, K. C., BISWAS, D., ACHARYYA, A., MAHARATNA, K., GAUTAM, A. & NAIK, G. R. CNN based approach for activity recognition using a wrist-worn accelerometer. *Engineering in Medicine and Biology Society (EMBC)*, 2017 39th Annual International Conference of the IEEE, 2017. IEEE, 2438-2441.
- PARKKA, J., ERMES, M., KORPIA, P., MANTYJARVI, J., PELTOLA, J. & KORHONEN, I. 2006. Activity classification using realistic data from wearable sensors. *IEEE Transactions on information technology in biomedicine*, 10, 119-128.
- PATEL, R., GOLDSTEIN, T., DYER, E., MIRHOSEINI, A. & BARANIUK, R. Deterministic Column Sampling for Low-Rank Matrix Approximation: Nyström vs. Incomplete Cholesky

- Decomposition. Proceedings of the 2016 SIAM International Conference on Data Mining, 2016. SIAM, 594-602.
- PATIL, T. R. & SHEREKAR, S. 2013. Performance analysis of Naive Bayes and J48 classification algorithm for data classification. *International Journal of Computer Science and Applications*, 6, 256-261.
- PAVEY, T. G., GILSON, N. D., GOMERSALL, S. R., CLARK, B. & TROST, S. G. 2017. Field evaluation of a random forest activity classifier for wrist-worn accelerometer data. *Journal of science and medicine in sport*, 20, 75-80.
- PENG, H., LONG, F. & DING, C. 2005. Feature selection based on mutual information criteria of max-dependency, max-relevance, and min-redundancy. *IEEE Transactions on pattern analysis and machine intelligence*, 27, 1226-1238.
- PENG, L., CHEN, L., WU, X., GUO, H. & CHEN, G. 2017. Hierarchical complex activity representation and recognition using topic model and classifier level fusion. *IEEE Transactions on Biomedical Engineering*, 64, 1369-1379.
- PHAM, M., YANG, D. & SHENG, W. 2018. A Sensor Fusion Approach to Indoor Human Localization Based on Environmental and Wearable Sensors. *IEEE Transactions on Automation Science and Engineering*.
- PHILLIPS, L. J., DEROCHE, C. B., RANTZ, M., ALEXANDER, G. L., SKUBIC, M., DESPINS, L., ABBOTT, C., HARRIS, B. H., GALAMBOS, C. & KOOPMAN, R. J. 2017. Using embedded sensors in independent living to predict gait changes and falls. *Western journal of nursing research*, 39, 78-94.
- PLÖTZ, T., HAMMERLA, N. Y. & OLIVIER, P. Feature learning for activity recognition in ubiquitous computing. *IJCAI Proceedings-International Joint Conference on Artificial Intelligence*, 2011. 1729.
- POURBABAEI, B., ROSHTKHARI, M. J. & KHORASANI, K. 2017. Deep Convolution Neural Networks and Learning ECG Features for Screening Paroxysmal Atrial Fibrillation Patients. *IEEE Transactions on Systems, Man, and Cybernetics: Systems*.
- QIU, S., WANG, Z., ZHAO, H. & HU, H. 2016. Using distributed wearable sensors to measure and evaluate human lower limb motions. *IEEE Transactions on Instrumentation and Measurement*, 65, 939-950.
- RAJA, K. B., RAGHAVENDRA, R., VEMURI, V. K. & BUSCH, C. 2015. Smartphone based visible iris recognition using deep sparse filtering. *Pattern Recognition Letters*, 57, 33-42.
- RAMOS-GARCIA, R. I. & HOOVER, A. W. A study of temporal action sequencing during consumption of a meal. Proceedings of the International Conference on Bioinformatics, Computational Biology and Biomedical Informatics, 2013. ACM, 68.
- RASHEED, M. B., JAVAID, N., ALGHAMDI, T. A., MUKHTAR, S., QASIM, U., KHAN, Z. A. & RAJA, M. H. B. Evaluation of human activity recognition and fall detection using android phone. *Advanced Information Networking and Applications (AINA), 2015 IEEE 29th International Conference on*, 2015. IEEE, 163-170.
- RAVI, D., WONG, C., LO, B. & YANG, G.-Z. Deep learning for human activity recognition: A resource efficient implementation on low-power devices. *Wearable and Implantable Body Sensor Networks (BSN), 2016 IEEE 13th International Conference on*, 2016. IEEE, 71-76.
- RAVI, N., DANDEKAR, N., MYSORE, P. & LITTMAN, M. L. Activity recognition from accelerometer data. *Aaai*, 2005. 1541-1546.
- REDDY, S., MUN, M., BURKE, J., ESTRIN, D., HANSEN, M. & SRIVASTAVA, M. 2010. Using mobile phones to determine transportation modes. *ACM Transactions on Sensor Networks (TOSN)*, 6, 13.

- REISS, A., HENDEBY, G. & STRICKER, D. 2015. A novel confidence-based multiclass boosting algorithm for mobile physical activity monitoring. *Personal and Ubiquitous Computing*, 19, 105-121.
- REISS, A. & STRICKER, D. Introducing a new benchmarked dataset for activity monitoring. *Wearable Computers (ISWC), 2012 16th International Symposium on*, 2012. IEEE, 108-109.
- RODRIGUEZ-MARTIN, D., SAMÀ, A., PEREZ-LOPEZ, C., CATALÀ, A., CABESTANY, J. & RODRIGUEZ-MOLINERO, A. 2013. SVM-based posture identification with a single waist-located triaxial accelerometer. *Expert Systems with Applications*, 40, 7203-7211.
- RONAO, C. A. & CHO, S.-B. Deep convolutional neural networks for human activity recognition with smartphone sensors. *International Conference on Neural Information Processing*, 2015. Springer, 46-53.
- RONAO, C. A. & CHO, S.-B. 2016. Human activity recognition with smartphone sensors using deep learning neural networks. *Expert Systems with Applications*, 59, 235-244.
- ROY, N., MISRA, A. & COOK, D. 2016. Ambient and smartphone sensor assisted ADL recognition in multi-inhabitant smart environments. *Journal of ambient intelligence and humanized computing*, 7, 1-19.
- SAKAR, C. O., KURSUN, O. & GURGEN, F. 2012. A feature selection method based on kernel canonical correlation analysis and the minimum Redundancy–Maximum Relevance filter method. *Expert Systems with Applications*, 39, 3432-3437.
- SANI, S., MASSIE, S., WIRATUNGA, N. & COOPER, K. Learning Deep and Shallow Features for Human Activity Recognition. *International Conference on Knowledge Science, Engineering and Management*, 2017. Springer, 469-482.
- SATHYANARAYANA, A., JOTY, S., FERNANDEZ-LUQUE, L., OFLI, F., SRIVASTAVA, J., ELMAGARMID, A., ARORA, T. & TAHERI, S. 2016a. Sleep quality prediction from wearable data using deep learning. *JMIR mHealth and uHealth*, 4.
- SATHYANARAYANA, A., JOTY, S., FERNANDEZ-LUQUE, L., OFLI, F., SRIVASTAVA, J., ELMAGARMID, A., TAHERI, S. & ARORA, T. 2016b. Impact of Physical Activity on Sleep: A Deep Learning Based Exploration. *arXiv preprint arXiv:1607.07034*.
- SCHÖLKOPF, B., SMOLA, A. & MÜLLER, K.-R. 1998. Nonlinear component analysis as a kernel eigenvalue problem. *Neural computation*, 10, 1299-1319.
- SHOAIB, M., BOSCH, S., INCEL, O. D., SCHOLTEN, H. & HAVINGA, P. J. 2014. Fusion of smartphone motion sensors for physical activity recognition. *Sensors*, 14, 10146-10176.
- SILVER, D., HUANG, A., MADDISON, C. J., GUEZ, A., SIFRE, L., VAN DEN DRIESSCHE, G., SCHRITTWIESER, J., ANTONOGLU, I., PANNEERSHELVAM, V. & LANCTOT, M. 2016. Mastering the game of Go with deep neural networks and tree search. *nature*, 529, 484-489.
- SONG, S., CHANDRASEKHAR, V., MANDAL, B., LI, L., LIM, J.-H., SATEESH BABU, G., PHYO SAN, P. & CHEUNG, N.-M. Multimodal multi-stream deep learning for egocentric activity recognition. *Proceedings of the IEEE Conference on Computer Vision and Pattern Recognition Workshops*, 2016. 24-31.
- STATES, U. 2015. 2015 United States of Aging Survey Executive Summary [Online]. Available: <http://www.unitedhealthgroup.com/~media/UHG/PDF/2015/USofAging-2015-Executive-Summary.ashx?la=en> [Accessed May 2017].

- STIKIC, M., LAERHOVEN, K. V. & SCHIELE, B. 2008. Exploring semi-supervised and active learning for activity recognition. *IEEE International Symposium on Wearable Computers*, 81-88.
- STONE, E. E. & SKUBIC, M. 2015. Fall detection in homes of older adults using the Microsoft Kinect. *IEEE journal of biomedical and health informatics*, 19, 290-301.
- SU, X., TONG, H. & JI, P. 2014. Activity recognition with smartphone sensors. *Tsinghua Science and Technology*, 19, 235-249.
- SUBRAHMANYA, N. & SHIN, Y. C. 2010. Sparse multiple kernel learning for signal processing applications. *IEEE Transactions on Pattern Analysis and Machine Intelligence*, 32, 788-798.
- SUN, L., ZHANG, D., LI, B., GUO, B. & LI, S. 2010. Activity recognition on an accelerometer embedded mobile phone with varying positions and orientations. *Ubiquitous intelligence and computing*, 548-562.
- SUTO, J., ONIGA, S., LUNG, C. & ORHA, I. Recognition rate difference between real-time and offline human activity recognition. *Internet of Things for the Global Community (IoTGC), 2017 International Conference on, 2017. IEEE*, 1-6.
- SUTO, J., ONIGA, S. & SITAR, P. P. 2016. Feature analysis to human activity recognition. *International Journal of Computers Communications & Control*, 12, 116-130.
- SZTYLER, T., STUCKENSCHMIDT, H. & PETRICH, W. 2017. Position-aware activity recognition with wearable devices. *Pervasive and Mobile Computing*, 38, 281-295.
- TANG, J., ALELYANI, S. & LIU, H. 2014. Feature selection for classification: A review. *Data Classification: Algorithms and Applications*, 37.
- TAPIA, E. M., INTILLE, S. S., HASKELL, W., LARSON, K., WRIGHT, J., KING, A. & FRIEDMAN, R. Real-time recognition of physical activities and their intensities using wireless accelerometers and a heart rate monitor. *Wearable Computers, 2007 11th IEEE International Symposium on, 2007. IEEE*, 37-40.
- TERADA, T. & TANAKA, K. A framework for constructing entertainment contents using flash and wearable sensors. *International Conference on Entertainment Computing, 2010. Springer*, 334-341.
- TUNCA, C., ALEMDAR, H., ERTAN, H., INCEL, O. D. & ERSOY, C. 2014. Multimodal wireless sensor network-based ambient assisted living in real homes with multiple residents. *Sensors*, 14, 9692-9719.
- UDDIN, M., SALEM, A., NAM, I. & NADEEM, T. Wearable sensing framework for human activity monitoring. *Proceedings of the 2015 workshop on Wearable Systems and Applications, 2015. ACM*, 21-26.
- UM, T. T., BABAKESHIZADEH, V. & KULIC, D. 2016. Exercise Motion Classification from Large-Scale Wearable Sensor Data Using Convolutional Neural Networks. *arXiv preprint arXiv:1610.07031*.
- UM, T. T., PFISTER, F. M., PICHLER, D., ENDO, S., LANG, M., HIRCHE, S., FIETZEK, U. & KULIĆ, D. Data augmentation of wearable sensor data for parkinson's disease monitoring using convolutional neural networks. *Proceedings of the 19th ACM International Conference on Multimodal Interaction, 2017. ACM*, 216-220.
- UNITED NATIONS. 2017. *World Population Prospects:Key findings & advance tables [Online]*. Available: https://esa.un.org/unpd/wpp/Publications/Files/WPP2017_KeyFindings.pdf [2017 Revision].
- URAY, M., SKOCAJ, D., ROTH, P. M., BISCHOF, H. & LEONARDIS, A. Incremental LDA Learning by Combining Reconstructive and Discriminative Approaches. *BMVC, 2007*. 272-281.

- URBANOWICZ, R. J., MEEKER, M., LACAVA, W., OLSON, R. S. & MOORE, J. H. 2017. Relief-based feature selection: introduction and review. arXiv preprint arXiv:1711.08421.
- USLU, G., DURSUNOGLU, H. I., ALTUN, O. & BAYDERE, S. 2013. Human activity monitoring with wearable sensors and hybrid classifiers. *International Journal of Computer Information Systems and Industrial Management Applications*, 5, 345-353.
- VACHER, M., FLEURY, A., PORTET, F., SERIGNAT, J.-F. & NOURY, N. 2010. Complete sound and speech recognition system for health smart homes: application to the recognition of activities of daily living. In-Tech.
- VAN DER MAATEN, L., POSTMA, E. & VAN DEN HERIK, J. 2009. Dimensionality reduction: a comparative. *J Mach Learn Res*, 10, 66-71.
- VAN KASTEREN, T., NOULAS, A., ENGLEBIENNE, G. & KRÖSE, B. Accurate activity recognition in a home setting. *Proceedings of the 10th international conference on Ubiquitous computing*, 2008. ACM, 1-9.
- VAN KASTEREN, Y., BRADFORD, D., ZHANG, Q., KARUNANITHI, M. & DING, H. 2017. Understanding Smart Home Sensor Data for Ageing in Place Through Everyday Household Routines: A Mixed Method Case Study. *JMIR mHealth and uHealth*, 5, e52.
- VEPAKOMMA, P., DE, D., DAS, S. K. & BHANSALI, S. A-Wristocracy: Deep learning on wrist-worn sensing for recognition of user complex activities. *Wearable and Implantable Body Sensor Networks (BSN)*, 2015 IEEE 12th International Conference on, 2015. IEEE, 1-6.
- WALLEN, M. P., GOMERSALL, S. R., KEATING, S. E., WISLØFF, U. & COOMBES, J. S. 2016. Accuracy of heart rate watches: implications for weight management. *PLoS One*, 11, e0154420.
- WANG, A., CHEN, G., YANG, J., ZHAO, S. & CHANG, C.-Y. 2016a. A comparative study on human activity recognition using inertial sensors in a smartphone. *IEEE Sensors Journal*, 16, 4566-4578.
- WANG, J., CHEN, Y., HAO, S., PENG, X. & HU, L. 2017a. Deep learning for sensor-based activity recognition: A survey. arXiv preprint arXiv:1707.03502.
- WANG, J., ZHANG, X., GAO, Q., YUE, H. & WANG, H. 2017b. Device-free wireless localization and activity recognition: A deep learning approach. *IEEE Transactions on Vehicular Technology*, 66, 6258-6267.
- WANG, L. 2016. Recognition of human activities using continuous autoencoders with wearable sensors. *Sensors*, 16, 189.
- WANG, L., GU, T., XIE, H., TAO, X., LU, J. & HUANG, Y. A wearable rfid system for real-time activity recognition using radio patterns. *International Conference on Mobile and Ubiquitous Systems: Computing, Networking, and Services*, 2013. Springer, 370-383.
- WANG, R., BLACKBURN, G., DESAI, M., PHELAN, D., GILLINOV, L., HOUGHTALING, P. & GILLINOV, M. 2017c. Accuracy of wrist-worn heart rate monitors. *Jama cardiology*, 2, 104-106.
- WANG, S., YANG, J., CHEN, N., CHEN, X. & ZHANG, Q. Human activity recognition with user-free accelerometers in the sensor networks. *Neural Networks and Brain*, 2005. ICNN&B'05. International Conference on, 2005. IEEE, 1212-1217.
- WANG, W. & LIVESCU, K. 2015. Large-scale approximate kernel canonical correlation analysis. arXiv preprint arXiv:1511.04773.
- WANG, Y., CANG, S. & YU, H. Realization of wearable sensors-based human activity recognition with an augmented feature group. *Automation and Computing (ICAC)*, 2016 22nd International Conference on, 2016b. IEEE, 473-478.

- WANG, Z., YANG, Z. & DONG, T. 2017d. A review of wearable technologies for elderly care that can accurately track indoor position, recognize physical activities and monitor vital signs in real time. *Sensors*, 17, 341.
- WILSON, D. H. & ATKESON, C. Simultaneous tracking and activity recognition (STAR) using many anonymous, binary sensors. *International Conference on Pervasive Computing*, 2005. Springer, 62-79.
- WU, G. & XUE, S. 2008. Portable preimpact fall detector with inertial sensors. *IEEE Transactions on Neural Systems and Rehabilitation Engineering*, 16, 178-183.
- WU, J., WANG, J. & LIU, L. 2007. Feature extraction via KPCA for classification of gait patterns. *Human movement science*, 26, 393-411.
- WU, W., DASGUPTA, S., RAMIREZ, E. E., PETERSON, C. & NORMAN, G. J. 2012. Classification accuracies of physical activities using smartphone motion sensors. *Journal of medical Internet research*, 14.
- WU, Z., XU, Q., LI, J., FU, C., XUAN, Q. & XIANG, Y. 2018. Passive indoor localization based on csi and naive bayes classification. *IEEE Transactions on Systems, Man, and Cybernetics: Systems*, 48, 1566-1577.
- XI, X., TANG, M., MIRAN, S. M. & LUO, Z. 2017. Evaluation of feature extraction and recognition for activity monitoring and fall detection based on wearable sEMG sensors. *Sensors*, 17, 1229.
- XU, S. Empirical research methods for software engineering: Keynote address. *IEEE International Conference on Software Engineering Research, Management and Applications*, 2017. 1-1.
- YANG, M., ZHENG, H., WANG, H., MCCLEAN, S., HALL, J. & HARRIS, N. 2012. A machine learning approach to assessing gait patterns for complex regional pain syndrome. *Medical Engineering and Physics*, 34, 740-746.
- YAO, S., HU, S., ZHAO, Y., ZHANG, A. & ABDELZAHER, T. Deepsense: A unified deep learning framework for time-series mobile sensing data processing. *Proceedings of the 26th International Conference on World Wide Web*, 2017. International World Wide Web Conferences Steering Committee, 351-360.
- YEKKEHKHANY, B., SAFARI, A., HOMAYOUNI, S. & HASANLOU, M. 2014. A comparison study of different kernel functions for SVM-based classification of multi-temporal polarimetry SAR data. *The International Archives of Photogrammetry, Remote Sensing and Spatial Information Sciences*, 40, 281.
- YOON, S., SIM, J. K. & CHO, Y.-H. 2016. A flexible and wearable human stress monitoring patch. *Scientific reports*, 6, 23468.
- YU, L., XIONG, D., GUO, L. & WANG, J. 2016. A compressed sensing-based wearable sensor network for quantitative assessment of stroke patients. *Sensors*, 16, 202.
- YUN, J. & LEE, S.-S. 2014. Human movement detection and identification using pyroelectric infrared sensors. *Sensors*, 14, 8057-8081.
- ZENG, M., NGUYEN, L. T., YU, B., MENGSHOEL, O. J., ZHU, J., WU, P. & ZHANG, J. Convolutional neural networks for human activity recognition using mobile sensors. *Mobile Computing, Applications and Services (MobiCASE)*, 2014 6th International Conference on, 2014. IEEE, 197-205.
- ZHAN, K., RAMOS, F. & FAUX, S. Activity recognition from a wearable camera. *Control Automation Robotics & Vision (ICARCV)*, 2012 12th International Conference on, 2012. IEEE, 365-370.

- ZHANG, J. & WU, Y. 2018. Automatic sleep stage classification of single-channel EEG by using complex-valued convolutional neural network. *Biomedical Engineering/Biomedizinische Technik*, 63, 177-190.
- ZHANG, M. & SAWCHUK, A. A. A customizable framework of body area sensor network for rehabilitation. *Applied Sciences in Biomedical and Communication Technologies*, 2009. ISABEL 2009. 2nd International Symposium on, 2009. IEEE, 1-6.
- ZHANG, M. & SAWCHUK, A. A. A feature selection-based framework for human activity recognition using wearable multimodal sensors. *Proceedings of the 6th International Conference on Body Area Networks*, 2011. ICST (Institute for Computer Sciences, Social-Informatics and Telecommunications Engineering), 92-98.
- ZHANG, M. & SAWCHUK, A. A. Motion primitive-based human activity recognition using a bag-of-features approach. *Proceedings of the 2nd ACM SIGHIT International Health Informatics Symposium*, 2012. ACM, 631-640.
- ZHANG, S., MCCULLAGH, P. & CALLAGHAN, V. An efficient feature selection method for activity classification. *Intelligent Environments (IE)*, 2014 International Conference on, 2014. IEEE, 16-22.
- ZHANG, S., WEI, Z., NIE, J., HUANG, L., WANG, S. & LI, Z. 2017. A Review on Human Activity Recognition Using Vision-Based Method. *Journal of healthcare engineering*, 2017.
- ZHENG, Y., LIU, Q., CHEN, E., GE, Y. & ZHAO, J. L. Time series classification using multi-channels deep convolutional neural networks. *International Conference on Web-Age Information Management*, 2014. Springer, 298-310.
- ZHENG, Y., WONG, W.-K., GUAN, X. & TROST, S. Physical Activity Recognition from Accelerometer Data Using a Multi-Scale Ensemble Method. *IAAI*, 2013.
- ZHOU, B., SUNDHOLM, M., CHENG, J., CRUZ, H. & LUKOWICZ, P. 2016. Measuring muscle activities during gym exercises with textile pressure mapping sensors. *Pervasive and Mobile Computing*.
- ZHU, C. & SHENG, W. 2011. Motion-and location-based online human daily activity recognition. *Pervasive and Mobile Computing*, 7, 256-269.
- ZHU, C. & SHENG, W. 2012. Realtime recognition of complex human daily activities using human motion and location data. *IEEE Transactions on Biomedical Engineering*, 59, 2422-2430.
- ZOLFAGHARI, S. & KEYVANPOUR, M. R. SARF: Smart activity recognition framework in Ambient Assisted Living. *Computer Science and Information Systems (FedCSIS)*, 2016 Federated Conference on, 2016. IEEE, 1435-1443.